Project Khepri:
Feasibility Study of Mining Asteroid Bennu

Final Engineering Design Report

August 26, 2022

Revision History

Revision	Revision Date	Description	Author(s)
1.0	August 26, 2022	Original version of this document	See List of Authors
2.0	September 19, 2022	Internal review comments incorporated	See List of Authors

List of Authors

University of Alberta
Gowtham Boyala
Adam Gremm
Ahmet Gungor
Amirhossein Taghipour

University of Arizona
Massimo Biella
Jiawei "Jackson" Qiu
Athip Thirupathi Raj

University of Toronto
Arjun Chhabra
Adam Gee
Saanjali Maharaj
Erin Richardson

University of Waterloo
Julia Empey

University of Western Ontario
Haidar Ali Abdul-Nabi
Erika Frost
Ariyaan Talukder
Lindsay Richards

Executive Summary

Water has been identified as a critical resource for development of robust cis-lunar infrastructure. Providing a potential source of clean-energy propellant and/or an essential consumable for humans or agriculture on crewed trips to the Moon or Mars while avoiding high costs of launching from Earth is thus a highly desirable element to cis-lunar infrastructure.

The OSIRIS-REx mission provided a complete survey of the asteroid Bennu and will return regolith samples to Earth in 2023, making this a well-understood and low-risk target that is estimated to be on average 6.3% water by mass. The Khepri Project comprises a team of international students, academics, and industry subject matter experts working on the technical design, business case, and political aspects of a feasibility study to mine asteroid Bennu for water.

This study included outlining a multi-year mining mission, where robotic explorers would be sent to both an orbit around Bennu as well as to Bennu's surface, culminating in tonnes of water extracted for transport back to cis-lunar space for immediate use. Mining asteroid Bennu is an unprecedented scientific opportunity to study the formation of our solar system - large scale operations could enable kilogram scale samples across Bennu's surface and subsurface.

Such an endeavor would provide new opportunities for synergy with other industries, such as Canada's well established mining sector. Future mining of near-earth asteroids provides additional resources (e.g. rare earth elements) to support Canada's manufacturing sector as well.

Pursuing such a mission provides an opportunity to demonstrate novel surface operations on small bodies leading to future asteroid mining endeavors. These include: use of autonomous robotic elements; improved in-situ resource utilization (ISRU) technologies; and deep space rendezvous. The Canadian Space Agency's leadership in this direction would engage Canadian academia, industry, and students, and would facilitate continued development of highly qualified personnel in planetary geology and space robotics & operations.

This document outlines the various elements considered in this feasibility study, culminating in mission and system design.

Acknowledgements

Project Khepri would like to thank the University of Alberta, University of Arizona, University of Toronto, Western University, and MDA for their support. Project Khepri would also like to thank all of the advisors that took time to help guide us and bring this mission concept to life, especially:

Project Facilitator

MDA/University of Toronto
Cameron Dickinson

Lecturers and Panelists

Geared Motion Engineering
Gavin Hay

Freelance
Dale Boucher

MDA
Ross Gillett
Peter Krimbalis
Joanne Leung
Adam Philip

University of Alberta
Chris Herd
Carlos Lange
Michael Lipsett
Benoit Rivard
Dan Sameoto

University of Arizona
Erik Asphaug
Dante Lauretta
Mike Nolan
Anjani Polit
Jekan Thanga
Leonard Vance

University of Toronto
Mark Barnet
Chris Damaren

University of Waterloo
Brandon DeHart

University of Western Ontario
Timothy Newson
Gordon “Oz” Osinski

Contents

List of Acronyms

AAM	Asteroid Approach Maneuver
ADC/ADCS	Attitude Determination and Control System
AGI	Analytical Graphics, Inc.
AMM	Asteroid Mining Mission
CAD	Computer Aided Design
CDH	Command and Data Handling
CFD	Computational Fluid Dynamics
CI	Ivuna-like Chondrites
CM	Mighei-like Chondrites
CNT	Carbon Nanotube
CR	Renazzo-like Chondrites
CSA	Canadian Space Agency
EGA	Earth Gravity Assist
EPS	Electrical Power System
ESA	European Space Agency
EML	Earth-Moon Lagrange Point
DART	Double Asteroid Redirect Test
DOF	Degrees of Freedom
DSM	Deep Space Maneuver
DSMC	Direct Simulation Monte Carlo
FFBD	Functional Flow Block Diagram
GEO	Geostationary Orbit
GMAT	General Mission Analysis Tool
GNC	Guidance Navigation and Controls
GTO	Geosynchonours Transfer Orbit
HDPE	High Density Polyethylene
H20	Water
ISRU	In-Situ Resource Utilization
ISS	International Space Station
JAXA	Japan Aerospace Exploration Agency
JPL	Jet Propulsion Laboratory
LDPE	Low Density Polyethylene
LEO	Low Earth Orbit
LH2	Liquid Hydrogen
LOX	Liquid Oxygen
MDA	MacDonald Dettwiler and Associates

MONTE	Mission Analysis, Operations, and Navigation Toolkit Environment
MLBD	Mission Level Block Diagram
MTBF	Mean Time Before Failure
MTO	Mars Transfer Orbit
NAM	Nominally Anhydrous Mineral
NASA	National Aeronautics and Space Administration
NEAR	Near Earth Asteroid Rendezvous
OSIRIS-REx	Origins, Spectral Interpretation, Resource Identification, Security, Regolith Explorer
OTES	OSIRIS-REx Thermal Emission Spectrometer
OVIRS	OSIRIS-REx Visible and InfraRed Spectrometer
PMD	Propellant Management Device
PV	Photovoltaic
RAP	Robotic Asteroid Prospector
RFP	Request for Proposal
SBD	System Block Diagram
SHD	System Hierarchy Diagram
SLS	Space Launch System
SPOF	Single Point of Failure
SSBD	Subsystem Block Diagram
STK	Systems Tool Kit
TAGSAM	Touch-and-Go Sampler
TBD	To Be Determined
TBM	Tunnel Boring Machine
TLI	Trans-Lunar Injection Orbit
TRL	Technology Readiness Level
TTC	Telemetry, Tracking and Command
T-VAC	Thermal Vacuum

List of Figures

List of Tables

Chapter 1: Introduction and Asteroid Mining Mission Concept

This project provides a concept for an asteroid mining mission to extract water from asteroid Bennu: Project Khepri. OSIRIS-REx's spectral analysis revealed that Bennu is composed of roughly 0.49% to 0.91% hydrogen by mass on the surface, and meaning between 4.4% and 8.1% water by mass [1]. While certain types of rocks or "boulders" are targeted with a known spectral abundance of hydrogen (higher end), an average value is roughly 6.26% by mass of water, meaning with a mass[1] of 73.29 billion kg, there is ∼4.588 billion kg of water. With a current valuation of launch costs being roughly 8000 USD/kg or $8000/kg (see Section 8.1), that values the water on Bennu at ∼$37 trillion. Given this valuation, this poses great economic value for a water mining mission at Bennu.

This paper is broken down into various chapters. Chapter 2 outlines all background information gathered by Project Khepri on past relevant space missions and considered methods/technologies, much like a technical literature review. Chapter 3 includes all high level trades relevant mission and system architecture. Chapter 4 breaks down the overall mission into segments and components, with each described in detail. Chapter 5 breaks down the mission systems and includes necessary requirements for these systems. Chapter 6 further breaks down those systems into key subsystems, highlighting their functions and requirements. Chapter 7 gives a detailed cost estimate of the various mission components. Finally, Chapter 9 summarizes the findings of this study and presents overall economic and humanitarian benefit.

[1] https://en.wikipedia.org/wiki/101955_Bennu

Chapter 2: Background

2 Preliminary Analysis: Missions To Date

Various asteroid-related missions have been conducted so far. A survey of these reference missions that completed surface operations on small bodies was conducted. They are summarized as follows:

OSIRIS-REx Touch and Go (Asteroid Sample Collection) - Bennu (2016-2023)
The OSIRIS-REx mission is the most representative mission and critical reference mission for this project, as it conducted a Touch and Go operation on Bennu's surface, with the goal of collecting at least 60g of material to be returned to Earth for analysis. It surveyed the asteroid, collecting vast amounts of data about Bennu and its environment. It conducted a touch-and-go landing where it "touched" the surface and sunk to a depth of approximately 50cm, using its robotic arm to collect a large sample of the material in the process[2]. It is estimated that 2kg of material were obtained[3], which far surpasses the initial goal of 60g.

Hayabusa (Asteroid Sample Collection) - Itokawa (2003-2010)
The goal of Hayabusa was to collect a sample from the asteroid Itokawa and return it to Earth for analysis, as well as study properties of the asteroid such as its shape, composition, and topography. The first touchdown attempt landed within 30m of the target site but no sample was collected. The second touchdown allowed for the collection of less than 1g of material via the use of sampling bullets fired at the surface. This mission marks not only the first controlled landing on and ascent from an asteroid, but also the first sample return from an asteroid.

Hayabusa 2 (Asteroid Sample Collection) - Ryugu (2014-2020)
This JAXA mission focused on sample collection and return from the asteroid Ryugu. Hayabusa 2 deployed two rovers and a lander. An artificial crater was created by firing an impactor at the surface. A sample of material was collected from this crater. 10% of the material was shared with NASA for analysis. Ryugu is similar to Bennu in that they are both carbonaceous asteroids.

Rosetta Mission and Philae Lander (Comet Landing) - 67P/Churyumov–Gerasimenko (2004-2016)
The goal of this ESA mission was to orbit and eventually land on the comet 67P for scientific study. The lander, Philae, descended to the designated Agiklia landing site. However, the lander's ice screws, which were designed for soft materials, did not penetrate the hard surface of the Agilkia region. Additionally, the thruster failed to fire due to a problem with a seal and the harpoons did not fire due to electrical issues. These failures led to a unsuccessful landing, but fortunately, the lander eventually settled on the surface. There, Philae was able to capture images and confirm the presence of complex molecules on the comet.

Stardust (Comet Sample Return) - Wild 2 (1999-2006)
This mission's primary focus was to collect dust from the coma of the Wild 2 comet. The sample return capsule used panels of aerogel to collect material. Additionally, some particles were collected during a flyby of asteroid 5535 Annefrank. Upon the culmination of this mission, more than 10,000 particles larger than 1 micrometer were returned to Earth for further study.

[2] https://www.scientificamerican.com/article/nasas-osiris-rex-is-overflowing-with-asteroid-samples/

[3] https://www.scientificamerican.com/article/NASAs-osiris-rex-probe-successfully-stows-space-rock-sample/

Deep Impact (Comet Impact) - Tempel 1 (2005-2013)
Unlike other previous cometary missions, Deep Impact's goal was to study the interior composition of a comet by means of, as the name suggests, an impact probe colliding with the Tempel 1 comet. The resulting crater was estimated to be have a diameter of 150 meters. The flyby spacecraft was able to capture images of the previously unseen inner composition of the comet.

Huygens (Saturn's Moon Landing) - Titan (1997-2017)
The ESA's Huygens Probe landed on Saturn's largest moon, Titan, as part of the Cassini mission. After a 2.5-hour descent, the probe survived on the surface for 72 minutes. This constitutes the milestone of the first landing in the outer solar system, and to date, the furthest landing from Earth.

NEAR Shoemaker (Asteroid Landing) - Eros (1996-2001)
This spacecraft, although not designed as a lander, survived a touchdown on the asteroid Eros and was able to transmit data for around two weeks.

Besides missions that completed surface operations on small bodies, a few additional relevant asteroid missions are discussed below:

Asteroid Redirect Mission (ARM)
This mission was proposed in 2013, but was subsequently defunded and cancelled in 2017. However, the goals of this mission would have been to retrieve a 4-metre diameter boulder from a Near Earth Asteroid's surface using a robotic arm with anchoring grippers. The boulder would have then been transported to a stable lunar orbit for further analysis. The spacecraft would have been propelled using solar electric propulsion. Bennu was one of the candidate parent asteroids for this mission.

Double Asteroid Redirect Test (DART) (2021-2022)
This first of its kind mission will attempt to demonstrate asteroid deflection (in terms of speed and path) by means of a kinetic impactor. The target for this test is Didymos, a binary asteroid system, which is not a threat for collision with Earth; it merely serves as a test bed. DART is planned to impact the smaller asteroid, Dimorphos, which is estimated to be 5 billion kilograms in mass. The expected result is a reduction in the altitude of Dimorphos' orbit around Didymos.

ISRU
While ISRU technologies have not yet been demonstrated in space, there have been some analog field tests on Earth with promising results and there are several plans for future space ISRU missions.

In 2008, the first lunar ISRU surface operations analog field test was performed in Hawaii at a site developed by NASA, the CSA, and DLR. The goal of this test was to demonstrate the prototype hardware and operations with the following functionalities: excavating material, producing oxygen, and storing the product. Due to limited system verification prior to the analog field test, neither system successfully electrolysed the extracted water. However, when tested with deionized water, the other system functions were effective. In 2010, a subsequent analog field test was carried out in Hawaii. The systems used in this test were the RESOLVE lunar polar resource characterization package, science instruments from CSA and NASA's Moon Mars Analog Mission Activity, as well as a mechanism for extraction using solar heating. This analog field test proved much more fruitful than the first - in 12 operations, 28g of oxygen was extracted via carbothermal reduction with a 9.6% average yield.

Looking ahead, NASA is investing in the Lunar Surface Innovation Initiative under the Artemis mission. This initiative focuses on increasing the TRL of lunar ISRU technologies by building machinery and electronics that are functional in extreme environments such as cryogenic permanently shadowed craters, developing strategies to mitigate lunar dust, and carrying out surface excavation and manufacturing operations. The ESA also has a lunar ISRU demonstration in development, with a target date of 2025. Slated to fly on NASA's Commercial Lunar Payload Services (CLPS) program is ESA's robotic drill, called Prospect, equipped with several scientific instruments to acquire lunar samples, which may prove useful in determining the presence and accessibility of lunar water for future ISRU missions.

This investigation revealed the current state of the art for missions focusing on landing on and sample collection from asteroids and other small celestial bodies, as well as ISRU technologies. This forms the background for the subsequent sections that are more specific to an Asteroid Mining Mission. This more in-depth investigation is outlined in Section 3, culminating in analysis and trade studies of the best current methods.

3 Overview of Considered Methods/Technologies

This section aims to investigate what is currently considered for ISRU and the current state-of-the-art technology and methods. It also assesses these various methods/technologies on various metrics, such as TRL, complexity and cost. It includes preliminary analysis relevant to the state-of-the-art knowledge.

3.1 Delta-V Calculator

Creating a Delta-V calculator involves many considerations. These are:

1. Launch vehicle design including fuel, type (serial/tandem), thrusters, characteristic energy, payload and mass breakdown among other variables.
2. Mission spacecraft design, again including fuel, thrusters, and mass breakdown.
3. The use of staging orbits, if at all, as a checkpoint between launch and transfer orbits.
4. Transfer orbit design, potentially including impulse maneuvers like Hohmann or Non-Hohmann transfers, deep space, phasing, chase and/or plane change maneuvers, and/or gravity assists.
5. Rendezvous maneuvers and/or orbit injection/deorbit burns with Bennu and relative motion mechanics.
6. Proximity operations near and around Bennu, including but not limited to, transfers to and from Bennu orbit and Bennu's surface and boulder operations on Bennu's surface.
7. Transfer orbit design back to Cis-Lunar space, similar to the previous transfer orbit design from Earth to Bennu.
8. Cis-Lunar orbit considerations, whether than be GEO, around one of the Earth-Moon system Lagrange points, typically EML1 or EML2, or any other Cis-Lunar orbit.

The most critical of these to this preliminary stage is launch vehicle design (1) which incorporates injection into transfer orbits (3), transfer orbit design to and from Bennu (4, 7) which includes rendezvous (5), and proximity operations around Bennu (6). Some preliminary information is known about the mission spacecraft at this stage, such as a mothership will be used, and a number of smaller spacecraft will be used for the mining operations. The only details of these spacecraft known at this stage are launch mass approximations, and rough thruster details. The mothership will use either a chemical or water-based propellant to propel the spacecraft during large delta-V maneuvers from Earth to Bennu and back, and the mining spacecraft will use water-based thrusters. This allows them to utilize product from the mission as fuel, and that the total amount of fuel for the entire mission does not need to be transported to Bennu.

Launch Design

OSIRIS-REx was launched using Atlas V 411 (no. AV-067). This launch vehicle consists of an Atlas first stage engine with a single additional strap-on solid rocket booster and a Centaur second stage engine. Centaur is a liquid hydrogen/liquid oxygen-fueled vehicle that produces 22,330 pounds of thrust (99,195 Newtons) using a single RL10-A-4-2 engine. The first stage burns RP-1 (Rocket Propellant-1) and liquid oxygen, and delivers 860,200 pounds of thrust at sea level (3.8 million Newtons). The solid rocket booster provides an additional 348,500 pounds of thrust at liftoff (1.6 million Newtons). Atlas V first lifted the

spacecraft into a parking orbit around Earth before firing its upper stage again to allow OSIRIS-REx to escape Earth's gravity. OSIRIS-REx then orbited the Sun for a year before using a gravity assist with Earth to travel to Bennu's vicinity. Although the reference design of OSIRIS-REx has been considered in Project Khepri, Altas V has since been decommissioned and thus cannot be used for this mission.

Future launch vehicles - New Glenn, Starship, and SLS - are possible alternatives for Project Khepri launch vehicles, considered in terms of their thrust and payload capacity. This payload must contain the mothership and any smaller spacecraft, including full or partial mission fuel for the mothership, and partial fuel for the smaller spacecraft. While these upcoming launch vehicles may be viable options when they become available, a current launch vehicle for consideration is the Falcon Heavy. This rocket can launch payloads up to 26700kg[4] to Geosynchronous Transfer Orbit (GTO), and subsequently on a hyperbolic escape trajectory to a heliocentric transfer orbit, similar to what OSIRIS-REx did with its launch from Atlas V in 2016[5]. The launch cost for Falcon Heavy is $150 million, which includes the price of fuel to incorporate into the economics of the mining mission.

Launch Vehicle	Thrust [MN]	Payload Capacity
Atlas V	5.5	8900 kg to GTO
Falcon Heavy	16.4	26700 kg to GTO
New Glenn	17.1	13000 kg to GTO
Vulcan Centaur	18.3	14400 kg to GTO
SLS	41	45000 kg to HCO, unknown to GTO
Starship	80.9	150000 kg to LEO, unknown to GTO

Table 3.1: Launch Vehicle Alternatives

A basic launch calculator was coded for this mission. It takes in the thrust inputs of the launch vehicle and calculates the delta-v for launch. It may be used for either a single-stage or multi-stage (serial or tandem) launch vehicle.

Transfer Orbit Design

As a starting point for transfer Orbit Design, OSIRIS-REx's trajectory was investigated. This outbound cruise trajectory of OSIRIS-REx is shown below in Figure 3.1.

[4] https://en.wikipedia.org/wiki/Falcon_Heavy
[5] https://en.wikipedia.org/wiki/Atlas_V

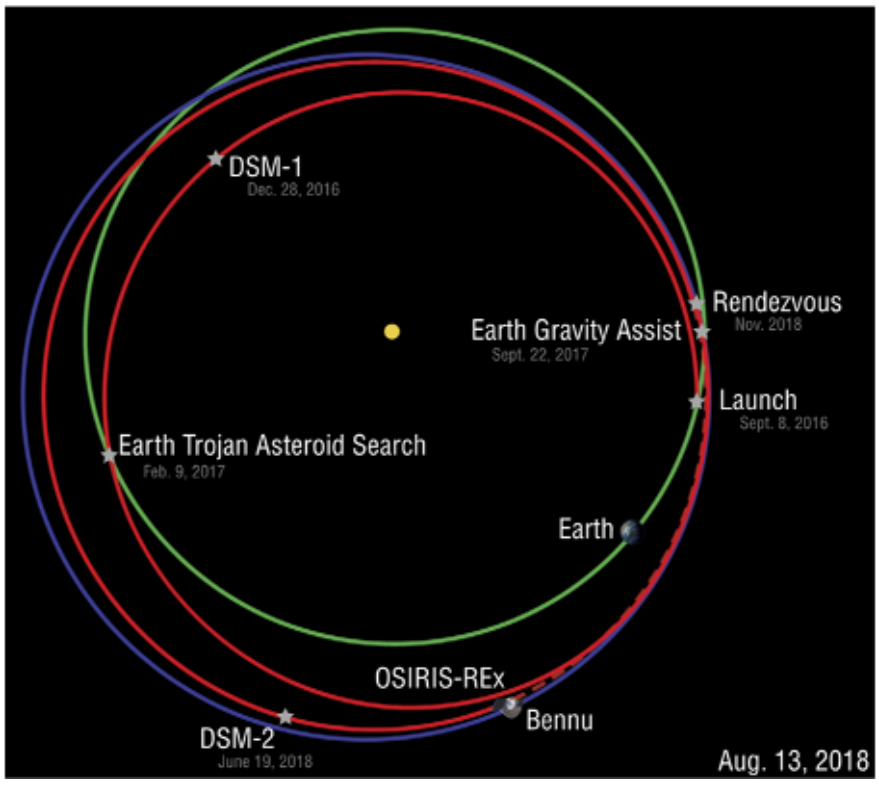

Figure 3.1: OSIRIS-REx's Transfer Orbit Trajectory from Earth to Bennu [2]

OSIRIS-REx's entire trajectory cost 1.4 km/s in delta-V[6]. The spacecraft[7] had a dry mass of 880kg and a wet mass of 2110kg. Their main Aeroject Rocketdyne MR-107S thrusters[8] also had a specific impulse between 225s to 236s. This means that with an average I_{sp} of 230.5s, the amount of fuel they carried allowed them 1.977 km/s of delta-V, meaning a safety factor of around 1.4. This is a good safety factor for consideration in fuel and delta-v allotment.

While the outbound cruise to Bennu is easily publicly findable information, details on the return cruise to Earth are not as much. Details of the Deep Space Maneuevers (DSMs)[9,10] and Rendezvous with Bennu, which was broken into four Asteroid Approach Maneuevers (AAMs)[11,12,13], are shown in Table 3.2 below.

[6] https://spaceflight101.com/osiris-rex/mission-flexibility/
[7] https://en.wikipedia.org/wiki/OSIRIS-REx
[8] https://spaceflight101.com/osiris-rex/osiris-rex-spacecraft-overview/
[9] https://www.nasa.gov/feature/goddard/2017/successful-deep-space-maneuver-for-nasa-s-osiris-rex-spacecraft
[10] https://www.nasa.gov/feature/goddard/2018/osiris-rex-executes-second-deep-space-maneuver
[11] https://www.nasa.gov/feature/goddard/2018/osiris-rex-executes-second-asteroid-approach-maneuver
[12] https://www.nasa.gov/feature/goddard/2018/nominal-aam3-preliminary-confirmation
[13] https://www.nasa.gov/feature/goddard/2018/osiris-rex-executes-fourth-asteroid-approach-maneuver

Table 3.2: Various DSM and AAM Delta-V Breakdowns

Maneuver	Delta-V (m/s)	Time after Launch (days)
DSM-1	431	111
EGA	-	379
DSM-2	16.7	658
AAM-1	351.3	753
AAM-2	135.8	767
AAM-3	5.1	781
AAM-4	0.1	795
Arrival (20km)	-	816
All Outbound Maneuvers	**940**	-

Members of the OSIRIS-REx team also explained that roughly 10 m/s of delta-V was expended in proximity operations around Bennu, meaning approximately 450 m/s of delta-V was used for the return trip from Bennu to Earth. The return trajectory is visualized in Figure 3.2[14], although the number of maneuvers and their delta-V requirement is unknown. The departure point from Bennu in the figure is nearly directly behind the arrival point shown at Earth, 2 revolutions around the Sun prior. This lower delta-V requirement is likely due to the trajectory design taking advantage of some gravity braking at Earth.

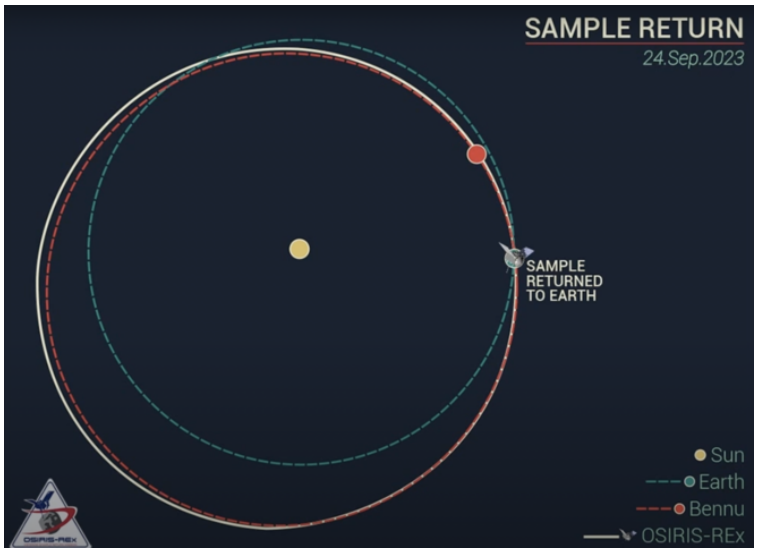

Figure 3.2: OSIRIS-REx's Transfer Orbit Trajectory from Bennu to Earth

From this initial investigation, an optimizer was created to try to determine the lowest-cost delta-V transfer orbit from Earth to Bennu via Matlab. Another sub-goal was to determine a range near the optimum, such that a variety of launch windows could be created to periodically send additional spacecraft for mining. Unfortunately, despite the successful completion of the optimizer, no optimum was found, with results varying widely depending on the initial conditions. Ultimately, a more complicated program like JPL's

[14] https://www.youtube.com/watch?v=zrRMoGrKkyU&ab_channel=OSIRIS-RExMission

MONTE[15], AGI's STK[16] or NASA's GMAT[17], must be used to determine such an optimal trajectory.

This optimization was completed by the OSIRIS-REx team and later found, with a minimum outbound cruise delta-V of 670 m/s, corresponding to 413 days, and 250 m/s return cruise corresponding to 856 days [3]. These trips correspond to specific dates that happen only once every 6 years. A faster but still low delta-V trip would consist of the same outbound cruise, but a 494 m/s return cruise corresponding to 422 days [3]. These two trajectories have are summarized below:

1. Delta-V: 920 m/s; Time: 1269 days or 3.47 years
2. Delta-V: 1092 m/s; Time: 835 days or 2.29 years

The reason why both of these are explored is that although one has a smaller delta-V, more water could be mined given the smaller amount of trip time, to make up for the difference. Moving forward, both of these trajectory delta-V values will be considered, and the best will be chosen as per mission requirements. It will also be assumed that there are multiple launch windows every 6.2 years (Bennu's synodic period with Earth) around that delta-V mark, so that there is not only one launch window for the mining mission.

This delta-V requirement is what the mothership must be capable of once it has been ejected from the launch vehicle following final separation of the payload capsule. As mothership thrusters have not been finalized, the mothership must carry at least enough fuel to get to Bennu, with a safety factor. Once the mothership has rendezvoused with Bennu, in will enter into a frozen terminator orbit of a TBD periapsis/radius.

Gravity Braking using Earth
Another maneuver was investigated where the spacecraft would simply depart from Bennu when near Earth at it's close approach every 6 years, and use Earth's gravity well to "brake" the spacecraft and be captured into a retrograde orbit around Earth. While this is technically possible, the delta-V required for the maneuver to depart Bennu onto such a hyperbolic trajectory around Earth would be greater than 5 km/s, as determined by analysis. This is in part due to the heliocentric orbital speeds of Earth and Bennu, which lie between 20 and 30 km/s depending on their position throughout their orbit, and also due to the maneuver taking place over such a short period, compared to the long two-year maneuver that OSIRIS-REx is performing to return to Earth from Bennu, that requires 2 full rotations around the Sun.

Proximity Operations

Once at Bennu, the smaller spacecraft must perform multiple proximity operations maneuvers as it interacts with Bennu's surface to collect material to "mine" for water many times over the mission timeline. At this stage, not much about these operations is fixed. As such, a generic proximity operations calculated was created for Hohmann and Non-Hohmann transfers, as well as escape maneuvers. Such a maneuver may look like one shown in Figure 3.3 below.

[15] https://montepy.jpl.nasa.gov/
[16] https://www.agi.com/products/stk
[17] https://opensource.gsfc.nasa.gov/projects/GMAT/

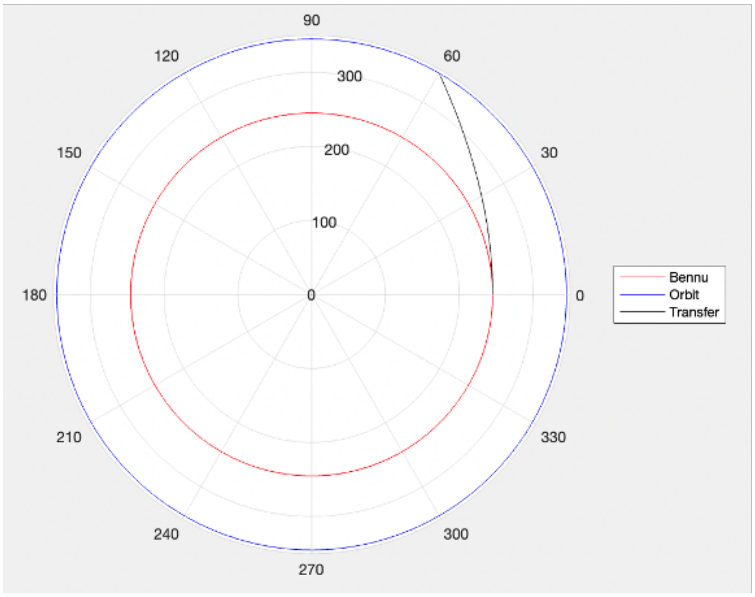

Figure 3.3: A Sample Proximity Operations Maneuver from Bennu to a Circle Orbit

In addition to this, a particle ejection calculator was created along the same lines to determine trajectories of debris/ejected particles. These descent operations can become highly involved and specific, leading to their optimization; however, due to the repeatable nature of an asteroid mining mission, those details were investigated yet have not been followed thus far.

Propellant Consumption

Calculators for propellant consumption for proximity operations, and orbit transfer to and from Bennu have also been created, utilizing the rocket equation as shown below:

$$m_{prop} = m_{dry}(e^{\frac{\Delta v}{I_{sp}\ g_0}} - 1) \tag{2.1}$$

where m_{prop} is the mass of propellant, m_{dry} is the dry mass of the spacecraft, Δv is the delta-v of the maneuver, I_{sp} is the specific impulse of the propellant, and $g_0 = 9.81\text{m/s}^2$.

3.2 Boulder Properties

Global Geology

Asteroid (101955) Bennu is a 0.5km diameter rubble pile carbonaceous chondrite asteroid that formed approximately one billion years ago from a large, differentiated parent body that was destroyed in a catastrophic impact [4]. The parent body itself likely formed early in the solar system's history 4.5 billion years ago and was tens to hundreds of kilometres in size, which allowed for extensive hydrothermal alteration to occur [5]. Bennu migrated to its current near-earth orbit 1.75 million years ago, before which it was a part of the main asteroid belt [6].

Although Bennu is relatively homogeneous on a global scale, there is considerable local variation 3.4. The Global geology can be split into two discrete units: An older smooth unit and a younger rough unit [4]. The smooth unit represents an older, relatively stable surface, while the rough unit represents areas with active

mass movement processes and resurfacing. The return of the OSIRIS-REx sample in 2023 will allow for the dating of formation, alteration, shock, and exposure ages for the various rock types on Bennu, which will provide more reliable absolute ages of the geologic units.

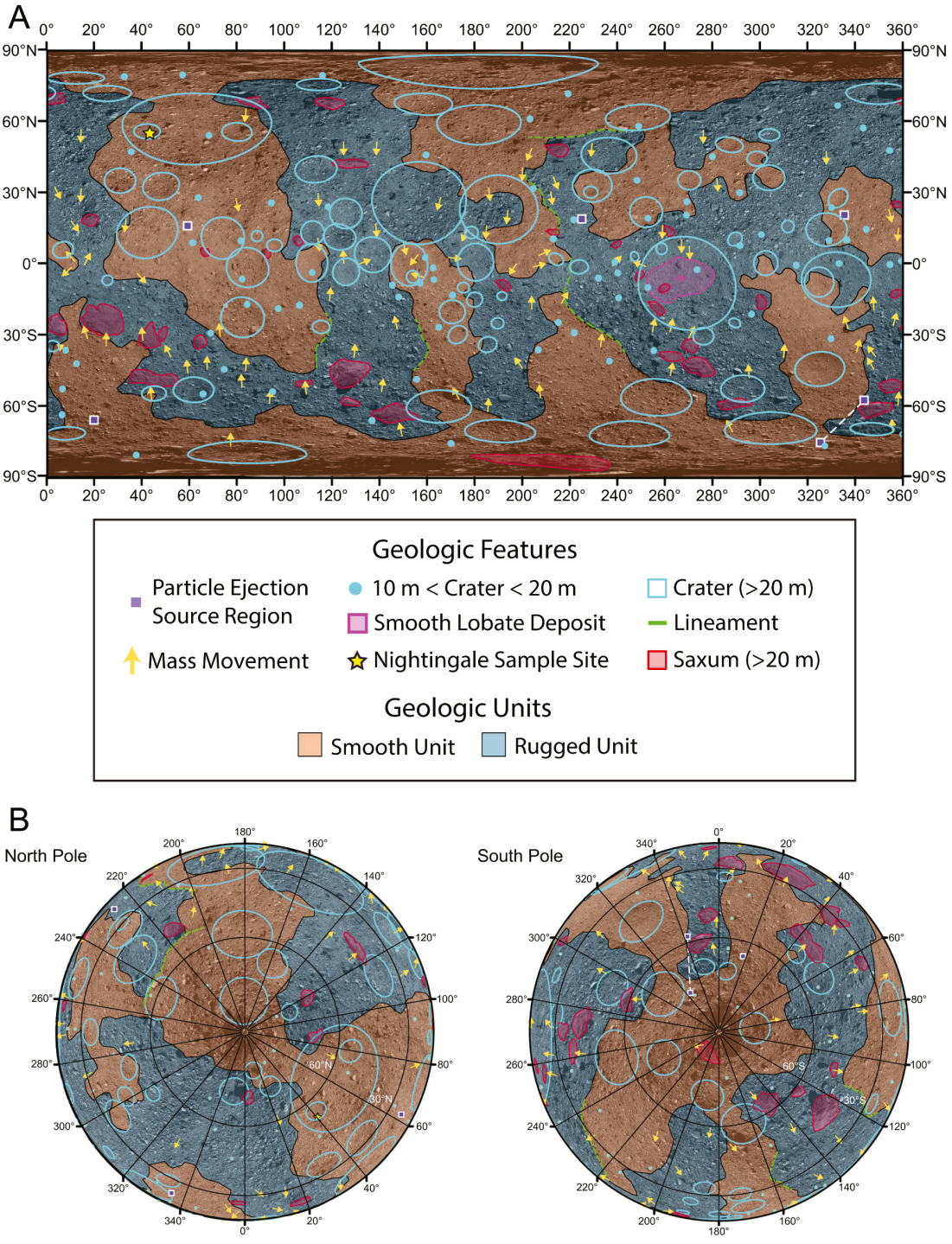

Figure 3.4: Global geologic map of Bennu from Jawin et al., 2022 [4]

The smooth unit is relatively old and formed between 10 and 65 million years ago, likely at the same time or immediately following formation of Bennu's prominent equatorial bulge. No resurfacing has occurred within the last 2 million years, which implies that the smooth unit is relatively geologically stable.

The surface of the rough unit is comparatively young and has been resurfaced by creep-style mass movement within the last 500,000 years, which is extremely recent in geologic time. The observation of particle ejection events by the OSIRIS-REx spacecraft demonstrates that Bennu is geologically active and the mass movement processes likely continue to the present day in the rough unit, although they have not been directly observed.

Bennu's surface is almost entirely cohesionless with a maximum compressive strength of approximately 2 Pa [7]. Due to the extremely low gravity, the shallow subsurface is not compresses and behaves like a granular fludized bed, analogous to a ball pit or quicksand. The low cohesion implies that capturing boulders from Bennu's surface will require very little force even if they are partially buried. It also suggests that anchoring to the surface of Bennu would be difficult or impossible, since any structure in the subsurface will not be able to exert significant force on the asteroid without disrupting it.

Boulder Types

At least four types of native boulders have been identified on Bennu 3.5 [8], along with exogenous, or type E boulders. Type E boulders are deposited by impactors and have varied compositions, but are typically brighter and stronger than Bennu's native material. The native boulders can be broadly categorized into high and low albedo types. The varied lithologies of Bennu's boulders are probably inherited from formation at different depths within the parent body [9] [10] [5]. Boulders with discrete layering off different lithologies have been observed, which implies that there was a vertical stratigraphic relationship between boulder types in the parent body [11].

Low albedo boulders include types A and B, which have a normal albedo between 3.5 and 4.9% [10]. Both have been interpreted as regolith breccias and formed near the surface of Bennu's parent body, although investigations are ongoing to evaluate if they could have instead formed through sediment deposition [12] [8]. The largest dark boulder (Roc Saxum) is 100m across which suggests that regolith breccia on Bennu's parent body extended at least 100m in depth and may have become sorted by grain size [8] [11]. Type A boulders have a rougher texture and larger visible clasts than type B. The clasts have varying compositions and albedo. High-albedo clasts are obvious in many type A boulders, which suggests that they formed at least in part after the parent body was hydrothermally altered. Type B boulders are similar to type A but have a much smoother texture and smaller visible clasts and visible polygonal fractures. The smoother surface often appears as a rind or coating on type A material, which suggests they are type A boulders that have been exposed at the surface for longer periods of time, becoming smoothed by micrometeorite impacts and fractured by impacts and thermal cycling. Thermal inertia data suggests that the dark boulders have a porosity of up to 50% and are comparatively weaker than the bright boulders [13].

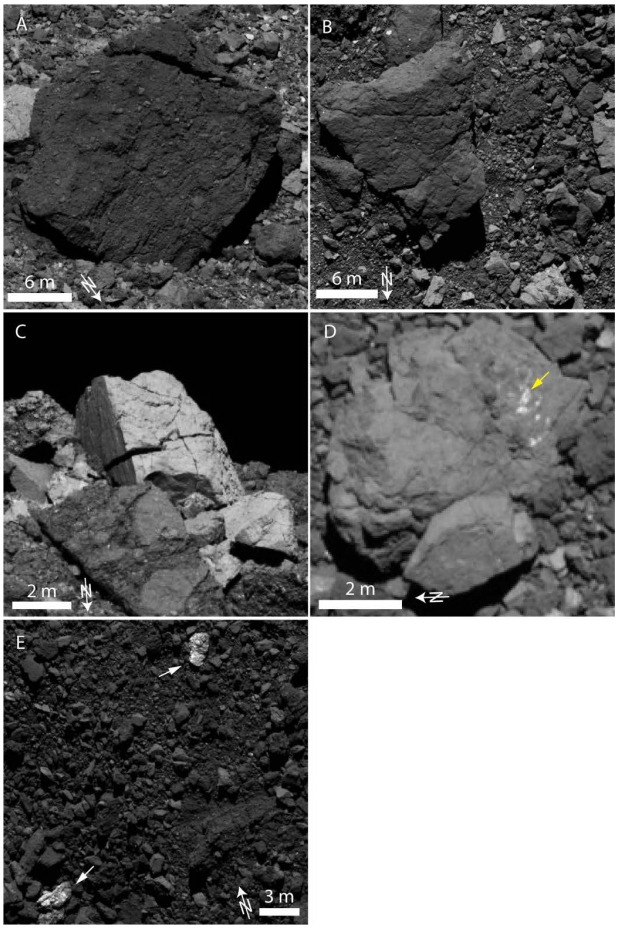

Figure 3.5: Types of boulders observed on Bennu from Jawin et al., 2022 [8]

The high-albedo boulders type C and D have a normal albedo between 4.9% and 7.4% and are much smaller on average than dark boulders [10]. Type C boulders exhibit smooth, angular surfaces and anastomosing fractures and have no visible clasts, implying that they are either very fine-grained or did not form through sedimentary or impact processes. Type D boulders are similar to type C but are slightly more rugged and contain visible carbonate veins [5]. The largest type C boulder is 12m in diameter [8] which suggests that they are more brittle than the dark boulders and more prone to fracturing from impacts and thermal cycling. This is supported by thermal inertia data [10] which shows they have up to 38% porosity, considerably less than the dark boulders. It is possible that the porosity has been infilled by alteration minerals [5], or it may not have existed to begin with.

Mineralogy

Bennu is a carbonaceous asteroid with a bulk composition most comparable to CM and some CI chondrite meteorites, although no exact analogue exists in the meteorite collection [14] [15] [16].

Until the OSIRIS-REx sample is returned, the best estimates of Bennu's composition come from visible to thermal infrared spectroscopy, thermography, and interpretation of meteorite analogues. Currently, Bennu is thought to be most analogous to the lowest Rubin petrologic subtype (most altered) CM chondrites, although some CI chondrites and one CR chondrite are also possible analogues. Bennu's spectra is

blue-sloped, which has been shown to correlate with an intimate mixture of phyllosilicate minerals, carbon species, and magnetite [17] [18].

Bennu is volumetrically dominated by hydrated phyllosilicate minerals and organic material. The exact proportion of phyllosilicate is debated, with an upper limited proposed at 67% based on spectral similarities to the CR1 chondrite Grosvenor Mountain (95577) [16]. Iron oxides (magenetite and goethite) probably comprise 5-10% of Bennu's surface, with anhydrous silicates such as olivine and pyroxene probably comprising 5%, although this may be an underestimation due to overprinting by phyllosilicate spectra. Large carbonate veins and probably disseminated carbonate are also present in high-albedo boulders, thought to be associated with rocks formed deeper in the parent body[5].

The phyllosilicates are probably dominated by serpentines with minor amounts of kaolinite and other clays[19]. Notably, no Mg-OH absorption band has been observed, which could suggest that the phyllosilicates are iron rich end members [20].

Water content ranges from 5.72-6.79% by weight and varies globally[1]. The OH absorption band that indicates the widespread hydrogen presence on Bennu cannot discriminate between hydroxylated and hydrated phyllosilicates but bennu's surface reaches 116 Celcius, which would be hot enough to cause dehydration [21]. Therefore, the hydrogen is almost certainly in the form of hydroxide, which require temperatures from 700-900 Celsius to liberate from phyllosilicates.

Two global spectral end members are observed [15]. One is consistant with a phyllosilite dominated, poorly crystalline or amorphous material and the other is consistant with fine particles. This discrepency could be explained by a coating of fine dust on larger boulders.

Mechanical Properties

The high and low albedo boulders have discrete physical properties , although the differences observed on a global scale may actually represent end-members of a continuum that is only apparent at higher resolutions [10] [13]. Ballouz et al., estimated the impact strength of Bennu's boulders at 0.44-1.7 MPa based on craters in metre-sized boulders [6]. This is slightly higher than the range of 0.10-0.78 MPa estimated by Rozitis et al. based on thermal inertia data [10].

The low-albedo boulders generally appear to be weaker and more porous, with 50% porosity and a tensile strength of 0.1-0.15 MPa. Despite the lower strength, dark boulders are on average much larger than bright boulders. This suggests that the more porous and weaker material may crumple and absorb small impacts rather than fracturing, which is also consistent with the observations by Jawin et al. of smoother type B material appearing as a coating on type A boulders [9].

High-albedo boulders appear to be stronger and less porous, with a porosity of 24-38% and tensile stregnth of 0.31-0.78MPa [10]. The smaller size and obvious fractures present in the bright boulders imply they are more prone to fracturing than the dark boulders. The higher strength and lower porosity likely results in a smaller capacity for internal deformation, leading to more frequent fracturing from impacts and thermal cycling. The low gravity of Bennu means that some of the heavily fractured bright boulders may be much weaker than the material's tensile strength and may break along fractures when moved.

3.3 Surface Impingement

Impingement of the vehicle on the surface of Bennu have several considerations that needs to be examined carefully to determine optimal landing conditions. These include but not limited to:

- Collisions between particles on the surface of Bennu that dislocated by the thruster's jet and the vehicle.
- Reduction in the visibility due to the particles fluttering around the vehicle.
- Formation of a crater which may result stability issues for the vehicle
- Blockage of solar panels by the cloud of particles since suspension of the particles may suspend around the spacecraft for hours due to the micro gravity conditions of Bennu
- Risk of penetration of the spacecraft into the surface in the case of impingement on the regolith

Inputs that are necessary to successfully explore the effects of the jet impingement can be classified into two categories:

- Landing conditions, e.g., landing type, landing speed, design of the thrusters, and mass of the vehicle
- Surface conditions, e.g., surface cohesion, size and density of the particles, and landing location

The following two approaches will be utilized for this purpose.

Empirical Correlations and Experimental Studies

There is an existing literature on the structures on the surface of Bennu and their interaction with a jet plume [22] [23]. Ballouz et al. recently developed granular impact force laws using in situ data from OSIRIS-REx mission [23] . Furthermore, there are other experimental studies that investigate the impact of jet plumes on the granular structures [24] [25]. It is aimed at utilizing the literature to develop basic understanding of geological characteristics of the materials on the asteroid's surface and their interaction with the approaching spacecraft. The preliminary analysis from the literature suggests that regolith, which covers some regions on the surface of Bennu, is not a suitable impingement location due to lack of strong resistance force applied by the particles (see Figure 3.6) on the solid body, e.g., spacecraft landing on the surface [23]. This may results in the burial of the spacecraft into the regolith. Similarly, jet plume impinging on the regolith may constitute a crater depending on the flow rate and height from the surface (see Figure 3.7) which may cause some stability considerations for the spacecraft as outlined above.

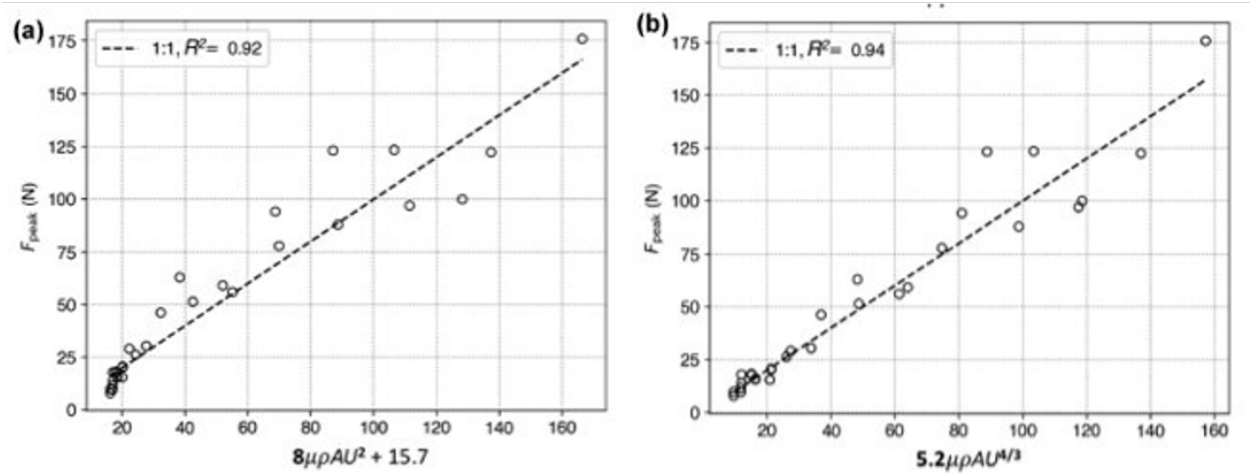

Figure 3.6: Empirical Correlations for Peak Force due to the Particles [23]

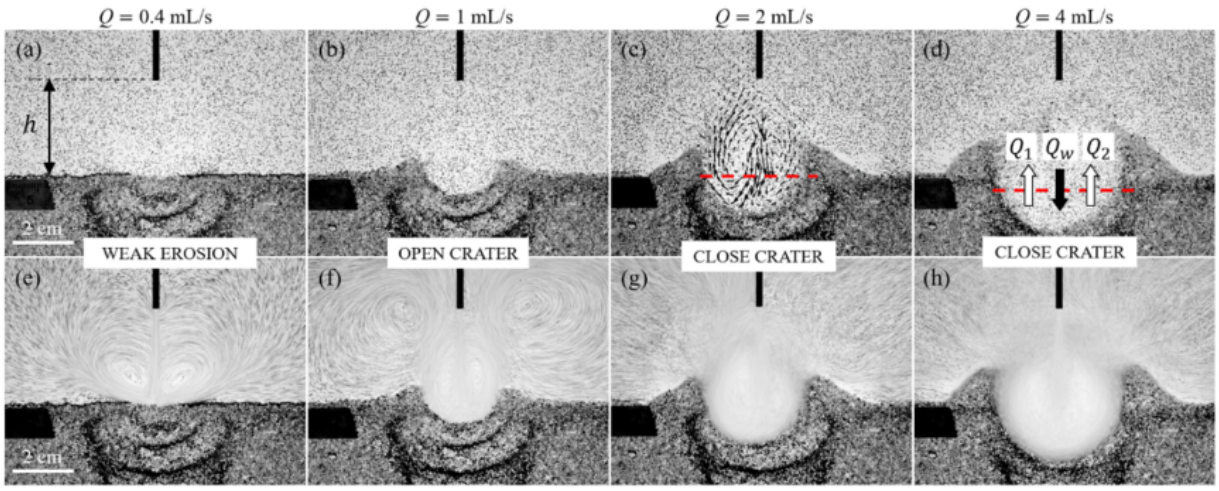

Figure 3.7: Crater morphology for different flow regimes [25]

Computational Fluid Dynamics (CFD) Simulations

Nature of the problem requires coupling between fluid flow and particle motion in order to realistically reflect the physics of interaction between jet plume and asteroid surface. Solution of this multi-physics problem would provide valuable data on the dynamics of the particles. This can be used in order to assess the damage on the spacecraft due to the particles, size of the crater formed by the jet plume, density of the particles around the spacecraft that reduces the visibility. These considerations are critical towards the success of the mission, therefore, a comprehensive analysis should be addressed to reveal their characteristics. However, effects of jet plume on the surface structures rely on several conditions including strength of the plume, height of the spacecraft from the surface, geological properties of the particles, and topology of the surface. Thus, numerical simulations, which are easier to conduct and provides faster results compared to the experiments, can be employed to deal with wide range of flow conditions.

The current multi-physics problem which involves the coupling of fluid dynamics and motion of the particles can be solved using CFD simulations. OpenFOAM which is an open-source CFD solver is determined for conducting the simulations. This approach aims at illuminating the physics behind the impingement of the vehicle for several surface and landing conditions.

Near-vacuum conditions on the surface of Bennu due to lack of atmosphere cause flow to contradict with the continuum hypothesis. Therefore, special attention should be paid to the selection of the solver since standard approaches that assumes continuum such as compressible, incompressible or potential flow solvers, can not be employed for simulating rarefied flows. Hence, Direct Simulation Monte Carlo (DSMC), which is a statistical approach based on the Boltzmann Equation, method is utilized to conduct the simulations. This method uncouples the motion and collision of the particles. The collisions between the particles are solved in each mesh cell in a probabilistic manner after the motions of the molecules are captured. It has been shown that DSMC performs perfectly in capturing the physics of jet plume development in near-vacuum conditions as well as other rarefied gas flows [26] [27] [28] [29] [30]. Note that the jet plume studies simulated the flow on the surface of the Moon rather than Bennu or any other asteroid. However, the flow physics of the jet plume on the Moon has no fundamental differences than that of on Bennu since both lack of an atmosphere.

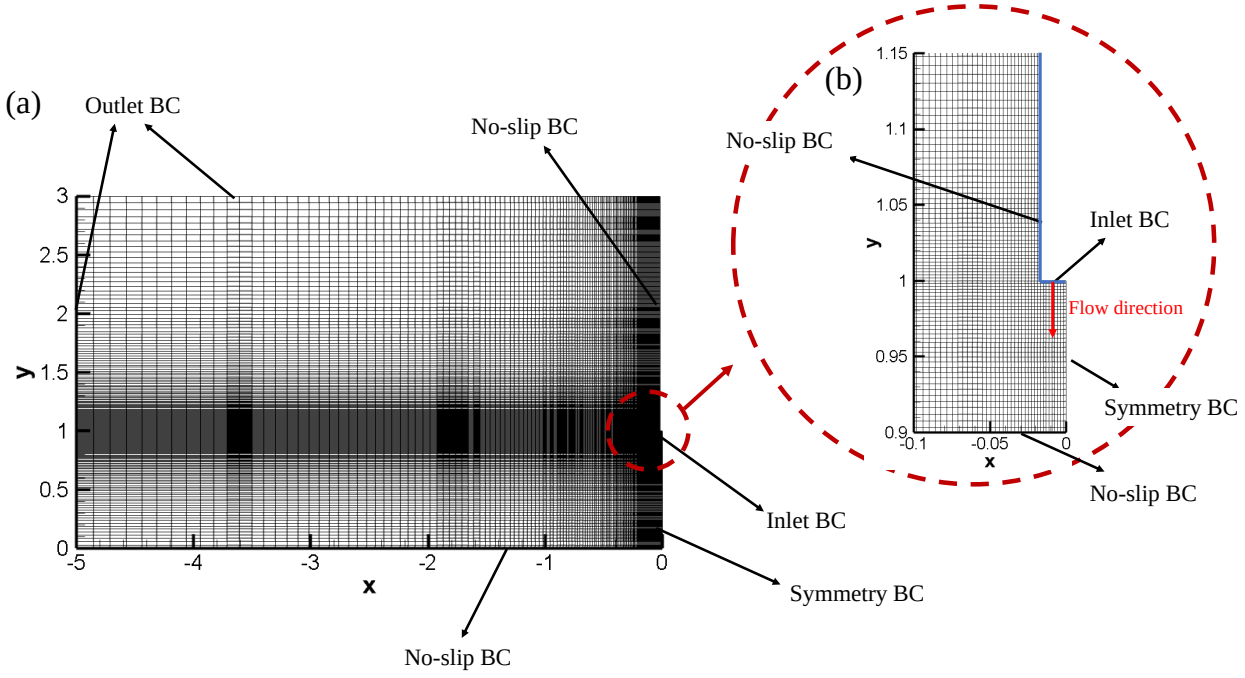

Figure 3.8: Computational domain and boundary conditions of 2d simulations for $h = 1m$ depicting (a) full view, (b) detailed view around the inlet.

We start our analysis by solving for the flow field only without coupling it with dynamics of the particles. This may seem to be a futile approach, since the motion of particles are responsible for the aforementioned risks for landing of the spacecraft. However, it is estimated that the sampling collection apparatus of OSIRIS-REx displaces considerable amount of material, which is mostly attributed to the low cohesion strength of the particles on the surface of Bennu [31]. This hints that a jet plume that can reach to the

surface will cause mobilization of the particles depending on its momentum. The high momentum jet, introduced by the thrusters, would try to expand in every direction because of the near-vacuum conditions of the medium. This results in diminishment of the jet as it approaches to the surface. Therefore, we aim at identifying the jet plume's ability to preserve its momentum when it reaches the surface. Hence, we run 2D simulations at a range of thruster height from the surface (h) and inlet jet velocity at the thruster outlet (v) to distinguish the conditions that yield a substantial interaction between the jet plume and particles.

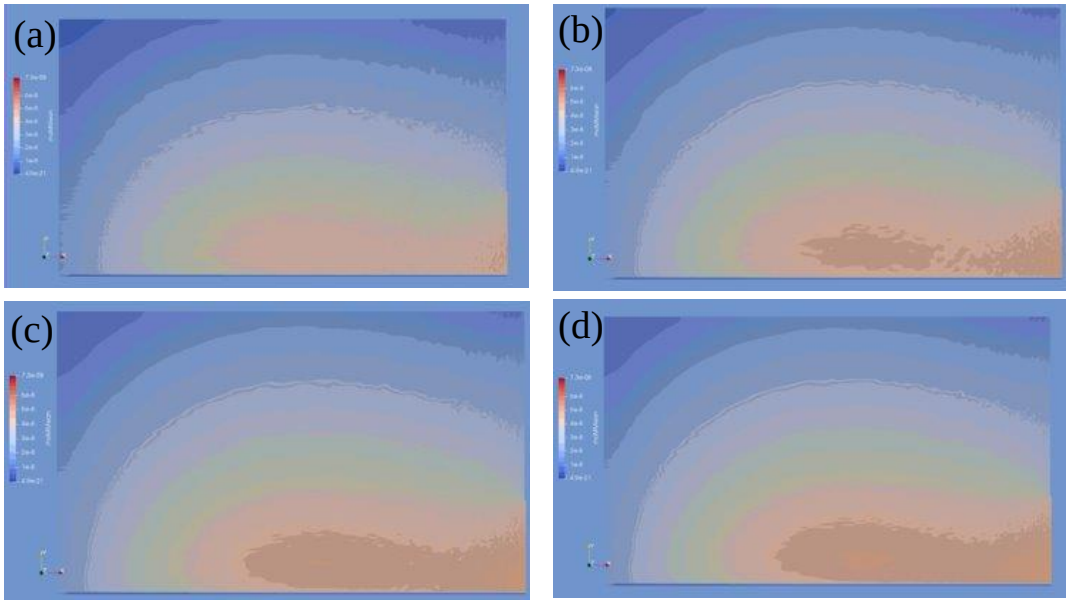

Figure 3.9: Preliminary results for the density of the jet plume for $h = 1m$ and $v = 1m/s$ at (a) $t_1 = 0.05s$, (a) $t_2 = 0.10s$, (a) $t_3 = 0.15s$, and (a) $t_4 = 0.20s$

Computational domain with detailed view around the inlet is given in Figure 3.8. Since there is a full symmetry in the flow, the symmetry boundary condition is applied at the thruster centerline to save computational effort. Preliminary results for the development of the flow density in the domain, that corresponds to the $h = 1m$ and $v = 1m/s$ case, is given in Figure 3.9. It is clear from the figure that the density of the flow is highest at the inlet and shrinks as the plume expands in other directions. This in inline with our intuition for the jet plume behaviour under near-vacuum conditions as explained above. Nevertheless, a comprehensive validation and verification study is still necessary to prove the reliability of the simulations.

3.4 Anchor

The anchoring system onto the surface of asteroid Bennu has several requirements that must be met to ensure success while doing operations on the surface. A failure in one or more of these systems could prove fatal to the system.

- Target Selection: For the anchor to succeed on the surface, it requires a boulder with low porosity.

- Landing Site: The landing site must be able to withstand high impact forces, and be able to provide the depth needed for the harpoon.
- Robust: The anchoring system must have a negligibly low rate of failure, and in the scenario it does fail, have a fail-safe to continue the mission

With the following conditions identified, it can be seen that the anchoring system is highly dependent on the location. Due to this, a large amount of unwanted variability is introduced to the success of the system. Though, if anchoring is the method of choice, there are a few options.

Philae Harpoon Anchor

The Philae mission's harpoon anchor was developed by the ESA (European Space Agency), though failed to be used during the mission due to deployment issues [32].

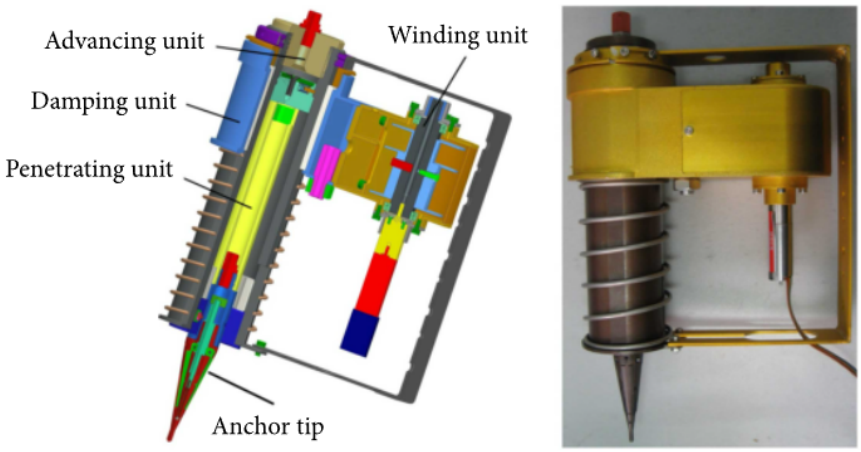

Figure 3.10: Harpoon Unit with Labeled Components

This unit consists of several components, including:

- Winding Unit: Tense cord attached to tail of penetration unit
- Damping Unit: Protects the motor from impact loads.
- Advancing Unit: High Pressure gas ignites and hits piston
- Penetrating Unit: Pyrotechnics ignite & create high pressure gas, the piston is hit and the claws and barb are opened. The anchor tip is dependent on the surface that is being penetrated.

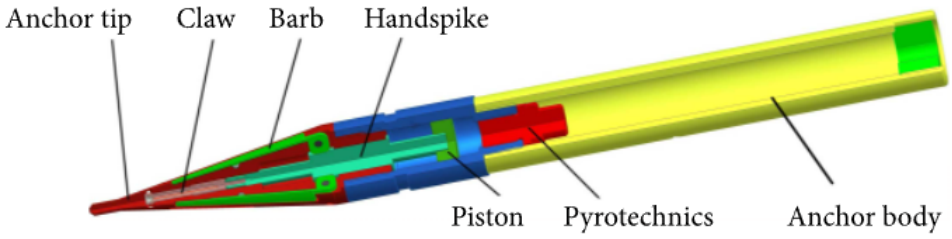

Figure 3.11: Harpoon with Labeled Elements

Inflatable Anchor

The inflatable anchor consists of two main components.

- Anchor Rod: Long member capable of withstanding a pullout force attached to
- Inflatable Membrane(s): responsible for securing the anchoring system into the surface of the asteroid

This method of anchoring relies almost solely on the properties of the surface, which are unknown. Current studies point toward an asteroid with a surface of high porosity, which will result in the fracturing of a boulder upon anchor penetration rather than a successful dig. Moreover, as discussed in the condition outlines, this could prove to be fatal to the mission [33].

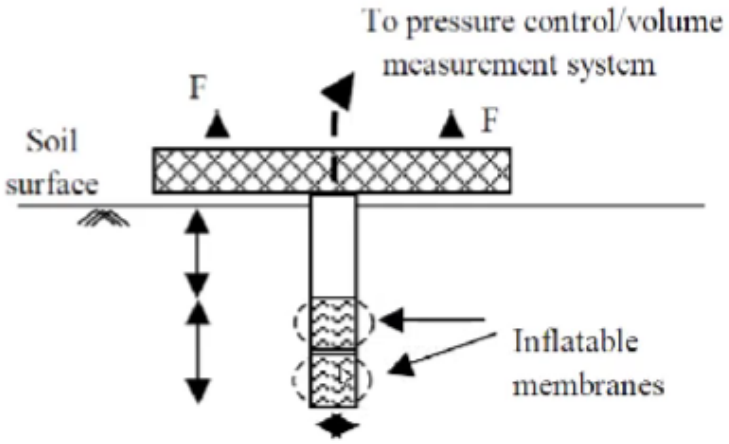

Figure 3.12: Inflatable Anchor with Labeled Elements

Plate Anchor

The plate anchoring method is another permanent anchor, that has a high level of stability. Though, this is another method that is highly dependent on the structural integrity within the depth of Bennu. It works by penetrating a plate deep within the surface, and then using the tension in the wire between the plate and the starting unit to create an anchor. The unit consists of:

- Penetrating Unit
- Plate to stay underneath surface
- Wire/Cable to hold tension

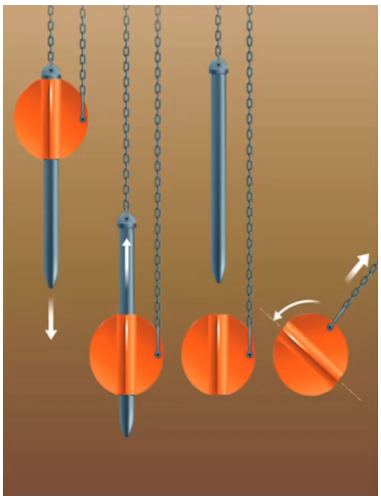

Figure 3.13: Plate Anchor with Outlined Operations

All the proposed surface anchoring methods are highly dependent on the composition of the surface of Bennu, and the chosen landing site. Hence, it becomes very difficult to determine the success of the penetrating anchoring methods without a sample of Bennu.

3.5 Gripping and Boulder Manipulation

Regardless of the decision of surface-ops vs orbit ops, the gripper is an essential system. To create a gripper there are a list of key requirements that must be achieved by the gripper. They are as follows:

- Have enough strength to lift boulder, while maintaining low power usage
- Not fracture the boulder under shear stress or crush the boulder
- Must be robust, endure large vibrations, and work effectively under extreme temperature conditions.
- Be able to pick up boulders of various sizes
- Be able to fit a variety of sensors on to the end effector of the system.

Soft Body Grippers

Soft body grippers are a technology that come very close to replicating how a human would interact with objects. They are very safe for humans to operate around, are simple and robust, and can be modified based on the scenario it is in. Despite this, there are some draw backs to soft body gripping mechanisms such as low precision, and effectiveness being highly dependent on the life cycle of the chosen material. Another factor to consider for the gripper is the amount of force being put upon the boulder. With soft body grippers, we avoid the challenge of fracturing the boulder through shear failure, but it introduces the challenge of avoiding failure by crushing. In addition to this problem, it is a challenge to include force moment sensors on a soft body gripper, this makes it hard to adapt grip strength for future grips.

If these presented challenges can be overcome, then soft body grippers would be the optimal choice. With the large added benefit of being able to conform to the object being picked up, it would ensure further success for the grippers task.

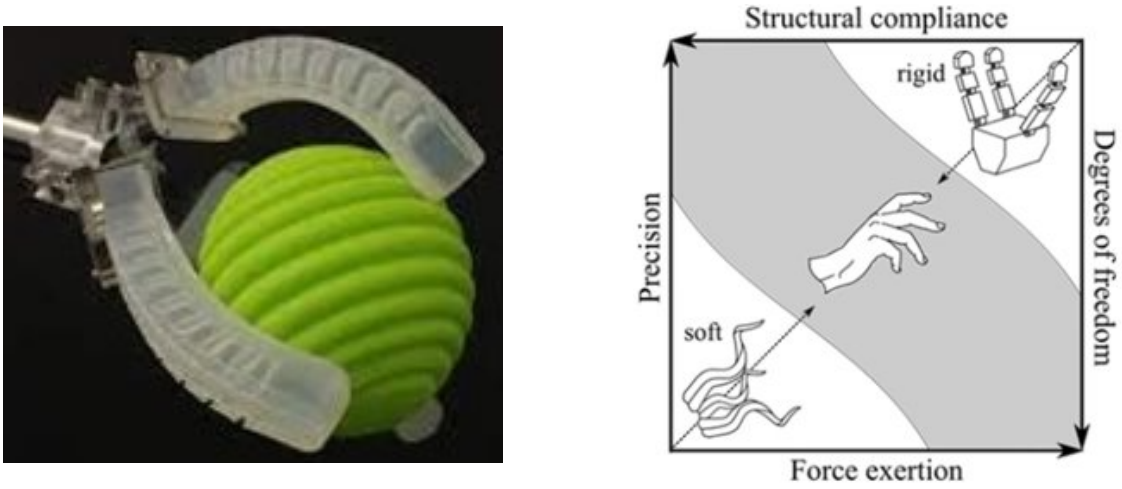

Figure 3.14: Example Soft Body (left) and Comparison Chart of Soft vs. Rigid Body Grippers (right)

Hard Body Grippers

The team have been able to narrow down to 2 possible hard body options

1. Microspine Gripper
2. Claw Mechanisms

With the hard body option, the gripper becomes a very robust system, but introduces the problem of weight limits, and power consumption. In addition, the maximum shear force that a boulder on Bennu can withstand has not been given a finite value yet, making it another mission-critical concern.

Microspine Grippers

The Microspine Gripper is a complex system constructed at the Jet Propulsion Lab which consist of a large number of small spines which seek to imitate insects which use this same concept to navigate a variety of terrain. The advantage of having these large number of spines is the distribution of force load. In a typical three finger claw mechanism, the total force is spread amongst 3 contact points. However, in a Microspine gripper the force is distributed amongst the total number of spines. This results in a lower force at each spine, and therefore each contact point, which will be an advantage when dealing with brittle boulders. Figure 3.15 shows the operation of a Microspine gripper.

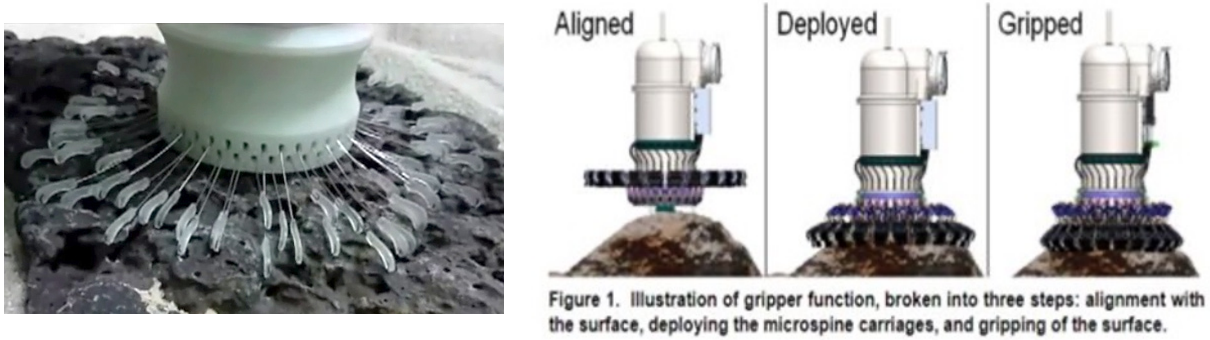

Figure 3.15: Microspine Gripper on Rocky Surface (left) and Microspine Actuation Process (right)

Further, due to the large number of spines, this allows this style of gripper to conform to small-scale roughness surfaces. As discussed, the maximum force a boulder can withstand is unknown, and therefore a boulder that is mostly buried into the surface of Bennu may have its exposed patch sheared-off upon Gripping, thereby skewing mission requirement calculations.

Claw Mechanisms

This system uses a satellite/probe mounted claws/arms to manipulate boulders, the claws may be just robotic arms with suitable end effectors or soft robotic capture mechanisms. Below in Figure 3.16 are some examples from available literature.

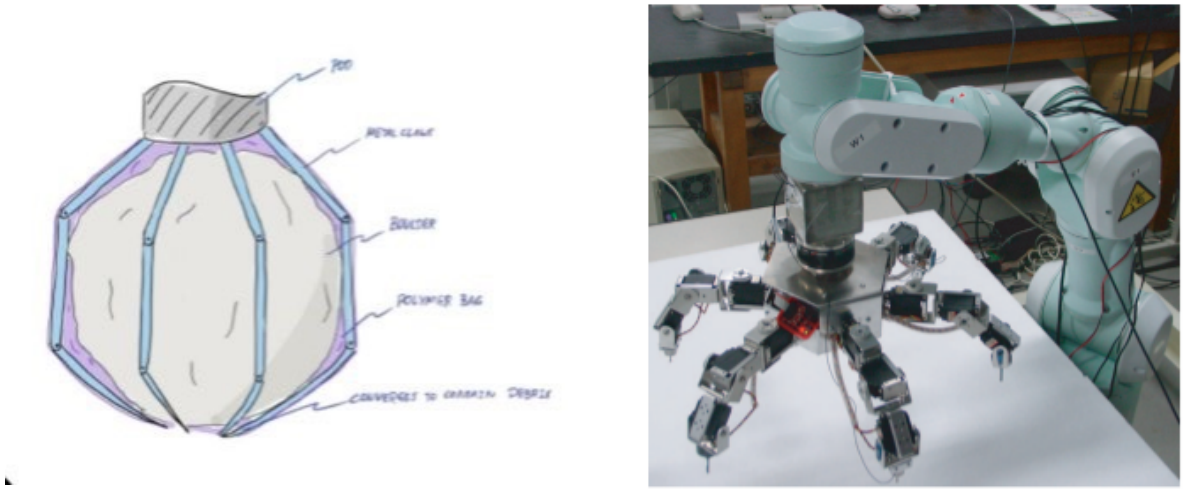

Figure 3.16: An artist depiction of a claw capturing a boulder (left) and a claw end effector attached to a robotic manipulator (right)

Manipulation once Gripped

Boulder manipulation physics must be understood to develop the control systems for any of the above manipulation techniques. This also requires knowledge of the boulder properties. An example of ways to manipulate the boulder is shown in Figure 3.17 below.

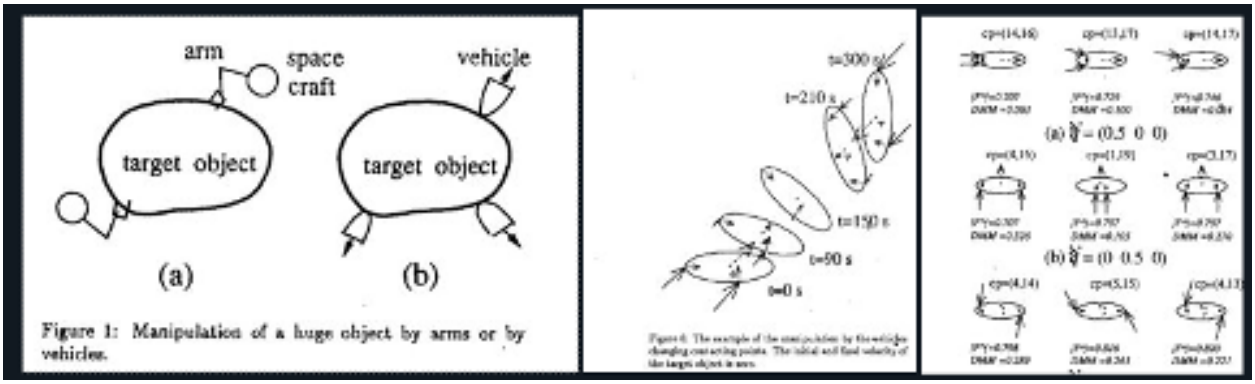

Figure 3.17: Sample Manipulation of a Target Object

3.6 Pneumatically Lofting Boulders

Another mechanism of boulder transport that was explored was pneumatically lofting boulders from the surface of Bennu into orbit. Further investigation into this mechanism revealed two possible scenarios:

1. Using compressed gas to create controlled explosions
2. Pneumatic regolith/boulder processing, using open and closed systems

Figures 3.18 to 3.20 below outline the process of pneumatic regolith processing.

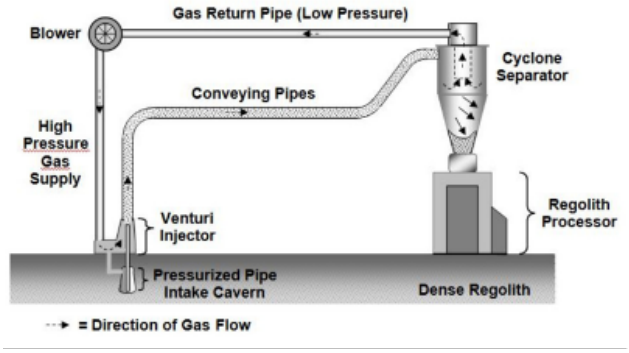

Figure 3.18: Concept of a Close Cycle Regolith Conveying

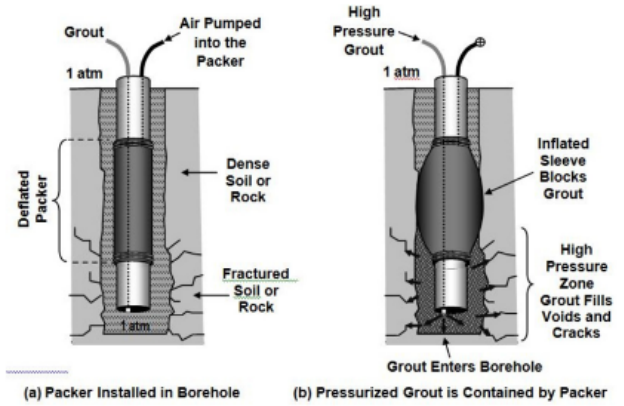

Figure 3.19: Principle of the Inflatable Borehole Packer

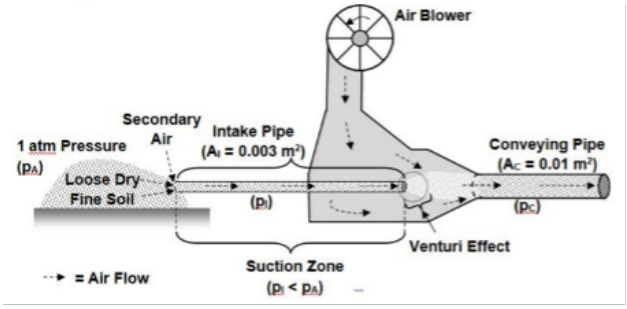

Figure 3.20: Charging Pneumatic Conveyor with an Air Injector

3.7 Move Boulders into Orbit

There are many potential methods for lifting boulders off the surface. These fall into two main categories:

- Spacecraft controlled boulder pick-up and transport into orbit
- Direct boulder launch into orbit

Of these, many potential concepts have been created for each. For spacecraft-controlled methods, these include:

- The use of grippers
- The use of claws
- The use of bags
- The use of harpoons with extendable "fishhooks" that bury under or besides boulders. These would retract back into orbit, pulling the boulder with it.

The above methods would be used in combination with thrusters and a guidance, navigation and controls system. For direct boulder launch methods, these include:

- Attaching thrusters to boulders via smaller autonomous spacecraft that land on the surface of Bennu and attach to boulders to lift them (Figure 3.21)

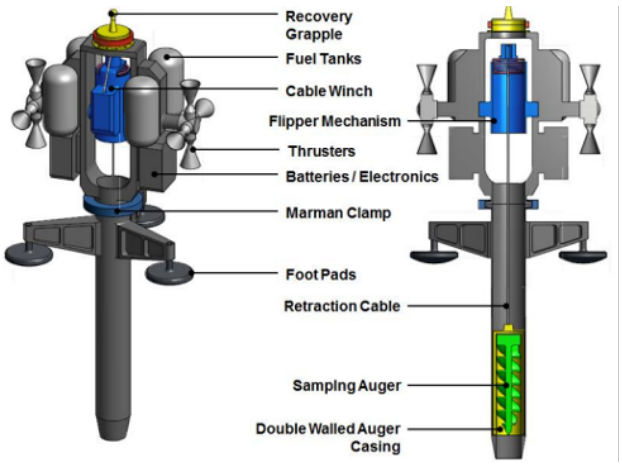

Figure 3.21: Autonomous Spacecraft with thruster system to attach to a boulder [34] [35]

- Catapulting boulders, which requires one end to be anchored to surface infrastructure,
- Spring launching (Figure 3.22)

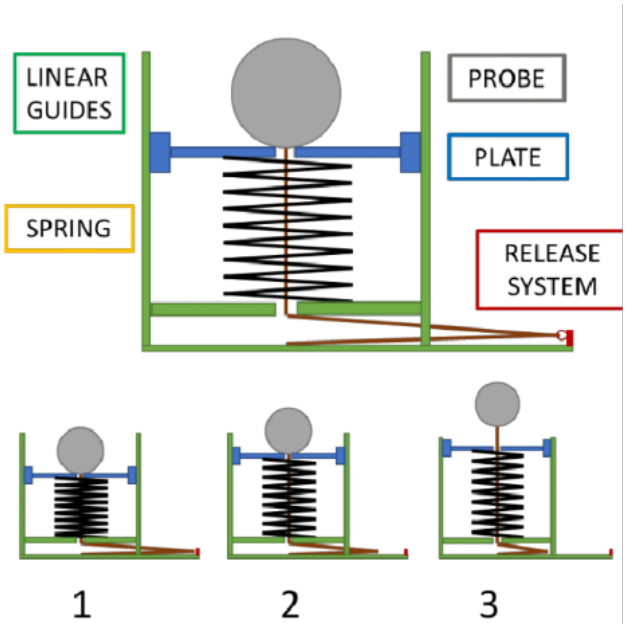

Figure 3.22: Concept of a Spring Launching Boulder System

- Controlled explosions underneath boulders to launch them into orbit, as mentioned in Section 3.6

Critical to all these potential methods is the creation and hazard of debris. This will be a major consideration is the trade-off of these mechanisms.

3.8 Processor Methods

Water on Asteroids

As a result of the research of the Solar system, water was discovered in cometary nuclei, asteroids, and dwarf planets, as well as on Mars [36]. Away from the Sun, water predominantly exists as ice [37]. There may be up to 2 million asteroids larger than 1 km in the Solar System; 19,500 medium-sized asteroids have been detected near the Earth. Estimates of the number of near-Earth asteroids that contain water are consistent with observations of their C-to-S population ratios. There are likely thousands of H2O-rich, near-Earth asteroids with diameters greater than 5 metres, and their number is growing year. Carbon-chondritic C-type asteroids are the most reliable water supply [37]. Their structure is loose and quite brittle. Therefore, drilling is unnecessary for such an object. To extract water, it will suffice to merely scrape the surface.

Carbonaceous chondrite meteorites experienced fluid flow within the past million years. Due to its primitive nature and distinctive chemical and physical features, the Tagish Lake meteorite is one of the most studied carbonaceous chondrites. Tagish Lake is a carbonaceous chondrite breccia of type 2.0 that is dark, organic-rich, ungrouped, and similar to CI and CM chondrites. Carbonaceous chondrites likely preserve a record of early Solar System processes that has been altered or obscured to variable degrees by subsequent processing [38]. The existence of minerals, such as hydrated silicates, magnetite, carbonates, sulphates, and halite, indicates that some carbonaceous chondrites (the CI and CM subtypes) have undergone aqueous alteration (reactions with liquid water) [38] [39]. Water ice has been observed on the

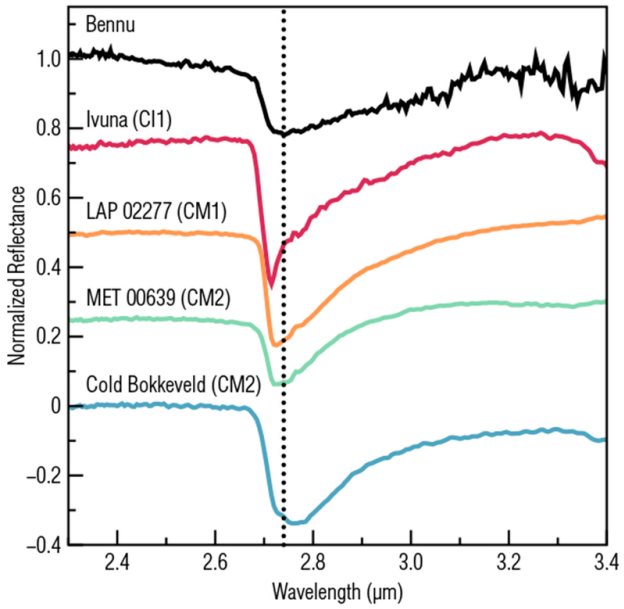

Figure 3.23: Average DOY 306 OVIRS spectrum between 2.3 and 3.5 microns compared to spectra of example carbonaceous chondrites [46]

surface of the asteroid(24) Themis, and the presence of radio-genic87Sr/86Sr in meteorite calcium sulfates indicates that fluid flow may have occurred recently [40] [41].

Water on Bennu

OSIRIS-REx spectroscopic observations from visible through thermal infrared wavelengths are highly complementary and show that the pristine sample that will be returned from Bennu has the potential to inform our understanding of water in the early solar system and its origins on Earth. Bennu's spectra indicate that the surface is consistent with and dominated volumetrically by some of the most aqueously altered CM chondrites. We cannot rule out the presence of a lesser component of CI material based on both the presence of magnetite and the visual variability among materials on the surface. Studying freshly collected, cleanly curated astroid materials returned by spacecraft reduces the ambiguity of terrestrial exposure that meteorite samples have typically experienced [42].

The meteorites shown in Figure 3.23 are Ivuna (CI1), LaPaz Icefield (LAP) 02277 (CM1), Meteorite Hills (MET) 00639 (CM2), and Cold Bokkeveld (CM2) [43]. Cold Bokkeveld may have been very mildly and briefly heated based on Raman spectroscopy of the insoluble organic material, but the evidence is somewhat ambiguous and there is no mineralogical evidence of heating that would change our interpretation of the observed 2.71-m feature (where mineralogy is the property to which the laboratory and remote sensing measurements shown here are sensitive) [44] [45]. Because meteorites have interacted with the Earth's environment, even if briefly, they are prone to mineralogical and chemical alteration, including the adsorption and absorption of terrestrial water (which can be recognized through oxygen isotope analysis). The spectra shown in Figure 2.8 were measured under vacuum after the samples were heated to between 400 and 475 K, which drives out adsorbed and absorbed terrestrial water [46].

Data obtained from the spacecraft's two spectrometers, the OSIRIS-REx Visible and Infrared Spectrometer (OVIRS) and the OSIRIS-REx Thermal Emission Spectrometer (OTES), reveal the presence of molecules that contain oxygen and hydrogen atoms bonded together, known as "hydroxyls." The team suspects that these hydroxyl groups exist globally across the asteroid in water-bearing clay minerals, meaning that at some point, Bennu's rocky material interacted with water. While Bennu itself is too small to have ever hosted liquid water, the finding does indicate that liquid water was present at some time on Bennu's parent body, a much larger asteroid [46].

The Hayabusa mission of the Japan Aerospace Exploration Agency (JAXA) is the most recently returned mission and has successfully collected thousands of regolith particles, ranging in size from 10 to 200 m (usually 50 mu in diameter), from the near-Earth S-type asteroid 25143 Itokawa in 2010 [47] [48]. More than 900 Itokawa particles have been separated and are curated in an ISO 6 cleanroom at the Planetary Material Sample Curation Facility of JAXA. The water contents of the nominally anhydrous minerals (NAMs) of two Itokawa particles have recently been determined to be 698–988 parts per million (ppm), which equates to a water content of 160–510 ppm for the entire Itokawa asteroid [49]. This estimated water content is at the upper end of the range estimated for inner solar system bodies (e.g., 30–300 ppm for S-type asteroids based on remote observations of 433 Eros and 1036 Ganymede [50]; 250-350 ppm for L and LL chondrites based on laboratory measurements [51]; 3–84 ppm in the bulk silicate Moon), except for Earth and possibly Venus, which contain up to 3000 ppm of water.

Extraction of water from Asteroids

On asteroids, water extraction is significantly simpler than metal processing. To harvest precious metals in space, new technology that operates in microgravity and maybe vacuum must be created. Methods of mineral extraction on Earth necessitate water, various chemicals, and gravity; therefore, they cannot be easily modified for use in space. However, extracting water just needs heating ice-encased regolith and trapping the resulting water vapour; therefore, it is quite possible with minimum technological investment [34] [52]. From the resource extraction standpoint, the carbonaceous C-type asteroids are most desirable; as they contain a mixture of volatiles, organic molecules, rock, and metals [53] [54] [55].

However, the required power to heat an asteroid material is high and is approximately estimated below. For the mission to be economical, efficient and to bring down the processing times, it is necessary to investigate methods to generate enough power to process asteroid material.

There are at least two methods for mining asteroids: a complete asteroid might be captured and hauled back to the Earth's or Moon's neighbourhood, or the valuable resource could be recovered and processed in-situ. Depending on the size of the target asteroid, it will be necessary to either transport the entire asteroid or process resources in-situ. Smaller asteroids would be easier to catch, de-spin, and transport to the Earth's vicinity, whereas larger asteroids would either have to be processed totally in-situ or only a portion of the asteroid could be returned. Moreover, very massive asteroids or smaller M-type asteroids are more likely to survive atmospheric entry and impact Earth because they are less likely to disintegrate in the atmosphere.

A recent study determined that it is possible to catch, de-spin, and transport a 7m diameter, over 500 tonne asteroid to a high lunar orbit. This expedition would cost around $2.6 billion dollars and would not necessitate the development of any new technologies [56]. Another study showed that retrieving an asteroid with a diameter of 2m to the International Space Station is also feasible [57].

Since bennu has a radius of 245m and due to high cost and lack of available technology, it was determined to process each boulder on bennu in situ and move the processed water to lunar orbit. A reasonable volume of boulder to be processed is estimated to be $1m^3$ to $2m^3$.

Assuming $1m^3$ boulder size, the power required to heat a boulder to 900°C to extract water from it is calculated using Equations (2.2) and (2.3) below.

$$Q = mC_p(T_2 - T_1) \tag{2.2}$$

$$Q = \rho V C_p(T_2 - T_1) \tag{2.3}$$

The surface temperature varies from 76.85°C to -73.15°C. Assuming ρ = 1190 kg/m^3, C_p = 750 J/Kg/K, T_2 = 900°C for dehydroxylation, and T_1 is the warmest surface temperature of 76.85°C, this gives: Q = 204 KWh.

To process a boulder of 1 m^3 we are assuming we would need over 250kWh - 300KWh of energy and to power additional infrastructure. This is a large amount of energy and it is necessary to investigate power source or methods to heat up the boulder to process a boulder fast. There are a number of available power sources:

1. Solar PV Panels
2. Nuclear Fuels
3. Direct Solar Concentration using Laser Ablation
4. Space Biomining

Solar PV Panels

Solar PV panels are extensively used to power satellites and other space infrastructure. The Technology has high TRL levels, however to supply enough power to process a boulder it would take a large array of PV panels and otherwise the time required to process a boulder would be very high. The International Space Station (ISS) employees eight solar array wings and can generate about 240 kilowatts in direct sunlight[18]. Together the arrays contain a total of 262,400 solar cells and cover an area of about 27,000 square feet (2,500 square meters) more than half the area of a football field[19].Additionally, other infrastructure like batteries and tracking devices add to the size of the system, solar arrays also degrade over time and requires frequent maintenance. The high power demand for heating asteroid material makes this system unpractical.

Nuclear Fuels

Radioisotope Thermoelectric Generators(RTGs) and Nuclear fission reactors for space are other excellent sources of power because they are compact and reliable. RTGs have been used as a main source of power by the US since 1961. High decay nuclear fuels like plutonium-238 and Americium-241 are used by both NASA and ESA to power over 25 space vehicles by converting the heat from the radioactive decay into

[18] https://en.wikipedia.org/wiki/Electrical_system_of_the_International_Space_Station#cite_note-4

[19] https://www.nasa.gov/mission_pages/station/structure/elements/solar_arrays-about.html

electricity through solid state thermocouples. With RTGs the power generated cannot be varied or shut down, therefore, they require supplementary batteries to store energy for peak times.

RTGs are reliable, safe and maintenance-free and can provide heat or electricity for decades. However, when the power required is over 100 kW, nuclear fission systems are much more cost-effective compared to RTG's. Nuclear fission systems can be launched cold with no radioactive hazards and can be started once the device is in orbit. The power can be varied and can be shut down depending on the thermal load. Russia has used over 30 nuclear fission reactors in space, whereas the USA has used only one on the SNAP-10A in 1965. Although recently there have been a revival of interest in the use of nuclear fission for space missions, the high cost of developing the reactor, and cost of nuclear raw material is a disadvantage for this mission. The estimated cost to make one pound of Plutonium-238 is about 4 million US dollars, and this does not include the cost of the reactor itself[20].

Optical mining

Optical mining uses concentrated solar power to excavate carbonaceous chondrite asteroid surfaces and reduce the asteroid to fragments while releasing volatiles. Experimental evidence is shown that supports the Optical Mining method. Asteroid simulant materials have been found to spall at 100 W/cm2 of light irradiation. Loosely bound or poorly connected fragments move and shift even as low as 11 W/cm2 . Furthermore, literature shown that water and carbon dioxide volatiles are released during illumination at these conditions [58]. The optical mining system was first trademarked and patented by TransAstra. The proposed design shown in figure 3.25 makes use of inflatable solar concentrators and optical elements like light-tubes and optical baffles to concentrate solar rays on to the asteroid material in a controlled process to extract and collect volatiles like water and carbon dioxide.

Reference Design: Optical Mining by TransAstra

- Uses telescopic optics (essentially large mirrors) to direct concentrated sunlight on target material to extract water
- Relatively high mass and volume due to the optical system but low power requirement since harvesting solar power
- Medium TRL since there is an existing design that was tested on Earth, however no such design has been used in a space mission to date
- Relatively low complexity since only requires a few simple actuated components
- Throughput rate is medium since dehydroxylation commences relatively quickly once sunlight beam hits boulder, but it requires the beam being directed throughout the boulder

Laser Ablation is a process where thousands of laser pulses heat up an object. Laser ablation meets the 900 degree heat requirement needed to extract water from the boulders. There are 2 methods to doing Laser Ablation:

1. Stand-On System : The Mining unit itself is being sent up with a large laser array. This allows for a quick mining of the desired boulder, though poses the problem of possible contamination due to the gas and debris from the asteroid.

[20] https://www.forbes.com/sites/williampentland/2015/11/08/peak-plutonium-238-u-s-starts-making-nuclear-fuel-for-deep-space-missions/?sh=5ce1280853b4

2. Another possible, though less viable method is to have a Stand-Off system, which orbits earth. Though the cost of this method makes it unviable, it would have the benefit of being able to be used on more than one mission

Though very effective, the Laser Ablation method requires a very large power source. This could possibly be addressed with a large solar concentrator on the mining unit to power the laser array unit.

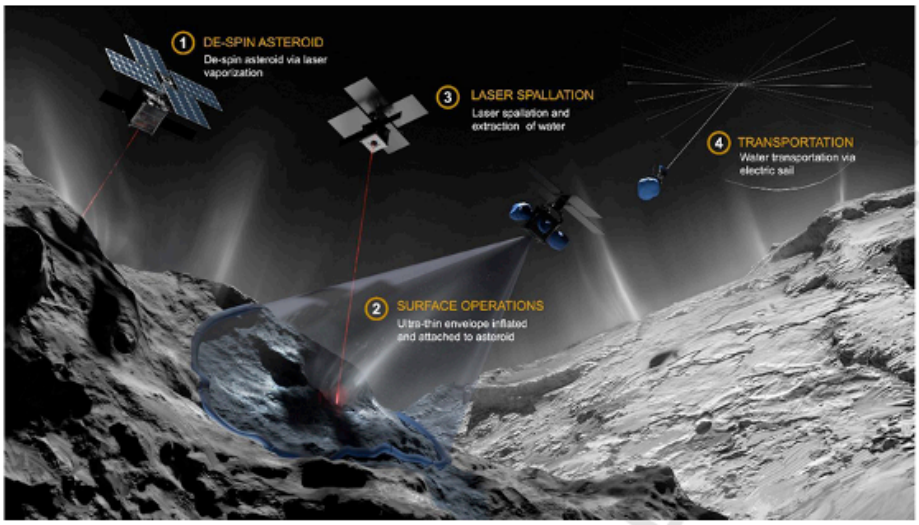

Fig. 8. Small spacecraft asteroid mining architecture for volatiles using lasers for extraction and electric sails for transportation (Image credit: Efflam Mercier).

Figure 3.24: Small spacecraft asteroid mining architecture for volatiles using lasers for extraction and electric sails for transportation [59]

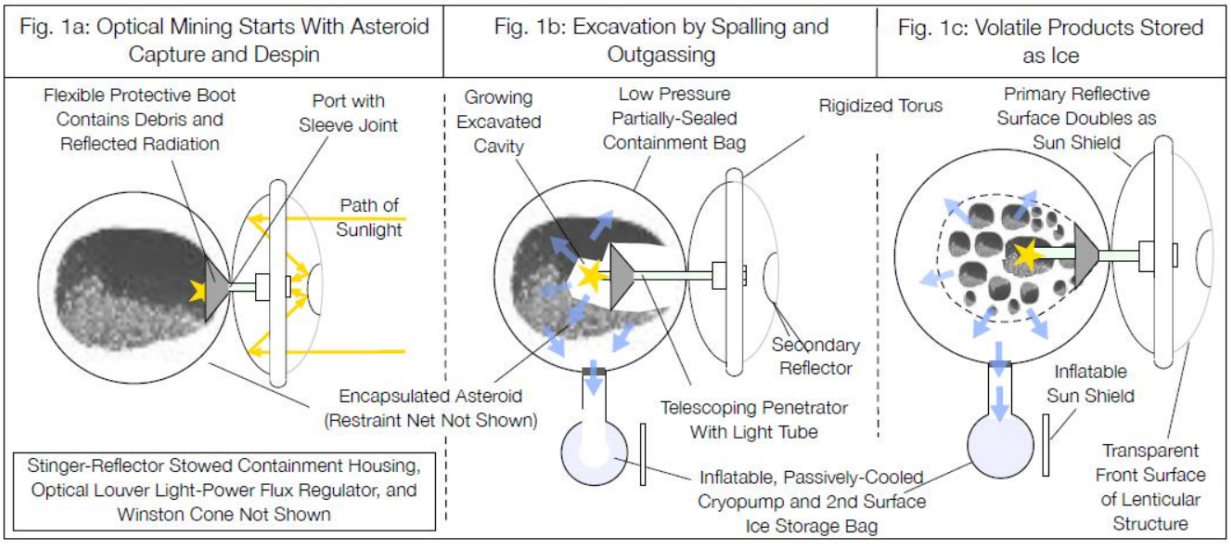

Figure 3.25: Concept of Optical Mining [60]

Space Biomining

This technology can be used to mine metals, and has been proven on the space station [61].

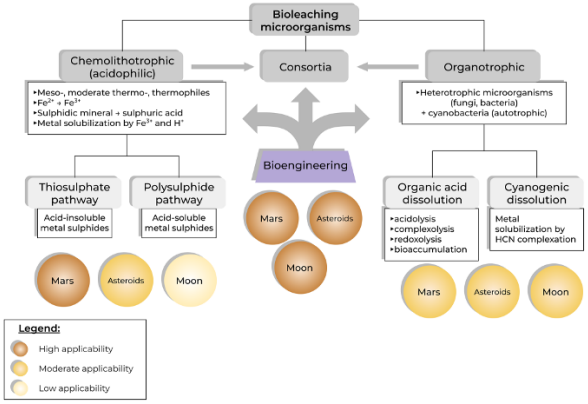

Figure 3.26: Diagram summarizing the main types of biomining/bioleaching microorganisms and mechanisms, and their potential space applicability taking into account the general surface composition and mineral content of Mars, Moon and asteroids [62]

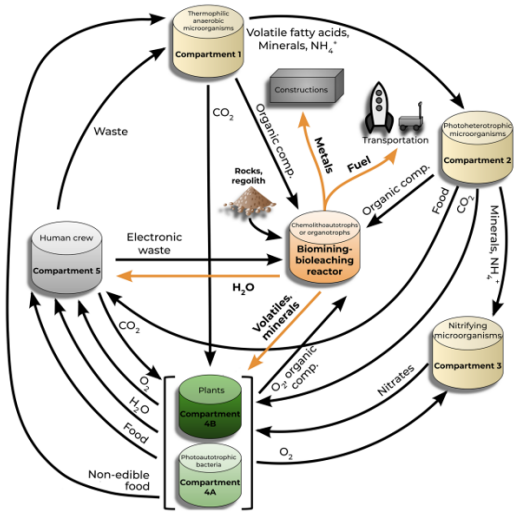

Figure 3.27: Conceptual figure of a biomining/bioleaching compartment in the context of Biological life support system, based on the regenerative life-support systems MELiSSA project design [62][63]

3.9 Processor Interfaces

With various processor methods outlined and considered, how these architectures interface with other components must be considered. This usually includes before the processing interfaces and after the processing interfaces. It often depends on the exact architecture used. One example found in the literature is for the Robotic Asteroid Prospector (RAP) as shown in Figure 3.28 below.

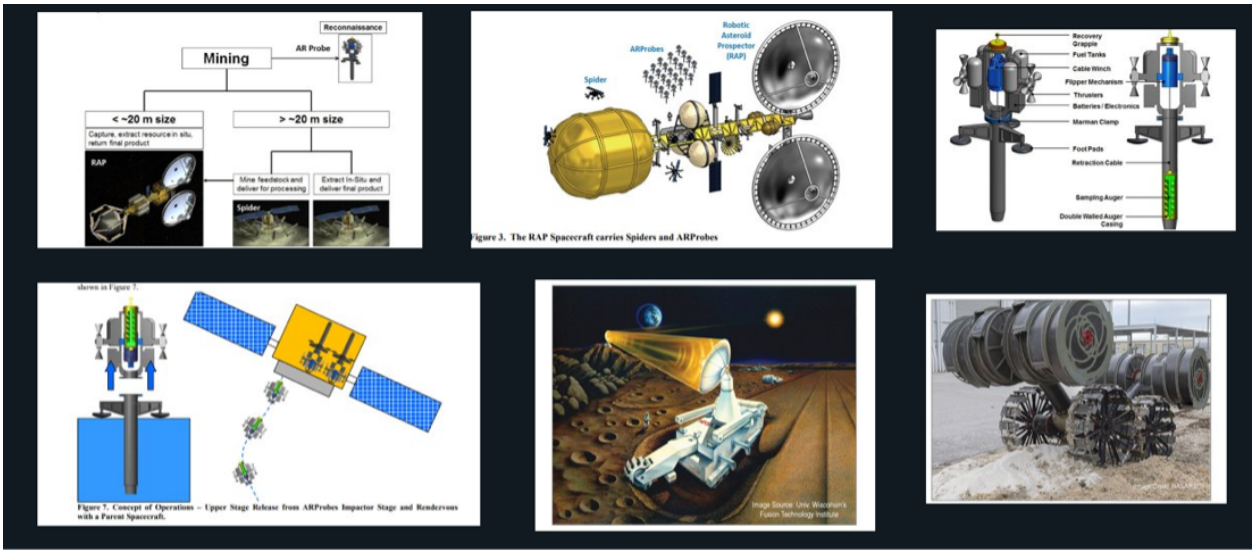

Figure 3.28: Example of various interfaces in Processing of Regolith

a
Two main interfaces that are critical to the processing of boulders are the:

- Loading
- Tailings

The loading interface is exactly how the boulder gets put into the processing chamber. This can be done with a variety of mechanisms and could be done by keeping the boulder as a whole, or by crushing it up into smaller components. Crushing into smaller components is a common practice for terrestrial mining of various ores. Some designs used in the literature are shown blow in Figure 3.29.

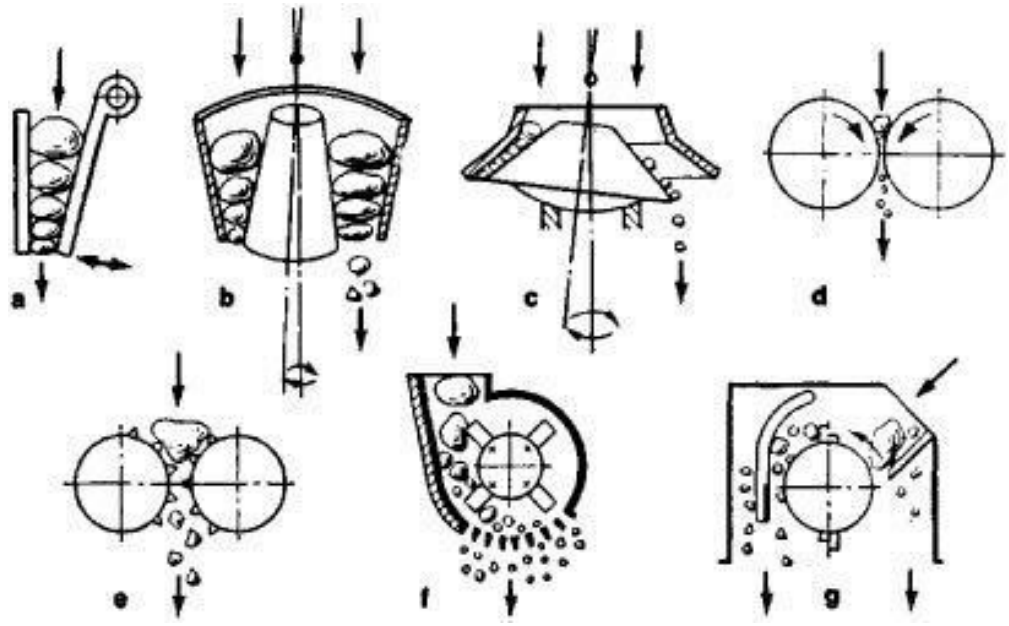

Figure 3.29: Mechanisms of Crushing Ore into Smaller Particles

Once the processing is complete, the "tailings" or waste material must be collected and disposed of somehow, hence another interface. This procedure can be done in a variety of ways. Depending on the design, both of these interfaces could be combined into one complex interface, if desired.

3.10 Move Water into Orbit

Moving water into orbit is dependent on a surface processing method. There are two potential ways that water can be moved into orbit from Bennu's surface:

1. Via a "pipeline-like" mechanism, with active or passive pumping.
2. Via a spacecraft that is loaded with the water taken from processing.

Both means require significant thermal design and considerations, as well as fluid mechanic and transport considerations.

Water is extracted from the asteroid regolith via the dehydroxylation process, which uses heat up to 900C to convert bound hydroxyl groups into gaseous water molecules. These molecules can be frozen out onto a dust grain surface [64]. While water can also be formed via oxygen and hydrogen atoms, and frozen onto the surfaces of the grains, which is a more dominant process, this is not how the dehydroxylation mechanism works. It was found that considerable optical shielding is required for freezing of the water molecules. Other devices such as Meissner traps (which turn water vapour into ice), that are used in Earth T-VAC chambers, could be used for ice collection.

One key decision is the state of matter of the water after processing. For the pipeline-like mechanism, the water must be in either a liquid or gaseous phase. As fluids are liquids or gases, this can only utilize these properties in these phases. "Pumping" in this mechanism can be done a variety of ways, such as:

- Using active powered pumps that are designed for space applications.
- The use of hydrophillic materials such as Zeolite A and ZSM-S coatings deposited via in-situ crystallization on stainless steel and aluminum alloys. These showed excellent hydrophilicity and adhesion which make them suitable materials for moving water based on non-gravitational force [65].
- The creation of electrostatic gradients (electric fields) via an electric emitter that charges gaseous water droplets and a reversely charged collector in the direction of the desired flow [66]. This is a commonly used mechanism is electrostatic precipitators.
- Using capillary flow forces in microgravity. As these and surface tension forces govern fluid flow in the absence of gravity, they can decrease pumping and power requirements. Capillary flow (with the underlying surface tension forces) can pull fluid for meters along pipe in microgravity environments, and would continue indefinitely in a perfectly weightless environment [67]. As Bennu as a near weightless environment, with a local gravity of $\sim 9.8 * 10^{-5}$ m/s^2, this is potentially an optimal mechanism.
- Using electrolytic gas evolution. This involves using electrolysis to make bubbles in a liquid to initiate fluid flow [67].

With all of these fluid transport modes, bubbles (in a liquid) can arise easily in microgravity when the fluid moves faster than the critical flowrate and cause damage to equipment. Bubble mitigation is critical, and mesh screens can be used to remove bubbles from the liquid. These can also be managed via Propellant Management Devices (PMDs).

Another consideration for the pipeline-like mechanism is the thermal requirement. As space is a cold environment, even around a hot thermal mass like Bennu, temperature control to keep water in a fluid phase is critical. Use of compounds such as Methanol can decrease the freezing point so that water stays a cold liquid, however this doesn't appear to do anything to the boiling point, which could still result in bubble formation in hot scenarios [68].

For spacecraft transport, water would most likely be transported as a liquid or solid. As the water would be in some container, pressure considerations would be more critical to ensure the container doesn't crack or burst under pressure variances due to the water phase, be that solid or gaseous). Spacecraft transport simplifies the transport mechanism to a propulsion and guidance, navigation and control problem. However, this still includes thermal difficulties. This could also introduce control difficulties if water is in the liquid phase, and the introduction of "sloshing" issues. While not seen in space applications, these have been encountered in drone applications [69]. Using a spacecraft also does not entirely eliminate the need for fluid transport, as there must be a means of transporting the water (in some phase) from the processor to the container, as well as to a larger storage vessel like a mothership if used.

3.11 Architectures

There are various architectures used on various space missions depending on the mission goals and applications. This section investigates the literature developed on how to decide on such an architecture - using what is known as a "Trade Study".

Multi-Vehicle Architecture

Evaluation of Multi-Vehicle Architectures for the Exploration of Planetary Bodies in the Solar System outlines a procedure to set up and evaluate a trade space for different mission architectures [70]. The process comprises four steps:

1. Functional decomposition of system goals
2. Generate possible solutions
3. Evaluate solutions against identified metrics
4. Downsize tradespace and evaluate remaining architectures in more detail

Steps 1-2 were completed as follows:

1. Functional decomposition of the system goal
    - System goal: mine water from Bennu
    - System subgoals:
        - Transit from earth
        - Collect boulders (or regolith?)

  - Process collected material to extract water
  - Store extracted water
  - Discard tailings safely
  - Transit to destination
  - Transit to & from Mothership (if Mothership exists)

2. Possible solutions:

   - One big spacecraft with full functionality
   - Many small spacecraft with full functionality
   - Many small spacecraft with distributed functionality
     - Independent vs. dependent
     - Coordinated vs. non-coordinated
     - Spatially distributed
     - Temporally distributed

Evaluation Process for Multi-Vehicle Architectures

Once the desired solutions are created, they can be evaluated using a variety of metrics. Some of these main metrics are listed below:

- Mass
  - Drives procurement and launch costs
  - Physical models (higher fidelity but increased computational complexity and cost) and parametric models
- Science Benefit
  - Metric reflects perceived benefit. Metric is unitless. Metric identifies the ability of each architecture to meet the mission's science and technology goals
  - Perceived benefit provided by an instrument for a given science objective. This can be weighted as shown in Table 3.3 below.

Table 3.3: Breakdown of Science Investigation Weightings

Weighting	Meaning
0	Does not address science investigation
1	Touches on the science investigation
2	Partially addresses the science investigation
3	Addresses most of the science investigation
4	Fully addresses the science investigation
5	Exceeds the science investigation

- Complexity
  - Structural complexity: the number and type of components, the number and type of connections, and the dependency structure (i.e. how the connections are arranged within the system)

  - Dependency structure: centrality/bus architecture; number and length of cycles; reachability; nesting depth; and entropy content
  - The above factors have been combined in Sinha's equation which includes:
    * Vehicle-level: Evaluates the design complexity of each individual vehicle within an architecture, depending on the subsystems and instruments they each possess
    * System-level: Includes intervehicle interactions, reflects operational and structural complexity

- Redundancy
  - Higher redundancy - Greater productivity through parallelization of tasks - greater coverage
  - Lower risk if the mission is not dependent on single vehicle (single point of failure, SPOF)

- Cost
  - Related to complexity and mass metrics
  - Alternatively, a ground-up or parametric cost model can be used to estimate the cost of a mission

- Productivity
  - The ability of an architecture to achieve the goals (i.e. its ability to successfully complete the mission goals) and its productivity during the mission (i.e. the amount of science done)
  - Non-trivial; redundancy and emergency behaviours affect it
  - One of the advantages of distributed systems is that they provide an opportunity to increase the mission reliability through the duplication of subsystems. In turn, this increases the productivity of the mission, since a more reliable system can operate for longer without failure.
  - Reliability is defined as the probability that a system will be in a functional state at the end of the nominal mission.

- Reliability
  - Can either be increased by higher component reliability or increasing redundancy

- Coverage
  - Typically, the larger the number of sites visited and the larger the area explored at each site, the greater the data return is for planetary surface vehicles
  - The coverage metric is assessed to be not driving for Khepri: our goal is to extract lots of water, not understand boulders from different areas

- Uncertainty and Risk
  - Risk is defined as the uncertainty associated with the science benefit, complexity and cost metrics.
  - It illustrates disagreements in the effectiveness of instruments in achieving the science goals, or uncertainties in technology and in integration difficulty. All these aspects have historically been shown to be associated with increased mission cost and schedule delays.
  - Each of the aforementioned metrics includes a set of weightings derived either from science goals, existing designs or expert opinions. Uncertainty in the metrics arises in differences in expert opinions. Each architecture therefore carries a certain amount of uncertainty.

3.12 Debris Creation

Debris creation on Bennu and within its orbit appears to be an issue that has implications for proximity operations and mission design. Literature has shown there are numerical simulation methods based on OSIRIS-REx data to model regolith and debris created by impingement mechanisms, such as the Touch-and-Go Sampler (TAGSAM) [23]. It is also evident that particle ejection events on Bennu (McMahon et al.), cause redistribution of regolith, with most particles ejected landing near Bennu's equatorial ridge. Thermal stresses over time can cause crack development in boulders, eventually resulting in breakage and regolith creation [71]. This is another consideration for debris creation.

Debris itself could lead to many issues, however the extent to which is currently unknown. This will impact the design of mission spacecraft, and mission operations. It is also unknown if there are any linkages between increased amounts of debris and the number of particle ejection events. If debris created from proximity operations tend to be ejected and land near the equatorial ridge, this could impact Bennu's environment.

Simulation

In order to model debris created by spacecraft interactions with the surface of Bennu, we chose to use the Rebound N-body integration package [72]. Previous efforts to model the granular impact dynamics on the surface of Bennu have used similar N-body integrators such as `pkdgrav` [23]. The Khepri team chose to use Rebound as it is open source and can easily be modified to suit the specific conditions for different simulation cases. Specifically, we chose to use the Rebound Ejecta Dynamics package [73], which was developed to model debris ejected from the surface of an asteroid. While the original code was intended to simulate the DART mission, we modified the following various components to model Bennu. In the Rebound file `bodyparams.py`, the following were changed:

Target Parameters

- Target radius ($rtarg$): 245.03 (Bennu's mean radius in m)
- Target mass ($mtarg$): 7.329e10 (Bennu's mass in kg)
- Constant ($K1$): 0.34 (Calculated via parameters below in Table 3.4 and Equation 19 [74])
- Equivalent Exponent (mu): 0.38 (Based on the porosity of the target body [75])
- Measure of the Tensile Strength of the Body (Ybar): 0.125 (Approximate tensile strength of low albedo boulders on Bennu, the vast majority of the surface, in MPa)
- Target Density ($rhoT$): 1190 (Bennu's bulk density in kg/m^3)
- Target Rotational Period ($perT$): 4.3*3600 (Bennu's rotational period in seconds)

Next, use the ellipsoid shape model, so set ellipsoid = True. The ellipsoid shape model parameters are:

Ellipsoid Shape Model

- Target Dimenion a (aT): 282.37 (Bennu's equatorial radius in m)
- Target Dimenion b (bT): 282.37 (Bennu's equatorial radius in m)

- Target Dimenion c (cT): 249.25 (Bennu's polar radius in m)

The binary model was not used, so set corresponding values were set to 0. The impactor parameters were:

Impactor Parameters

- Outer radius of impactor (a): 0.16 (TAGSAM head diameter in m)
- Impactor material density ($rhoi$): 2700 (Density of aluminum in kg/m^3, TAGSAM head material)
- Impactor velocity (vi): 0.1 (Speed in m/s of TAGSAM impact)
- Impactor mass (mi): 11 (Mass calculated from Table 3.4 in kg)
- Strength-Regime Emergence Position Proportionality Constant ($Cvps$): 0 (The strength regime is negligible compared to the gravity dominated regime due to the near cohesion less surface of Bennu.)
- Gravity-Regime Transient Crater Proportionality Constant (Ctg): 0.8 (Calculated via Table 3.4 from Equations 19 and 20 [76])

Finally, the debris parameters were:

Debris Parameters

- Mass excavated (mex): 2e3 (Mass of ejected particles in kg)
- Number of particles ($Nparts$): 1e3 (Number of Particles ejected)
- Maximum particle radius ($rmax$): 1e2 (Maximum particle radius, up to 10s of meters of boulders)
- Particle Density (rho): 1332 (Approximate boulder density based on CM-Chondrites, Section 8.3)

Table 3.4: Debris Parameters Calculation

Parameter	**Value**
Tensile Strength - low Albedo (Ybar, MPa)	**0.125**
Tensile Strength - high Albedo (Ybar, MPa)	**0.545**
mu - low Albedo	**0.375**
mu - high Albedo	**0.43**
Just Tag crater, not thruster	
Tagsam crater depth (H, m)	0.488
Crater radius (R, m)	0.16
Crater volume (V, m3)	0.04
Tg (crater formation time, s)	50
Ktg	0.77
Ctg	0.78
Impactor radius (a, m) - TAGSAM	0.16
mass of impactor (mi, kg)	10.52
density of impactor (rhoi, kg/m3)	2700
velocity of impactor (vi, m/s)	0.1
density of target (rhot, kg/m3)	1190
K1 (low albedo)	**0.344**
K1 (high albedo)	**0.608**
Tagsam Head	
Outer radius (m)	0.16
Inner Radius (m)	0.105
Annulus Height (m)	0.05
Cap height (m)	0.02
Volume (m3)	0.0039
Mass excavated	
Volume (m3)	0.04
Mass (kg)	46.7

One thing to notice is that the calculated mass excavated in Table 3.4 from the crater ejecta mass and the value used for mi in the Impactor parameters are different. This is because the simulator would not run for ejecta masses smaller than the used value, due to issues with the velocity distribution that had not yet been determined.

Despite some shortcomings in the overall feasibility of the model, some general conclusions were drawn from the plotted results. Figure 3.30 and Figure 3.31 below shows the debris created with the smallest possible run mass of 2000 kg, at the equator, 3 minutes and 15 minutes after the surface impact, respectively.

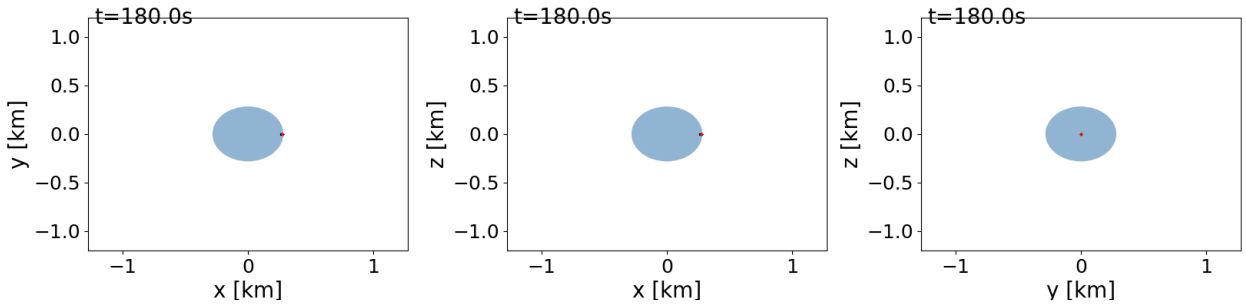

Figure 3.30: Debris Field 3 minutes after impact at the equator for an ejecta mass of 2000kg. Note the impact site (particles that have re-impacted the surface) is in red and the debris particles are in black

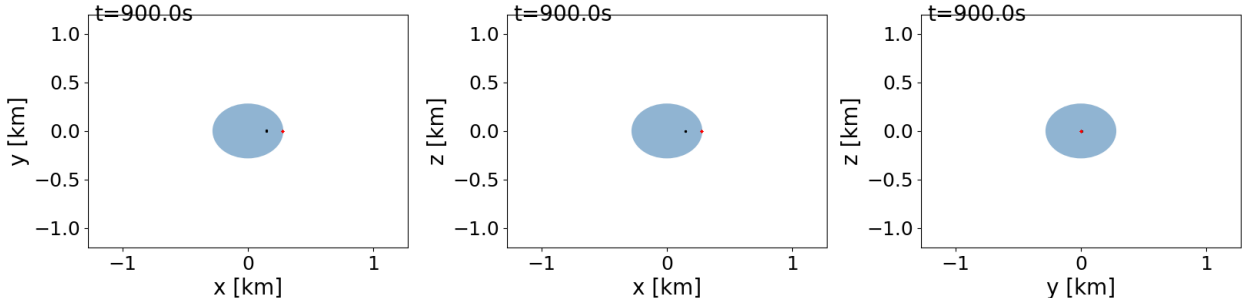

Figure 3.31: Debris Field 15 minutes after impact at the equator for an ejecta mass of 2000kg. Note the impact site (particles that have re-impacted the surface) is in red and the debris particles are in black

The above simulation only ran for 15 minutes, even though the results for long times are desired. Figure 3.32 and Figure 3.33 below shows the debris created with the smallest possible run mass that shows significant debris, 200000 kg, at the equator, 3 and 15 minutes after the surface impact, respectively, at the equator.

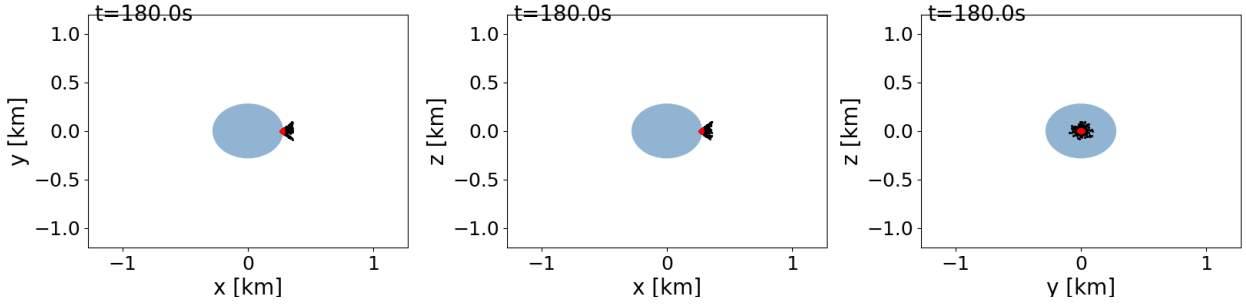

Figure 3.32: Debris Field 3 minutes after impact at the equator for an ejecta mass of 200000kg. Note the impact site (particles that have re-impacted the surface) is in red and the debris particles are in black

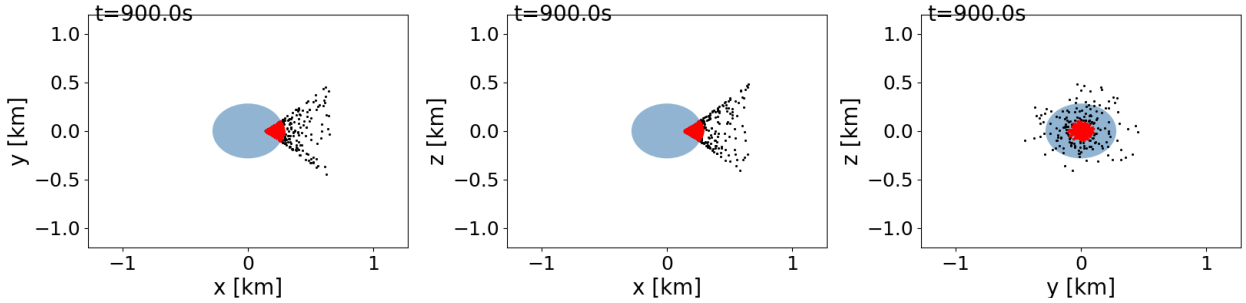

Figure 3.33: Debris Field 15 minutes after impact at the equator for an ejecta mass of 200000kg

Figure 3.34 below shows the same case as Figures 3.32 and 3.33, but this also shows an example trajectory of the spacecraft after the surface impact. The spacecraft coordinates are in red, and the debris particles are in black, with lines connecting the trajectories of each respective item.

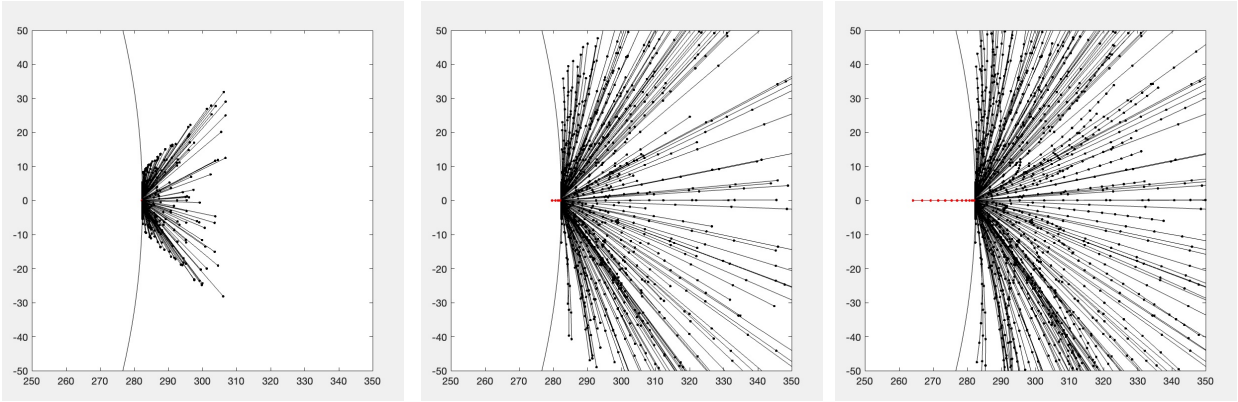

Figure 3.34: Debris Field at 1 minute, 5 minutes and 13 minutes after impact, respectively, at the equator for an ejecta mass of 200000kg. Note the axes are in m from the origin of Bennu

Figure 3.35 and Figure 3.36 below shows the debris created with the smallest possible run mass that shows significant debris, 200000 kg, at the equator, 3 minutes and 21 minutes after the surface impact, respectively, at a latitude of 45 degrees.

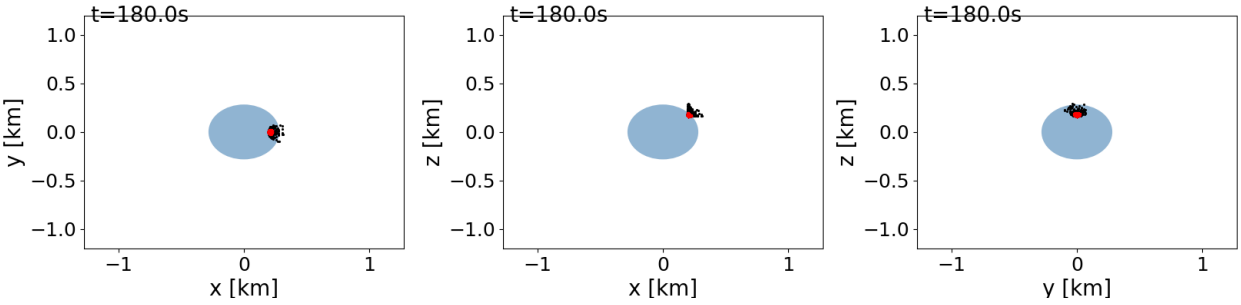

Figure 3.35: Debris Field 3 minutes after impact at the equator for an ejecta mass of 200000kg. Note the impact site (particles that have re-impacted the surface) is in red and the debris particles are in black

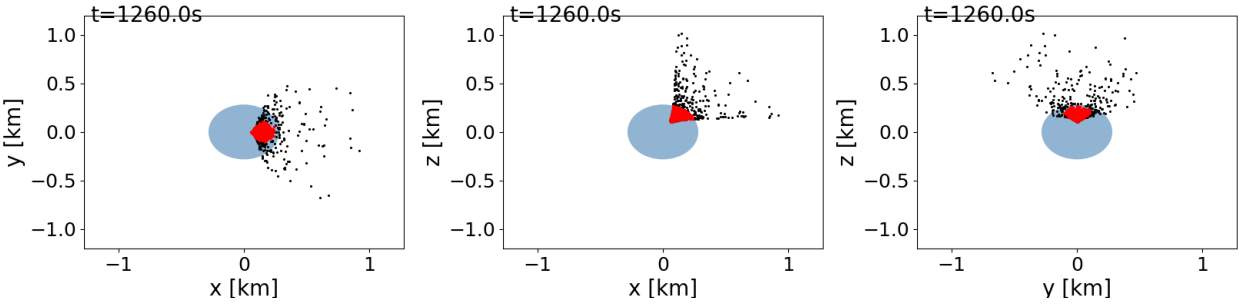

Figure 3.36: Debris Field 15 minutes after impact at the equator for an ejecta mass of 200000kg

Figure 3.37 and Figure 3.38 below shows the debris created with the smallest possible run mass that shows significant debris, 200000 kg, at the equator, 3 minutes and 28 minutes after the surface impact, respectively, at a latitude of 90 degrees, or at Bennu's north pole.

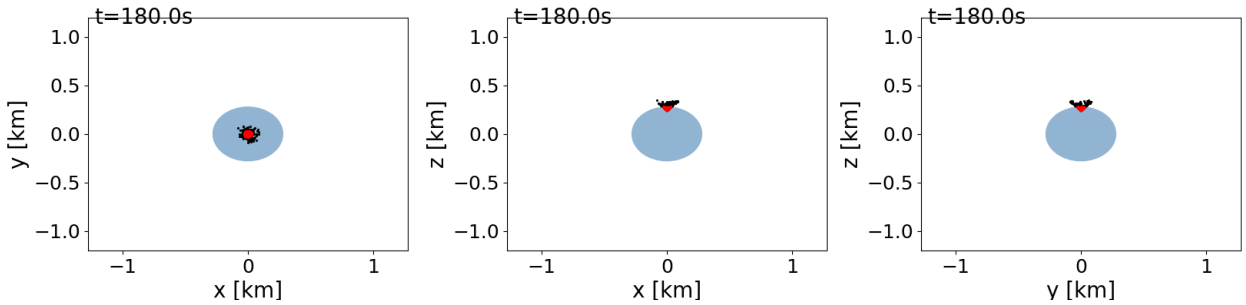

Figure 3.37: Debris Field 3 minutes after impact at the equator for an ejecta mass of 200000kg. Note the impact site (particles that have re-impacted the surface) is in red and the debris particles are in black

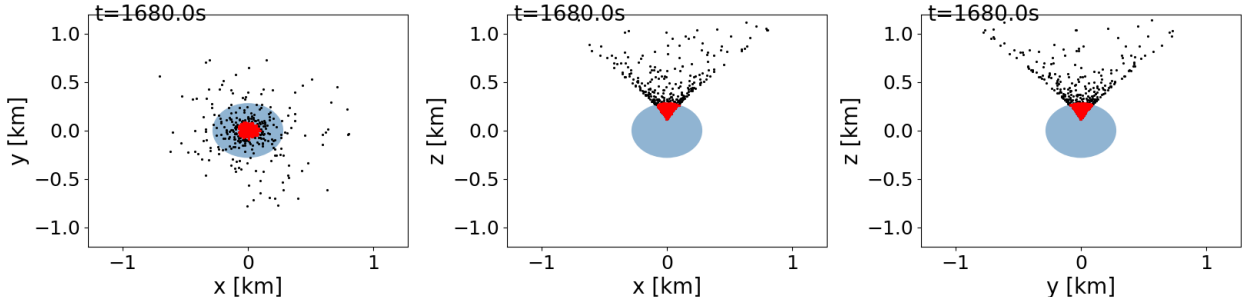

Figure 3.38: Debris Field 15 minutes after impact at the equator for an ejecta mass of 200000kg

The main conclusions from these simulations are as follows:

- Even though the small ejecta masses not do not produce much on the plots, the large ejecta masses can be used as representative.
- The ejecta varies depending on the latitude and longitude of the impact site.
- Even after nearly 30 minutes, there is still significant debris in the atmosphere within 1km of Bennu's center (roughly within 750m from Bennu's surface).
- Even if the spacecraft attempts to quickly divert from the impact site (Figure 3.34), there is debris created in the x-z plane that would impact the spacecraft. To this end, impacting the surface as little as possible and as slow as possible, to prevent any debris creation as much as possible is recommended for proximity operations.

Chapter 3: Trade Studies based on the State-of-the-Art

4 Mission Architecture Trades

4.1 Mission Architecture Definition

First, functions instrumental to completing the mission were identified. These include arriving at Bennu, acquiring boulder material, processing the boulder material into water, disposing tailings, and departing Bennu.

Next, different mission architectures incorporating these functions were generated. Alternatives varied the number of involved spacecraft from a monolithic to highly distributed systems and also varied the location of certain operations such as processing and disposal of tailings, considering locations such as Bennu's surface, an orbit around Bennu, and in transit to cis-Lunar space.

The architecture alternatives were discussed and anticipated concerns and challenges for each were noted. The Mission Architecture team then met with advisors to discuss the options and their benefits and drawbacks and eventually selected two options to keep, "Orbit Ops" and "Surface Ops".

"Orbit Ops", illustrated in Figure 4.1, sees a picker spacecraft collect a boulder from Bennu's surface, but processing operations occur in an orbit around Bennu.

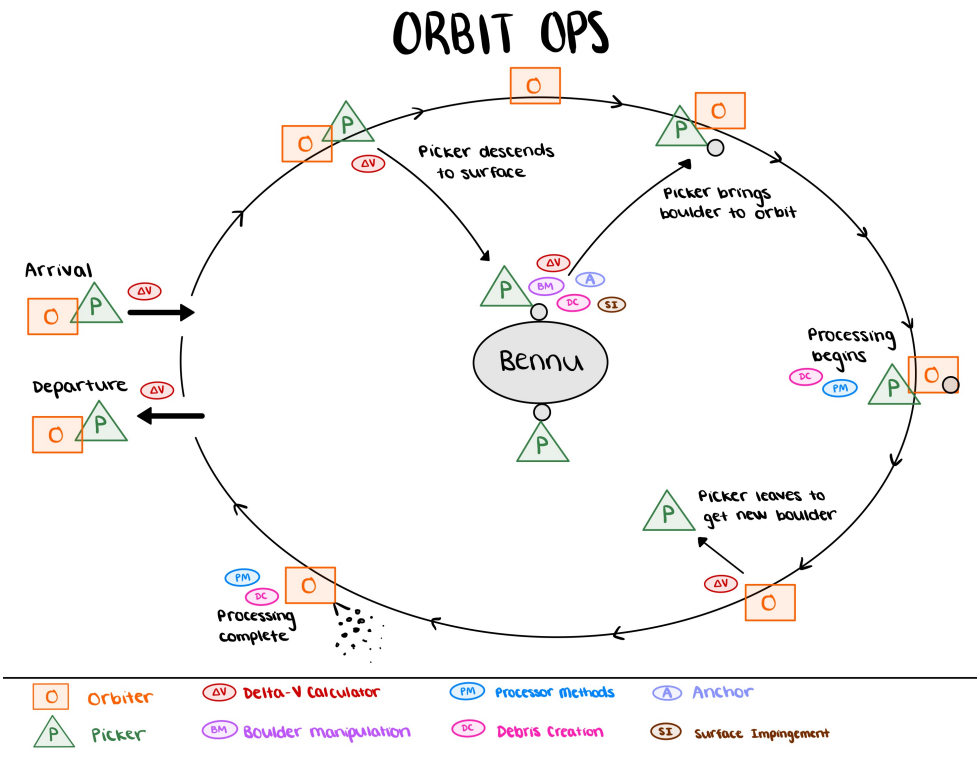

Figure 4.1: Sketch of high level mission architecture with primarily orbital operations.

"Surface Ops", illustrated in Figure 4.2 sees a lander anchor to Bennu's surface more permanently. Boulders are processed on the surface and only water is transported to an orbit around Bennu.

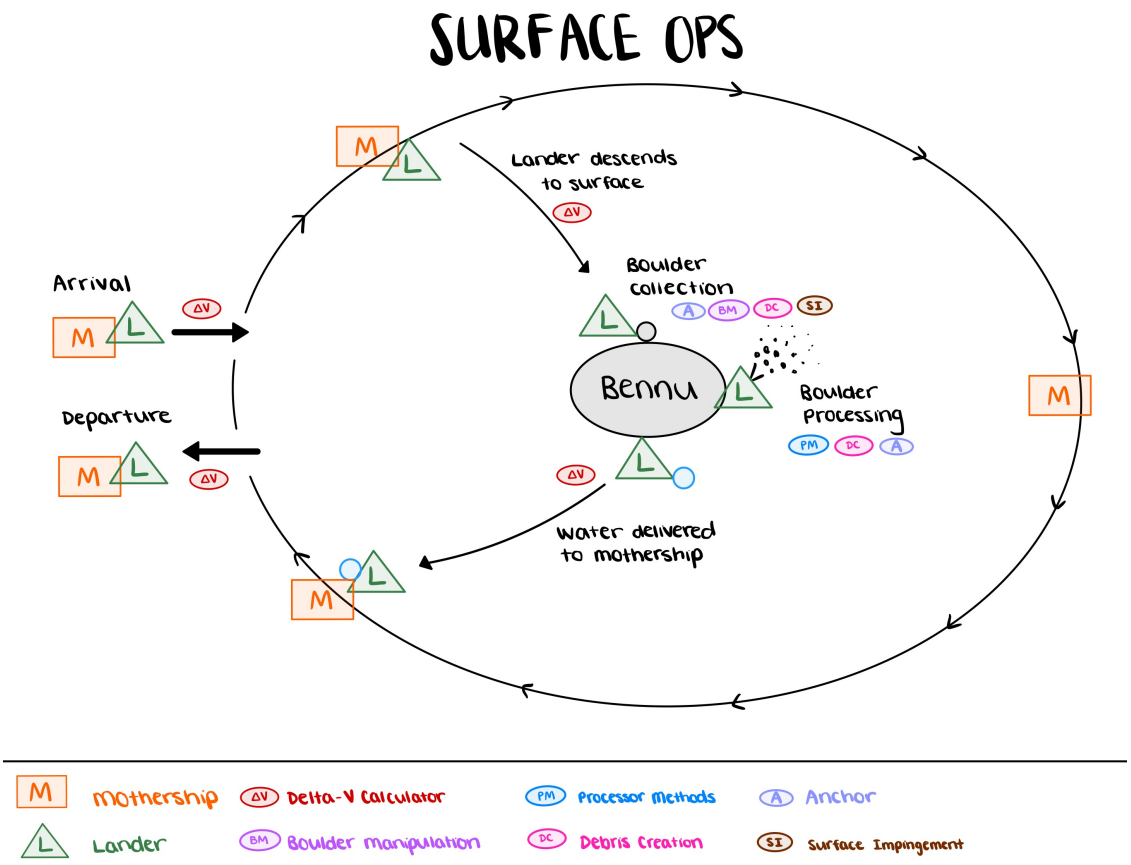

Figure 4.2: Sketch of high level mission architecture with primarily surface operations.

An architecture-level trade study was set up with the metrics listed in Table 4.1. With this work done quite early on in the project, the metrics, while vague, aim for coverage of important preferences while avoiding overlap between them.

Table 4.1: Metrics for selecting a mission architecture.

Metric	Rationale
Water Yield	Architectures that deliver more water are preferred.
Fuel Consumption	Lower cost architectures are preferred.
Debris Impact	Architectures that have less of an impact on space near Bennu and Earth are preferred.
Complexity	Architectures that are more reliable and less complex are preferred.
Duration	Architectures that process material more quickly are preferred.

Input was solicited from relevant other subteams to help evaluate the architecture alternatives against each of the metrics. A discussion on each is provided below.

Water Yield

Water yield is defined as the mass of water expected to be yielded from the same amount of boulder material mass. Using the same processing method, the amount of water created from a given amount of boulder mass was assumed to be the same on the surface or on-orbit.

The transportation of material from surface to orbit should also be considered. Assuming a non-perfectly sealed transportation container (such as gripper claws), some regolith will likely break off of boulders while they are moved. This means that on-orbit processing might result in slightly less water yielded from the same boulder as surface processing.

Fuel Consumption

The following was considered for fuel consumption. Surface operations would require a surface processing plant, whereas orbit processing would not. Using an approximate density of 1332 kg/m^3 for Bennu regolith, 2002 trips harvesting a 1m^3 boulder are necessary to harvest the required amount of water (Section 8). Note all calculations used a $I_{sp} = 230.5s$ which is the hydrazine propellant used by OSIRIS-REx and a orbit of 920m above Bennu's surface.

The analysis is broken into 2 sections: fuel consumption on the initial transit from Earth to Bennu and over all of the mining operations. The totals of the various methods are compared for the two scenarios with equal launch masses.

Earth to Bennu

Surface Ops (6 pods, mothership and plant) or **Orbit Ops** (8 pods and mothership)

- Total Dry Mass = 48000kg
- Propellant: 41152 kg

Operations on Bennu

Orbit processing

- 2002 trips, carrying a 1m^3 1332 kg boulder to 920m Orbit in Hohmann Transfer - Propellant: 363 kg

Surface processing

- Bring plant to surface: Negligible Propellant
- Do small trips (same amount of water as boulder water harvested) - Propellant: 292 kg
- Do large trips (Full boulder mass in water) - Propellant: 36 kg

Total Mission

- **Surface Ops** (less pods): 41188 to 41444 kg depending on trip (slower since 6 pods)
- **Orbit Ops**: 41515 kg (faster since 8 pods)

While very close overall, the surface ops would have slightly less fuel consumption.

Debris Impact

The metric to measure debris created was the number of impingements with the surface, with the specific type of impingement impact each having a different effect on the surface and so have different scaling factors to represent the severity of the debris created. These are:

- Gripper: Little if any. Weight x1
- Thruster: Large cloud. Weight x2.
- Anchor: Blow large hole, very large cloud. Weight x3.

Various architecture combinations were thought of to compare the amount of debris by each. There were ones exclusive to on-orbit processing, and ones where processing could be done on the surface or on-orbit. Like for the Fuel Consumption analysis, 2002 (rounded to 2000) trips/boulders are necessary.

Orbit Processing: No plant

- 2000 main impingements from thrusters
- 2000 impingements to grab boulders

Surface Processing: Plant anchors once, Spacecraft collects boulders to bring to plant

- Assume 4 impingements to anchor (square/rectangular configuration)
- 2000 for gripper and 2000 for thrusters

Surface/Orbit Processing: Plant anchors and collects boulders itself

- Assume 4 impingements to anchor (square/rectangular configuration)
- Assume only 20 boulders near each anchor site - plant needs to be moved 100 times to get 2000 boulders - 400 anchor impingements
- No thruster impingements to move the plant as spacecraft is far enough away from surface
- 2000 impingements to grab boulders

The final weighted results of the 4 cases are shown in Table 4.2 below.

Table 4.2: Debris Creation input to Architecture Assessment

Scenario	Weighted Impingements
Orbit Ops: No plant	6000
Surface Ops: With plant, spacecraft bring boulders	$\sim$6000
Surface/Orbit Ops: With plant, plant collects boulders	3200

With this information, debris creation seems equally risky for both surface and orbit operations. One caveat is that, for surface operations with a plant collecting boulders, there may be more debris due to not being able to “cherry-pick” boulders that would likely create fewer debris. This makes orbit operations slightly more attractive to mitigate debris creation.

Complexity

Anchoring may not be possible, and it adds significant contribution to surface ops complexity. Some requirements for the anchoring system were as follows:

- Must penetrate the surface with enough depth to keep the unit stable on the asteroid.
- System must provide at least 0.5MPa of upward reacting force to hold unit on asteroid
- Unit can easily detach from anchor
- Withstand the extreme temperature requirements
- Be able to fit in a compact space

Based on the above requirements, these metrics were used to identify the optimal technology:

- Power Consumption
- Mass
- TRL
- Redundancy
- Failure Tolerance
- Number of Mechanisms per Spacecraft

These trade results were summarized in Table 4.3 below.

Table 4.3: Anchoring Trade

Parameter	Weight	Microspine	Harpoon	Inflatable	Rationale
Economic Factors:					
Power Consumption per Cycle	0.1	-1	0	1	Scored with calculations of power needed for each technology
Complexity/ Risk Factors:					
Mass	0.2	1	-1	-1	Taking into account all equipment required to fully deploy the anchoring system
TRL	0.2	1	1	-1	Assuming tests performed on earth are a good/decent indicator for what to expect on surface of Bennu
Failure Tolerance	0.2	1	0	-1	Scoring based on units ability to have a component of the anchor fail and the mission still succeed
Number of Mechanisms per Spacecraft	0.2	-1	0	1	Considering the number of units needed to be attached the unit on Bennu
TOTALS	1	0.3	0	-0.3	

Through this trade study, it could be deduced that the optimal technology for the anchor were the microspines. They have a high failure tolerance and can be fit into a compact space whilst being able to withstand the harsh conditions upon deployment. Though this is the best option, there was still large uncertainty if the microspine grippers would be able to grip on the nearly cohesionless surface of Bennu, which made anchoring too uncertain [7]. This subsequently was a critical driver in determining the type of operations.

Duration

Two main factors affect the overall duration: the time required to more shipments to orbit, and the time required to process. These two are compared for surface and orbit ops.

Shipping water vs. regolith to orbit:

- Each round trip from Bennu to orbit: 7.4 hours
- Shipping required water to orbit: 200 trips
- Shipping equivalent required boulders to orbit: 2000 trips
- Time saved by shipping only water: $\sim$555 days

Processing on-orbit vs. on surface:

- Processing a Boulder of $1m^3$ requires roughly 300 kWh of power
- Power is available for half of the time on the surface vs. orbiting in a terminator orbit (always in sunlight), so it would likely take longer to process on surface
- Solar concentrator-based laser power is the most feasible options considering the amount of power needed, and with 4m diameter reflectors it takes $\sim$2.3 Earth days to process a boulder
- Time saved by processing in orbit (2000 boulders): 4600 days

Net savings in time by orbit processing: $\sim$4000 days = $\sim$11 years

Overall Trade Study
The overall trade study gave scores of -1, 0 or 1 to each option based on the results of the above analysis. The better option is On-Orbit Operations as shown in Table 4.4 below.

Table 4.4: Mission Architecture Trade Study

Parameter	Weight	Rationale	On-Orbit Ops	Surface Ops
Water yield	0.3	We prefer architectures that deliver more water	-1	1
Fuel consumption	0.15	We prefer lower cost architectures	-1	1
Debris impact	0.15	We prefer architectures that have less of an impact on space near Bennu and Earth	1	-1
Complexity	0.25	We prefer architectures that are more reliable and less complex	1	-1
Duration	0.15	We prefer architectures that process material more quickly	1	-1
Total Score	1		**0.1**	**-0.1**

Qualitative Thoughts on Benefits of On-Orbit Processing
Some qualitative thoughts are also included on the benefits of On-Orbit processing, in addition to the results of the trade study:

- Removes anchoring issue
- Better power availability for processing
- Can dispose of tailings on either surface or orbit
- Provides broader range of target boulders

4.2 Khepri Multi-Vehicle Evaluation

With On-Orbit operations chosen as the mission level architecture, the vehicle architecture should be chosen as well. A mothership can be considered for multi-vehicle architectures where necessary. This was considered and is shown in Figure 4.3 below.

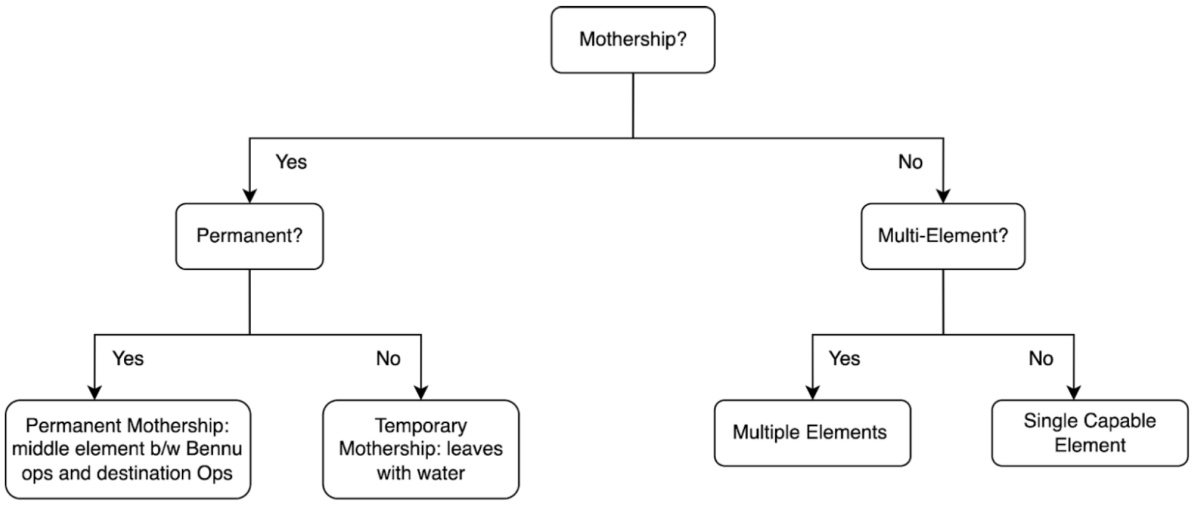

Figure 4.3: Mothership Decision Tree

Four main options were considered as shown below:

1. Minecart & Mothership Architecture - Minecarts collect boulders from Bennu and bring them to a Mothership in orbit that processes
2. Minecart-Processor Architecture - Minecarts collect boulders and have a processor on board that processes in orbit, the final water is delivered to the Mothership
3. Minecart & Processor Architecture - Minecarts collect boulders, interface with a Processor spacecraft (like the TransAstra Honeybee) that processes in orbit, and the processor delivers the final water is delivered to the Mothership
4. Super Mothership Architecture - Mothership collects boulders, processes, and stores all water

Table 4.5 below summarizes the trade, with metrics selected in relation to those described in Section 3.11. The Minecart & Mothership Architecture was selected. Note that throughout the remainder of this document, spacecraft refered to as “Minecarts” or “Pickers” are the same vehicle.

Table 4.5: Vehicle Architecture Trade Study

Metric	Weight	#1	Justification for Minecart & Mothership (#1)	#2	Justification for Minecart/ Processor (#2)	#3	Justification for Minecart & Processor (#3)	#4	Justification for Super Mothership (#4)
Fuel Usage	0.225	1	Minimum, give water to mothership/ mailman and don't haul around	1	Minimum, give water to mothership/ mailman and don't haul around	0	More than Minecart/ Processors, give water to mothership/ mailman and don't haul around	-1	Maximum, have to haul water processed around
Number of Spacecraft	0.1	0	10=1 Mothership with 4 processors and 2 tanks, 1 Mailman, 8 Minecarts	0	10=1 Mothership with 2 tanks, 1 mailman, 8 processors/ Minecarts	-1	18=1 Mothership with 2 tanks, 1 mailman, 8 Minecarts, 8 Processors	1	2=1 Mothership with processor and Minecart, 1 Mailman
Number of Different Interfaces	0.1	0	2=1 interface between mothership and Minecarts, 1 between mailman and mothership	0	2=1 interface between mothership and Minecarts, 1 between mailman and mothership	-1	3=1 interface between Minecart and processor, 1 between mothership and processor, 1 between mailman and mothership	1	1 interface between mailman and mothership
Total Mass	0.05	0	Middle	0	Middle	-1	Most, between all spacecraft	1	Least, only 2 spacecraft
Power Complexity	0.225	1	Mothership and mailman produce, Minecarts just store	0	Mothership, mailman and Minecarts produce	-1	Mothership, mailman, processors and Minecarts produce	1	Mothership and mailman produce
Redundancy	0.3	1	Lots	1	Lots	1	Lots	-1	None
Total Score	**1**	**0.75**		**0.525**		**-0.175**		**-0.05**	

4.3 Number of Minecarts

While not explicitly a trade study, the number of minecarts that were necessary was evaluated. This came down to the initial loading of the processors, as both processors need to loaded with a boulder at the same time, so that the processor tensioning systems can even out the mass distribution and ensure the center of gravity of the mothership stays at the geometric center, to prevent the need for adverse ADC control to keep

the mothership stable. This meant that a minimum of 2 minecarts are needed, but an additional 2 minecarts were also chosen for redundancy concerns, totalling 4 minecarts.

4.4 Mission Level Thruster Trade

This trade seems like a detailed design trade; however, it is necessary at this stage of mission design because it determines mission parameters and rates.

Four different types of thrusters were considered for this trade study. These were chosen based on the amount of thrust required to leave Bennu with an approximate 170 tonnes of water for the final return trip (outlined in more detail in Table 4.7). This means that for an approximate impulse lasting 21 minutes, slightly longer than OSIRIS-REx's departure maneuver lasting 7 minutes, a thrust of around 66 kN is required with a delta-V of 494 m/s (fast return trip). These thrusters are outlined below:

1. Hydrazine Thrusters: Specifically, the MR-80B Aerojet Rocketdyne thrusters, would be the hydrazine thruster of choice. These have a maximum thrust of 3.6kN. These thrusters have a TRL-7, having been used on NASA's Skycrane for the Perserverance Rover[21]. Using 8 MR-80B thrusters gives 28.8kN of thrust[22], meaning the maneuver would take around 20 minutes. This is longer than previous continuous firing of these thrusters in space, and adds concern to the feasibility. Hydrazine is an attractive fuel as it is stable and has a lot of history in space flight. The main drawback with hydrazine is that all the propellant would need to be brought to Bennu for the return trip of the Mailman, as mined water could not be used as propellant, meaning a lot of fuel would be consumed on the trip to Bennu from Cis-Lunar space. While water could be split into hydrogen and oxygen, and if nitrogen was brought to Bennu hydrazine could be created, the amount of nitrogen necessary would be 88% of the mass of the hydrazine, so nearly all propellant would need to be brought.

2. Hydros-C Thrusters[23]: These are some of the most advanced high-TRL water thrusters to date. Although these are used for cubesats and have low thrust, high thrust could be achieved by using many of them, or in theory developing one of the same cumulative mass that delivers the same cumulative thrust. For one of approximately equivalent mass to 8 MR-80B thrusters, it would deliver 2.4kN of thrust, about 8% of the MR-80B thrust. These could use the mined water from Bennu directly, provided it was rigorously purified. This means no extra fuel would need to be brought to Bennu.

3. BE-7 or RL10C-11 Thrusters: These thrusters are LH2-LOX thrusters with the RL10C-11 having much history on Atlas V Vulcan, and the BE-7 being a successor to the BE-3, also with history on the New Shephard[24] launch vehicle. BE-7 is designed for the Blue Moon lander and has a maximum thrust[25] of 44 kN. While the mass is unknown, it has a very similar specific impulse to the RL10C-11 thruster[26], so a scaled mass was used based on the amount of thrust, 78 kg. While this thrust is attractive, and this fuel could be created from purified mined water, storing LH2 is not an easy task. Liquid hydrogen boils off with slight temperature variation as it must be kept a very cold temperature

[21] https://www.globenewswire.com/news-release/2021/02/17/2177546/0/en/Aerojet-Rocketdyne-Propulsion-to-Enable-NASA-Perseverance-Rover-s-Landing-on-Mars.html

[22] https://www.rocket.com/sites/default/files/documents/In-Space%20Data%20Sheets%204.8.20.pdf

[23] https://satsearch.co/products/tui-hydros-c-water-propulsion-system

[24] https://en.wikipedia.org/wiki/New_Shepard

[25] https://www.blueorigin.com/engines/be-7/

[26] https://en.wikipedia.org/wiki/RL10

of 20K. This can be dangerous, and in addition hydrogen molecules can leak through tank walls as they are so small. This can cause leakage rates up to 1% per day, so storage of liquid hydrogen for long term missions is almost impossible. This storage issue could be avoided, if purified water was stored aboard the spacecraft, and electrolysis and cold storage occurred during transit to create the amounts of liquid hydrogen and oxygen necessary for the various maneuvers throughout the transit to and from Bennu.

4. Omnivore Thrusters: These are a current in-development thruster that uses concentrated sunlight to heat up propellant for use in essentially a hot-gas thruster. The propellant can be unpurified water, so the mined water could be used directly. The amount of thrust is directly related to the power generated by the solar condenser, with a 250 kW or 15m diameter solar condenser, producing 146N of thrust [60]. For a scaled condenser of 2.5m in diameter, this would produce 6.9 kW and around 4N of thrust. This value was used as this size condenser is roughly necessary to meet the rates for water extraction (outlined below in Section 8.3. Even if you had multiple of these for redundancy, for example 4 thrusters, this is only 40N of thrust. This is vastly smaller than the previously alternatives, and the large delta-V maneuvers would take days to complete. This may violate the impulse approximation for the trajectory maneuvers, as these would simulate more continuous thrust maneuvers.

To compare these thrusters mathematically, the amount of raw water required was compared, as some of these would use water as their propellant. The BE-7 needs components of water from electrolysis, where 1kg of water produces 0.888kg of oxygen and 0.112 kg of hydrogen, giving a mixture ratio of 7.93:1 of oxygen to hydrogen. The RL10C-11 takes a fuel ratio of 5.88:1 for oxygen to hydrogen, meaning to get enough hydrogen necessary for the overall propellant required, more water must be consumed. Assuming BE-7 has the same fuel ratio, for 1 kg of LOX-LH2, 0.1453kg (1/6.88) of it will be hydrogen, and 0.8547kg will be oxygen. Therefore, 1.298kg of water is necessary to produce enough hydrogen for 1kg of LOX-LH2, giving 0.145kg of hydrogen and 1.153kg of oxygen. This means that the propellant amounts need to be multiplied by this factor of 1.298 to compare to the other water thrusters. Since the MR-80B uses hydrazine thrusters, it is not consuming water, but the hydrazine needs to be brought as a payload, so this increases the overall mass. Calculations were done for two scenarios: to Bennu and to Cis-Lunar space. These are summarized in Tables 4.6 and 4.7 below. Note that 1970 m/s is required from Cis-Lunar space as 1.3 km/s is required to escape Earth from GEO[27], with the additional 670 m/s required to get to Bennu. Note also the various delta-V values derived from the analysis in Beckman et. al [3], and that the trip fuel masses have a safety factor of 1.4 applied.

Table 4.6: Overall Architecture Assumptions and Delta-Vs

Mailman Mass (kg)	2000
Delta-V to Bennu fro GEO (m/s)	1970
Delta-V to Cis-Lunar, Trips 1 & 2 (m/s)	250
Delta-V to Cis-Lunar, Trip 3 (m/s)	494
Safety Factor for Fuel	1.4

[27] https://en.wikipedia.org/wiki/Delta-v_budget

Table 4.7: Thruster Trade Comparisons

First Water Cycle				
Thruster	MR-80B	Scaled Hydros-C	BE-7	Omnivore
Specific Impulse (s)	212.5	310	453.8	375
Deliver per cycle (kg)	60391	60391	60391	60391
Fuel to get to Cis-Lunar (kg)	11129	7484	6548	6142
Initial Mass Leaving Bennu (kg)	73521	72427	70962	84694
Fuel to get Back to Bennu (kg)	61445	2552	2023	16161
Initial Mass Leaving Cis-Lunar (kg)	63445	4552	4023	18161
Raw water necessary (kg)	60391	70427	68962	82694
Second Water Cycle				
Thruster	MR-80B	Scaled Hydros-C	BE-7	Omnivore
Specific Impulse (s)	212.5	310	453.8	375
Deliver per cycle (kg)	143221	143221	143221	143221
Fuel to get to Cis-Lunar (kg)	25904	17420	15241	14297
Initial Mass Leaving Bennu (kg)	171125	165192	162484	178428
Fuel to get Back to Bennu (kg)	72508	2552	2023	18910
Initial Mass Leaving Cis-Lunar (kg)	74508	4552	4023	20910
Raw water necessary (kg)	143221	163192	160484	176428
Third Water Cycle				
Thruster	MR-80B	Scaled Hydros-C	BE-7	Omnivore
Specific Impulse (s)	212.5	310	453.8	375
Deliver per cycle (kg)	171388	171388	171388	171388
Fuel to get to Cis-Lunar (kg)	64911	42815	36970	34887
Initial Mass Leaving Bennu (kg)	238299	216202	210358	208274
Raw water necessary (kg)	171388	214202	208358	206274
Return Manuever (Third Cycle)				
Return Initial Mass (kg)	238299	216202	210358	208274
Number of Thrusters	8	8	4	4
Maximum Thrust per Thruster (N)	3603	300	44000	6.9
Total Max Thrust (N)	28824	2400	176000	27.6
Approximate Mass of Thruster (kg)	168	164	78	100
Total Thruster Mass (kg)	1344	1309	312	400
Firing Time for Return Manuever (494 m/s) (min)	68.1	741.7	9.8	62130.1
Main Outbound Manuever (Last Outbound)				
Post-DSM1 Mass (kg)	146499	4492	3987	38161
Number of Thrusters	8	8	4	4
Maximum Thrust per Thruster (N)	3603	300	44000	6.9
Total Max Thrust (N)	28824	2400	176000	27.6
Approximate Mass of Thruster (kg)	168	164	78	100
Total Thruster Mass (kg)	1344	1309	312	400
Firing Time for Biggest Manuever, AAM1 after DSM1 (444 m/s) (min)	37.6	13.9	0.2	10231.6
Totals				
Prox Ops Consumption	3586	2458	1679	2032
Total Raw Necessary	375000	447822	437804	483065
Total Water Delivered	375000	375000	375000	375000
Efficiency	1.000	1.194	1.167	1.288
Amount of Fuel Used	310727	72822	62804	108065
Cost of Fuel (M)	2486	583	502	865

From this study, the cost of fuel is the main end result. While hydrazine is very feasible, the cost of this option is very unattractive compared to the other options. As outlined above, there are various risks with each of the remaining three options, but given the most feasibility and lowest cost with the LOX-LH2 option, the BE-7 thrusters are chosen.

Recall that the architecture consists of three components: Mothership, Minecarts, and a Mailman. It is important to note that the result of the above trade, using the BE-7 thruster and LOX-LH2, is for the Mailman, as it is the one travelling back and forth to Cis-Lunar space. For the mothership, it could be fitted with hydrazine thrusters, but given that the technology for electrolysis and hydrogen storage would be necessary for the Mailman and the fuel is more mass efficient, it could use the same thrusters as well.

Also worth noting, the Minecart spacecraft should be designed, so they don't have to haul all of their fuel over the many trips necessary to collect boulders from Bennu's surface. This means they utilize water thrusters, as the propellant is readily available. As these delta-V maneuvers are very small, only small thrust maneuvers are necessary and wanted in Bennu's microgravity environment. Since the Minecarts are not fitted with solar condensors, and the LOX-LH2 thrusters cannot do small thrust maneuvers, this leaves Hydros-C thrusters, scaled or not, as the optimal choice.

4.5 Boulder Size Trade

A final trade that was completed for the mission architecture was determining the size of boulders that should be collected and harvested. This ultimately determines the size of necessary processing equipment in order to meet the mission requirements laid out in detail in Section 8. From Rozitis et. al [10], it is shown that there is the most abundance of 1-2m boulders, and this drops off as the boulder size is increased. However, from analysis the team has done on boulder counting, there are enough boulders of any whole number size to meet the mission requirements. The constraint is then on the mass and volume of the design capable of handling large boulders, as well as the complexity involved. Some pros for handling large boulders are:

- Fewer trips to the surface and hence less failure risk
- More efficient (more processing mass per trip), as well as more fuel efficient since fewer trips
- More modular, system can handle smaller boulders too

Whereas some pros of handling smaller boulders are:

- If processing architecture is fixed in nature, more redundancy due to smaller components
- More flexibility for gripper design and Minecart size
- Easier to fit Minecarts in payload fairing

The concern of fitting the necessary architecture in the payload fairing ultimately played a large role in this trade. If the architecture is fixed, smaller boulders should be collected to ensure redundancy. However, most space architecture is expandable/deployable, so it can be assumed that the processors can be as well. Two important parameters for this discussion are the number of trips and boulder mass (and hence required lifting thrust). These parameters are shown for boulder sizes of 1-5m, as above 5m was determined to be too complicated and risky an architecture, from an operations point of view and fitting inside the payload fairing:

- 1m Boulders: 11224 trips, 697 kg, 0.06N
- 2m Boulders: 1403 trips, 5579 kg, 0.45N
- 3m Boulders: 416 trips, 18831 kg, 1.53N
- 4m Boulders: 175 trips, 44636 kg, 3.64N
- 5m Boulders: 90 trips, 87189 kg, 7.10N

The three biggest drivers in finalizing this trade were:

1. Minimize the number of trips ($\sim$<1000)
2. Ensure that the boulder can be lifted by 4 Hydros-C thrusters (maximum thrust of 4.8N)
3. Have a range of boulders for more flexibility in boulder target selection

The boulder sizes that met these drivers were in the range of 2-4m, so the gripper, Minecart and mothership processors will be designed to handle any boulder size at or within this range.

4.6 Mothership Truss Design Trade Study

One main design decision was the type of mothership truss structure. Further detailed in Section 8.4, the mothership must be collapsable for launch, but large enough to process 4m boulders. This means the mothership architecture must be a deployable truss of some form, to give the overall spacecraft some structure and rigidity. This means a few options can be considered:

- Telescoping Truss Members: This structure benefits from collapsability for storage or transportation. However, because of the many joints and the nested structure, it lacks stiffness compared to other structural designs. One benefit is you can have nested structures within the overall telescoping architecture, so you could have an outer shell for structure, and an inner shell for fluid flow.
- Scissor-Lift Style Truss Members: This type of structure will likely have more stiffness. One possible complication is integrating a piping system where the joint be flexible in angle so that the scissor-lift style truss can collapse and deploy.

This trade is too difficult to complete at this stage, and would require further testing and analysis, but has been outlined here to show the considerations to both options.

5 Gripping and Manipulation Trades

5.1 Gripper Trade

The gripping mechanism is essential regardless of the choice of surface or orbit operations. Below are the following metrics to identify which gripper mechanism is used.

- Must provide enough force to pick up boulder from surface no matter boulder shape/orientation
- Avoid crushing boulder
- Be able to have sensors on board to send data to picker
- Withstand the extreme temperature requirements
- Be able to fit in a compact space on mothership

Based on the above requirements, these metrics were used to identify the optimal technology:

- Power Consumption
- Mass
- TRL
- Redundancy
- Failure Tolerance
- Number of Mechanisms per Spacecraft

Using these metrics a trade study was completed as shown in Table 5.1 below to determine the optimal gripper, comparing microspines, rigid body grippers and soft body grippers.

Table 5.1: Gripper Trade Study

Factors	Weighting	Microspines	X # Finger Claw	Soft bodies
Mass	0.3	-1	1	1 + needs gas.
TRL	0.2	-1	1	1
Redundancy	0.1	1	0	-1
Failure Tolerance	0.1	0	0	-1
Complexity	0.1	-1	1	0
Interfacing with the boulder	0.2	-1	1	1
TOTAL	1	-0.7	0.8	0.5

Through this trade, the team was able to deduce that the optimal method was the finger claw, with the fingertips being a soft body type material to minimize the stress applied on to the boulder. After the trade study was completed, it was deduced that even though the soft bodies did not win the trade, combining the two methods would leave less uncertainty if the boulder would be crushed or not upon grasping. With a soft body design that was patented by MDA, the gripper has a high TRL level and has the benefit of already being developed, lowering mission costs. This new proposed gripper also has the benefit of not needing

any gas to operate, and can be used with relatively low power consumption. Another benefit to this method is that it can be stowed away in a compact form to further reduce launch costs. Unknown elements about the soft body element of the gripper include its life cycle, and how prone it is to degradation. Tests for these must be conducted to ensure mission success.

5.2 Robotic Manipulator Degrees of Freedom (DOF) Trade

With the new proposed gripper, the team must perform a trade on the degrees of freedom of the robotic arm connected to the minecart unit. A trade was conducted the degree needed to not interface with the surface or impact the gripper's payload. It was concluded that the gripper arm would have a stationary shoulder joint that would be the main connection to the minecart unit. The elbow joint on the gripper arm will have one degree of freedom, helping lift the boulder up and for reducing size for mission launch. Finally, the wrist joint attached to the claw would have two degrees of freedom. This will help the picker align more precisely with the boulder for the optimal attack angle. In total, the team assessed that the arm would have a total of 3 degrees of freedom, as shown in Figure 5.1 below.

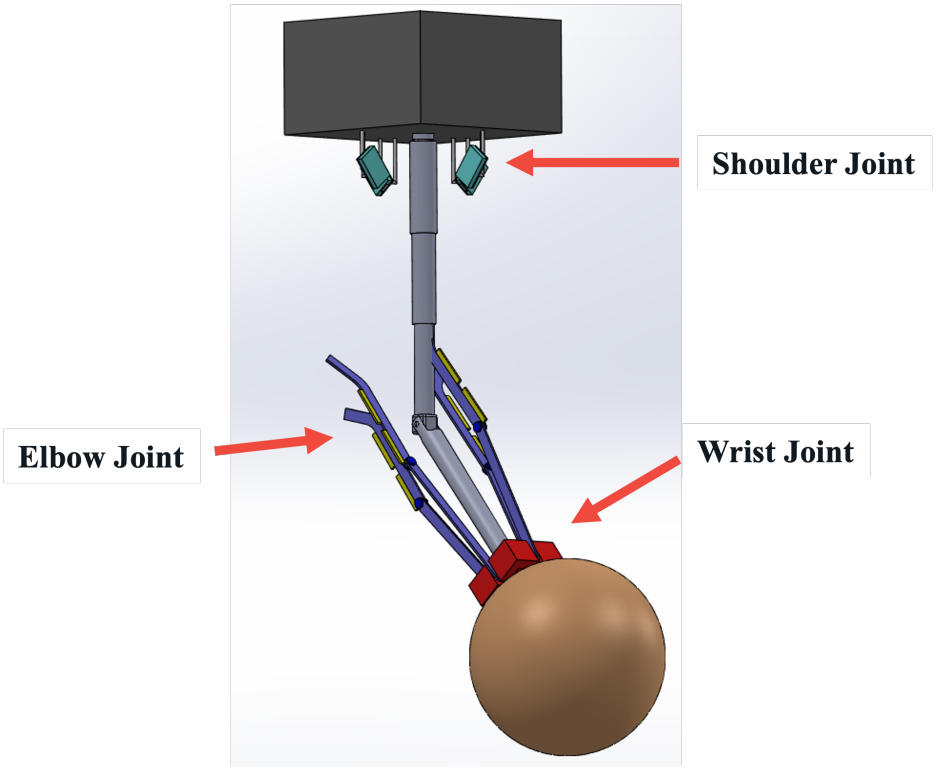

Figure 5.1: Various joints and DOF on Robotic Manipulator

5.3 Braided Manipulator and Bag Trade

After the concerns of the rigidity of the boulders (see Section 3.2 and Section 6.4), the team consider possibilities for enclosing the claw in transit from surface to orbit. This protection system must align with the mission requirements for loss of material and maintain the minecart's power and mass budgets. The

team explored possible bag or netting technologies, but all have a low TRL level and would need to be tested along with the team's gripper design.

6 Loading, Crushing and Processing Trades

6.1 Overall Processing Architecture

With the mothership doing the processing, the means by which this processing was accomplished needed to be determined. While smaller spacecraft may be able to only process one boulder at a time, the intent with mothership processing was to have multiple boulders being processed simultaneously. This can be done various ways either with a whole boulder or crushed regolith. Crushed regolith was chosen as this increases the overall surface area of the boulder, as the rate of heat transfer is directly proportional to the surface area through which the heat applied, whether that be conductively, convectively or radiatively. This effectively decreases the time to process the material. This then requires a method to crush the boulder into smaller particles.

Initial concepts took inspiration from "washing machines" where the drum would spin and bash around the boulder to break it up. A modified concept, which began a series of comparisons, used the spinning method as the source, to create "artificial gravity" by centrifugal motion, to help facilitate pseudo-flow of particulate through the processing steps. This initial concept is shown below in Figure 6.1.

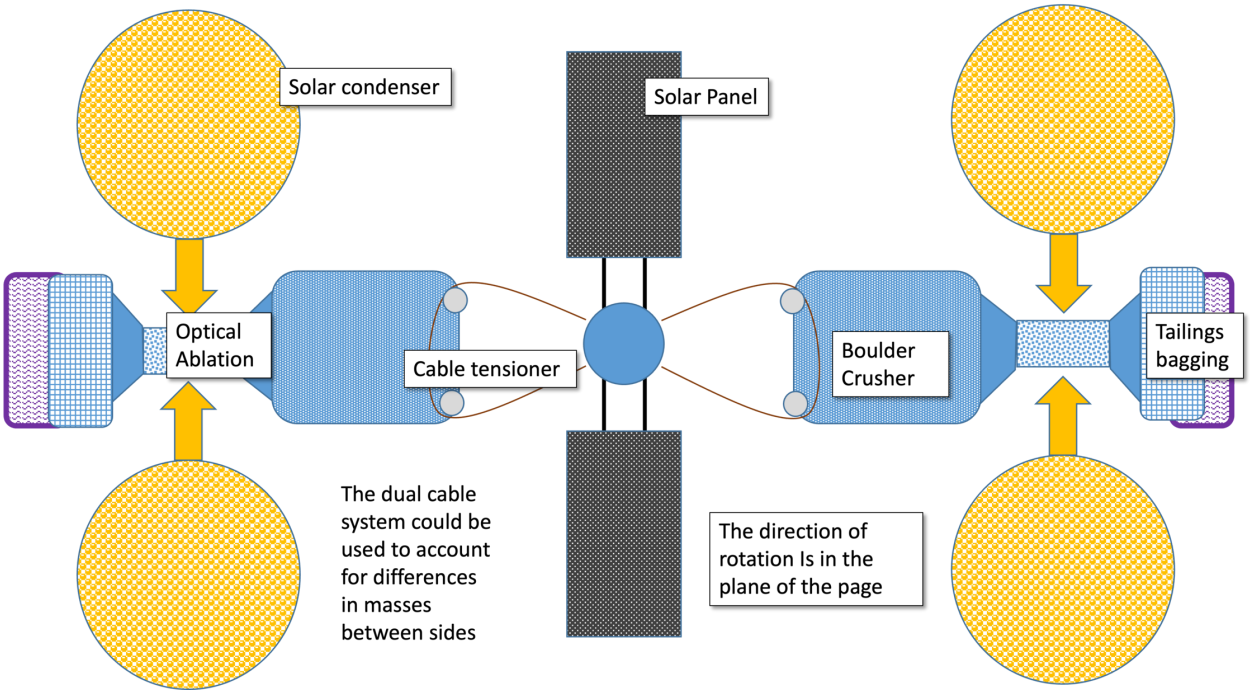

Figure 6.1: Initial Artificial-Gravity Processing Concept

Please note that the above figure assumes Optical Mining as the processing mechanism of choice, which was decided concurrently, and this trade is evaluated and described in Section 6.5 below.

The start of the processing cycle begins some sort of "loading" of boulders into the processors, some sort of "crushing" of the boulders into smaller particulate, and finally the processing takes place. Many different concepts were discussed throughout the design process, with trade study outlined in more detail in the following sections. The below flow chart in Figure 6.2 outlines some of the main ideas considered and how

the process would work.

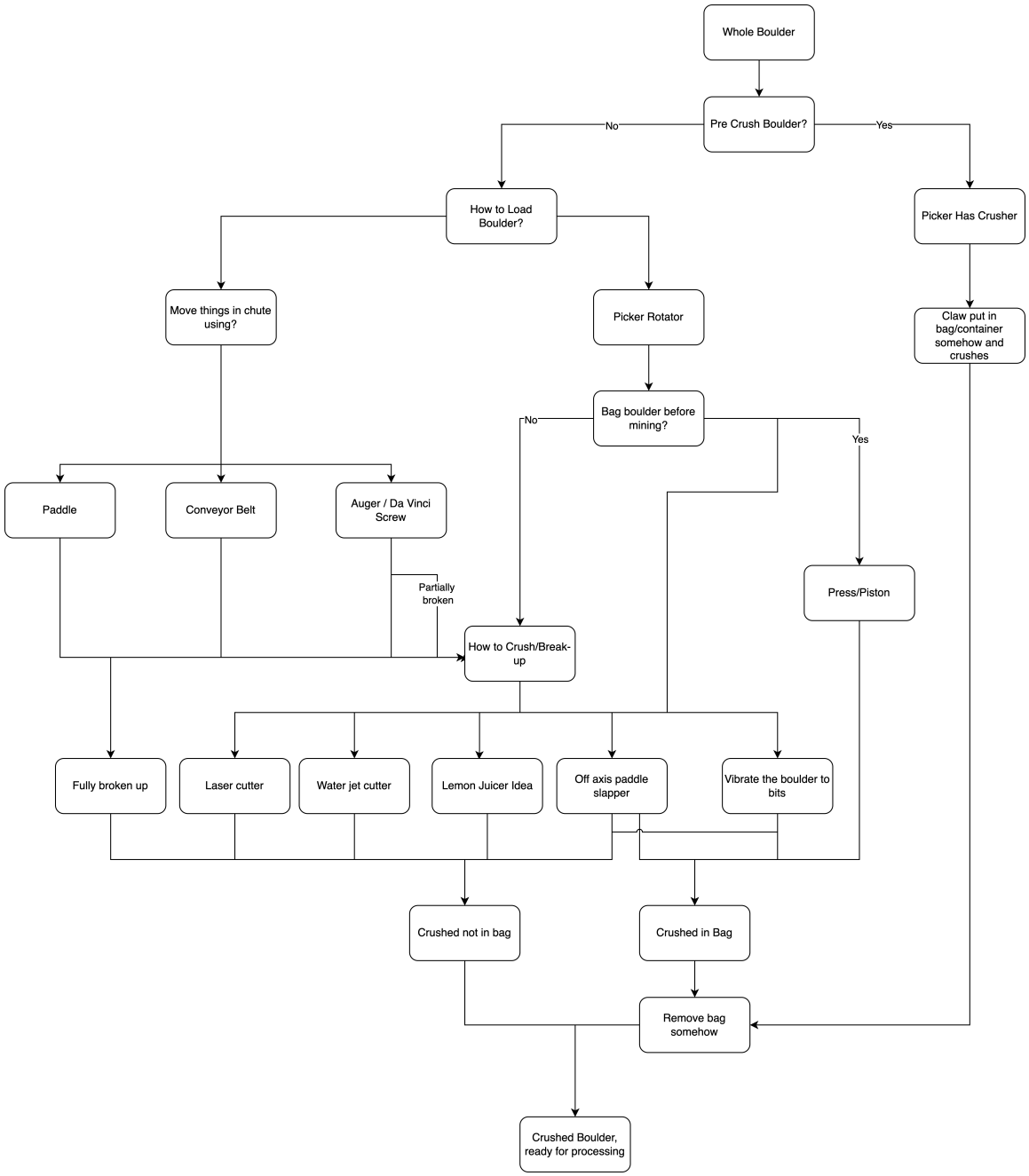

Figure 6.2: Loading and Crushing Design Flow Chart

Once the boulder is crushed, two more elements of the architecture remain. These are, the water collection via a kinetic method, and tailings collection and disposal. Water collection will be accomplished via cold-fingers, which will allow for sublimation of the water from gas to ice on their surface, which creates a pressure gradient (partial vacuum) that acts on water vapour downstream to pull the water in the direction of the cold finger. This pressure force is aided by the large temperature gradient between the hot gas and the cold-finger. The tailings collection method is outlined in Section 7.

6.2 Boulder Loading Interface Trade Study

As described in Section 3.9, there are many ways a boulder could be loaded into the processing unit. As the processor resides on the mothership, but the pickers collect the boulders, there must be some interface between the two to deposit the boulder into the processor. Various methods for this were considered, from robotic arms to "slides", with inspiration from common everyday items. The three main options considered are:

- Picker-Boulder Rotation
- PEZ Dispenser
- Drum Door

Each of these concepts was drawn to investigate visually and more in-depth for feasibility. These are shown in respective order in Figure 6.3 to Figure 6.6 below. Note for those drawings that depict a similar centrifugal configuration to Figure 6.1, only the left side of the design has been drawn. Note also the crushing concepts shown in Figure 6.3 to Figure 6.5 were not finalized at this point of the design, and a trade was also completed on these concepts in Section 6.3 below.

The Picker-Boulder Rotation concept could have a mechanism that rotates the entire unit on the mothership, or if the picker claw were to have an attached dexterous manipulator with an elbow joint, this elbow could position the boulder once docked.

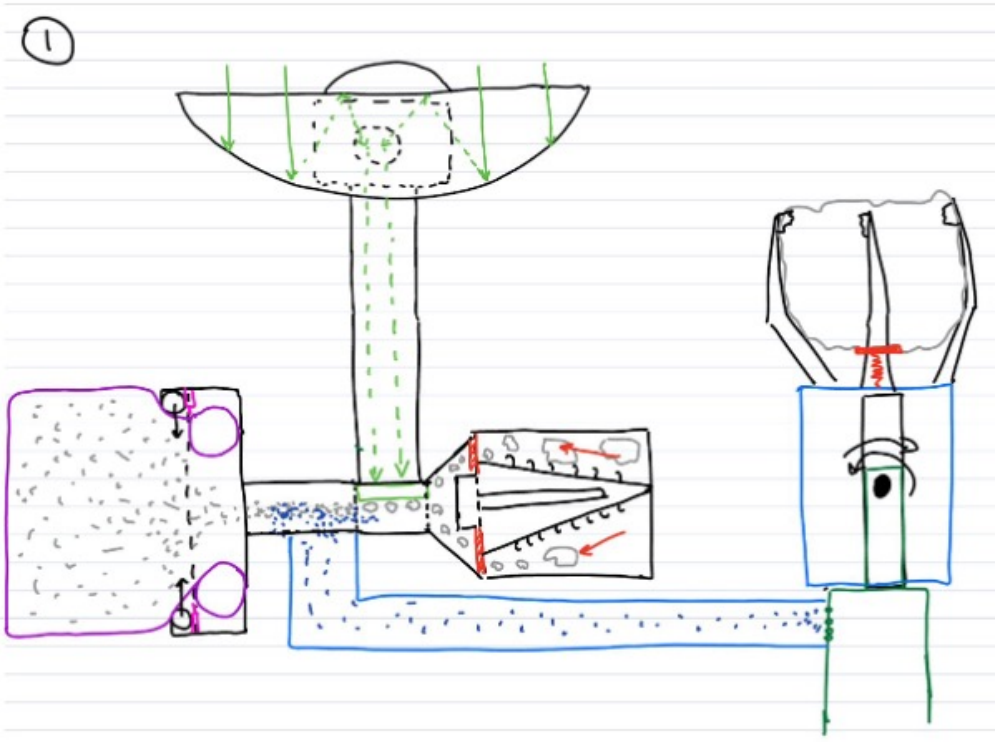

Figure 6.3: Docking of Picker to Mothership with Boulder: Step #1

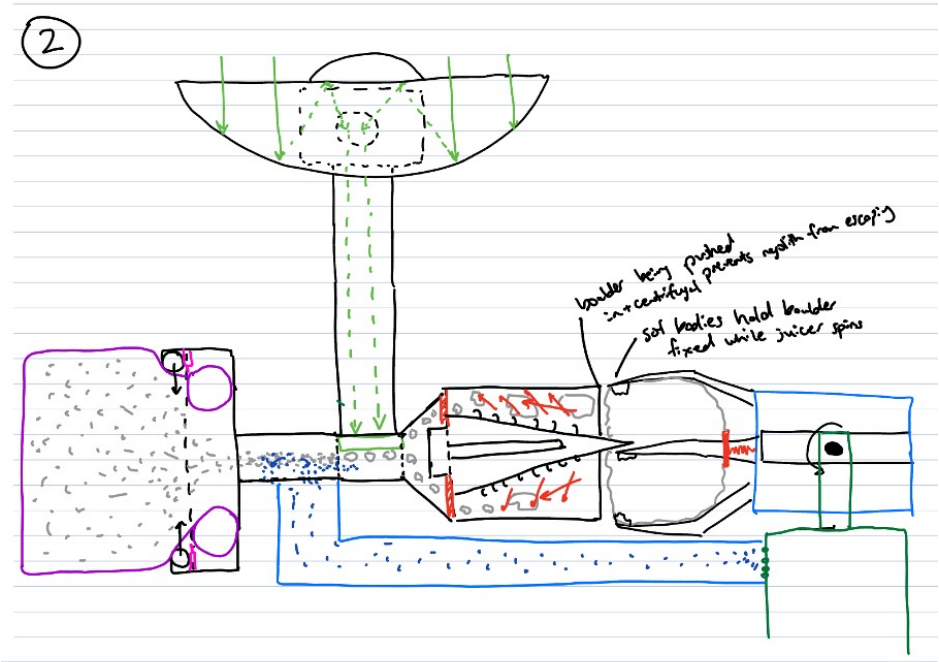

Figure 6.4: Picker Rotation with Boulder: Step #2

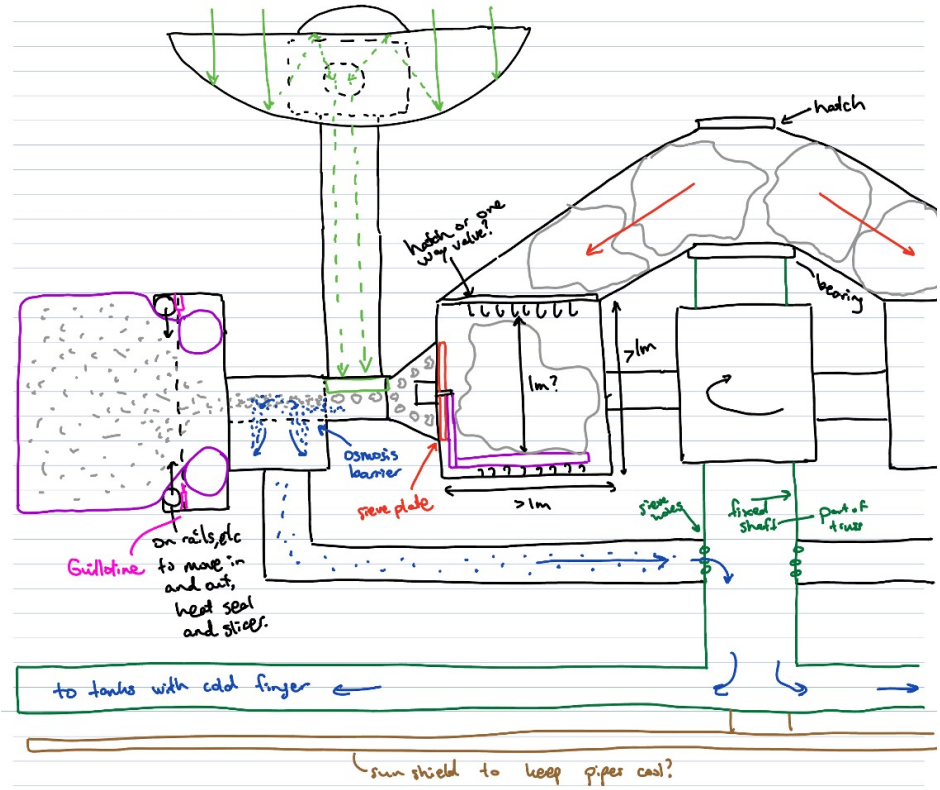

Figure 6.5: PEZ Dispenser Loading Concept

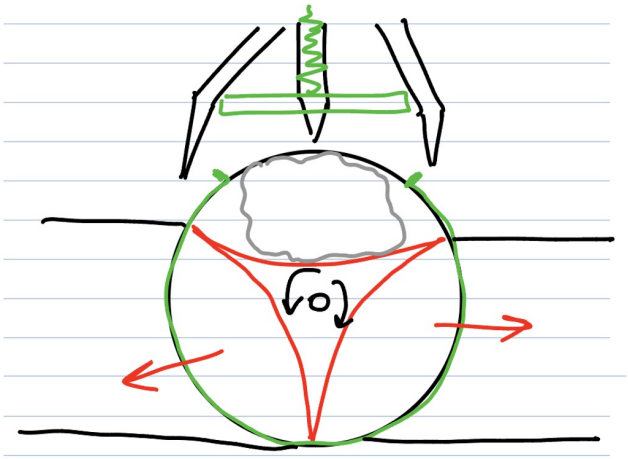

Figure 6.6: Drum Door Loading Concept

These above mechanisms take advantage of the centrifugal force to move the boulders in one regard or another. For the Boulder-Picker Rotation concept, once the boulder has been rotated in line with the processor, the centrifugal force will pull the boulder along. Similarly, for the PEZ concept, once the boulder has been moved off-axis after loading through the hatch, the centrifugal force will pull it along. For the drum door, once the boulder has been rotated to the left or right chamber and is off-axis, the centrifugal force will again act on the boulder.

For the latter of the two concepts, there are difficulties with moving the boulder. For the PEZ dispenser, this is the off-axis movement, which could be accomplished by further mechanisms, but this increases complexity and failure risk. For the drum door, moving off-axis is simple enough, but containing the boulder in the first chamber long enough to seal off the drum via the rotation is not trivial, and comes down to precise boulder release/rotation timing, or additional mechanisms/timing to seal the loading chamber after the boulder has been deposited. It was also thought the size of the drum pocket would need to be at least twice as large as the boulder diameter, meaning the drum diameter would be at least 4 times the boulder diameter. As 2-4m boulder are sought after, this would make the chamber 16m in diameter, which would be very difficult to fit in the payload fairing even with a collapsible design.

Ultimately a trade study was conducted comparing these three options. This is shown in Table 6.1 below, with the Boulder-Picker Rotation concept being selected.

Table 6.1: Boulder Loading Trade Study

		Score			Rationale		
Metric	Weight	Dock & Rotate Picker	PEZ Dispenser	Drum Door	Dock & Rotate Picker	PEZ Dispenser	Drum Door
Complexity							
Is timing critical and complex?	0.3	1	1	-1	No	No	Yes
Number of Mechanisms	0.1	-1	1	1	2+= 1 to dock and latch, 1 to rotate picker, maybe 1 to seal door/picker deals with	1+ = 1+ to move boulder down chute, maybe 1 to seal door	1+ = 1 to rotate drum, maybe 1 to seal door
Risk							
Is boulder ever not held, with only force previously applied by picker?	0.3	1	-1	-1	Has centrifugal force when released	Even if point force from picker, boulder size/shape will affect movement and rotation	Even if point force from picker, boulder size/shape will affect movement and rotation
Faith in mechanics, is this realistic in zero-g?	0.3	1	-1	-1	Seems feasible as long as forces on picker during rotation are not significant, can protect joints	Moving down the chute is not simple, more mechanisms adds complexity and risk of jamming	Timing is critical and if even slightly off will not work
Totals	1	0.8	-0.2	-0.8			

6.3 Boulder Crushing Trade Study

Once the boulders are loaded from the picker to the mothership processing unit, there must be a way to "crush" or break up the boulders into smaller particulate for the actual processing system to dehydroxylate the regolith and extract the water. As outlined in Figure 6.2, there were many crushing options considered. With the Picker-Boulder Rotation concept chosen for loading, this limited the design to certain crushing concepts. The main contenders were:

- #1: Lemon Juicer
  - The lemon juicer is a concept shown above in Figure 6.3 and 6.4. The boulder would be held either by the gripper or microspine-like fixtures inside the crushing chamber and the centrifugal force would push the boulder onto the "juicer", breaking it apart, much like how a lemon is juiced.
- #2: Self-Feeding Auger

- The self-feeding auger concept is shown below in Figure 6.7. This had the added benefit of an additional force acting in the direction of the flow.

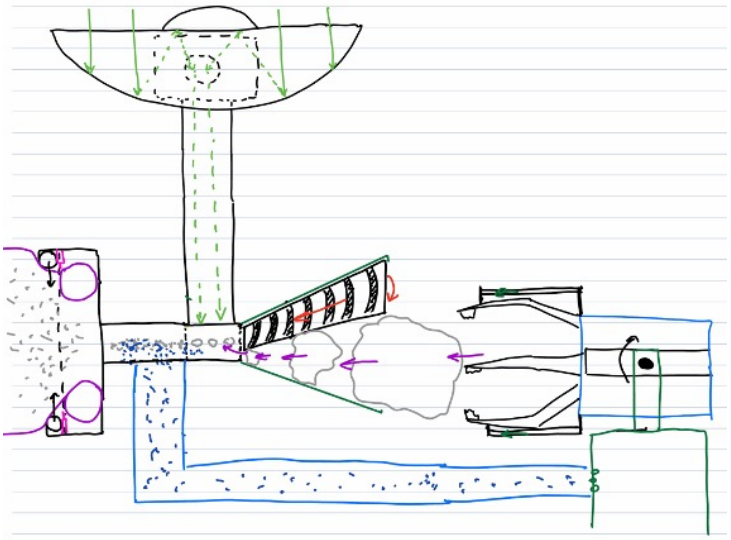

Figure 6.7: Self-Feeding Auger Concept

- #3: Tunnel Boring Machine (TBM)
  - The TBM concept draws inspiration from tunnel boring machine faces which exert tremendous pressure underground on rock to bore tunnels. This concept is highly modular, and a version is shown in Figure 6.8 below.

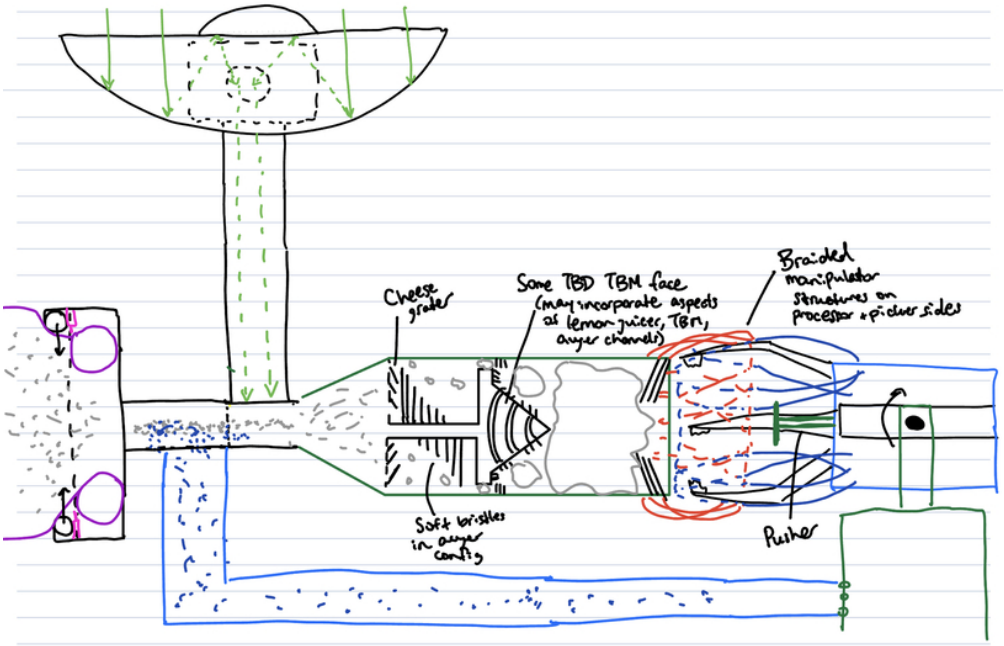

Figure 6.8: TBM Concept

- #4: Nutating Engine
  - The nutating engine is a modification to the lemon juicer concept, but here the juicer spins off axis. This precession acts to pinch the boulder between the juicer and the side of the crushing chamber, exerting increased pressure. This could be accomplished via one drive shaft like a nutating disc engine[28]. This is shown in Figure 6.9.

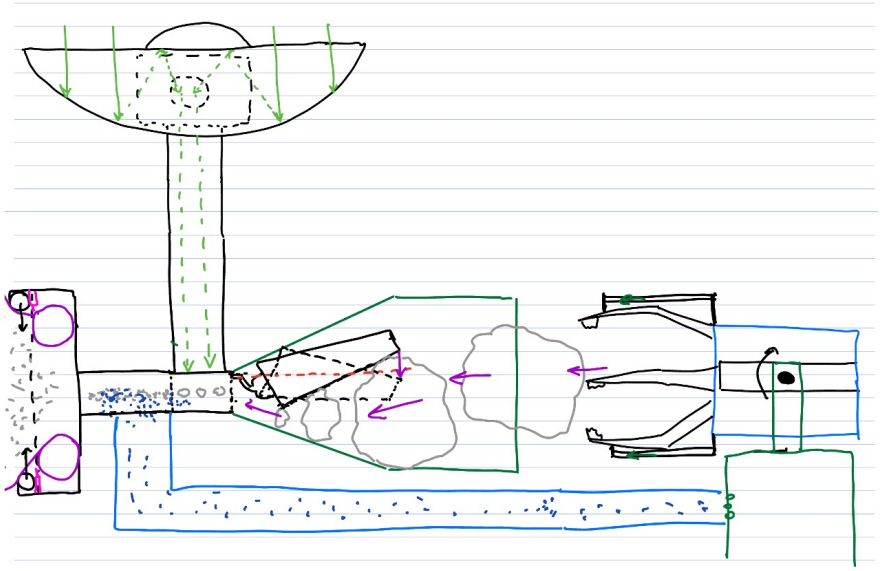

Figure 6.9: Nutating Engine Concept

These concepts all took into consideration a variety of things:

- Pressure: While studies have shown the pressure required to crush Bennu's boulder is less than 1MPa, which is very low in comparsion to rock crushing pressures on Earth, the boulders are non-homogeneous bodies. Some may have other particulates from other meteoroids that may be unexpected. Therefore, it is best to error on the side of higher required pressures.
- Failure: Failure could occur from any number of causes, but most likely from if the system becomes jammed. Therefore, ways to reduce the likelihood of jamming, or introducing ways to unjam the system, were preferred.
- Risk: As these concepts are unproven technologies in a foreign environment interacting with boulders with fairly unknown mechanical properties, the risk is significant. Risk is lowered by leveraging technologies used on Earth that could be modified for such applications. Risk also includes the risk the design poses to other aspects of the processor. One key item is the creation of debris/dust which could damage or reduce the efficiency of the solar collection for processing (as discussed in Section 6.5 below). This introduced the concept of sealing off the chamber, or mitigating any material from escaping the crusher. Another risk item is how cohesive the boulder is to begin with. Image analysis of the boulders on Bennu has shown large cracks like fault-lines in the boulders, begging the question if they will break apart into chunks when gripped by the picker. The crushing chamber should then

[28] https://en.wikipedia.org/wiki/Nutating_disc_engine

be able to accommodate and crush up smaller than 2m boulder sizes if the boulder fractures naturally into smaller chunks.

- Timing: If the boulder needs to be held by the picker during the crushing process, this is disadvantageous. Separation of the various steps in the processing cycle is ideal for optimization of the process.

The trade study investigating these factors for the described contenders is shown in Table 6.2 below. Note that both the TBM and Nutating Engine tie for the best option, but because of the increased modularity of TBM face, this concept was selected.

Table 6.2: Crusher Trade Study

		Scores				Justification				Notes
	Weight	#1	#2	#3	#4	Lemon Juicer (#1)	Auger (#2)	TBM (#3)	Nutating Engine (#4)	
Complexity										
Number of Mechanisms	0.1	0	0	0	0	1 driveshaft	1 driveshaft	1 driveshaft	1 driveshaft	
Risk										
Does the chamber need to be sealed? Risk of debris, or can you apply the bristle concept?	0.1	0	0	0	0	Can apply bristles	Can apply bristles	Can apply bristles	Can apply bristles	
Is there a secondary force always acting in direction of flow when the boulder is released?	0.3	-1	1	-1	-1	No	Auger pulls in direction of centrifugal force	No	No	Increase insurance of boulder movement
Do you need to hold onto the boulder whilst processing?	0.1	0	0	0	0	Can use microspines on chamber walls	Can use microspines on chamber walls	Can use microspines on chamber walls	Can use microspines on chamber walls	
Does this exert enough pressure to crush the boulder up?	0.4	-1	-1	1	1	Only contact on two sides	Only contact on two sides	Contact on whole face	Contact on sides but varies due to nutation	Most important that it actually gets broken up
Can you spin the mechanism the other way to remove jams?	0.1	0	0	0	0	Yes	Yes	Yes	Yes	
Totals	1	-0.7	-0.1	0.1	0.1					

The TBM face depicted in Figure 6.8 is just one of many possibilities. One concept discussed was to modify the TBM face like that of a "cheese grater" so the boulder is pushed against the face and a combination of the pressure and "grater holes" strip pieces of the boulder off. This arose from a discussion of two counter-rotating faces to grind up the boulder like the outlet of traditional "meat grinder", much like scissors if they rotated a full 360°. This design would need to be further defined and refined with simulation and testing, or ultimately with a feasibility study.

6.4 Crusher Chamber and Sealing Trade Study

Sealing of the crushing chamber was another discussion topic when trying to design the crushing chamber. Even with the acting centrifugal force, pieces of debris may exit the chamber non-optimally due to inter-debris collisions, and may hit and damage the picker or other parts of the processor, or worst of all settle on the solar condensers and damage them or impede optimal solar collection and reduce the efficiency to a level below that required for mission completion. Also note that the crushing chamber must be collapsible and expandable for the launch configuration, see Section 8.4.

The chamber wall options considered were:

- A flexible bag-like structure with:
  - A polygonal actuated outlet that can collapse and expand
  - An inflatable torus to the desired outlet diameter
- A braided-deployable structure that can be collapsed via actuators or pulleys

Using similar concepts, the sealing could be done completely passively using a soft bristle or brush structure, or more mechanically like:

- An inflatable torus to seal off the chamber
- An actuated latch, either with a hinge or a slider that moves out of the way
- A braided manipulator on the end of the crushing chamber that could effectively seal at the outlet

Other options considered including having the picker side of the loading interface seal against the crushing chamber; however, this was disadvantageous as it requires the picker to seal the chamber during the entire crushing process, instead of departing for the collection of another boulder.

The exact mechanism has not been rigorously chosen, but a tightly braided-deployable structure that can seal its own end, much like a “Chinese finger trap”, and be collapsed via pulleys is the top contender. Current research is being conducted on similar actuators by Stoy et. al [77], but nothing of the size nor braid density required for this application has been created to date.

As discussed in Section 5, this will interface directly with a similar mechanism on the bottom of the picker, that surrounds the gripper to enclose the boulder and/or boulder fragments during transit from Bennu to the Mothership.

6.5 Processor Requirements and Trade Study

The requirements for the processor method were outlined as follows:

- Shall attain 900 deg C in order to extract the water from the phyllosilicates
- Shall yield at minimum 6.26% water of the boulder mass
- Shall interface with picker that transports boulders to the Mothership for processing
- Shall minimize tailings

Based on the above requirements and typical mission constraints, the metrics to evaluate various processor method alternatives were identified:

- Mass
- Volume
- Cost
- TRL
- Resource recovery efficiency
- Power requirement

The alternatives outlined below for processor methods were researched in further detail to evaluate their feasibility as a chosen method for this project. These metrics are outlined in more detail in Table 6.3 below. Each of these options could be designed for the desired redundancy and extraction rate, so these metrics were not considered between options.

Table 6.3: Power source selection metrics

Technology	Solar + battery	Nuclear	Solar Concentration
Power (250-300 kWh + additional power to operate)	308W per day = 12.83W per hour	2000 W heat (Perseverance)	Honey bee - 250KW
Space (Size)	1000x1100 per panel - total 14 strings = 15.4 m2	Compact	15m X 2
Weight	@4.2kg/m2 = 64kgs	45kg = 4kg fuel used	130.53
Time to process 1m3 boulder (days)	1136.65 days	6.25	2 days
TRL	7	7	3
Equipment cost	Assuming 1100 $ per cell ?	perseverance - 75 Million	TBD
Degradation	High	Low	Low
System Efficiency	Low	High	High
Crushing boulder	Recommended for improved processor efficiency	May be Recommended for improved processor efficiency	Not needed, but optional
Development cost	Low	Low	High
Launch cost ($8k/kg)	512000	360000	1044240

With these metrics evaluated for each option, scores were assigned in a trade study below in Table 6.4.

Table 6.4: Processor Power source trade study

Technology	Weight	Solar + battery	Nuclear	Solar Concentration
Power	0.2	-1	1	1
Space (Size)	0.1	-1	1	0
Weight	0.1	-1	1	0
Time to process 1m3 boulder	0.1	-1	0	1
TRL	0.05	1	1	0
Equipment cost	0.1	0	-1	1
Degradation	0.05	-1	1	0
System Efficiency	0.1	-1	0	1
Crushing boulder	0.05	1	1	1
Development cost	0.05	1	0	-1
Launch cost	0.1	-1	1	1
Totals	1	-0.65	0.55	0.6

Ultimately, Solar Concentration was chosen both because of its trade score, and also since nuclear fuels are very limited in supply.

7 Tailings Disposal Trades

The section focuses on the design of a mechanism by for the disposal of the tailings, which are the materials left over after processing the regolith to extract water. For the purposes of this design, the following assumptions on the nature of the tailings were made:

- The amount of tailings generated is assumed to be 90% of the boulder mass
  - Including a factor of safety, the tailings bags shall be designed to accommodate 100% of the boulder mass i.e. for $4m^3$ diameter boulders
- The tailings will be at 900°C upon exit from the processor unit
  - This influences the tailings disposal design: either need a cooling unit before transferring tailings to bag, or need to design the bag to accommodate this high temperature
- The tailings are solid particulate matter
- The tailings are not charged particles

The high-level requirements were identified as follows:

- Shall not affect Bennu's orbit
- Shall adhere to Outer Space Treaty and other space policies regarding space debris
- Shall minimize creation of additional debris

The alternatives were divided into surface and orbital methods. For the former, the tailings could be disposed of, as is or in a sealed bag, on the surface. The option of burying the tailings on Bennu is eliminated due to its surface properties, such as the high distribution of boulders, making this infeasible. For the orbital methods, the tailings could be disposed of, as is or in a sealed bag, in a stable orbit. These options are not inherently linked to whether processing is done on the surface or in orbit, as the tailings disposal may just require an additional transit step (with low delta-v, given Bennu's microgravity environment) if processing was in orbit and tailings disposal on the surface, or vice versa. Thus, the high-level trade below was conducted independently. Four options were considered:

1. Surface Ops: Bag (#1)
2. Surface Ops: No Bag (#2)
3. Orbit Ops: No Bag (#3)
4. Orbit Ops: Bag (#4)

Table 7.1: High-Level Trade Study on High-Level Design of Tailings Disposal Mechanism

Parameter	Weight	Rationale	#1	#2	#3	#4	Notes/Justification for scoring
Economic Factors:							
Capacity per Cycle	0.05	Not as important since the bag size can be optimized	0	1	1	0	Bag method limited by bag volume, other methods can dispose of any volume
Fuel Consumption per Cycle	0.1	Fairly important for efficient operations	1	1	-1	-1	Depends on whether processing is done in the same place (surface vs. orbit) as disposal, either way it would be a small delta-v due to microgravity environment. Orbit for stable satellites is equatorial but spacecraft is more stable in polar orbit so would require orbit change.
Power Consumption per Cycle	0.05	Not as important since the power difference between methods would be negligible compared to power requirements to process	0	1	1	0	More power required to seal bag? Might be negligible depending on the mechanism chosen
Cycle Time	0.1	Need to work according to cycles designated by mission arch so fairly important to minimize time for disposal, more time for processing	0	1	1	0	More time required to seal bag? And time to compact tailings to fit into bag's predetermined finite volume, if necessary
Complexity/Risk Factors:							
Mass	0.1	Generally want to minimize mass for space mission -> fairly important	0	1	1	0	mass of bags
Redundancy	0.1	Minimize risk of subsystem failure ->fairly important	1	0	0	1	maybe pack extra bags to increase redundancy
Failure Tolerance	0.1	Minimize impact of subsystem failure ->fairly important	0	1	1	0	bags require more mechanisms
Security of Disposal	0.25	Most important since this is the primary objective of this subsystem	1	-1	-1	1	bag method is the most secure
Risk of Instability	0.15	Linked to primary objective, we want the tailings to STAY securely disposed of and not pose further risk to mission -> second most important	1	1	-1	-1	orbit: debris or spacecraft collisions may deorbit, surface: risk of debris hitting spacecraft but mitigate by stowing sensitive components
TOTAL SCORE	1		0.6	0.4	-0.1	0.1	

Based on the trade study above, the **surface sealed bag** alternative was selected. The detailed design of this mechanism involved several further trades, including the material selection for the bag and the method to seal the bag. Note that the method to load the bag with tailings was considered in the overall mission architecture - this design facilitates the loading of the tailings using centrifugal forces. The detailed design options for material type are presented below:

1. LDPE (#1)
2. Beta Cloth (#2)
3. Polymer Based (#3)
4. HDPE (#4)
5. Aluminum Foil (#5)
6. CNT Based (#6)

As shown in Table 7.2, the highest rated alternatives in the trade was **CNT**, particularly because of its ability to withstand the high temperature of the tailings upon exit from the processor. It was also selected because of its strength, flexibility, durability and porosity.

The sealing mechanism alternatives are as follows:

1. Velcro (#1)
2. Ziploc (#2)
3. Magnetic Tape (#3)
4. Thermal Seal (#4)
5. Stitcher (#5)
6. Hot Wire (#6)
7. Drawstring (#7)

As shown in Table 7.3, the highest rated alternatives in the trade were Thermal Seal and Stitcher. The design will proceed with **Stitcher** since a heat-independent and purely mechanical method was preferred given the assumption that the tailings would enter the disposal bag at 900°C.

Table 7.2: Material Selection Trade for Tailings Disposal Bags

Parameter	Weight	Rationale	#1	#2	#3	#4	#5	#6	Notes/Justification For Scoring
Economic Factors:									
Cost per yard	0.1	Fairly important since the difference in cost for these alternatives is not negligible	1	-1	1	1	0	0	Values were determined and scored
Complexity/Risk Factors:									
Mass/Density	0.05	Generally want to minimize mass for space mission -> kinda important	0	1	0	-1	-1	-1	depends on density of material (adjustable)
TRL	0.1	Minimize risk of failure ->fairly important	0	1	1	1	1	0	has it flown in space before?
Porosity	0.15	Need tailings to be secure ->very important	0	1	1	0	-1	1	More porosity, less weight, and higher flexibility; but not porous enough to allow particulate tailings to escape
Decomposition Temperature	0.15	keep tailings secure in harsh thermal environment ->very important	-1	1	1	0	-1	1	Should be valued if hot tailings directly come out from the processor
Flexibility	0.05	bag can accomodate tailings ->kinda important	1	1	1	0	0	1	inverse of stiffness (can be adjusted easily in case we use woven structures like woven fabrics)
Durability	0.1	need to withstand force of loading ->fairly important	0	0	0	1	0	1	
Yield Strength	0.05	not very important, we care more about ultimate tensile strength as shape of bag is not important once it does its job	-1	1	-1	0	-1	1	
Thickness	0.05	ease of packing but not that mission critical	0	0	0	-1	1	0	Can be adjusted for CNT based and polymeric materials
Tensile Strength	0.1	important as we don't want bag to burst and release tailings prematurely	0	0	0	0	-1	1	
Strain to Failure	0.05	not very important as shape of bag is not important once it does its job	0	0	0	0	-1	1	
Coefficient of Thermal Expansion	0.05	not very important, we care more about decomposition temperature as shape of bag is not important once it does its job	-1	1	-1	0	1	0	
Radiation Resistance	0.1	important to survive in harsh environment	0	1	0	0	1	0	Based on the literature radiation resistant materials can be used directly or the existing materials can be coated by radiation proof coatings
TOTAL SCORE	1		-0.1	0.5	0.45	0.2	-0.25	0.6	

Table 7.3: Trade for Sealing Mechanism for Tailings Disposal Bags

Parameter	Weight	Rationale	#1	#2	#3	#4	#5	#6	#7	Notes/Justification For scoring
Economic Factors:										
Power Consumption per Cycle	0.05	Not as important since the power difference between methods would be negligible compared to power requirements to process	1	1	1	0	0	0	1	thermal methods require power for heating, complex mechanical methods also require power for various mechanisms
Cost	0.05	Good to consider to minimize overall mission costs but likely not a huge factor considering the order of magnitude of these costs	1	0	-1	0	1	1	1	velcro, hot wire, string and adhesive tape all cheap, ziploc slightly pricier, mag tape and thermal seal mechanism more expensive but only need one thermal seal mechanism
Cycle Time	0.05	Need to work according to cycles designated by mission arch so fairly important to minimize time for disposal, more time for processing	1	0	1	0	0	0	0	”slap together” mechanisms are the quickest, other mechanisms take slightly more time like ziploc along edge of bag or pulling drawstring, twisting and then taping is a two-step process and requires the most time
Complexity/Risk Factors:										
Mass	0.05	Generally want to minimize mass for space mission -> fairly important	1	1	0	0	0	1	1	mag tape slightly heavier than velcro and ziploc and strings, twist & thermal methods require additional mechanism hence additional weight
Redundancy	0.05	Minimize risk of subsystem failure ->fairly important	1	1	1	-1	-1	-1	0	can have extra velcro, mag tape, ziploc, adhesive tape; drawstring pulling mechanism may not be redundant, neither twist mechanism even though string and tape may be redundant; might not be able to add extra thermal mechanisms
Operational Complexity	0.3	Less steps in the procedure and less mechanisms needed is preferred	-1	-1	-1	1	1	-1	1	ranked according to number of steps
Failure Tolerance	0.05	Minimize impact of subsystem failure ->very important	1	1	1	-1	-1	-1	-1	if complex mechanisms stop working, none of the bags will seal; if simple mechanisms fail, try another bag eg. velcro misalignment
Security of Disposal	0.4	Most important since this is the primary objective of this subsystem	0	0	0	1	1	1	-1	velcro & drawstring may allow for gaps in seal if misaligned velcro or not fully pulled strings; twist&tape may be susceptible to unravelling; all others secure
TOTAL SCORE	1		0	-0.1	-0.15	0.6	0.65	0.1	0	

Chapter 4: Mission Concept

8 Mission-Level Requirements Derivation

Mission-level requirements derivation aimed to provide subsystem teams bounds of the range mission components will need to perform in. To provide useful guidelines, preliminary analysis was performed to answer the following questions:

- How much water do we need to extract?
- How fast do we need to extract water?
- How much boulder regolith do we need to process?
- How much mass can we launch?

This activity sparked additional analysis to plan water collection and delivery cycle timelines, estimate water required for propellant. Derived quantities and justifications are outlined below.

8.1 Required Revenue and Cost of Water

It is assumed that the entire mission will have a budget of $1.5B. Assuming that a 100% return on investment is necessary to make the mission worthwhile, we require enough water to generate $3B in revenue.

To determine how much water is required to generate $3B in revenue a launch vehicle analysis was completed to determine launch costs per kg into various orbits, to determine the equivalent launch cost of water. These results are shown in Tables 8.1 and 8.2.

Table 8.1: Launch Cost Analysis Part 1

Launch Vehicle Comparison	Cost (M)	Payload to LEO (t)	Payload to GTO (t)	Payload to TLI (t)	Payload to MTO (t)	Cost per kg (LEO)	Cost per kg (GTO)	Cost per kg (TLI)	Cost per kg (MTO)	GTO/LEO	TLI/LEO	MTO/LEO
Falcon 9 (Reusable)	50	16.3	5.5			3067.5	9090.9			2.96		
Falcon 9 (Expendable)	67	22.8	8.3		4	2938.6	8072.3		16750	2.75		5.70
Falcon Heavy (Reusable)	97	63.8	26.7		16.8	1520.4	3633.0		5773.81	2.39		3.80
Falcon Heavy (Expendable)	150	63.8	26.7		16.8	2351.1	5618.0		8928.571	2.39		3.80
SLS Block 1	2000	95		27		21052.6		74074.1			3.52	
SLS Block 1B	2000	105		42		19047.6		47619.0			2.50	
SLS Block 2	2000	130		46		15384.6		43478.3			2.83	
Starship	10	150				66.7						
New Glenn	68	45	13.6			1511.1	5000.0			3.31		
Vulcan Centaur	141	27.2	14.4	12.1		5183.8	9791.7	11652.9		1.89	2.25	
Average Cost per kg										2.61	2.77	4.43

Table 8.2: Launch Cost Analysis Part 2

		Cost per kg (LEO)	Cost per kg (GTO)	Cost per kg (TLI)	Cost per kg (MTO)
Tax	20%				
Average Cost of Tested Spacecraft		3086.7	8070.5	8559.9	13679.6
Rounded Cost		3000	8000	9000	14000

Assuming the target customers will be in High Earth Orbit (just above GEO), this gives a launch cost of $8000/kg of water, meaning 375,000 kg of water must be delivered to customers; however, some water will be used as propellant for use in mission elements. Depending on the type of propellant, discussed in Section 4.4, an extra amount of water must be allocated for propellant use. This propellant and thruster trade, while detailed design, was one necessary at this stage, in order to determine mission level requirements.

8.2 Timescale Derivation

Bennu makes a close approach with Earth roughly every 6 years. OSIRIS-REx took advantage of this to have a low delta-V requirement to get to Bennu, as well as return to Earth. Their mission roughly spanned 7 years, with 2.2 years of outbound cruise, 2.4 years at Bennu, and 2.4 years of return cruise, meaning their mission was not exactly optimal from a delta-V perspective. An optimal mission would mirror Bennu's synodic period, and this was explored by Beckman et. al [3]. A simple mission design would include a whole number of years of mining. Since it takes approximately 1 year for outbound cruise (1.13 years), there could be approximately 3 years of mining (2.53 years) before a 2 year return trip (2.34 years), such that the outbound cruise and return cruise take advantage of Bennu's close approach with Earth. Similarly, the mission could be extended in 6 year increments, and after the first 3 years of mining, the mining period would be 6 years long. It was decided that the mission duration would span 18 years, as this is a whole number of 6 year periods. THe final 6 year period takes advantage of a more costly but faster delta-V trip back to cis-Lunar space, which actually allows for a net increase in water (more water produced in that time than consumed by the increase in fuel). This means the final cycle is roughly 7 years of mining (7.18 years), followed by a return trip of roughly 1 year (1.16 years). This is summarized in the Gantt chart in Figure 8.1 below.

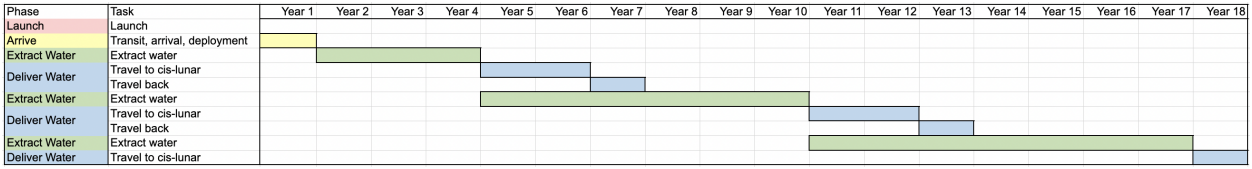

Figure 8.1: Mission Timeline Gantt Chart

These specific trip times were outlined in Section 3.1. Two options for the trip were a faster, less delta-V efficient trip and a slower, more delta-V efficient, shown below:

1. Delta-V: 920 m/s; Time: 1269 days or 3.47 years
2. Delta-V: 1092 m/s; Time: 835 days or 2.29 years

While more delta-V is necessary for the second option, since an extra 1.18 years can be spent mining during the first 6 years, it is actually the better option from a mining rate perspective. This will be further outlined in Section 8.3. This means that there will be 15.71 years of useful water extraction, compared to 14.53 years. For the first and second return trips, the delta-V of the trip should be minimized to maximize product delivery, so the longer return trip can be used. However, to get the 15.71 year timeline, the final return trip should use the faster but more costly delta-V trip. This was shown in Figure 8.1.

While this 6 year cycle is optimal for fuel consumption, it creates large periods between product delivery from an economic point of view. This is traded against delivering more often, where more fuel would be required for these less optimal trips. This would effectively decrease your ROI. As these less optimal trip

delta-v requirements are unknown and would require highly specific analysis, the 6 year cycle as outlined in the Gantt chart will be used for mission design.

It is also useful to know the times that the various maneuvers are occuring after the launch date. Using Beckman et al's analysis, as well as true OSIRIS-REx date data, the following dates were determined and shown in Table 8.3 below.

Table 8.3: DSM and AAM Delta-V and Time Breakdowns

Maneuver	**Delta-V (m/s)**	**Time after Departure from Earth/Cis-Lunar (days)**
DSM	39.7	276
AAM-1	444.4	371
AAM-2	180.8	385
AAM-3	4.7	399
Arrival (20km)	-	413
All Outbound Maneuvers	**669.6**	-

8.3 Required Performance Rates and Regolith Mass

Given the 15.71 years of useful water extraction time derived in Section 8.2, required performance rates can be derived. These rates are dependent on the type of boulder selected. As a range of 2-4m boulders will be selected, this will effectively give a range of regolith and water to be processed. These are included in Table 8.4 below, with the average over 2-4m included as well. Note that the fuel required is for all the pickers combined.

Table 8.4: Rates and Boulder Information

Boulder Diameter (m)	1	2	3	4	2-4 Average
Factor	3219	811	569	510	1076
Amount of Water Required	441023	438615	438373	438314	438434
Net Recovered Water after Picker Fuel (kg)	437804	437804	437804	437804	437804
Water Percentage	6.26%				
Amount of Regolith contained in (kg)	**7045100**	**7006633**	**7002767**	**7001825**	**7003742**
Efficiency	0.9				
Amount of Regolith Total (kg)	7827889	7785148	7780853	7779805	7781935
Useful Ops Time (yrs)	15.71				
Amount of Water Required per Year (kg/yr)	28073	27919	27904	27900	27908
Amount of Water Required per Hour (L/hr) or (kg/hr)	3.202	3.185	3.183	3.183	3.184
Regolith per hour (kg/hr)	56.842	56.531	56.500	56.493	56.508
Boulder Density (kg/m3)	1332				
Boulder Volume (m3)	0.52	4.19	14.14	33.51	17.28
Boulder Mass (kg)	697.43	5579	18831	44636	23015
Bennu Mass (kg)	7.33E+10				
Bennu Average Radius (m)	245.00				
Bennu Gravity (m/s^2)	8.14E-05				
Force to Lift of Surface (N)	0.057	0.454	1.53	3.64	1.87
Equivalent Earth weight (g)	5.8	46.3	156.3	370.6	191.1
Amount of Boulders to Process per Year	714	89	26	11	42
How often a boulder needs to be processed (days)	0.51	4.09	13.80	32.72	16.87
Number of Trips/Boulders	11224	1403	416	175	665
Percent of Boulder per day (%)	**195.6%**	**24.5%**	**7.2%**	**3.1%**	**5.9%**
Delta-V (for slow Hohmann Transfer) (m/s)	0.0669				
Picker Mass (kg)	3980				
SF on Fuel	1.4				
Hydros-C Specific Impulse (s)	310				
Total delta-V (m/s)	785	98.068	29	12	46
Fuel Required by Pickers per trip to Mothership (kg)	0.144	0.294	0.703	1.497	0.831
Fuel Required by Pickers per trip to Bennu (kg)	0.143	0.284	0.666	1.411	0.787
Fuel for One trip (kg)	0.287	0.578	1.369	2.909	1.618
Fuel Required total (kg)	3219	811	569	510	1076

The amount of raw water using the thrusters as specified above to get 375,000kg of deliverable water, for the average 2-4m case is 438,126kg. An additional small amount is necessary for the pickers, although this is dependent on the number of trips, which is dependent on boulder size. Assuming boulders on Bennu are $\sim$6.26% water by mass, the required water yield is contained in 6,998,816 kg of regolith. Assuming that the water extraction process is 90% efficient, the mission will need to process 7,776,463 kg of regolith.

Since 438,126kg of water must be created in total, 27,888 kg of water must be created per year. Typical CM chondrite density is 2960 kg/m^3 [10]. The two types of boulders on Bennu either have low porosity and high albedo, from 24% to 38%, or high porosity and low albedo, from 49% to 55% [10]. Similarly, this gives density ranges of 1835 kg/m^3 to 2250 kg/m^3 for high albedo, and 1332 kg/m^3 to 1510 kg/m^3 for low albedo ones. The target boulders will be ones with high albedo, as those tend to have high concentrations of water, meaning that should be the density estimate used. However, to ensure that the boulder processing rate is sufficient or even over designed, the low density figure will be used, of 1332 kg/m^3. This also allows for

margin to process both high and low albedo boulders if desired. Given a boulder density of 1332 kg/m^3, the number of boulders to harvest is dependent on the boulder size. Since the system is designed to be capable of handling between 2-4m spherical boulders, the number of trips of each and the required processing rate is shown below:

- 2m Boulders: 1403 trips, 24.5% of a boulder per day
- 3m Boulders: 415 trips, 7.2% of a boulder per day
- 4m Boulders: 175 trips, 3.1% of a boulder per day

As the system is designed for this range, it will likely make somewhere between 175-1403 trips to meet or exceed this requirement.

8.4 Launch Breakdown

As stated in Section 8.1, the entire mission is assumed to have a budget of $1.5B. For early design requirements derivation, 20% of this budget, or $300M is allocated to the cost of launching mission components from Earth. The Falcon Heavy is currently the most cost-per-mass efficient launch vehicle and is treated as the selected launch vehicle. Expendable Falcon Heavy launches (as reusable launches of the Falcon Heavy have not yet been demonstrated) cost about $150M per launch, meaning 2 launches can be afforded. The Falcon Heavy's launch capacity of 26,700 kg per launch results in the overall mission mass budget of 53,400 kg. Each launch also has a payload fairing volume of 5m in diameter by 13.1m as shown below in Figure 8.2; however, this is not the full volume of a cylinder due to the payload fairing tapering.

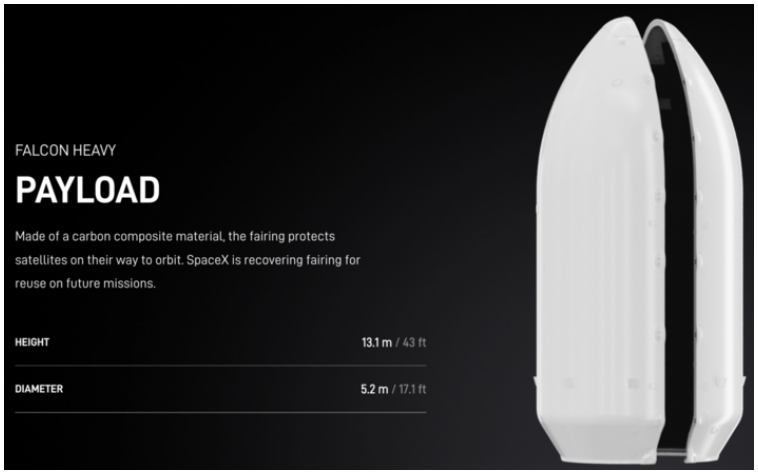

Figure 8.2: Falcon Heavy Payload Fairing Size

As described above, two launches are allocated from the mission economics. One of these launches will launch the mothership, and the second launch will launch the remaining components. The main governing constraint of the architecture is launch volume. As boulders up to 4m in diameter will be processed, the architecture must be compactible, and then deploy to full size upon arrival at Bennu. Due to this volume constraint, the water tanks will be launched with the second launch. This also provides the added benefit of providing a docking interface for the pickers for launch, as the pickers will already need to dock to the water tanks to refuel.

Launch 1 Configuration

Figure 8.3 shows the mothership collapse for the launch configuration. Figure 8.4 shows the mothership once fully deployed after arrival at Bennu. Note that after the mothership has been ejected from the payload fairing, the solar arrays and supporting trusses on both sides must be deployed in egress, to keep the mothership in optimal temperature ranges. The mothership's ADC system must also keep the mothership aligned with the sun for the solar arrays to be effective. Also note that only 80% of the launch volume dimensions have been used, to allow for margin and growth during launch.

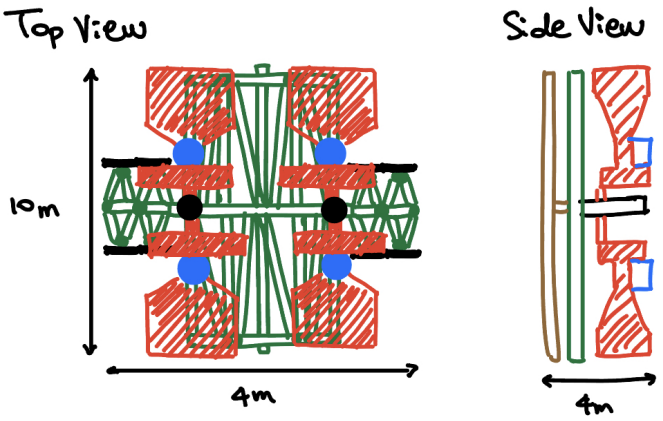

Figure 8.3: Stowed Mothership

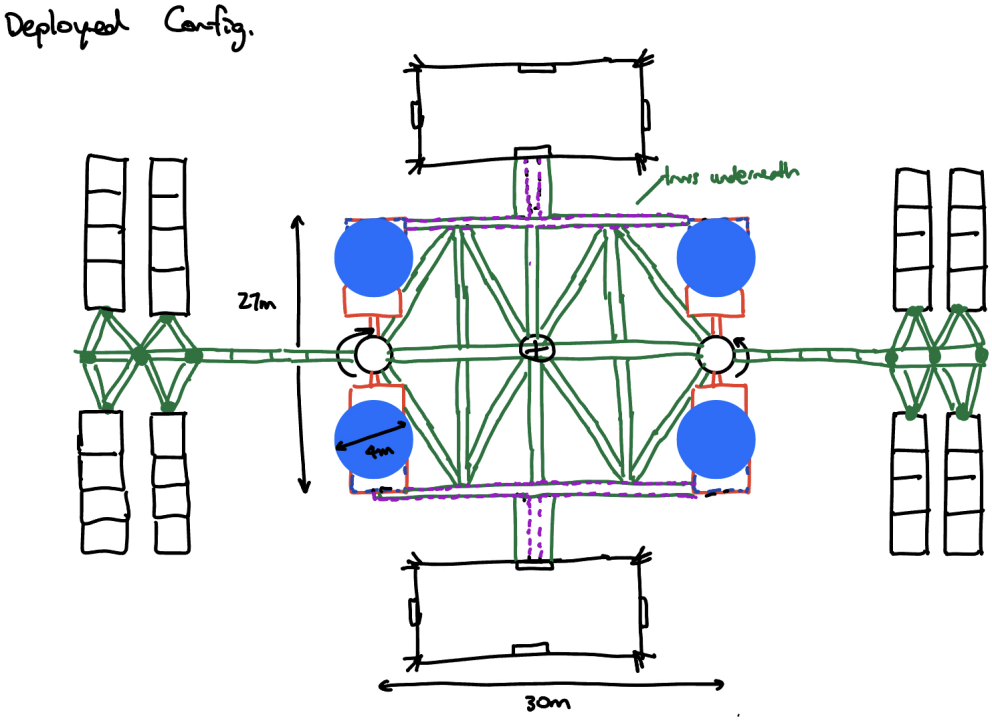

Figure 8.4: Deployed Mothership

In addition to the volume constraints, a preliminary mass budget was completed for the mothership based on typical subsystems from a Space Mission Engineering design textbook, that overlap well with the subsystems outlined for the mothership. This is shown in Table 8.5 below. Note this is for the dry mass.

Table 8.5: Mothership Mass Budget

Mass Budget			Per Unit				Total			
	Maturity code	% MGA	Basic Mass	MGA	Best Estimated Mass	Units	Basic Mass	MGA	Best Estimated Mass	Percent of Total
Payload (Processor)	1	25	2241	747	2988	1	2241	747	2988	15%
Structure and Mechanisms	1	25	3735	1245	4980	1	3735	1245	4980	25%
Thermal Control	1	25	896	299	1195	1	896	299	1195	6%
Power (including wiring harness)	1	25	3138	1046	4184	1	3138	1046	4184	21%
TT&C (Comms)	1	25	1046	349	1395	1	1046	349	1395	7%
On-Board processing (C&D)	1	25	598	199	797	1	598	199	797	4%
Attitude Determination and Control (ADC)	1	25	896	299	1195	1	896	299	1195	6%
Propulsion	1	25	1942	647	2590	1	1942	647	2590	13%
Other (Balance + and Launch)	1	25	448	149	598	1	448	149	598	3%
Total									19922	100%

Launch 2 Configuration

The second launch configuration is much more complicated as this launch includes the water tanks, pickers and mailman as one cohesive launch unit. Upon arrival at Bennu, these units separate for mission operations to begin. Two prospective configurations were considered, with configuration #1 as shown in Figure 8.5 below being selected for its symmetrical advantages.

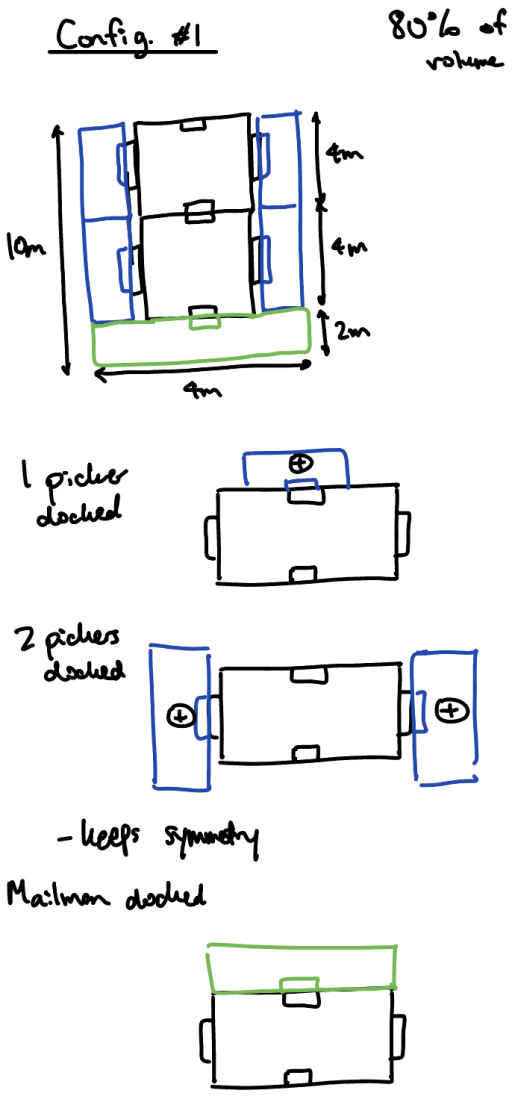

Figure 8.5: Second Launch Configurations

The mailman must be capable of holding enough water as fuel for the journey. For the 26.7 tonnes total launch wet mass, this is roughly 6800kg of water, with a safety factor of 1.4 like OSIRIS-REx used. This means a volume of 6.8m^3 or greater is necessary, so a flexible container with a launch size of 2m by 4m by 4m fits this specification. The mailman would look in this configuration as shown in Figure 8.6 below.

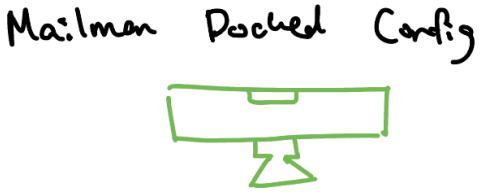

Figure 8.6: Mailman Launch Configuration

This mailman has a flexible water tank because it must be capable of holding much more water for its delivery trips. For the third and largest delivery trip, it must be able to hold around 192m^3 of water. This volume could be met by many geometrical combinations, but it definitely means that the container must be able to expand in size.

Due to the mailman size for launch, this restricts the water tank diameter for launch as well. The water tanks will also be flexible in nature, but for launch must compact to 0.5m by 4m by 4m in total volume.

There are a variety of ways that the picker could be configured for launch and likely similarly for docking and charging. The configuration that is most in line with the design requirements will be chosen, but the launch configuration must fit inside a 1.75m by 1.75m by 4m rectangular prism. While technically it could fit in a 1.75m by 4m by 4m volume, it is good to ensure a square or circular design for good mass distribution, although this could be updated in the future if not all components for the minecart can fit.

The mass budget breakdown for the second launch is summarized in Table 8.6 below.

Table 8.6: Second Launch Mass Breakdown

Launch #2 Mass	
Total Launch Mass (kg)	26700
Fuel (kg)	4841
Fuel Safety Factor	1.4
Fuel with Safety Factor (kg)	6778
Total Launch Mass Dry (kg)	19922
Launch Items	
Mailman (kg)	2000
Number of Tanks	2
Water Tank (kg)	1000
Number of Minecarts	4
Minecarts (kg)	3980

8.5 Customer and Mission Level Requirements

With everything defined and outlined, the customer and mission level requirements were derived. These are shown with various rationales and trace-ups in Tables 8.7, 8.8 and 8.9 below.

Table 8.7: Customer Requirements

ID	Text	Rationale
KHEPRI-001	The mission must deliver at least 375,000 kg of water to cis-lunar space over 18 years.	Cost upperbound = $1.5B. 100% ROI = $3B. Assuming $8k/kg, we require 375,000kg, or 375 tonnes.
KHEPRI-002	Delivered material must be at least 99% (TBC) water by mass.	WAG, chat with Mark Barnet and Mike Lipsett

Table 8.8: Mission Level Requirements

ID	Text	Rationale	Trace Up
Physical Requirements			
KHEPRI-003	The first launch components must be able to be stowed in a 4m x 4m x 10m volume	80% of launch volume	-
KHEPRI-004	The second launch components must be able to be stowed in a 4m x 4m x 10m volume	80% of launch volume	-
KHEPRI-005	The total mass of the first launch components must not exceed 26,700kg.	Launch mass max of 26.7 kg, 2 allocated launches	-
KHEPRI-006	The total mass of the second launch components must not exceed 26,700kg.	Launch mass max of 26.7 kg, 2 allocated launches	-
KHEPRI-007	The first launch components must be attached to the payload fairing by one powered launch adapter.		-
KHEPRI-008	The second launch components must be attached to the payload fairing by one powered launch adapter.		-
KHEPRI-009	The mission components must be able to withstand TBM Hz of vibration at launch.		-
KHEPRI-010	The mission components must be kept between TBD K and TBD K over the course of the mission.		-
KHEPRI-011	The mission components must be able to withstand at least TBD Grays of radiation.		-
Performance Requirements			-
KHEPRI-012	The mission components must be capable of nominally operating for at least 15.71 years	Worst case = 2.31+6+5.78 =14.09 yrs vs. 15.71, SF = 1.11	KHEPRI-001
KHEPRI-013	The mission components must transit from Earth to Bennu within 1.13 years	Margin of 1.0 as this is worst case scenario, Raw time is 1.13 years	KHEPRI-001
KHEPRI-014	The mission components must extract water from asteroid material at a rate of at least 5.07 L/hour	Worst case for 171388 in 5.78 yrs (worst case trip back), with SF of 1.5	KHEPRI-001
KHEPRI-015	The mission components must collect at least 8,600,000 kg of regolith	Derivation sheet, 7778066 kg max for only 2m boulders collected, SF of 1.1	KHEPRI-001

Table 8.9: Mission Level Requirements

ID	Text	Rationale	Trace Up
Environmental Requirements			
KHEPRI-016	The mission must not disturb Bennu's orbit by more than 3microns/s.	Bennu orbital delta-v uncertainty spec, could be measured by momentum impacts of pickers, Farnocchia2021 (average), Total momentum change of Bennu must be less than 2.2*10^5 kgm/s, or roughly 55 m/s of collisions for a 4000 kg picker	-
KHEPRI-017	The mission must not generate any single piece of debris larger than 1 tonne further than 38.9km from Bennu.	Size of debris matters, if small doesnt matter (less than a tonne item - will burn up in Earth's atmosphere), 38.9 km is Bennu's hill sphere	-
KHEPRI-018	The mission must not generate any single piece of debris larger than 30cm within 2 km of Bennu.	Polluting environment, spacecraft requirement for impact tolerance (30cm size particles were the maximum for O-REx)	-
KHEPRI-019	The mission components must be capable of withstanding an environment of TBD becquerels.		-

9 Boulder Target Selection

9.1 Background

The distribution of water across Bennu's surface is not homogeneous, with concentrations ranging from 5.72 wt% to 6.79wt%, a 17% variation relative to the mean 9.1 [1]. Error in the measurement of hydrogen content may increase the relative variation to approximately 60%. Such a large variation means that targeting high-grade boulders can significantly reduce the number of processing cycles needed to meet production targets, in turn reducing mission time, and risk.

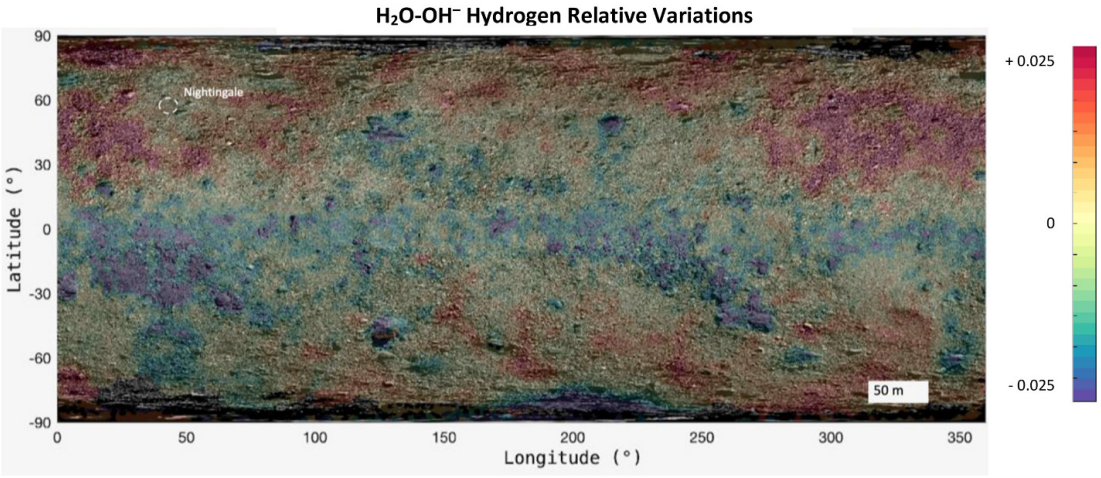

Figure 9.1: Global hydrogen abundance map of Bennu from Praet et al., 2021. [1]

High-grading is an established technique in the terrestrial mining industry whereby the highest grade portion of a deposit is mined first, providing operating capital to profitably develop lower-grade areas later in the mine's life cycle [78]. A similar approach to mining Bennu is logical. Although future missions may be able to profitably extract water from even the lowest-grade boulders on Bennu, maximizing profit requires maximizing the throughput rate, and therefore early missions should focus on mining boulders with the highest concentrations of water. Additionally, since servicing the mining and processing equipment at Bennu will be difficult or impossible, reducing the number of cycles is critical for reducing wear on systems and by extension the risk of mechanical failures.

Previous works have identified a relationship between increased hydrogen content and higher albedo and between albedo, thermal inertia and lithology [1] [9] [8] [10] [13]. These relationships imply a potential link between lithology and hydrogen enrichment. As described in the Boulder Properties section of this report, smooth, high albedo boulders are interpreted as being more hydrothermally altered than the dark regolith breccia boulders which could explain the apparent relationship.

The team investigated the relationship between boulder types, thermal inertia, albedo, and hydrogen abundance to evaluate if specific boulder types can be high-graded and if specific areas of Bennu should be preferentially targeted. Using texture-based image classification and manual boulder counts, it is proposed that bright, brittle boulders contain significantly more water than the dark regolith breccia boulders and should be targeted first. Bright boulders are clustered in patches and concentrated in the Northern Hemisphere.

9.2 Previous Work

A global map of the hydrogen distribution on Bennu was produced by Praet et al. using the depth of the OH- absorption band in OVIRS spectroscopic data [1]. The hydrogen abundance varies from 0.64 to 0.76 wt% with an accuracy of plus or minus 0.15 wt%. This map highlights several regions of elevated hydrogen abundance, especially in the Northern Hemisphere. The concentration generally increases towards the poles, which may be a result of greater insolation and longer periods of space weathering near the equator. The areas with the highest concentration of hydrogen are associated with the brightest parts of Bennu's surface, while the lowest concentrations are associated with the darkest areas including several areas that are associated with individual dark boulders. The paper concludes that a combination of initial composition and space weathering are possible causes of the variation in initial hydrogen content.

The types of boulders on Bennu are described by Jawin et al. and are discussed in detail in the boulder properties section of this report [8]. There are at least four types of boulders identified on Bennu. Type A and B boulders are dark, clastic rocks that have been interpreted as a regolith breccia. They have a normal albedo of 3.5-4.9% and are characterized by rough surfaces, with tybe B being somewhat smoother than type A. Type C and D boulders are considerably brighter with a normal albedo of 4.9-7.4% and have no visible clasts. They also contain considerably more anastomosing fractures, which implies a more brittle composition, which is supported by thermal inertia data [10]. In the case of type D boulders, carbonate veins up to metres in length are present. Kaplan et al. concluded that a hydrothermal system on the order of hundreds of kilometers would be required to form the veins, implying that these boulders have undergone extensive aqueous alteration [5].

9.3 Methodology

To investigate the relationship between lithology and hydrogen content, the team developed an automatic texture-based classifier that can reliably separate type C and D boulders from dark boulders and regolith. To classify boulder types, the 60 degree north to 60 degree south global albedo mosaic produced by Golish et al [79] was used as an input. Two boulder classes were defined: "High Albedo", consisting of type C and D boulders and "Low Albedo" consisting of type A and B boulders. A class was also defined for fine-grained material with clasts smaller than 0.5m regardless of composition. The albedo histograms for each of these classes are provided in Figures 9.2 and 9.3.

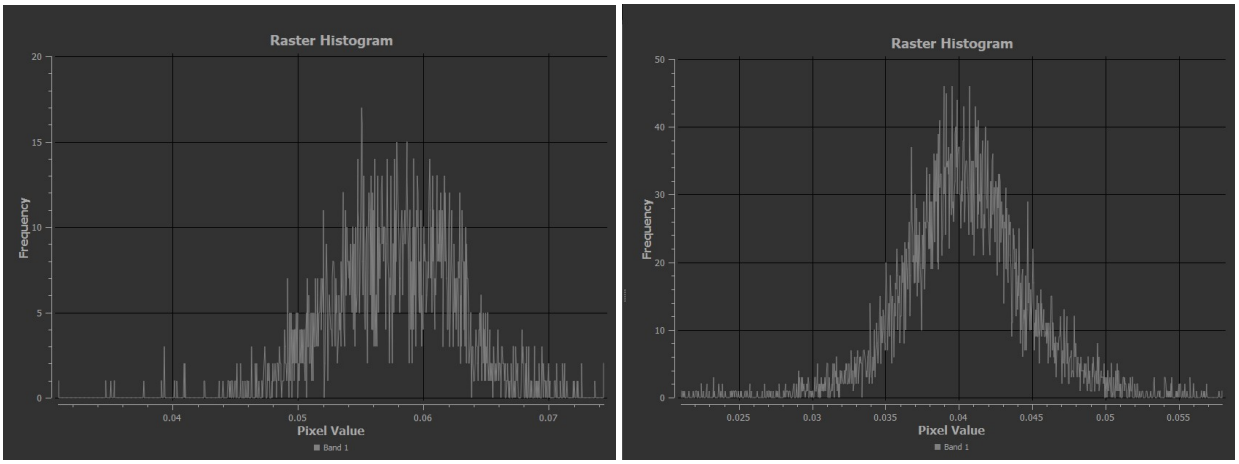

Figure 9.2: High Albedo Histogram (left) and Low Albedo Histogram (right)

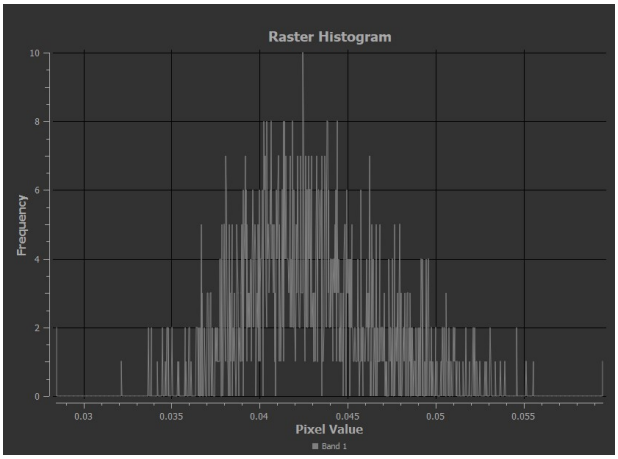

Figure 9.3: Regolith (Fine-Grain) Histogram

Direct classification of the albedo map was tested using Support Vector Machine and K-Nearest Neighbour supervised classifiers and K-means and Isodata unsupervised classifiers. In each case, little to no discrimination between boulder classes was achieved. These poor results may be due to similarities in albedo between the high-albedo boulder individual clasts in regolith breccia.

To overcome the limitations of direct albedo based classification, the team used a textural analysis approach called Structural Feature Set analysis (SFS). SFS was first developed by Huang et al. [80] for the classification of urban features with significant within-class spectral variation in high spatial resolution multispectral imagery. SFS operates by extending a series of lines outwards in many directions from a given pixel and computing histogram statistics for each line. The lines terminate after either a specified number of pixels (spatial threshold) or a specified change in pixel value (spectral threshold). The statistics computed are Length (the maximum histogram value along the line), Width (the minimum histogram value along the line), Pixel Shape Index (PSI), w-mean, SFS ratio (which describes the shape formed by the lines), and standard deviation.

An advantage of SFS analysis for the application of boulder mapping is that there is generally a significant difference between pixel values at the edge of a boulder, especially in the high-albedo boulder class. Therefore, the lines along which statistics are calculated typically terminate at the margins of boulders, providing an accurate statistical representation of the boulder itself rather than a combination of the boulder and adjacent surface as is obtained from traditional shifting-window based texture analysis. The end result is that the classified image captures individual boulders much more accurately than other methods.

Because the dark boulders are a regolith breccia, they incorporate clasts of the bright boulder material, and therefore the maximum albedo for both boulder classes is similar. Similarly, the w-mean is not always representative of the boulder's true composition, since large high-albedo clasts can cause in a similar value some boulders of both classes. For this reason, the SFS length and w-mean are excluded from the image classification.

SFS analysis was performed on a 1-255 linear stretch of the original normal albedo map and extracted each statistical map into a separate raster [79]. A multiband raster was created from the 1-255 albedo map, SFS width, PSI, SFS ratio, and standard deviation. To classify the resultant image, a per-pixel Support Vector

Machine (SVM) classifier was used. SVM classifiers have been shown to be the most effective standard classifier for SFS datasets [80]. Because dark fractures within rocks tend to be misclassified, a smoothing algorithm was applied to the resultant image and it was reclassified using the same training regions, which helped improve accuracy in large boulders. The complete workflow is shown in Figure 9.4. The results from the classifier clearly highlight global variations in the size and density of high-albedo boulders, as shown in Figure 9.5.

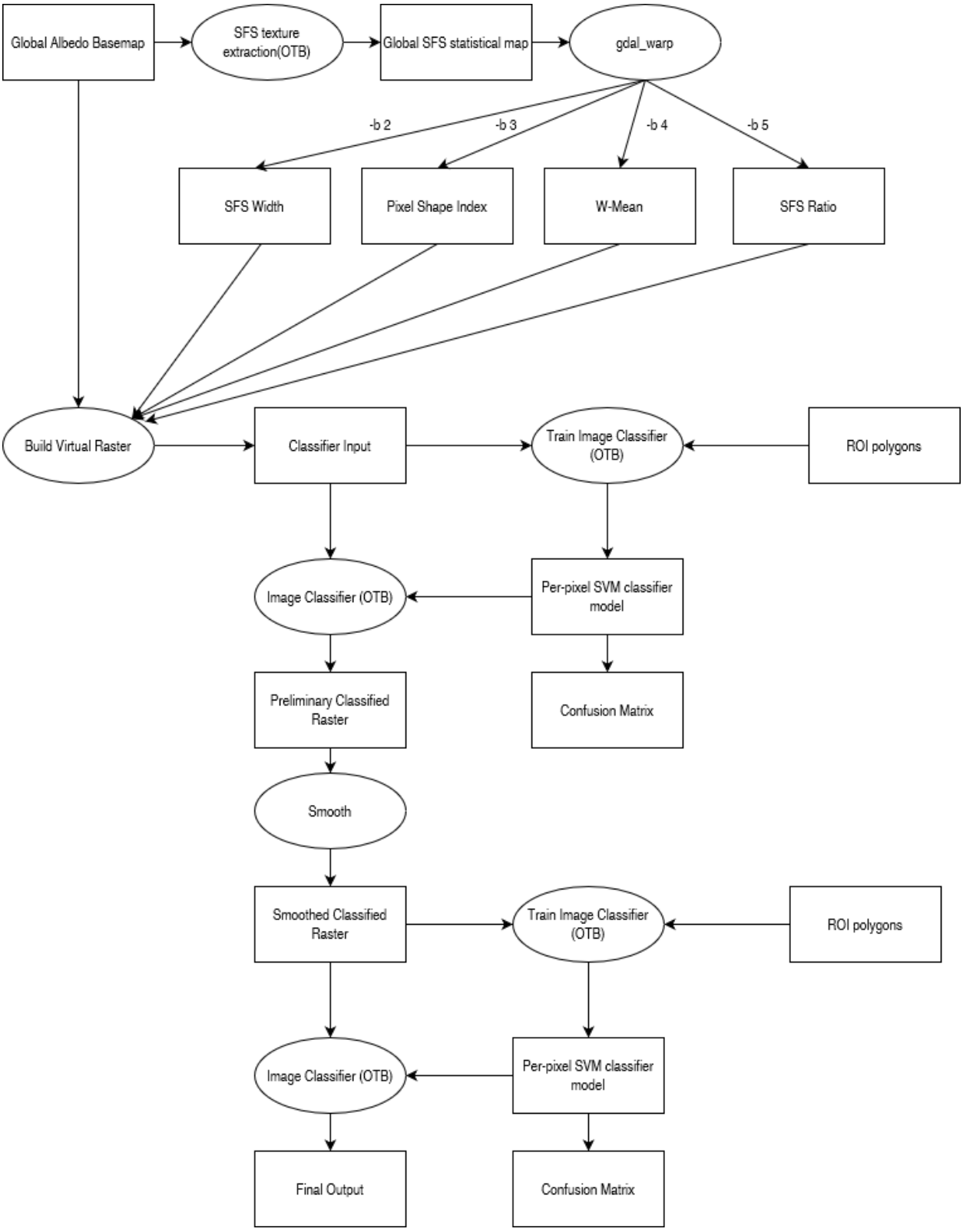

Figure 9.4: Classifier Workflow Diagram

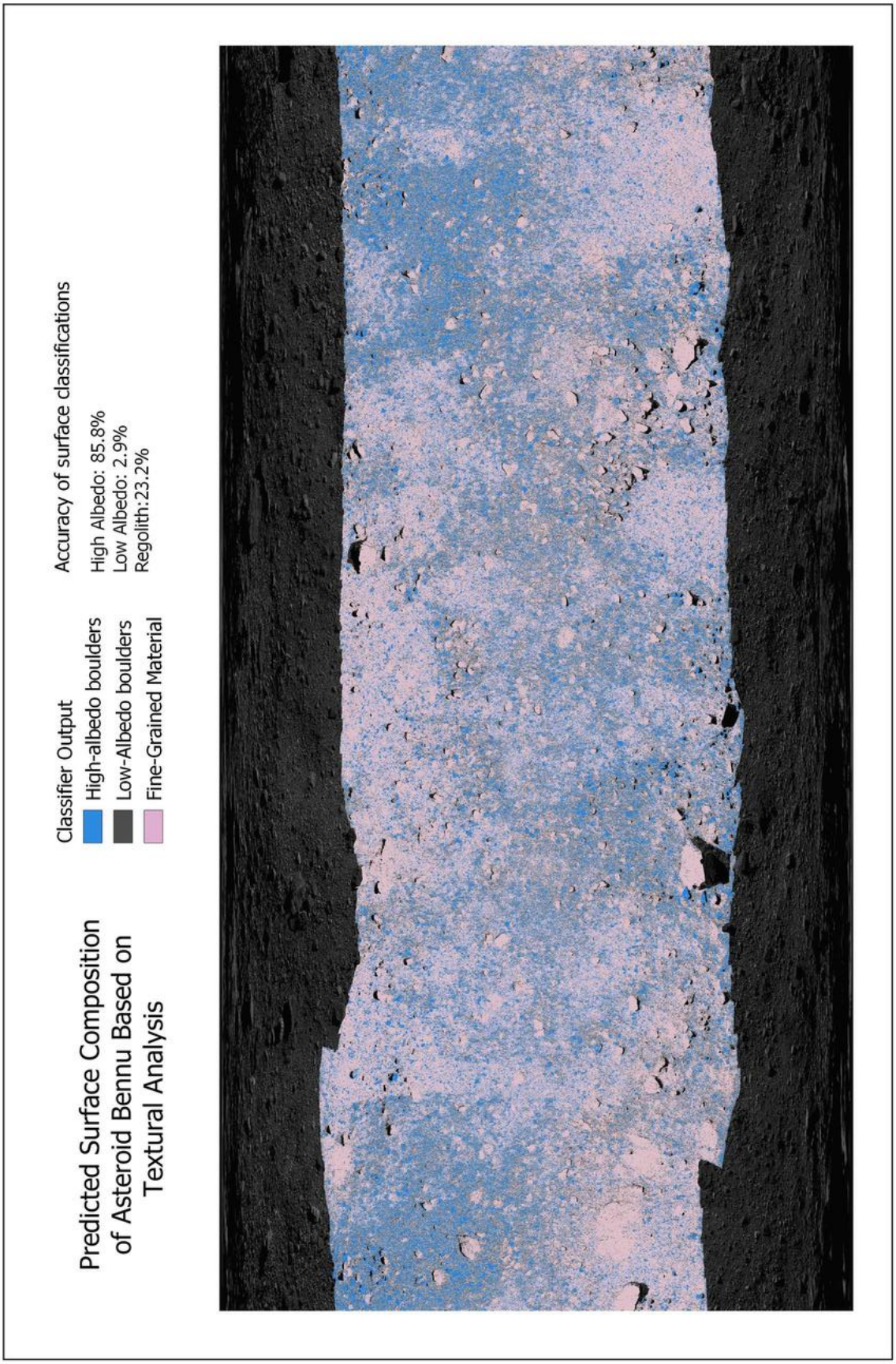

Figure 9.5: Classifier Map of High vs. Low Albedo Boulders

9.4 Results

The results show that there is a strong correlation between high densities of high-albedo boulders and high hydrogen concentrations, as shown in Figure 9.6. This relationship suggests that high albedo boulders contain significantly more hydrogen than the low-albedo boulders. Previous works have identified evidence of significant hydrothermal alteration in high-albedo boulders, so the higher hydrogen content may suggest higher phyllosilicate content as a result of this alteration. There is no apparent correlation between hydrogen content or the number of high-albedo boulders with the geologic units identified by Jawin et al. [4]. Both the rough and smooth units contain anomalously high and low hydrogen concentrations, which suggests that exposure time and space weathering is not a controlling factor for observed variations in water concentration.

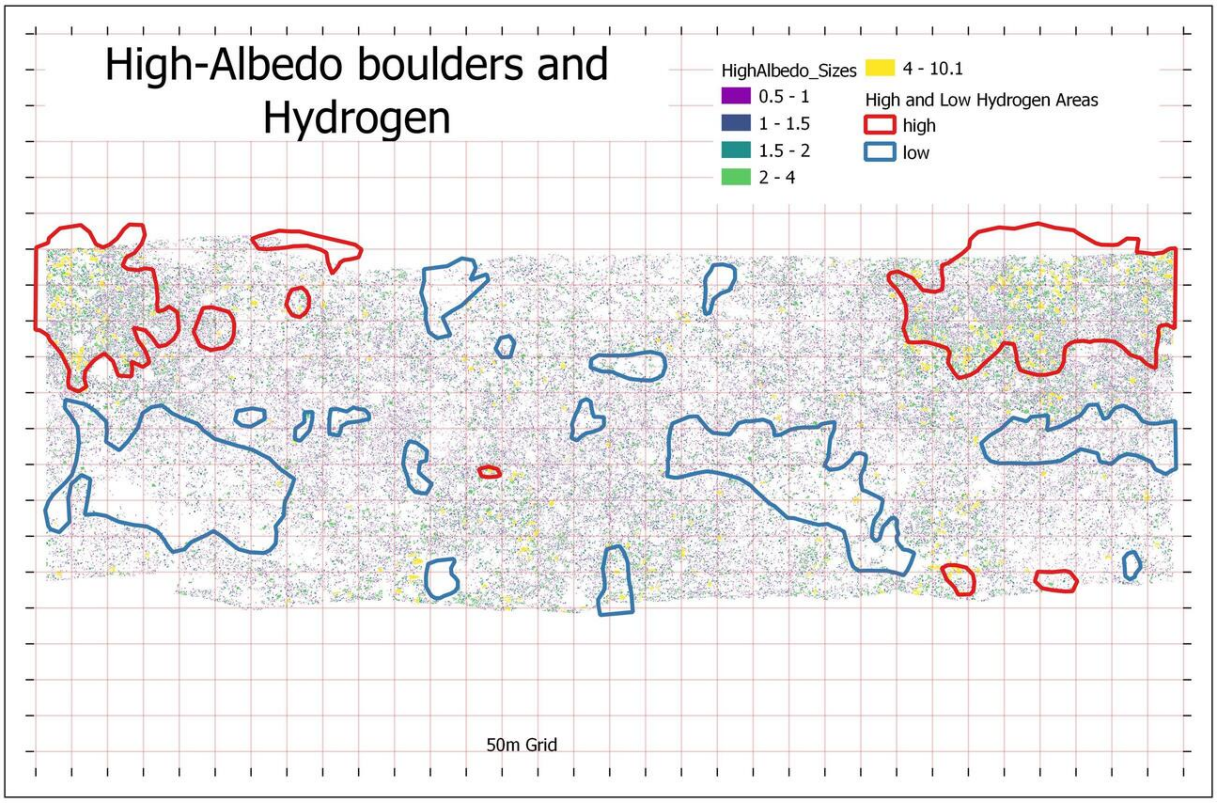

Figure 9.6: Correlation Map between High-Albdeo Boulders and Hydrogren Content

Based on the correlation between high-albedo boulders to hydrogen content, it seems logical that a water mining mission should target high-albedo boulders. The classifier predicts that there are approximately 61,700 high-albedo boulders in the 1-2m diameter size fraction comprising approximately 74% of the total population, as seen in Figure 9.6. However, this is likely an overestimate due to fractued large boulders being misclassified as several smaller boulders. Even if this value is overestimated by a factor of 10, which is unlikely, there would still be a sufficient number of boulders in the 1-2m size fraction to enable a profitable mining mission. Additionally, larger boulders are more reliably identified by the classifier, with approximately 13,400 2-3m boulders (16%), 4,600 3-4m boulders (5.5%), and 3,900 boulders larger than 4m (4.5%), as shown in Figure 9.7 below. A tiny fraction of these size ranges can produce sufficient volumes of water for the proposed mission.

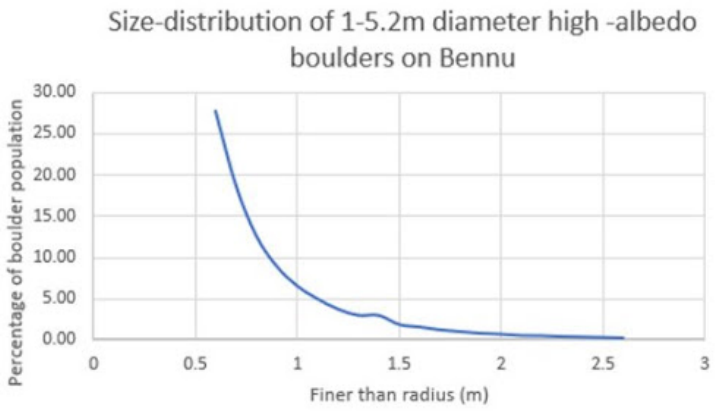

Figure 9.7: Plot of Bennu's Grain Size Distribution

9.5 Accuracy Assessment

Accuracy was assessed on a per-pixel basis using a confusion matrix generated with a unique set of validation data not used for training the classifier. This confusion matrix is shown below in Figure 9.8. Discrimination of regolith and low-albedo boulders is extremely poor due to the similarities in their textures. Since the low-albedo boulders are formed from cemented regolith, there is little to no difference in the surface texture between them and regolith. Discrimination of high-albedo boulders is significantly better, with an accuracy of 85.8%.

Classifier Interpretation

True Class	Shadow	High Albedo Boulders	Low Albedo Boulders	Regolith
Shadow	46368	0	0	0
High Albedo Boulders	26	26584	2951	303
Low Albedo Boulders	651	637	3534	111614
Regolith	62	507	449	34074

- High Albedo: 85.8% accurate
- Low Albedo: 2.9% accurate
- Regolith:23.2% accurate

Figure 9.8: Classifier Confusion Matrix

Per-boulder accuracy can likely be improved by integrating data from the OSIRIS-REx Laser Altimeter

(OLA) to delineate boulder boundaries. The number of small 1-2m boulders identified by the textural analysis method is likely an overestimation due to the identification of small parts of larger boulders as individual boulders.

10 Concept of Operations

10.1 Mission Overview

As described in Section 8.2, the mission takes place over 18 years. This 18 year time frame is further broken down in this section, first with the Mission Diagram in Figure 10.1 below, and later in Section 10.5.

10.2 Operational Environment

There are many parameters and characteristics about Bennu's environment to note. These are listed below:

- **Temperature on Bennu**: The temperature[1] on Bennu is highly varying, ranging between -73 $^{\circ}$C and 116 $^{\circ}$C.
- **Temperature in Space**: While in space, the spacecraft will be subjected to the lowest temperature it will face during its mission. The temperature within the solar system[29] is approximately 2.7 K.
- **Radiation**: Energetic particles can reach electronics of the spacecrafts and cause unexpected failures.
- **Debris Hazards**: Nominal operations may cause material on the surface of Bennu to rise and damage to the components of the proposed system. The escape velocity of Bennu is estimated to be 0.2 m/s, which is very low. Consequently, any small initial velocity imparted on the surface of Bennu will result in the displaced asteroid material covering significant distances with an unpredictable path, which creates a debris hazard. Additionally, as the heating process continues to extract water, the wasteful byproducts (mostly pieces of regolith) will inevitably begin to accumulate and pose a further debris hazard if not contained or controlled.
- **Loss of Signal (LOS)**: During nominal operations, unforeseen periods of LOS could occur due to attenuation of signals caused by solar radiation or other environmental factors. These could result in a temporary loss of internal communications between components of the system and to and from Earth.
- **Low Gravity**: Bennu has a low gravitational acceleration[1] of $9.807 \times 10^{-5} m/s^2$, which makes it difficult to remain on the surface without drifting into space.
- **Landing Sites:** When delivering components of the proposed system onto the surface of Bennu it is important to choose an appropriate landing site, as landing on boulders and other difficult terrain could cause physical damage.

10.3 Modes of Operation

The modes of operation for the proposed system and its components are defined below.

- **Idle:** In this mode, the system is idle and conserving power. Only critical systems are running, and the system awaits further instructions from external inputs. Systems will enter this mode during launch and transit to orbit, when refuelling or recharging, or at other instances when they are not performing operations for long periods of time.

[29] https://en.wikipedia.org/wiki/Outer_space

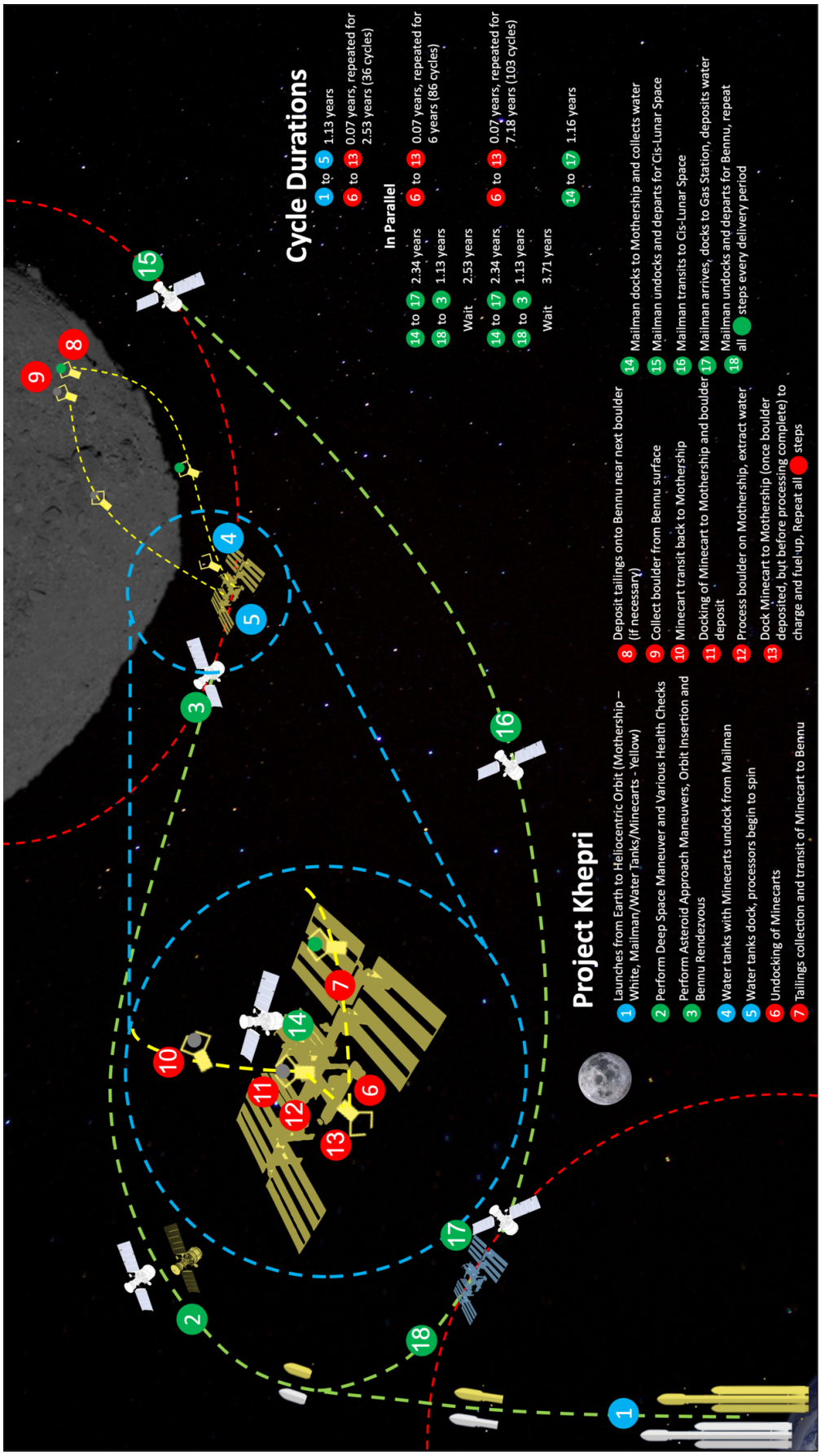

Figure 10.1: Mission Diagram

- **Initialization:** This mode will be utilized to set up the components of the system as they transition from Idle mode to Nominal Operation mode. Systems that were shut off in Idle mode are restarted, and system health checks are conducted to ensure all components are working properly before beginning nominal operations.
- **Nominal Operation:** All components of the system are functioning as expected. This is the normal mode of operation for systems performing boulder collection, processing, or water delivery.
- **Maintenance:** The system will enter Maintenance mode when it is undergoing scheduled maintenance operations. A system health check will be conducted once the maintenance is complete to ensure that all components are working as expected, and maintenance logs will be transmitted to Earth.
- **Emergency:** The system will enter Emergency mode in case of system failure, any detected physical damage, or low fuel. This mode can be activated at any point during the mission, and will cease nominal operation until the issue has been addressed.
- **Standby:** Standby mode is used when the system is idle for short periods of time. This may be used as required between other modes, such as during gaps in nominal operation while the system is awaiting instructions.

10.4 User Classes and Other Involved Personnel

The user classes for the proposed system and its components are defined below.

- **Mission Control Team:** The mission control team will be responsible for the planning and execution of the system's flight operations. They will communicate with components of the system and will monitor telemetry and other mission-critical information. The team must be familiar with flight planning for trips between the Mothership and Bennu, docking interfaces and operations, and the system's nominal and emergency operations.
- **Water Extraction Team:** The water extraction team is responsible for helping the system achieve it's primary goal of mining Bennu for water. They will monitor the system's nominal operations on Bennu and will work with the mission control team to identify and enact any required changes to the extraction mechanisms to optimize the water yield. The team must be familiar with the capabilities, interfaces, and operating environments of the proposed system, as well as with the mission plans and components.
- **Maintenance Team:** The maintenance team is responsible for the maintenance of the proposed system such that it may satisfy mission requirements. They must maintain safe operations during the mission, and therefore must be familiar with mission procedures for servicing and repairs.
- **Launch Team:** The launch team is responsible for delivering the system to its orbit around Bennu. They must be familiar with the physical constraints of the system and the launch vehicle.
- **Science Teams:** During this mission, our understanding of Bennu may evolve, and various aspects of the mission may need to be adapted in light of new findings. Teams of scientists and domain experts may need to analyse data and imagery sent by the proposed system, and inform the mission control team of their findings and recommendations. These teams must be familiar with Bennu and its characteristics, as well as with the mission at a broader level.

10.5 Operational Scenarios

Overview of Operational Scenarios

Figure 10.2 outlines the mission operations at the highest level. The mission is split into four phases: Launch, Arrival, Water Extraction, and Water Delivery. Operations in each mission phase are described in Sections 10.5 through 10.5. The modes of operation and user classes referenced in descriptions of operational scenarios are as defined in Sections 10.3 and 10.4 respectively.

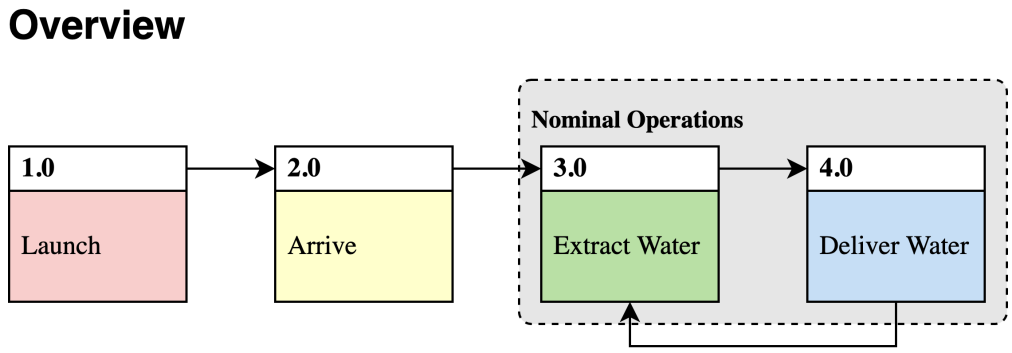

Figure 10.2: Mission-level FFBD.

Timeline

The overall mission timeline is shown in Figure 10.3.

Figure 10.3: Mission-level Gantt Chart.

Launch and Transit

This phase encompasses all activity from launch off of Earth's surface to arrival at Bennu. Components are in idle mode for the majority of this phase, and operations are limited to periodically powering up components to initialization mode to conduct system health checks before reverting them back to idle mode. Operations for periodic health checks are detailed in Figure 10.4.

Operating Environment

This phase has a difficult operational environment. The spacecraft must be capable of withstanding the severe vibrations and forces of launch, and once the payload has been jettisoned from the capsule, the spacecraft must be capable of withstanding the frigid temperatures of space and the radiation environment.

Sequence of Operations

Launch and transit operations are described in Figure 10.4.

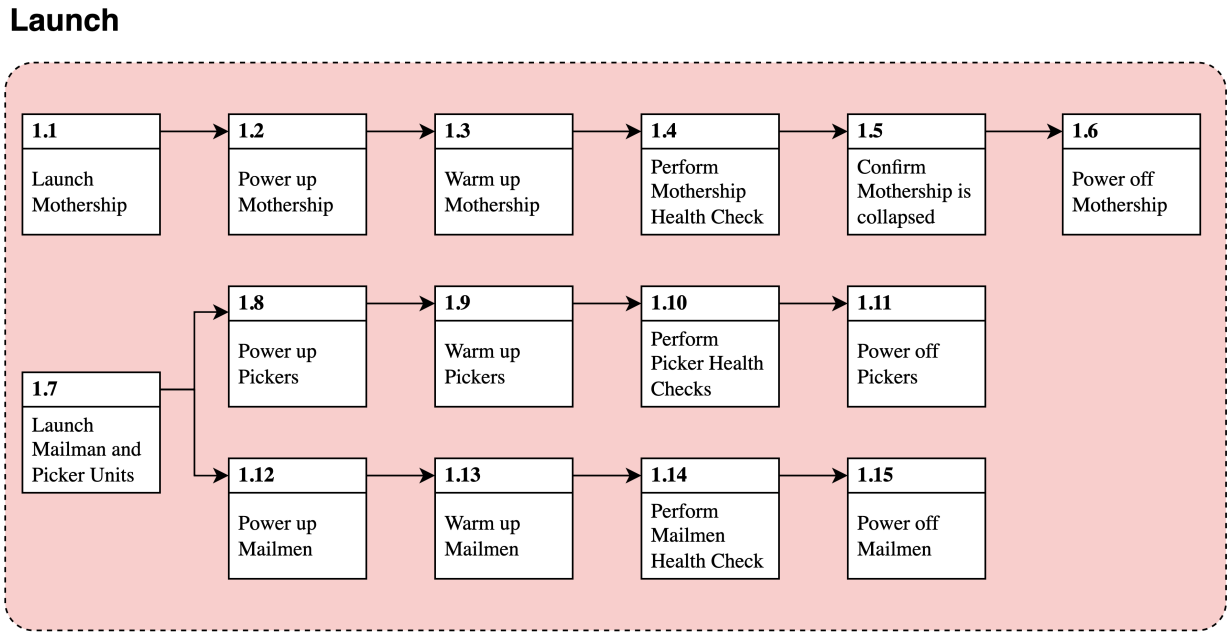

Figure 10.4: FFBD for launch and transit operations.

Timeline

The launch and transit timeline is shown in Figure 10.5.

Phase	Task	Month 0	Month 1	Month 2-7	Month 8	Month 9	Month 10	Month 11	Month 12	Month 13
Launch & Transit	Launch Mothership									
	Power up Mothership									
	Warm up Mothership									
	Perform Mothership health check									
	Confirm Mothership is collapsed									
	Power off Mothership									
	Complete Mothership Manuever									
	Launch Mailman and Pickers									
	Power up Pickers									
	Warm up Pickers									
	Perform Picker health checks									
	Power off Pickers									
	Power up Mailman									
	Warm up Mailman									
	Perform Mailman health check									
	Power off Mailman									
	Complete Mailman Manuever									
	Calibrate Mothership systems									
	Calibrate Mailmen systems									
	Calibrate Picker systems									

Figure 10.5: Gantt Chart for launch and transit operations.

Assumptions and Risks

It is assumed that the launch window has enough flexibility worked into the safety factors for the overall mission timeline. It is also assumed that after launch, both the mothership and mailman deploy their solar arrays to generate power to keep themselves and the other vehicles warm, and be able to complete the health checks.

Deployment

This phase encompasses all activity from arrival at Bennu's orbit to the start of the water collection cycle. During transport, the mission elements will remain Idle Mode. After arrival, they will enter initialization mode to prepare for nominal operations. Launch holddowns will be released. The Mothership will deploy into its operational configuration. Once the Mailman and Tanks arrive, the Mailman will pull the Tanks and facilitate their docking to the Mothership. The Pickers will undock from the Mothership and begin their descent to the surface. Arrival operations are outlined in Figure 10.6. The key users in this phase include the Mission Control Team and the Science Team. The Mission Control Team will monitor the Tugboats' flight to Bennu's surface and ensure successful undocking of each component. The Science Team will be prepared to process data collected during the arrival phase, and use it to inform future operations planning, if necessary.

Operating Environment

During launch and transit, all mission elements will be inside of launch vehicles. They will be held in place with launch holddowns. System elements may additionally have hold down release mechanisms. During this phase, elements will experience high gravitational and vibrational loads.

Sequence of Operations

Arrival and deployment operations are described in Figure 10.6.

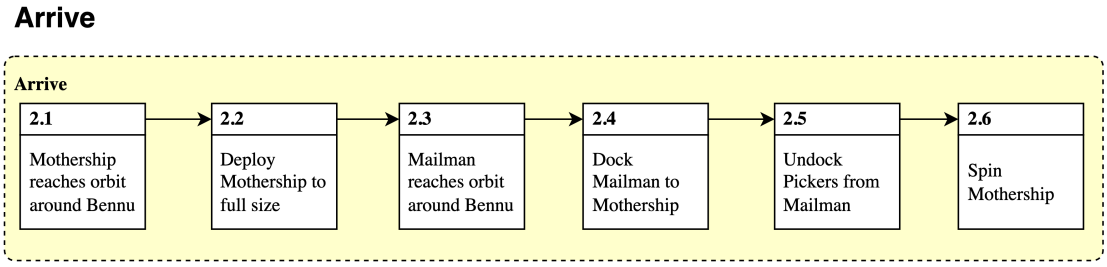

Figure 10.6: FFBD for arrival and deployment operations.

Timeline

The launch and transit timeline is shown in Figure 10.7.

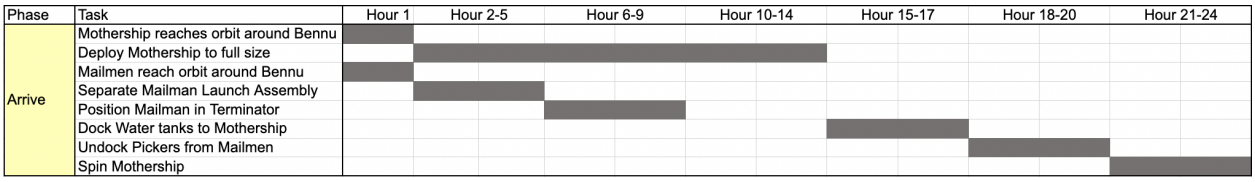

Figure 10.7: Gantt Chart for arrival and deployment operations.

Assumptions and Risks

These operations assumed to take place relatively quickly, and that the launches are close enough apart that all the vehicles reach Bennu at approximately the same time.

Boulder Collection

Each component will be operating in Nominal Mode in this phase. All user classes will be involved in this phase, excluding the Launch Team.

Operating Environment

The boulder collection occurs in Bennu's operating environment, where there are large temperature swings between Bennu's hot side, cold side and surrounding space. There is also the ionizing radiation environment to consider, and the lighting conditions. As the minecart will be interacting with the surface, the debris kicked up may modify the environment for periods of time until it all settles.

Sequence of Operations

Boulder collection operations are described in Figure 10.8.

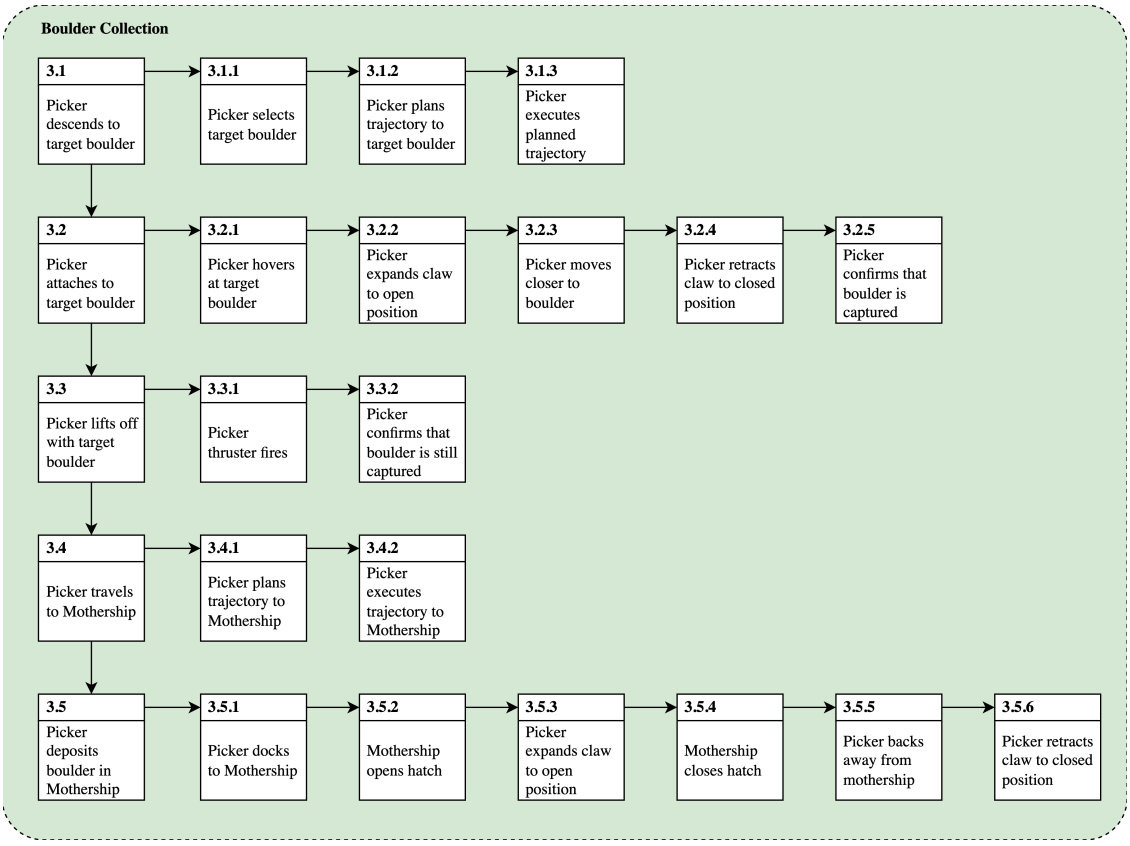

Figure 10.8: FFBD for boulder collection operations.

Timeline

The launch and transit timeline is shown in Figure 10.9.

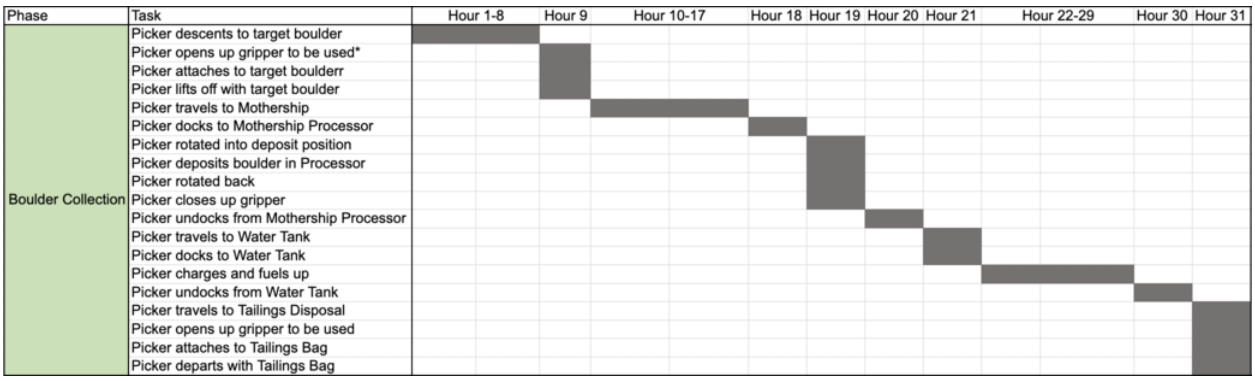

Figure 10.9: Gantt Chart for boulder collection operations.

Assumptions and Risks
The following assumptions and risks were identified:

- Boulders that are from meteorite impacts can be identified and avoided
- The minecart has a list of boulders and their locations for the spacecraft to go and pick them up
- Albedo is a meaningful proxy for boulder composition
- High-albedo boulders contain significantly more water than low-albedo boulders and regolith
- Boulder shape is close to a sphere
- Boulders are only slightly buried into the regolith (20% or less)
- Thrusters of the picker is far away from the surface so that they don't create a huge debris

Water Extraction

Each component will be operating in Nominal Mode in this phase. All user classes will be involved in this phase, excluding the Launch Team.

Operating Environment
The water extraction environment is the same as the boulder collection environment for the collection operations, but is in an orbital environment around Bennu for the extraction process. The mothership will be in a terminator orbit, always in the sun, and so the front side of the mothership will be very hot compared to the back. This will cause thermal stresses in the spacecraft that must be designed for. Similar points to ionizing radiation as the boulder collection environment must be considered.

Sequence of Operations
Water extraction operations are described in Figure 10.10.

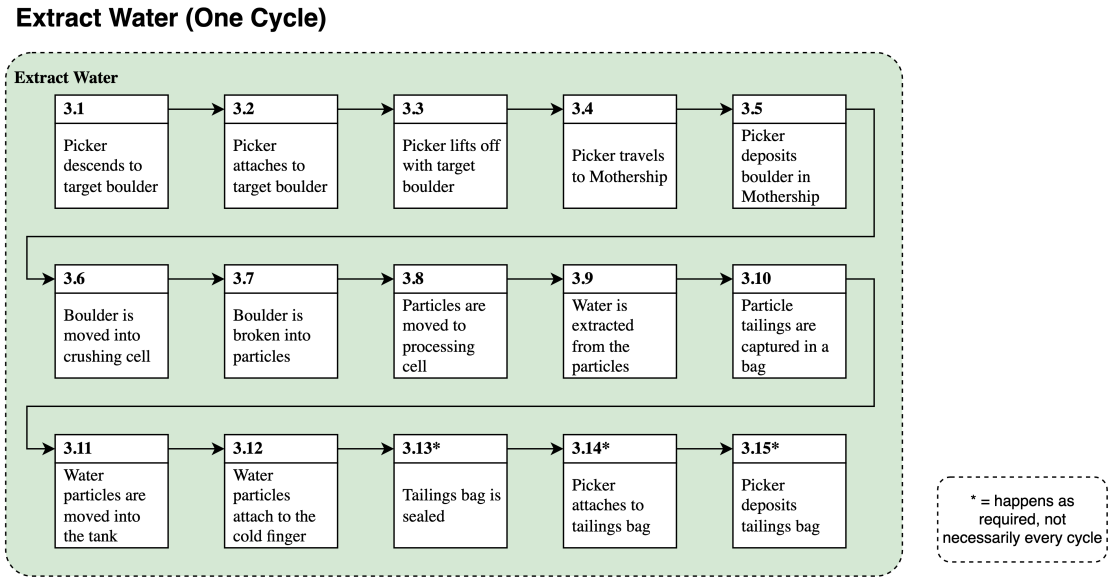

Figure 10.10: FFBD for water extraction operations.

Timeline

The launch and transit timeline is shown in Figure 10.11.

Phase	Task	Hour 1	Hour 2	Hour 3	Hour 4	Hours 5-10	Hours 11-571	Hour 572
Water Extraction	Picker deposits boulder in crushing cell							
	Boulder is moved through crushing cell							
	Particles move into filtering chamber							
	Particles are moved to processing cell							
	Water is extracted from the particles							
	Particle tailings are captured in a bag							
	Water particles are moved into the tank							
	Water particles attach to the cold finger							
	Tailings bag is sealed							

Figure 10.11: Gantt Chart for water extraction operations.

Assumptions and Risks

The following assumptions and risks were identified:

- The temp required to process is a min 900C
- There boulders are relatively crushed into smaller chunks to maintain 1-2kg/min processing rates
- Boulders have a 6.3% water content (on Average)
- Solar collectors have an efficiency of at least 30%
- Power to operate other equipment other than processor is delivered from the motherships Solar array
- The amount of tailings generated is assumed to be 94% of the boulder mass
- Including a factor of safety, the tailings bags shall be designed to accommodate 100% of the boulder mass i.e. for 2-4m diameter boulders
- The tailings will be at 900C upon exit from the processor unit

  - This influences the tailings disposal design: either need a cooling unit before transferring tailings to bag, or need to design the bag to accommodate this high temp

- The tailings are solid particulate matter
- The tailings are not charged particles

Water Delivery

Each component will be operating in Nominal Mode in this phase. All user classes will be involved in this phase, excluding the Launch Team.

Operating Environment
During this phase, water is transported from the Mothership's orbit around Bennu to cis-Lunar space. Water transfer operations occur in the Mothership's orbit, deep space, and cis-Lunar space. These three operating environments vary in temperature, ionizing radiation, and potentials for debris impacts, so the mailman must be designed accordingly.

Sequence of Operations
Water delivery operations are described in Figure 10.12.

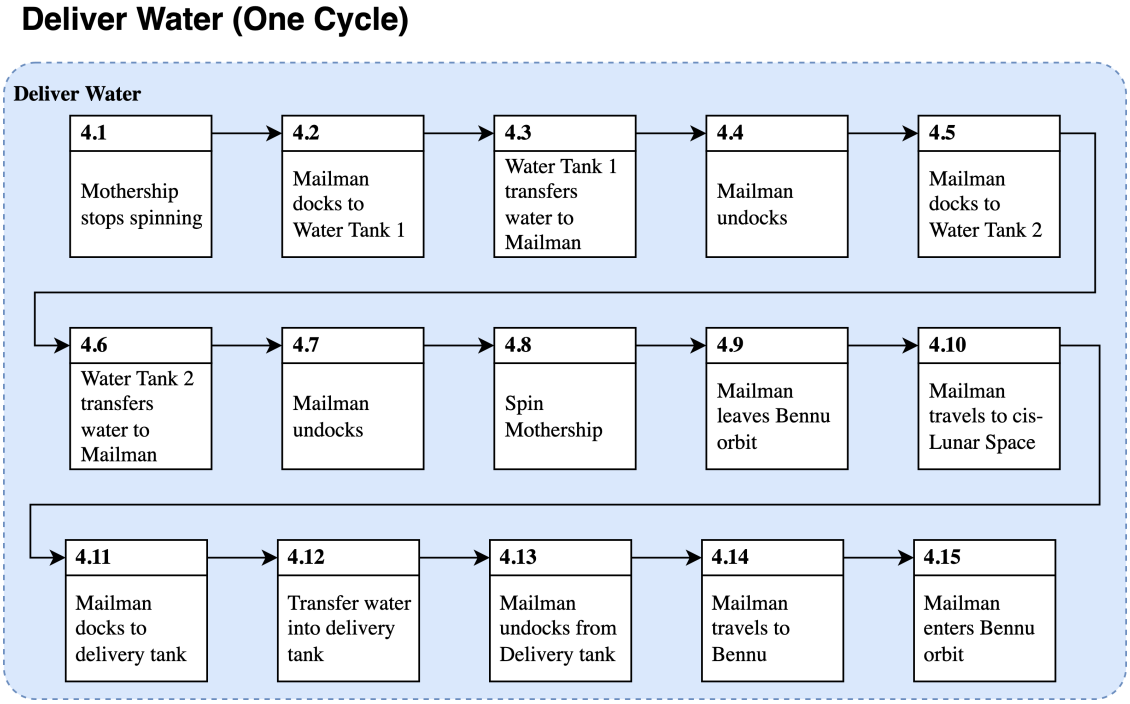

Figure 10.12: FFBD for water delivery operations.

Timeline
The launch and transit timeline is shown in Figure 10.13.

Phase	Task	Month 1	Month 2	Month 3	Month 4	Month 5	Months 6-33	Month 34	Months 35-47	Month 48
Water Deliver	Mothership stops spinning									
	Mailman docks to Water Tank 1									
	Water Tank 1 transfers water to Mailman									
	Mailman undocks									
	Mailman docks to Water Tank 2									
	Water Tank 2 transfers water to Mailman									
	Mailman undocks									
	Spin Mothership									
	Mailmain leaves Bennu orbit									
	Mailman travels to delivery location									
	Mailman docks to delivery tank									
	Transfer water into delivery tank									
	Mailman undocks from delivery tank									
	Mailman travels to Bennu									
	Mailman enters Bennu orbit									

Figure 10.13: Gantt Chart for water delivery operations.

Assumptions and Risks

It is assumed that the mailman water transfer operations take a long time to give margin to the operations, even though they may occur much faster. It is risky that there are only 2 water tanks and 1 mailman, as if one water tank fails, the mothership will be off balance, and if the mailman fails the water cannot be returned or may be lost. It is assumed that these systems will be designed with adequate robustness to prevent these failures.

Chapter 5: System Overview

10 System Overview

10.1 Mothership

As described in previous sections, the mothership is a truss-like structure which serves the main function of housing and performing the processing of boulders into tailings, and extracting the water from the regolith during this process. Below in Figures 10.1 and 10.2 are System Hierarchy and System Block Diagrams for the mothership, outlining the main subsystems of the mothership architecture. The functions of these subsystems are outlined in Figure 10.2.

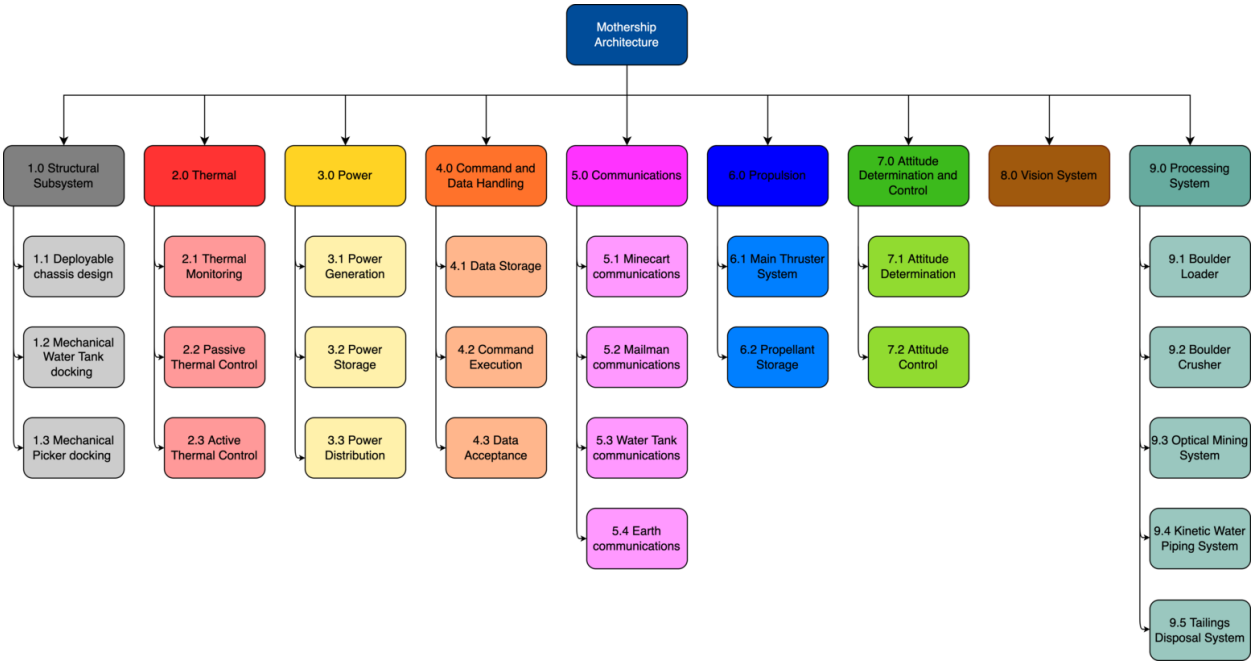

Figure 10.1: Mothership SHD

The mothership system has been designed in CAD, outlining the main structure, the processing systems, and aspects of the thermal, power and propulsion subsystems. This is shown in the stowed configuration in Figure 10.3 and in the fully deployed configuration in Figures 10.4 and 10.5 below.

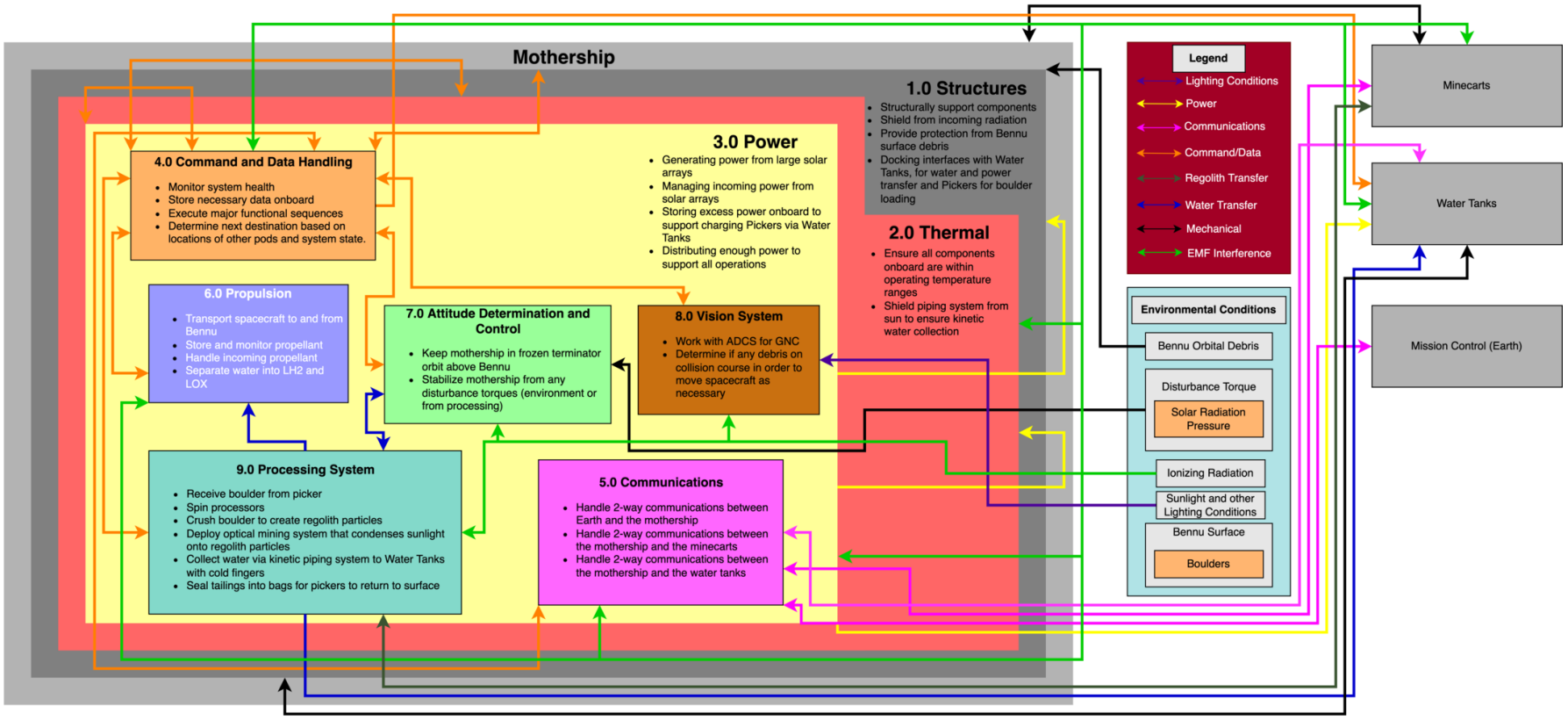

Figure 10.2: Mothership SBD

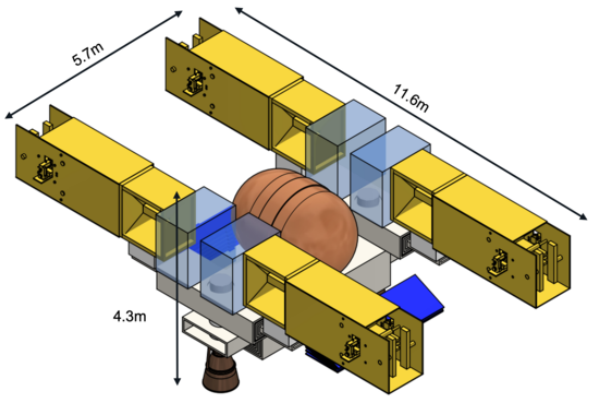

Figure 10.3: Mothership Stowed Configuration with Dimensions

Note that the stowed configuration is slightly larger than the payload fairing volume outlined in Figure 8.2; however, further optimization and iteration of the design would be able to fit the mothership inside the payload fairing. A visualization of the deployment of the mothership from the stowed to fully deployed configuration, as well as spinning of the processors, is shown in the following video: `https://www.youtube.com/watch?v=4Etz-5KBirk&ab_channel=GowthamNaidu`.

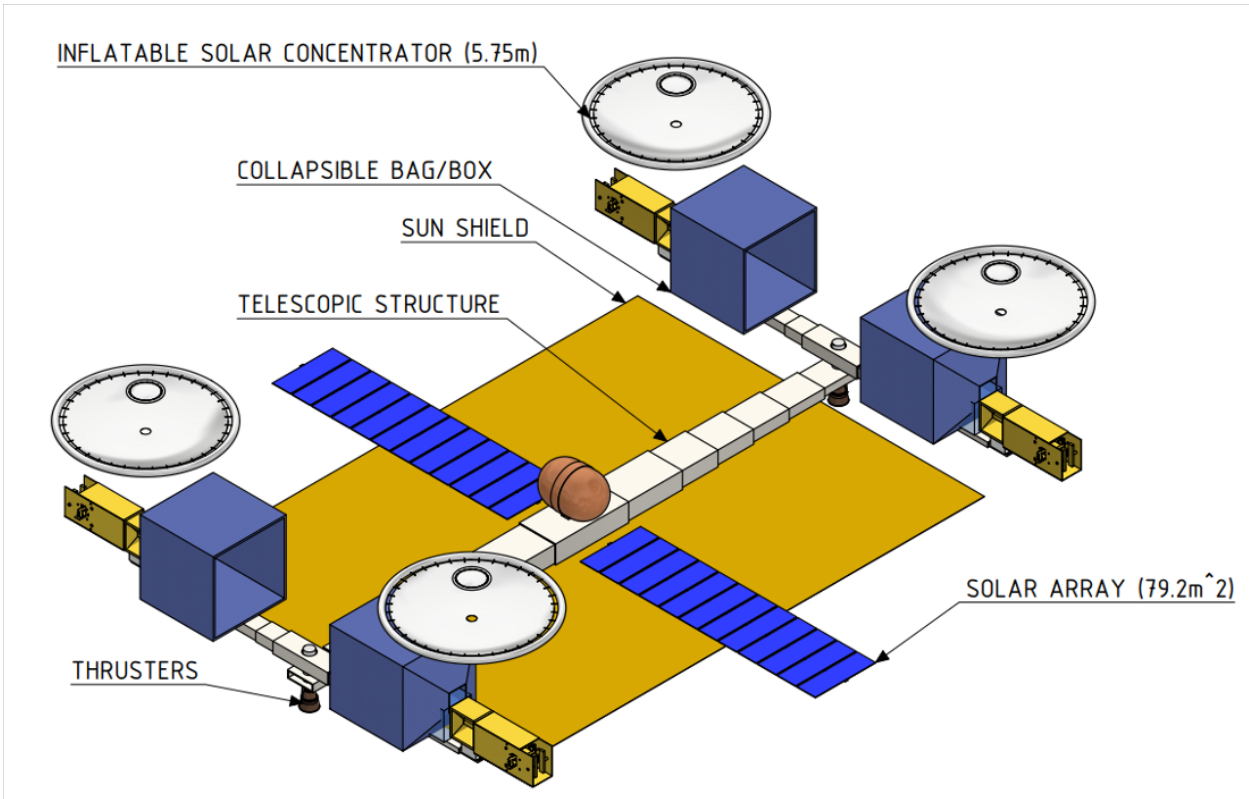

Figure 10.4: Mothership Deployed Configuration with Labeled Components

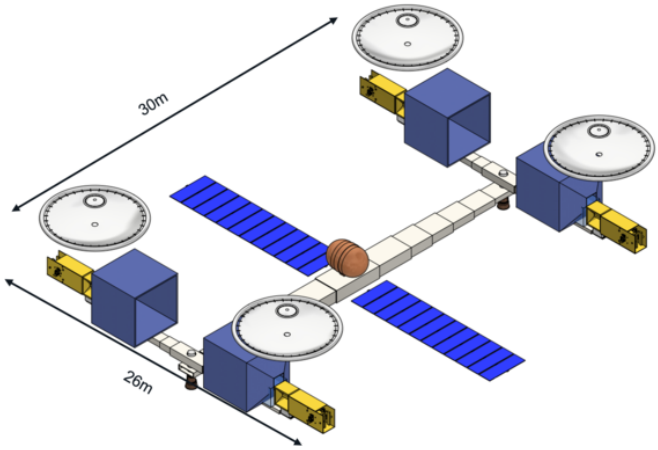

Figure 10.5: Mothership Deployed Configuration with Dimensions

The relevant preliminary mothership system requirements are shown below in Tables 10.1 and 10.2.

Table 10.1: Mothership Requirements

ID	Text	Rationale	Trace Up
Physical Requirements			
MOTHERSHIP-001	The Mothership must be able to be stowed in a 4m x 4m x 10m volume	80% of launch volume	KHEPRI-003
MOTHERSHIP-002	The total wet mass of the Mothership must not exceed 26,700kg.	Launch mass max of 26700 kg, 2 allocated launches	KHEPRI-005
MOTHERSHIP-003	The mothership must be attached to the payload fairing by one powered launch adapter.		KHEPRI-007
MOTHERSHIP-004	The mothership must be able to withstand TBM Hz of vibration at launch.		KHEPRI-009
MOTHERSHIP-005	The mothership must be kept between TBD K and TBD K over the course of the mission.		KHEPRI-010
MOTHERSHIP-006	The mothership must be able to withstand at least TBD Grays of radiation.		KHEPRI-011
Performance Requirements			
MOTHERSHIP-007	The Mothership must be capable of nominally operating for at least 16.84 years	Operate for all 18 years minus return trip of mailman	KHEPRI-012
MOTHERSHIP-008	The Mothership must transit from Earth to Bennu within 1.13 years	Margin of 1.0 as this is worst case scenario, Raw time is 1.13 years	KHEPRI-013
MOTHERSHIP-009	The Mothership must extract water from asteroid material at a rate of at least 5.07 L/hour	Worst case for 171388 in 5.78 yrs (worst case trip back), with SF of 1.5	KHEPRI-014
MOTHERSHIP-010	The Mothership must process at least 8,600,000 kg of regolith	Derivation sheet	KHEPRI-015
MOTHERSHIP-011	The Mothership must generate TBD W of power.		Derived
MOTHERSHIP-012	The Mothership's average power consumption must not exceed TBD W.		Derived
MOTHERSHIP-013	The Mothership's peak power consumption must not exceed TBD W.		Derived

Table 10.2: Mothership Requirements Continued

ID	Text	Rationale	Trace Up
Environmental Requirements			
MOTHERSHIP-014	The mothership must not allow particles greater than TBD cm to escape the processor.	Polluting environment, spacecraft requirement for impact tolerance (30cm size particles was max for O-REx)	KHEPRI-018
MOTHERSHIP-015	The mission components must be capable of withstanding an environment of TBD becquerels.		KHEPRI-019

10.2 Water Tank

As described in previous sections, the water tank is technically a subsystem of the mothership, which is responsible for collecting and storing the water from the processor. Below in Figures 10.6 and 10.7 are System Hierarchy and System Block Diagrams for the water tank, outlining the main subsystems of the water tank architecture. The functions of these subsystems are outlined in Figure 10.7.

Figure 10.6: Water Tank SHD

No detailed CAD drawings were created for the water tank at this stage, with only the dimensions, allocated overall dry mass, and collapsible container structure being detailed at this stage.

The relevant preliminary water tank system requirements are shown below in Table 10.3.

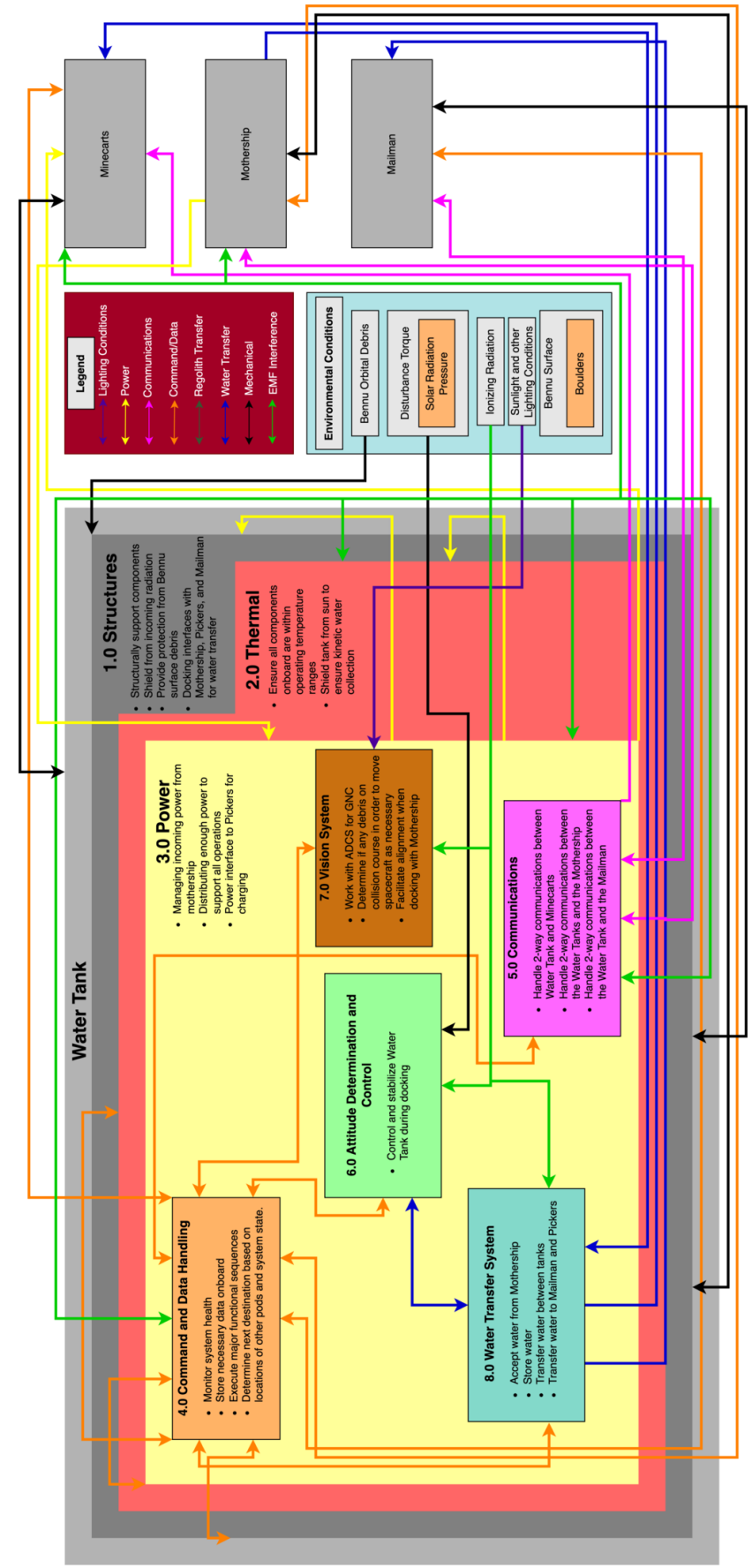

Figure 10.7: Water Tank SBD

Table 10.3: Water Tank Requirements

ID	Text	Rationale	Trace Up
Physical Requirements			
TANK-001	The water tank must be able to be stowed in a 0.5m x 4m x 4m volume	80% of launch volume	KHEPRI-004
TANK-002	The water tank must have a wet mass less than 1000kg.	Launch mass max of 26700 kg, 2 allocated launches	KHEPRI-006
TANK-003	The water tank spacecraft must be attached via a powered interface to the mailman for launch.		KHEPRI-008
TANK-004	The water tank must be able to withstand TBM Hz of vibration at launch.		KHEPRI-009
TANK-005	The water tank must be kept between TBD K and TBD K over the course of the mission.		KHEPRI-010
TANK-006	The water tank must be able to withstand at least TBD Grays of radiation.		KHEPRI-011
Performance Requirements			
TANK-007	The water tank must be capable of nominally operating for at least 15.71 years	Worst case = 2.31+6+5.78 =14.09 yrs vs. 15.71, SF = 1.11	KHEPRI-012
TANK-008	The water tank's average power consumption must not exceed TBD W.		Derived
TANK-009	The water tank's peak power consumption must not exceed TBD W.		Derived
Environmental Requirements			
TANK-010	The water tank must be capable of withstanding an environment of TBD becquerels.		KHEPRI-019

10.3 Minecart

As described in previous sections, the minecart is the spacecraft that collects boulders from the surface of Bennu to hand-off to the mothership for processing. This is accomplished via its robotic manipulator gripper, the main subsystem. Below in Figures 10.8 is the System Hierarchy Diagram for the minecart, outlining the main subsystems of the mothership architecture.

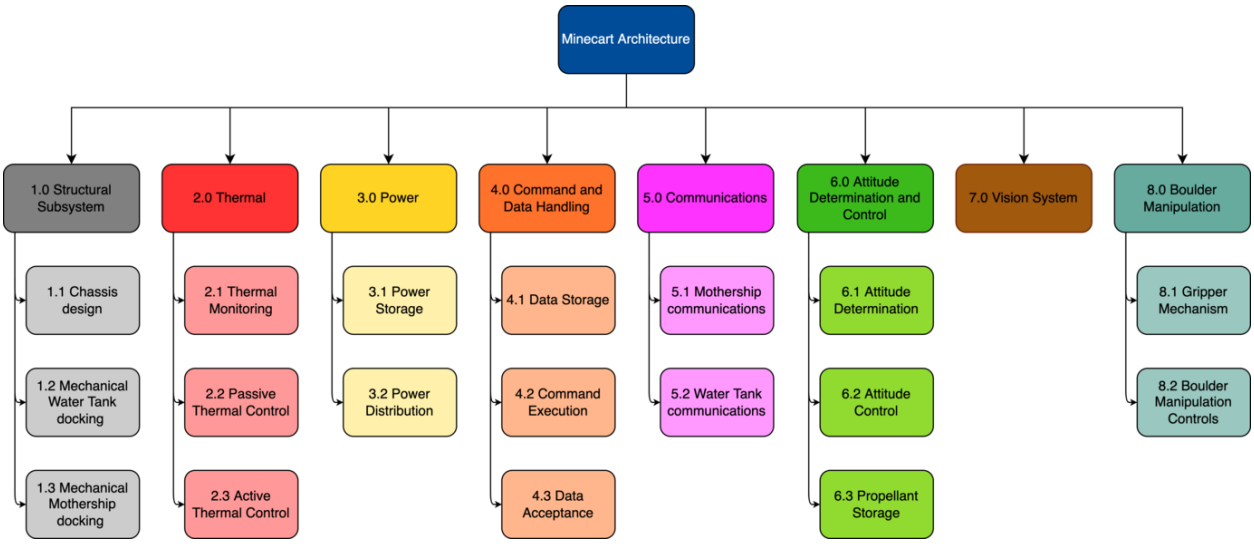

Figure 10.8: Minecart SHD

The minecart and gripper has been modelled in CAD, and is shown below in Figure 10.9. The System Block Diagram is shown in Figure 10.10 for the minecart. While the functions of these subsystems are not outlined in this figure, they are mostly self-explanatory given the previous subsystem descriptions for the Mothership and Water Tank. Note there will be significant overlap between the ADC and Propulsion subsystems, as there is no significant propulsion needed to get to Bennu due to the minecart hitching a ride via the mailman.

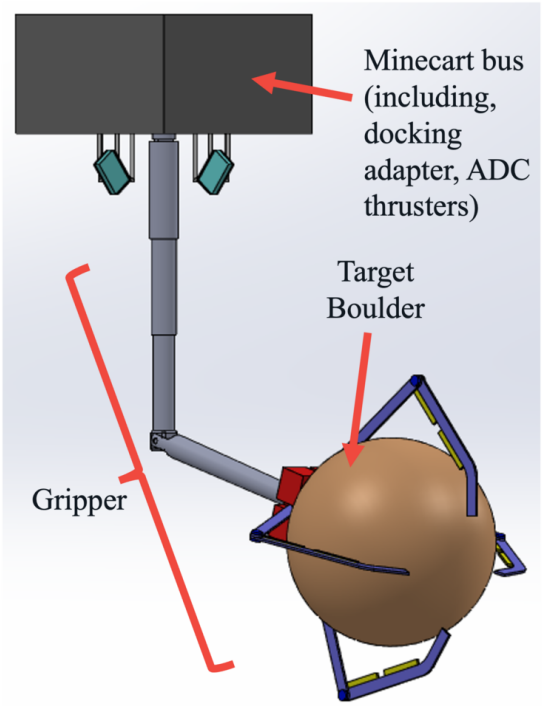

Figure 10.9: Minecart CAD

The relevant preliminary minecart system requirements are as shown below in Tables 10.4 and 10.5.

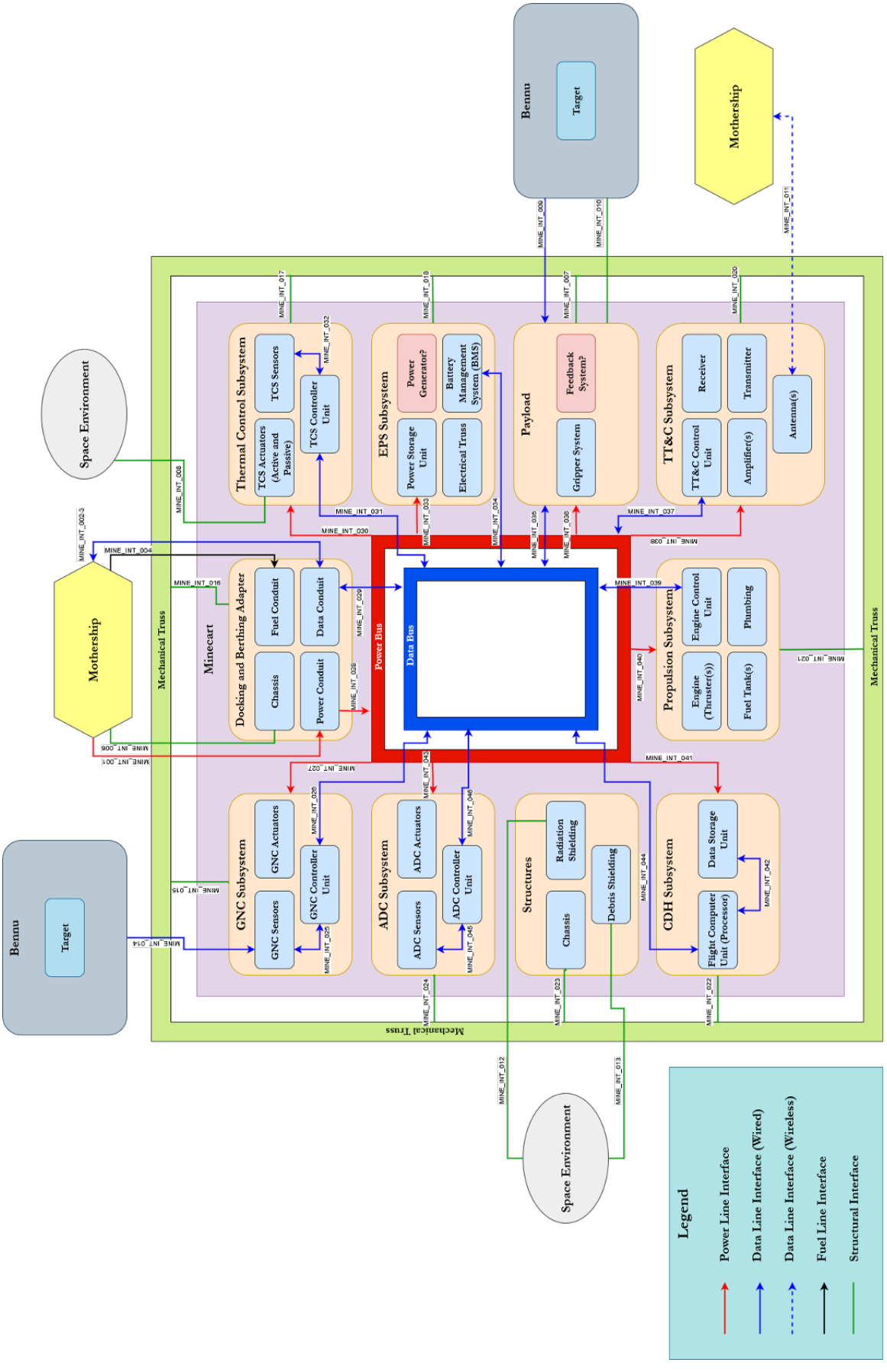

Figure 10.10: Minecart SBD

Table 10.4: Minecart Requirements

ID	Text	Rationale	Trace Up
Physical Requirements			
MINECART-001	There must be 4 minecart spacecraft		Derived
MINECART-002	The minecart must be able to be stowed in a 1.75m x 1.75m x 4m volume	Derived from launch configurations, includes 1.25 SF in volume	KHEPRI-004, MINECART-001
MINECART-003	The minecart spacecraft must have a wet mass less than 3980kg	Mass budget	KHEPRI-006, MINECART-001
MINECART-004	The minecart spacecraft must be attached via a powered interface to a water tank for launch.		KHEPRI-008
MINECART-005	The minecart must be able to withstand TBM Hz of vibration at launch.		KHEPRI-009
MINECART-006	The minecart must be kept between TBD K and TBD K over the course of the mission.		KHEPRI-010
MINECART-007	The minecart must be able to withstand at least TBD Grays of radiation.		KHEPRI-011
Performance Requirements			
MINECART-008	Each minecart must be capable of nominally operating for at least 15.71 years	Worst case = 2.31+6 +5.78=14.09 yrs vs. 15.71, SF = 1.11	KHEPRI-010
MINECART-009	One boulder collection cycle should take no longer than 10.91 days.	16.4 days with max 1403 boulders 2m boulders, 4 pickers, SF of 1.5	KHEPRI-014
MINECART-010	Each minecart must be capable of handling between 2m and 4m diameter boulders.	Max boulder size	Derived
MINECART-011	The minecarts must make be capable of completing minimum of 1403 trips with boulders at least 2m in diameter.	Need between 175-1403 for mission, could be more	KHEPRI-015, MINECART-010
MINECART-012	Each minecart must have at least TBD battery capacity for operations.		Derived
MINECART-013	Each minecart must have an average discharge rate of no more than TBD C.		Derived
MINECART-014	Each minecart must have a peak discharge rate of no more than TBD C.		Derived
MINECART-015	Each minecart must cease operations and return to the mothership if less than TBD% of capacity.		Derived
MINECART-016	Each minecart must be capable of charging TBD battery capacity at TBD C rate.		Derived
MINECART-017	Each minecart must be fully charged before undocking from the Mothership.		Derived
MINECART-018	The minecart must stay within an operation volume of TBD m x TBD m x TBD m.		Derived
MINECART-019	The minecart must have a nominal telemetry rate of TBD Hz.		Derived

Table 10.5: Minecart Requirements Continued

ID	Text	Rationale	Trace Up
Performance Requirements			
MINECART-020	The minecart must communicate with the mothership every TBD seconds.		Derived
MINECART-021	The minecart must communicate with the water tank every TBD seconds.		Derived
MINECART-022	The minecart must have a viewing angle range between TBD degrees and TBD degrees.		Derived
Environmental Requirements			
MINECART-023	The minecarts must not impart a cumulative momentum change greater than 2.2*10^5 kgm/s over the entire mission	Bennu orbital delta-v uncertainty spec, could be measured by momentum impacts of minecarts, roughly 55 m/s of collisions for a 4000 kg minecart	KHEPRI-016
MINECART-024	The minecarts must not impart a cumulative delta-v on Bennu of more than 55 m/s over the entire mission		MINECART-023
MINECART-025	The minecarts must not generate any single piece of debris larger than 1 tonne further then 38.9km from Bennu.	Size of debris matters, if small doesn't matter (less then a tonne item - will burn up in Earth's atmosphere), 38.9 km is Bennu's hill sphere	KHEPRI-017
MINECART-026	The minecarts must not generate any single piece of debris larger than 30cm within 2 km of Bennu.	Polluting environment, spacecraft requirement for impact tolerance (30cm size particles was the maximum for O-REx)	KHEPRI-018
MINECART-027	The mission components must be capable of withstanding an environment of TBD becquerels.		KHEPRI-019

10.4 Mailman

As described in previous sections, the mailman is essentially a large water tank with a more involved power system and propulsion system. The mailman is responsible for transporting itself, the minecarts, and the water tanks to Bennu, and transporting water back to cis-Lunar space. Below in Figures 10.11 and 10.12 are System Hierarchy and System Block Diagrams for the mailman, outlining the main subsystems of the mailman architecture. The functions of these subsystems are outlined in Figure 10.12. No detailed CAD drawings were created for the mailman at this stage, with only the dimensions, allocated overall dry mass, and collapsable container structure being detailed so far. The relevant preliminary mailman system requirements are shown below in Table 10.6.

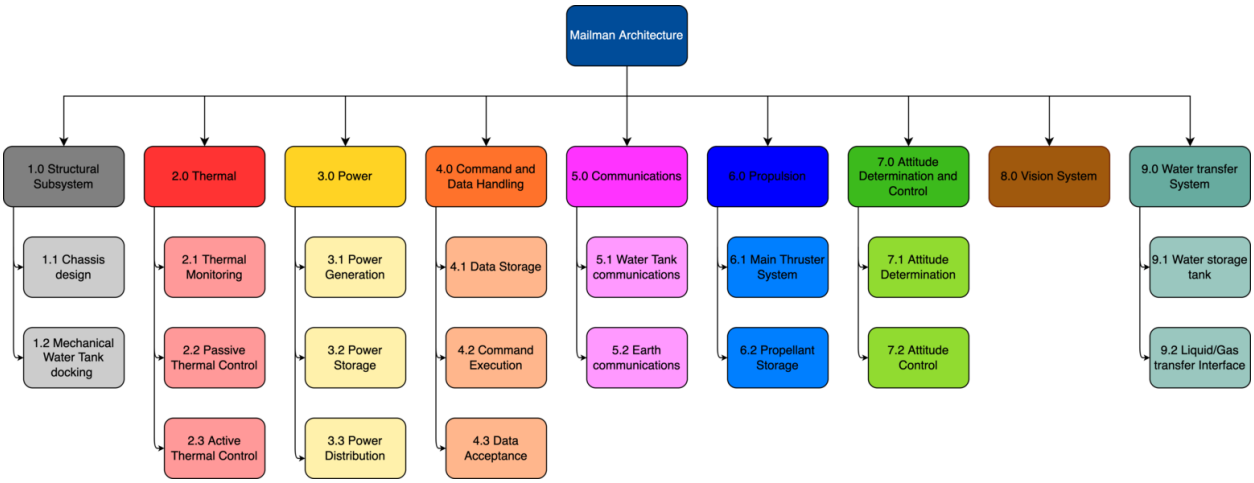

Figure 10.11: Mailman SHD

Table 10.6: Mailman Requirements

ID	Text	Rationale	Trace Up
Physical Requirements			
MAILMAN-001	The mailman must be able to be stowed in a 2m x 4m x 4m volume	80% of launch volume	KHEPRI-004
MAILMAN-002	The mailman must have a dry mass less than 2000kg.	Launch mass max of 26700 kg, 2 allocated launches	KHEPRI-006
MAILMAN-003	The mailman must be attached to the payload fairing by one powered launch adapter.		KHEPRI-008
MAILMAN-004	The mailman must be able to withstand TBM Hz of vibration at launch.		KHEPRI-009
MAILMAN-005	The mailman must be kept between TBD K and TBD K over the course of the mission.		KHEPRI-010
MAILMAN-006	The water tank must be able to withstand at least TBD Grays of radiation.		KHEPRI-011
Performance Requirements			
MAILMAN-007	The mailman must be capable of nominally operating for at least 18 years	Worst case = 2.31+6+5.78 =14.09 yrs vs. 15.71, SF = 1.11	KHEPRI-012
MAILMAN-008	The mailman must transit from Earth to Bennu within 1.13 years	Margin of 1.0 as this is worst case scenario, Raw time is 1.13 years	KHEPRI-013
MAILMAN-009	The mailman must be capable of making a round trip from Bennu to cis-lunar space within 3.69 years	Worst case is 2.56 years back and 1.13 years there, so 3.69	KHEPRI-014
MAILMAN-010	The mailman must be capable of making a return trip from Bennu to cis-lunar space within 2.56 years	Worst case is 2.56 years, best is 1.16	KHEPRI-015
MAILMAN-011	The mailman must generate TBD W of power.		Derived
MAILMAN-012	The mailman's average power consumption must not exceed TBD W.		Derived
MAILMAN-013	The mailman's peak power consumption must not exceed TBD W.		Derived
Environmental Requirements			
MAILMAN-014	The mailman must be capable of withstanding an environment of TBD becquerels.		KHEPRI-019

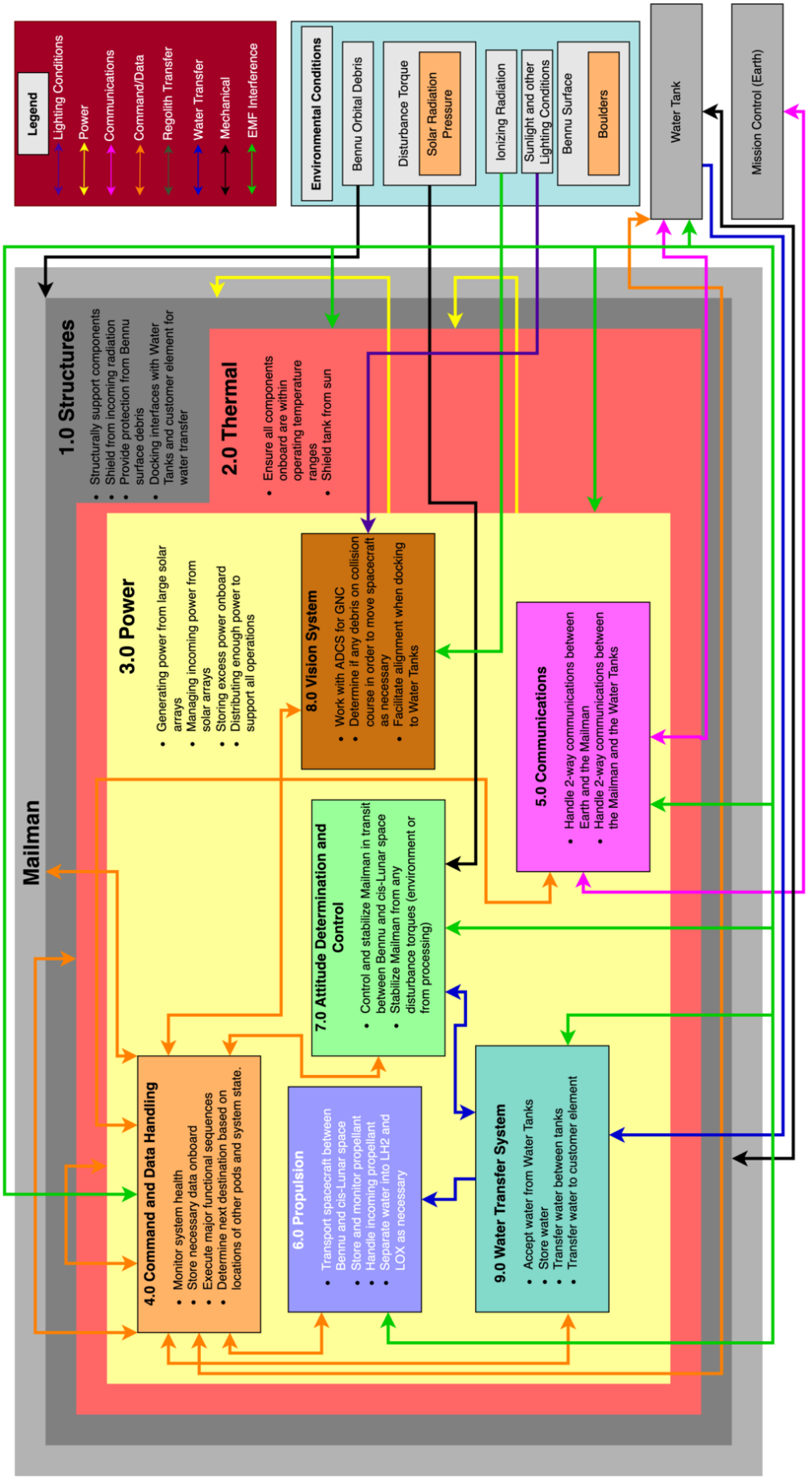

Figure 10.12: Mailman SBD

Chapter 6: Key Subsystem Overview

11 Gripper Subsystem Breakdown

11.1 Gripper Description

The main functionality of the gripper subsystem has already been described in detail in Section 5. The functionality and relationships of the various subsubsystems is outlined in the Gripper SSBD in Figure 11.1 below.

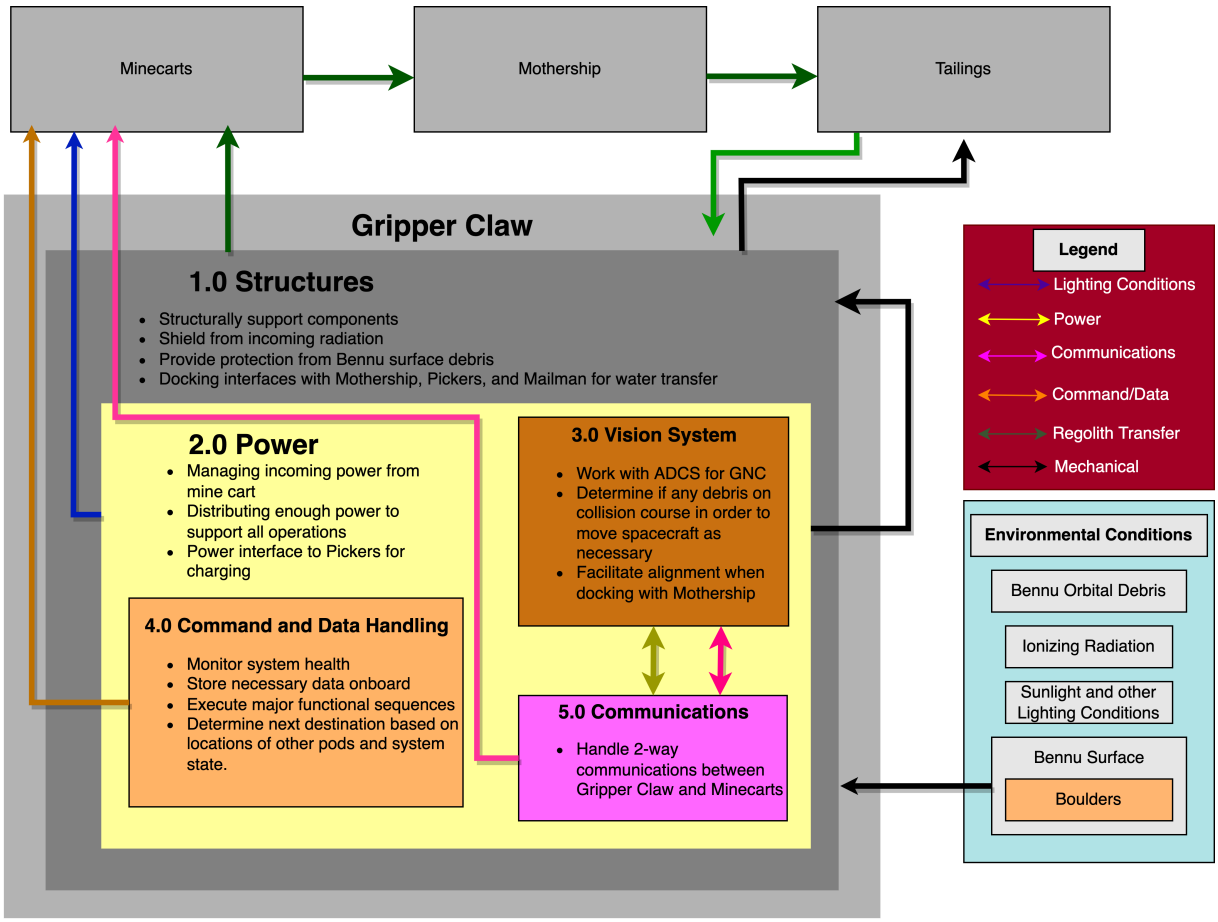

Figure 11.1: Gripper Subsystem SSBD

The Gripper features 4 main mechanisms namely, an elbow joint with 2 degrees of freedom, a telescoping bicep, soft bodies, and a clamping mechanism that holds the finger claws in place during transportation. The telescoping bicep, as shown below in Figure 11.2, allows for the unit to achieve overall stored dimensions of 1.75m in width and depth, and 3.95m in height. This is just less than the maximum volume capacity of 1.75m in width and depth and 4m in height. Furthermore, as shown in the top of Figure 11.2 the clamping mechanism is similar to that of an automobile brake pad system, which will securely hold the finger claws in place during transportation ensuring no damage is done to the claws themselves or any other instruments throughout the duration of the mission. Moreover, the elbow joint connected to the bicep and

forearm is capable of 3 degrees of freedom. Lastly, the presence of the soft bodies attached to the extremities of the finger claws are for the boulders, which are fragile in nature. These ensure that upon engagement the boulders do not fracture.

Thanks to the finger claws and the elbow joint, the Gripper is able to approach a boulder from any angle which will save both time and money on the mission, as this expands the number of boulders that can be selected from due to the shrinking compliance to boulder positioning. In Figure 11.2 we can see this mechanism being engaged.

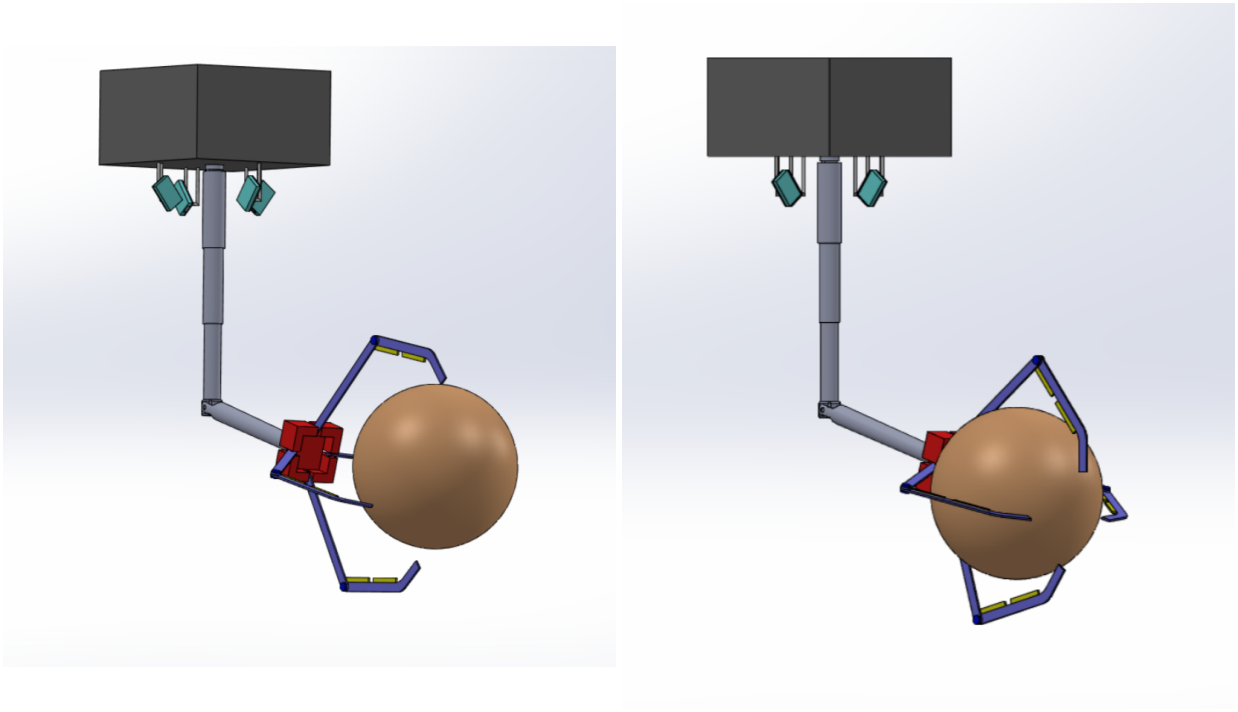

Figure 11.2: Gripper Position Before Grasping Boulder (left) vs. After (right)

Gripper Stowage

As mentioned previously, the finger claws are secured via the clamping mechanism, with its stowed configuration shown in Figure 11.3. The pressure lines shown in the figure are responsible for applying pressure onto the pads located in the clamping shell, which will secure the position shown throughout launch and return. Further, each of the four finger claws are made of two pieces, to allow for a full 180 degree rotation, enough for the finger claws to rotate backward and into their shells.

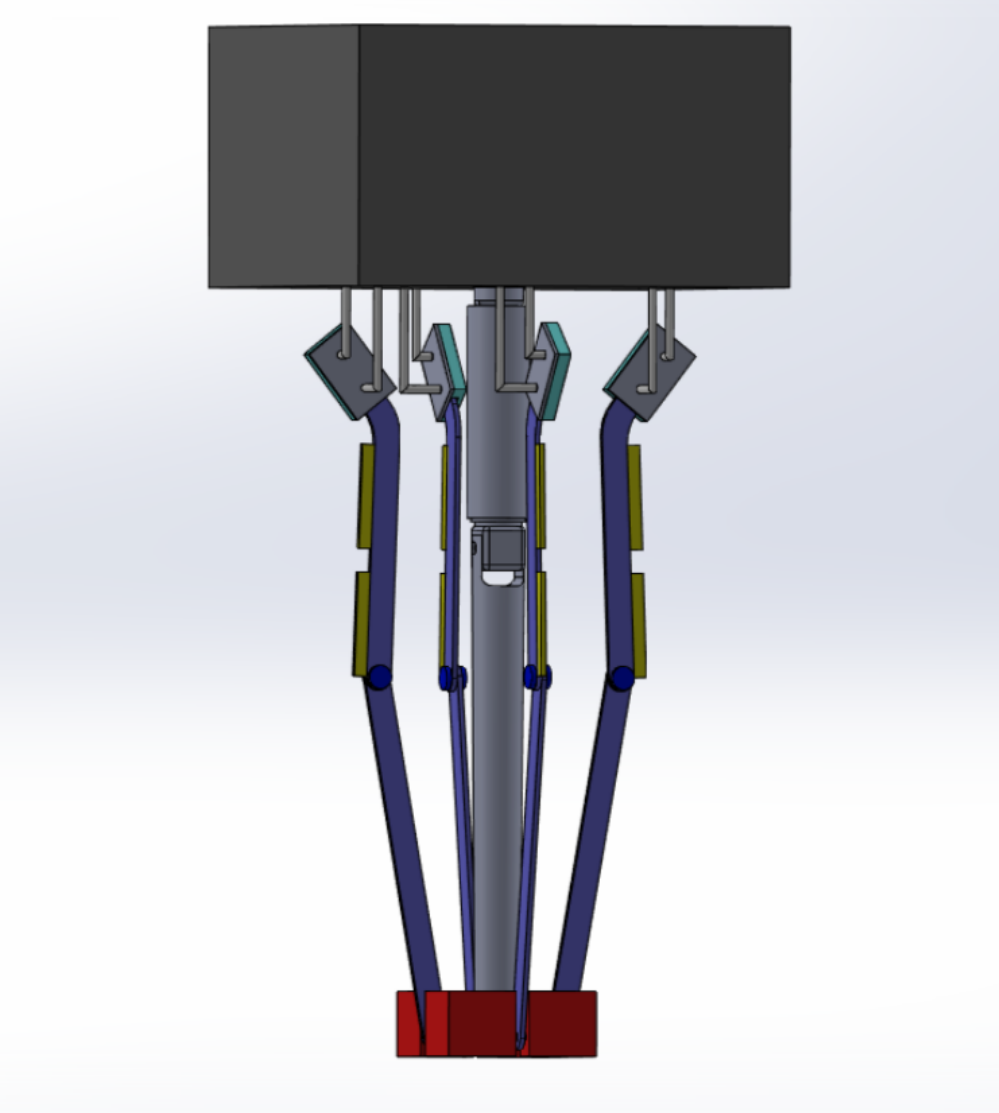

Figure 11.3: Stowed Configuration of the Gripper and Minecart

11.2 Gripper Requirements

Tables 11.1 and 11.2 outline the various physical, performance and environmental requirements that govern the gripper subsystem. Many of these are related to mine cart requirements or are self-derived for the gripper.

Table 11.1: Gripper Requirements

ID	Text	Rationale	Trace Up
Physical Requirements			
GRIPPER-001	The gripper subsystem must have a stowed volume of less than TBD m3	80% of launch volume	MINECART-002
GRIPPER-002	The gripper subsystem must have a mass less than TBD kg	Launch mass max of 26700 kg, 2 allocated launches	MINECART-003
GRIPPER-003	The gripper must have a powered, data and structural interface with the minecart.		Derived
GRIPPER-004	The gripper must be able to withstand TBM Hz of vibration at launch.		MINECART-005
GRIPPER-005	The gripper must be kept between TBD K and TBD K over the course of the mission.		MINECART-006
GRIPPER-006	The gripper must be able to withstand at least TBD Grays of radiation.		MINECART-007
Performance Requirements			
GRIPPER-007	Each gripper must be capable of nominally operating for at least 15.71 years	Worst case = 2.31+6+5.78 =14.09 yrs vs. 15.71, SF = 1.11	KHEPRI-012
GRIPPER-008	Each gripper must be capable of handling between 2m and 4m diameter boulders.	Max boulder size	MINECART-010
GRIPPER-009	The gripper must contact Bennu's surface no faster than TBD m/s.		MINECART-024
GRIPPER-010	One boulder collection cycle should take no longer than 10.91 days.	16.4 days with maximum 1403 boulders 2m boulders, 4 pickers, SF of 1.5	MINECART-009, MINECART-011
GRIPPER-011	The gripper must not apply more than TBD MPa to the boulder in order not to crush it.		Derived
GRIPPER-012	The gripper's average power consumption must not exceed TBD W.		MINECART-013
GRIPPER-013	The gripper's peak power consumption must not exceed TBD W.		MINECART-014

Table 11.2: Gripper Requirements Continued

ID	Text	Rationale	Trace Up
Environmental Requirements			
GRIPPER-014	The grippers must not impart a cumulative momentum change greater than 2.2*10^5 kgm/s over the mission.	Bennu orbital delta-v uncertainty spec, could be measured by momentum impacts of pickers, Total momentum change of Bennu must be less than 2.2*10^5 kgm/s	KHEPRI-016
GRIPPER-015	The gripper must not generate any single piece of debris larger than 1 tonne further than 38.9km from Bennu.	Size of debris matters, if small doesn't matter (less than a tonne item - will burn up in Earth's atmosphere), 38.9 km is Bennu's hill sphere	KHEPRI-017
GRIPPER-016	The gripper must not generate any single piece of debris larger than 30cm within 2 km of Bennu.	Polluting environment, spacecraft requirement for impact tolerance (30cm size particles was the maximum for O-REx)	KHEPRI-018
GRIPPER-017	The gripper braid must not let out particles greater than TBD cm.		GRIPPER-016
GRIPPER-018	The mission components must be capable of withstanding an environment of TBD becquerels.		KHEPRI-012

11.3 Minecart Controls

While no preliminary controls analysis for the gripper was completed at this stage, some acknowledgements of various control systems onboard the minecart were outlined. These are summarized for the various components/subsystems of the minecart as shown below in Table 11.3.

Table 11.3: Acknowledged Minecart Component/Subsystem Controls

Control	Function
Attitude and determination control	Keep spacecraft properly oriented, move between orbits
Telescopic arms	Deploy gripper
Gripper joints and fingers	Achieve correct angles for boulder collection
Temperature control	Keep all electrical components within operating temperatures
Docking and undocking on other vehicles	Autonomous controls to dock and undock

12 Processor Subsystem Breakdown

12.1 Docking and Loading Description

Most of the minecart docking and loading process was outlined in the trade studies in Section 6.2. Not much more of this has been explored at this stage, and docking points have not yet been integrated into the mothership CAD. The CAD does allocate enough room for the picker to fit on the axis of rotation of each processor. The rotation loading will not be due to direct rotation of the minecart, but rather by using the dexterous nature of the gripper arm,as it already has the DOF integrated for this functionality. One the minecart has docked, the arm will rotate and align to position the boulder directly in line with the crushing chamber.

12.2 Crusher Description

As defined is Section 6.3, the crusher accepts boulders from the minecart and crushes them into small particles for the processor to extract the water from. As noted in that section, the “finalized” design is still very rough at this stage, with the TBM crusher face being roughly outlined, but with little certainty in the functionality. This will be described more in Section 16.1. As of now, the TBM face can be visualized from a head-on and side view, shown in Figure 12.1 below. Note the Wedge structure is stationary, while the ”grader” section rotates boulders against (underneath) the wedge to create a surface against which the grader can operate.

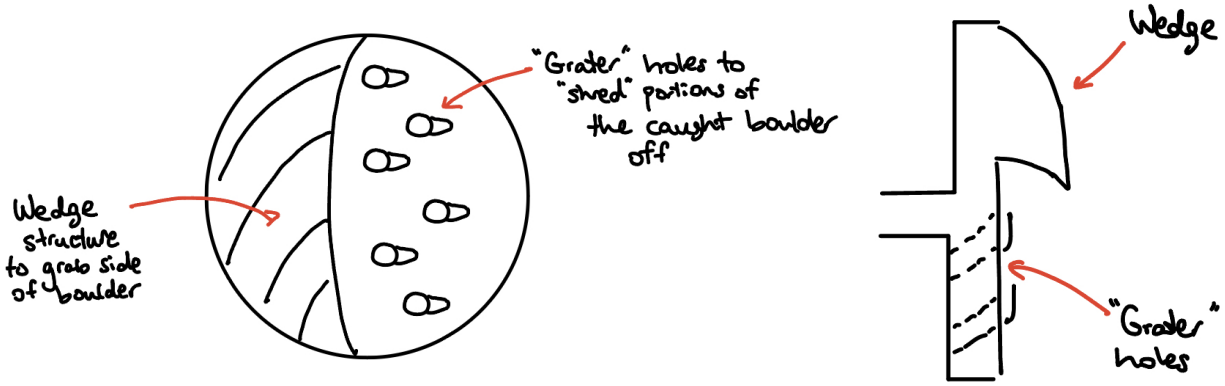

Figure 12.1: TBM Face Head-on (left) and From the Side (right)

The overall crusher, integrating with the processor and loading from the minecart is shown below in Figure 12.2. The braided structures on the end of the crusher and minecart prevent debris from escaping. Note that this drawing only depicts half of one dual-processor, and there are two of these structures on the mothership.

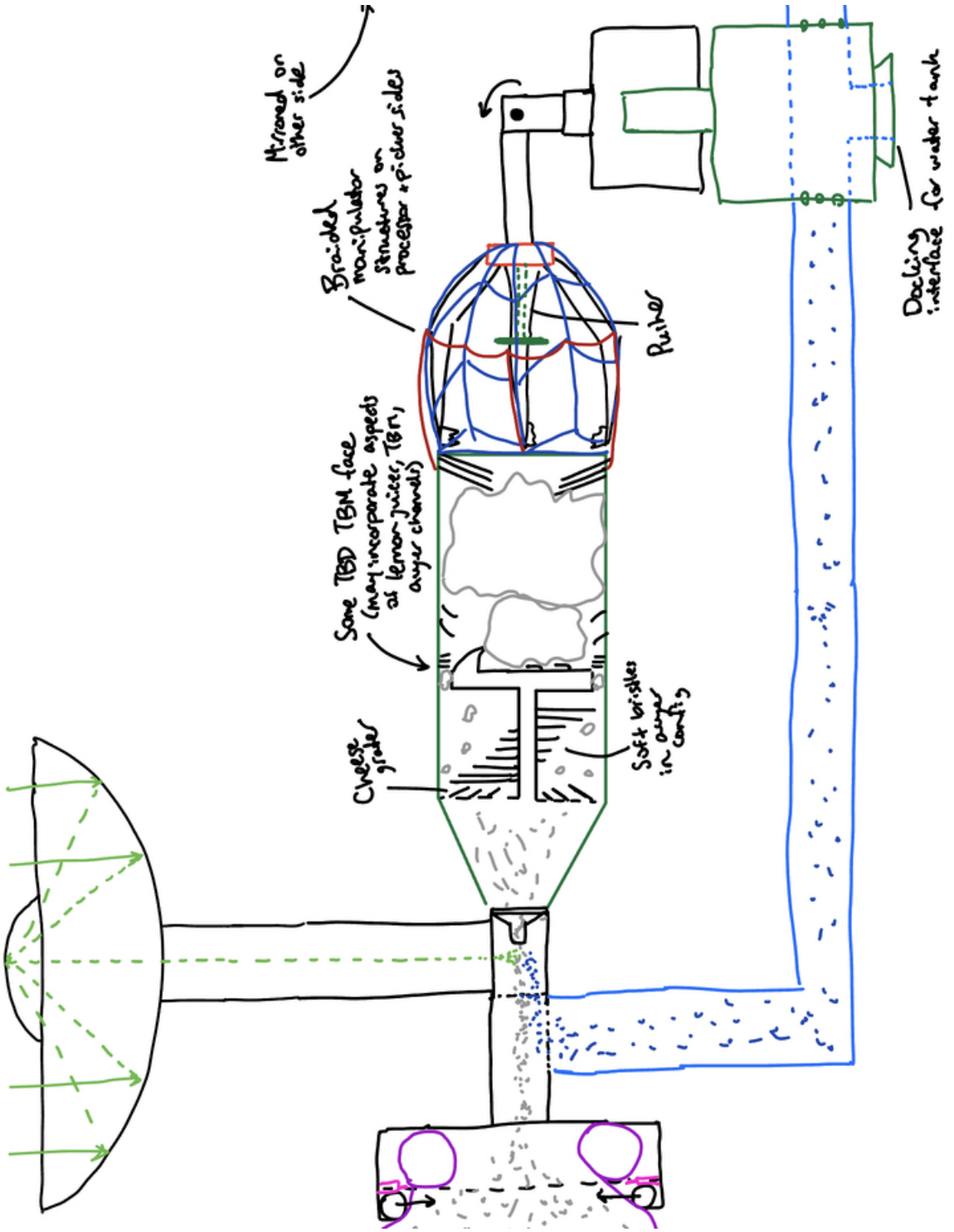

Figure 12.2: Drawing of the Finalized Processor with Minecart Loading and Crushier Side view

12.3 Crusher Requirements

Table 12.1 below outlines the preliminary crusher requirements derived at this stage in terms of physical, performance and environmental requirements.

Table 12.1: Crusher Requirements

ID	Text	Rationale	Trace Up
Physical Requirements			
CRUSHER-001	The crusher components must be fit inside the stowed crusher chamber, in a TBDm x TBDm x TBDm volume.	80% of launch volume	KHEPRI-003
CRUSHER-002	The total mass of the crusher system must not exceed TBD kg.	Launch mass max of 26700 kg, 2 allocated launches	KHEPRI-005
CRUSHER-003	The crusher system must have a power, data and structural interface to the Mothership		Derived
CRUSHER-004	The crusher system must be able to withstand TBM Hz of vibration at launch.		KHEPRI-009
CRUSHER-005	The crusher system must be kept between TBD K and TBD K over the course of the mission.		KHEPRI-010
CRUSHER-006	The crusher system must be able to withstand at least TBD Grays of radiation.		KHEPRI-011
Performance Requirements			
CRUSHER-007	The crusher must be capable of nominally operating for at least 15.71 years	Worst case = 2.31+6+5.78 =14.09 yrs vs. 15.71, SF = 1.11	KHEPRI-012
CRUSHER-008	The crusher must ensure a feedrate of TBD kg/hour into the processing system.	Extraction rate is governed by crushing rate	KHEPRI-014
CRUSHER-009	The crusher system must crush at least 8,600,000 kg of regolith	Derivation sheet, 7778066 kg max for only 2m boulders collected, SF of 1.1	KHEPRI-015
Environmental Requirements			
CRUSHER-010	The crusher must not generate any single piece of debris larger than 1 tonne further than 38.9km from Bennu.	Size of debris matters, if small doesn't matter (less than a tonne item - will burn up in Earth's atmosphere), 38.9 km is Bennu's hill sphere	KHEPRI-017
CRUSHER-011	The crusher must not generate any single piece of debris larger than 30cm within 2 km of Bennu.	Polluting environment, spacecraft requirement for impact tolerance (O-REx max was 30cm size particles)	KHEPRI-018
CRUSHER-012	The crusher components must be capable of withstanding an environment of TBD becquerels.		KHEPRI-019

12.4 Processor Description

The main functionality of the processor subsystem has already been described in great detail in Section 6. The functionality and relationships of the various subsubsystems is outlined in the Processor SSBD in Figure 12.3 below.

12.5 Processor Requirements

Table 12.2 below outlines the preliminary processor requirements derived at this stage in terms of physical, performance and environmental requirements.

Table 12.2: Processor Requirements

ID	Text	Rationale	Trace Up
Physical Requirements			
PROCESSOR-001	The processor system must fit in a TBD m3 stowed volume	80% of launch volume	KHEPRI-003
PROCESSOR-002	The total mass of the processor must not exceed TBDkg.	Launch mass max of 26700 kg, 2 allocated launches	KHEPRI-005
PROCESSOR-003	The processor system must have a power, data and structural interface to the Mothership		Derived
PROCESSOR-004	The processor system must be able to withstand TBM Hz of vibration at launch.		KHEPRI-009
PROCESSOR-005	The processor system must be kept between TBD K and TBD K over the course of the mission.		KHEPRI-010
PROCESSOR-006	The processor system must be able to withstand at least TBD Grays of radiation.		KHEPRI-011
Performance Requirements			
PROCESSOR-007	The processor must be capable of nominally operating for at least 15.71 years	Worst case = 2.31+6+5.78 =14.09 yrs vs. 15.71, SF = 1.11	KHEPRI-012
PROCESSOR-008	The processor must spin at 4 RPM to ensure the proper extraction rate.	Spin rate to get at least 5.07 kg/hr	KHEPRI-014
PROCESSOR-009	The processor must mine at least 8,600,000 kg of regolith	Derivation sheet, 7778066 kg max for only 2m boulders collected, SF of 1.1	KHEPRI-015
Environmental Requirements			
PROCESSOR-010	The processor not generate any single piece of debris larger than 30cm within 2 km of Bennu.	Polluting environment, spacecraft requirement for impact tolerance (O-REx max was 30cm particles)	KHEPRI-018
PROCESSOR-011	The processor system must be capable of withstanding an environment of TBD becquerels.		KHEPRI-019

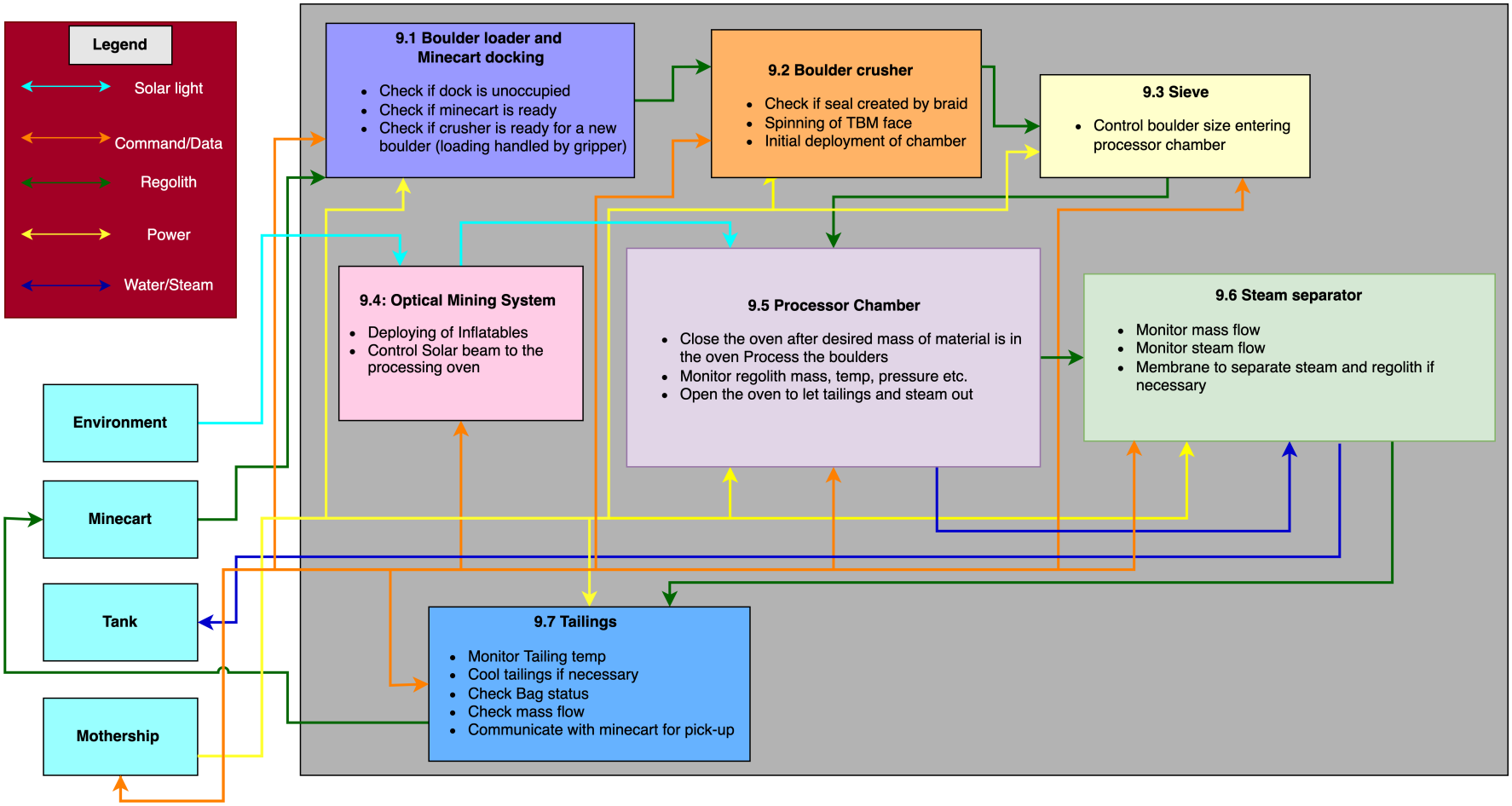

Figure 12.3: Processor SSBD

12.6 Processor Detailed Design and Calculations

In order to mothership and processor detail the design via CAD, many aspects of the processor system needed to be calculated. This included:

- Sizing of the Optical Mining Discs via Simulations
- Calculation of Water Extraction Rates
- Calculation of Processor Forces

Sizing of the Optical Mining Disks
The thermal power required to process asteroid material is provided by four 5.75 meter inflatable solar concentrators, with one for each processor oven. After several rounds of brainstorming, the team determined four processors were necessary to meet the required processing times and mission requirements. An optical analysis of the system was performed on an open source Monte Carlo Ray Trace modelling software, Tonatiuh. The simulation was performed for a simple cassegrain optical system to determine the correct size of the concentrator to deliver the required power and processing rates. This simulation view is shown below in Figure 12.4, with the final simulation results shown in Figure 12.5.

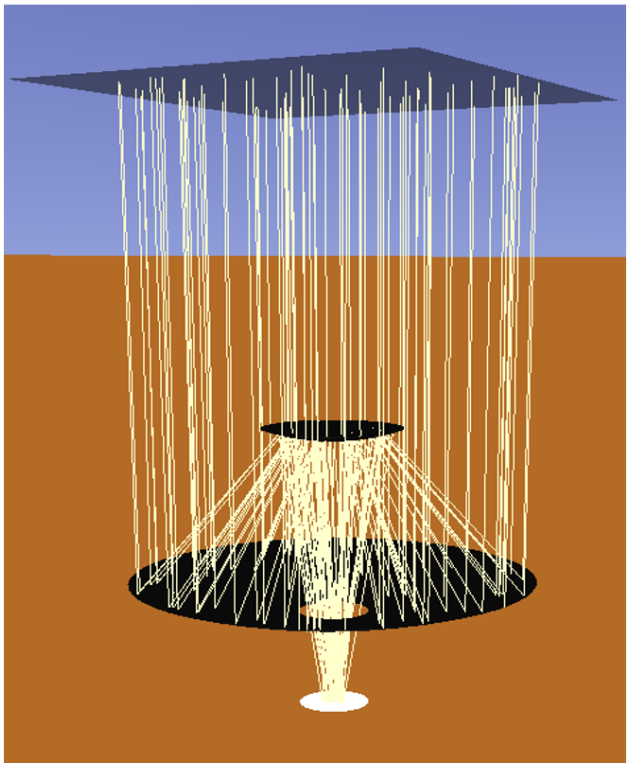

Figure 12.4: Optical Mining Simulation View with Incoming Solar Radiation

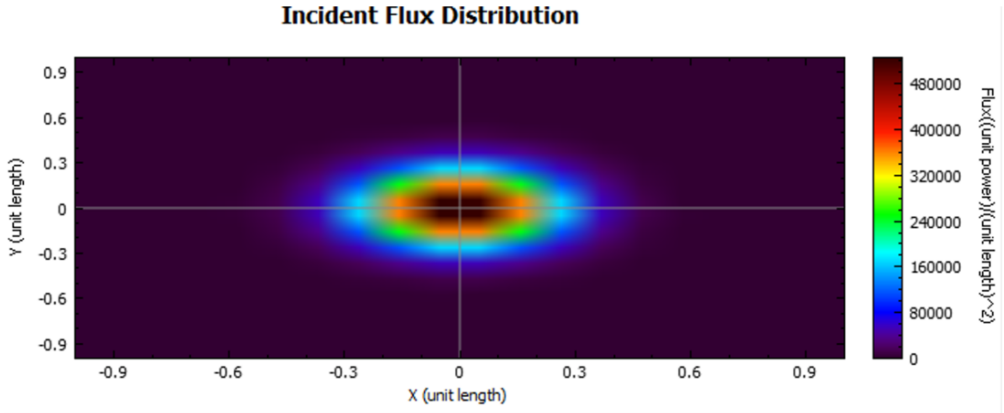

Total Power:	94966.9
Minimum Flux:	0
Average Flux:	23741.7
Maximum Flux:	526882
Maximum Flux Coordinates:	0.05 ; -0.05
Error:	0.0906979
Uniformity:	3.34804
Centroid:	-0.000123624 ; 7.64137e-05

Figure 12.5: Optical Mining Flux Map and Parameters

Important parameters necessary for the simulation were:

- Solar Radiation Constant: 1300 W/m^2 (Roughly similar to at Earth, as Bennu has a mean orbital distance only slightly larger than Earth)
- Thetamax: 0.00465 (A parameter that captures the very slight ellipsoidal shape of the sun compared to a perfect sphere)

The initial modeling of the optical surfaces was assumed to be ideal, and then a safety factor was considered for the surface reflectivity to estimate the concentrator size and flux maps. The parameters used in the modelling are shown in the Table 12.3. For all simulations, 10 million rays were traced. The results show that the simple Cassegrain configuration can deliver a peak intensity of 527 kW/m^2 on a spot size of 50mm diameter. It should be noted that other optical systems might be needed to direct the rays to the processor oven like light tubes depending on the location of the concentrators, however the optical simulations show we can generate enough power to process the regolith material.

Table 12.3: Simple Optical Configuration Parameters

Parameter	Value
Parabolic Primary Aperture Diameter	5.75m
Primary Focal Length	7.5m
Parabolic Secondary Aperture Diameter	1.5m
Secondary Focal Length	2.75m
Flat Receiver	-

Calculation of Water Extraction Rates

The water extraction rate had been determined by the mission requirements, namely 5.07 kg/hr. This now had to be verified via calculations that the discs were sized properly to meet this requirement. The calculations determining this rate and the effective processor revolution speed to yield this rate are shown below in Table 12.4.

Table 12.4: Processor Rate Calculations

Disc Diameter (m)	5.75
Number of Processors	4
Power Density (kW/m^2)	525
Power Density (W/cm^2)	52.5
Spot size ellipse semi-major axis (m)	0.05
Spot size ellipse semi-minor axis (m)	0.05
Spot size ellipse area (m^2)	0.0079
Power over Spot Size (W)	4123
Regolith Specific Heat Capacity (J/kg)	750
Regolith Initial Temperature (C)	0
Regolith Final Temperature (C)	900
Heat of Fusion of Water (J/kg)	333550
Heat of Vaporization of Water (J/kg)	225700
Diameter of Particle to be Processed (m)	0.005
Mass of above diameter spherical particle (kg)	0.000
Required Energy to Heat Particle (J)	62
Time to fully Extract Water/Heat Particle (s)	0.015
Water extraction Rate (kg/s)	0.00036
Water extraction Rate (kg/hr)	1.30877
Effective Water extraction Rate (kg/hr) (of all processors)	5.24
Factor on regolith flow rate	160.00
Speed over spot size (m/s) (8m from central axis)	3.33
Time in beam (s)	0.015
Processor Flow rate (kg/s)	0.000036
Angular velocity (rad/s)	0.416
Speed of Processor (rpm)	3.98

The end results from this calculation show that if the boulder is broken up into 5mm particles, the particle will be fully ablated in 0.015 seconds, the exact same amount of time that the particle will be in the 5cm spot size (at the maximum diameter) when the processor is spinning at $\sim$4 RPM. If the processor is

spinning slowed, which would just create a slight backlog in the "queue" for the extraction particles, larger particles could be mined as well. Note that it is assumed the spot size is roughly 8m from the central axis of the entire processor system on the mothership.

Calculation of Processor Forces

Now knowing the ∼4 RPM spin rate, it is useful to see the speeds, accelerations and forces on the fine particulate, and on the boulders themselves that would be loaded into the crushing chamber, ranging from 2-4m in size. This data is summarized in Table 12.5 below.

Table 12.5: Processor Distance, Velocity, Acceleration and Force Data

Radius from center (m)	Velocity (m/s)	Centrifugal acceleration (m/sˆ2)	Forces (N) on 5mm particle	Forces (N) on 2m boulder	Forces (N) on 3m boulder	Forces (N) on 4m boulder
1	0.416	0.173	0.00002	967.2	3264.2	7737.3
2	0.833	0.347	0.00003	1934.3	6528.3	15474.5
3	1.249	0.520	0.00005	2901.5	9792.5	23211.8
4	1.665	0.693	0.00006	3868.6	13056.6	30949.1
5	2.082	0.867	0.00008	4835.8	16320.8	38686.3
6	2.498	1.040	0.00009	5803.0	19585.0	46423.6
7	2.914	1.213	0.00011	6770.1	22849.1	54160.9
8	3.331	1.387	0.00012	7737.3	26113.3	61898.2
9	3.747	1.560	0.00014	8704.4	29377.4	69635.4
10	4.163	1.733	0.00015	9671.6	32641.6	77372.7
11	4.580	1.907	0.00017	10638.7	35905.8	85110.0
12	4.996	2.080	0.00018	11605.9	39169.9	92847.2
13	5.412	2.253	0.00020	12573.1	42434.1	100584.5
14	5.829	2.427	0.00021	13540.2	45698.2	108321.8
15	6.245	2.600	0.00023	14507.4	48962.4	116059.0

12.7 Tailings Disposal Subsystem Description

- There will be two spools of the bag material, CNT (as decided in Table 7.2) separated to give a bag width of 1m
- The horizontal stitcher will seal the bottom edge of the bag
- The material will roll out from each spool to the designated length of the bag
- The two vertical stitchers will seal the left and right edges of the bag
- The tailings will be loaded into the bag from the processor unit via centrifugal force
- When the bag is full, the horizontal stitcher will seal the top edge of the bag
- The full bag will be cut using a guillotine
- The full bag will be released to the picker for disposal on Bennu's surface
- The process will be repeated for the subsequent boulder

Based on the assumption that the tailings would be at 900°C upon exit from the processor unit (as described in Section 7), a subsystem block diagram was generated including a cooling unit before the tailings enter the disposal bag.

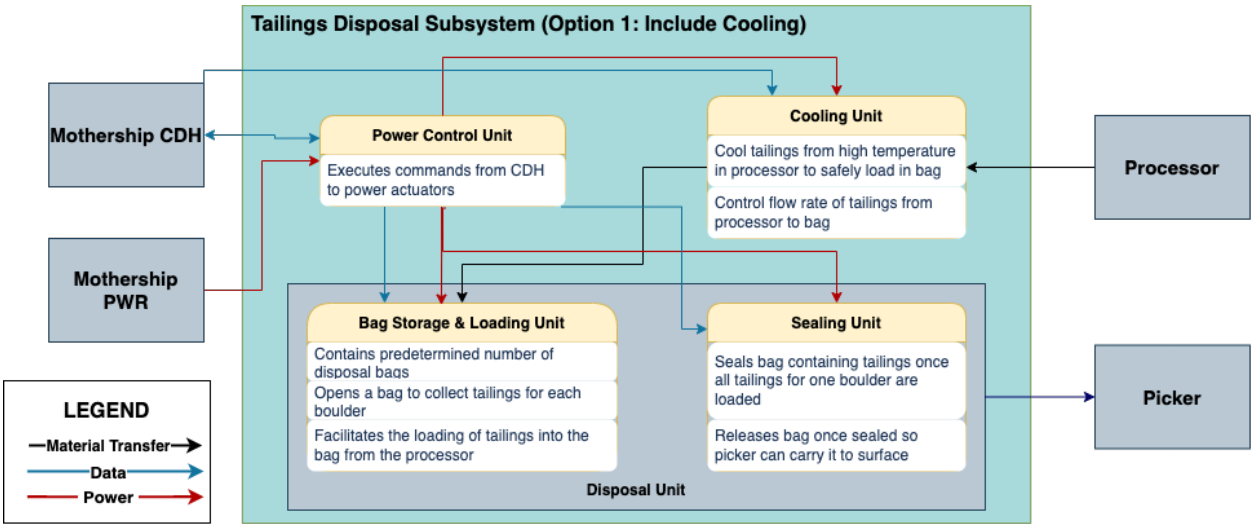

Figure 12.6: Tailings Disposal Subsystem Block Diagram with Cooling Unit

An alternative subsystem block diagram was generated in the case that the disposal bag was designed to handle the high temperatures and a cooling unit was therefore unnecessary.

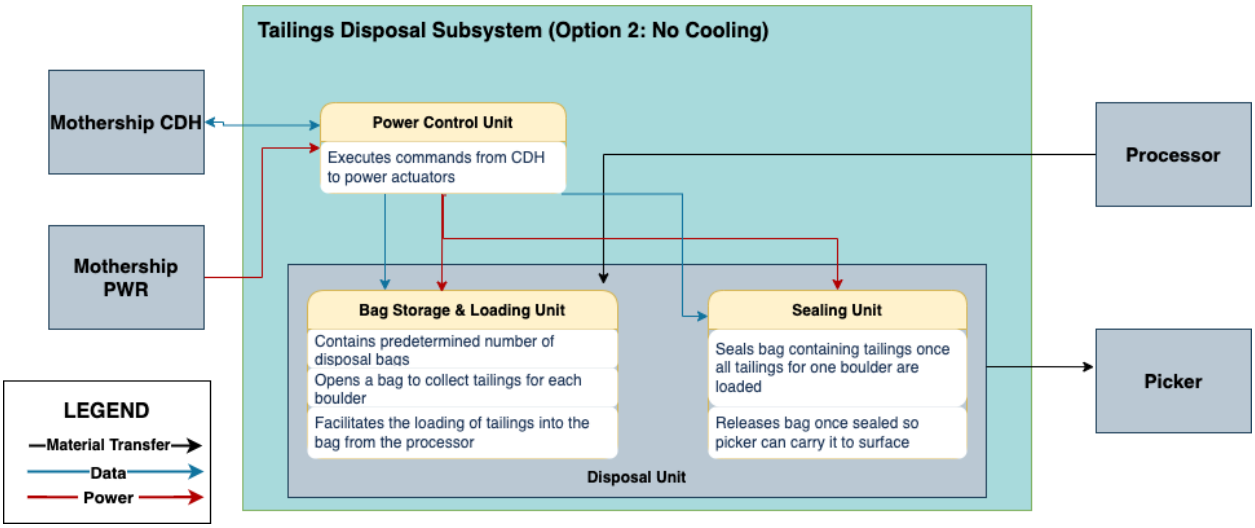

Figure 12.7: Tailings Disposal Subsystem Block Diagram without Cooling Unit

Since the bag material was chosen to be CNT according to the trade in Table 12.6, it was unnecessary to include a cooling unit as CNT can withstand the high temperature of the material. Thus, the subsystem block diagram used in the design is the one shown in Figure 12.7.

12.8 Tailings Disposal Requirements

Tables 12.6 and 12.7 below outline the preliminary tailings disposal requirements derived at this stage in terms of physical, performance, functional, and environmental requirements.

Table 12.6: Tailings Disposal Requirements

ID	Text	Rationale	Trace Up
Physical Requirements			
TAILINGS-001	The tailings disposal system must fit in a TBD m3 stowed volume	80% of launch volume	KHEPRI-003
TAILINGS-002	The total mass of the tailings disposal system must not exceed TBD kg.	Launch mass max of 26.7 kg, 2 allocated launches	KHEPRI-005
TAILINGS-003	The tailings disposal system must have a power, data and structural interface to the Mothership		Derived
TAILINGS-004	The tailings disposal system must be able to withstand TBD Hz of vibration at launch.		KHEPRI-009
TAILINGS-005	The tailings disposal system must be kept between TBD K and TBD K over the course of the mission.		KHEPRI-010
TAILINGS-006	The tailings disposal system must be able to withstand at least TBD Grays of radiation.		KHEPRI-011
Performance Requirements			
TAILINGS-007	The tailings disposal system must be capable of nominally operating for at least 15.71 years	Worst case = 2.31+6+5.78=14.09 yrs vs. 15.71, SF = 1.11	KHEPRI-012
TAILINGS-008	The tailings disposal system must be able to accomodate a tailings flowrate of TBD kg/s.	Flow rate from processor into tailings	KHEPRI-014
TAILINGS-009	The tailings disposal system must collect at least 8,050,000 kg of tailings	93.6% of 8,600,000 kg of regolith	KHEPRI-015
TAILINGS-010	The tailings disposal system must be able to withstand tailing temperatures of 900C	Tailings exit the processor unit at 900C	Derived
TAILINGS-011	The tailings disposal system must comprise a tailings storage unit for surface disposal	Result of surface vs. orbital disposal trade study (Table 7.1)	TAILINGS-009
TAILINGS-012	The tailings storage unit must have a sealing mechanism	The tailings must be secured so they remain where they are disposed of, regardless of the microgravity conditions	TAILINGS-015

Table 12.7: Tailings Disposal Requirements Continued

ID	Text	Rationale	Trace Up
Environmental Requirements			
TAILINGS-013	The placement of tailings on Bennu's surface must not disturb Bennu's orbit by more than 3microns/s.	Bennu orbital delta-v uncertainty spec, could be measured by momentum impacts of pickers, Total momentum change of Bennu must be less than 2.2*10^5 kgm/s	
TAILINGS-014	The tailings disposal system must not generate any single piece of debris larger than 1 tonne further than 38.9km from Bennu.	Size of debris matters, unless small (less than a tonne item - will burn up in Earth's atmosphere), 38.9 km is Bennu's hill sphere	KHEPRI-017
TAILINGS-015	The tailings disposal system must not generate any single piece of debris larger than 30cm within 2 km of Bennu.	Polluting environment, spacecraft requirement for impact tolerance (30cm size particles was max for O-REx)	KHEPRI-018
TAILINGS-016	The tailings disposal system must be capable of withstanding an environment of TBD becquerels.		KHEPRI-019

12.9 Tailings Disposal Detailed Design

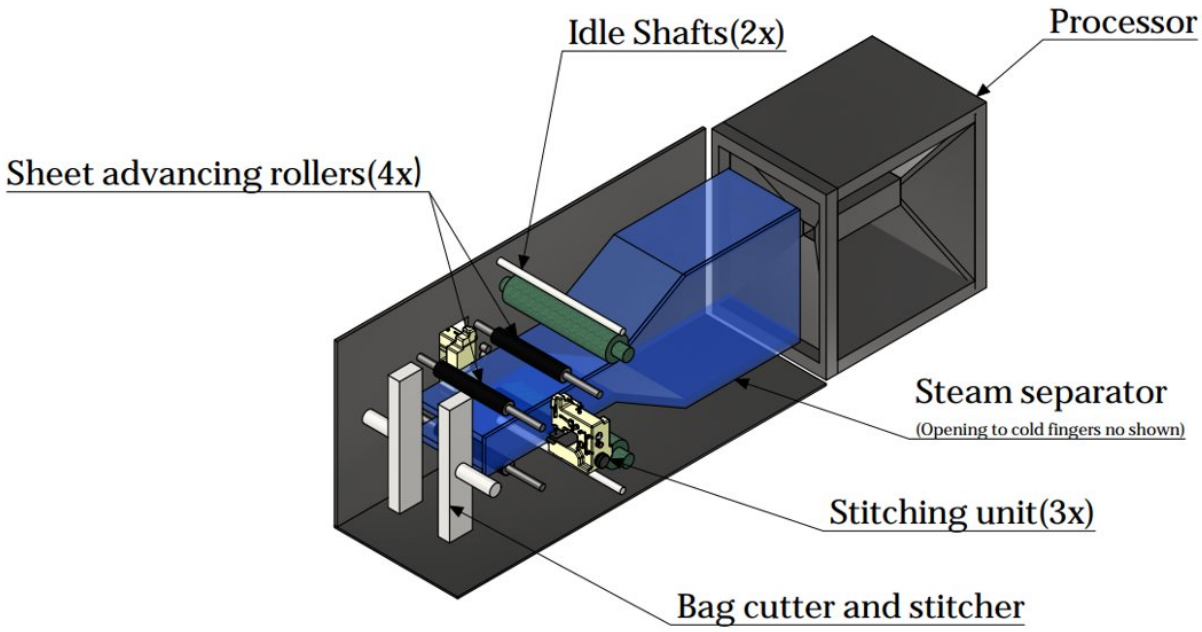

Figure 12.8: Tailings Disposal CAD

The figure above demonstrates the tailings disposal subsystem as described in Section 7.

The mass budget was calculated as follows, taking into account the volume loss by stitching (0.05 shown in Figure 12.9) and the porosity of the CNT bag (assumed to be 0.36):

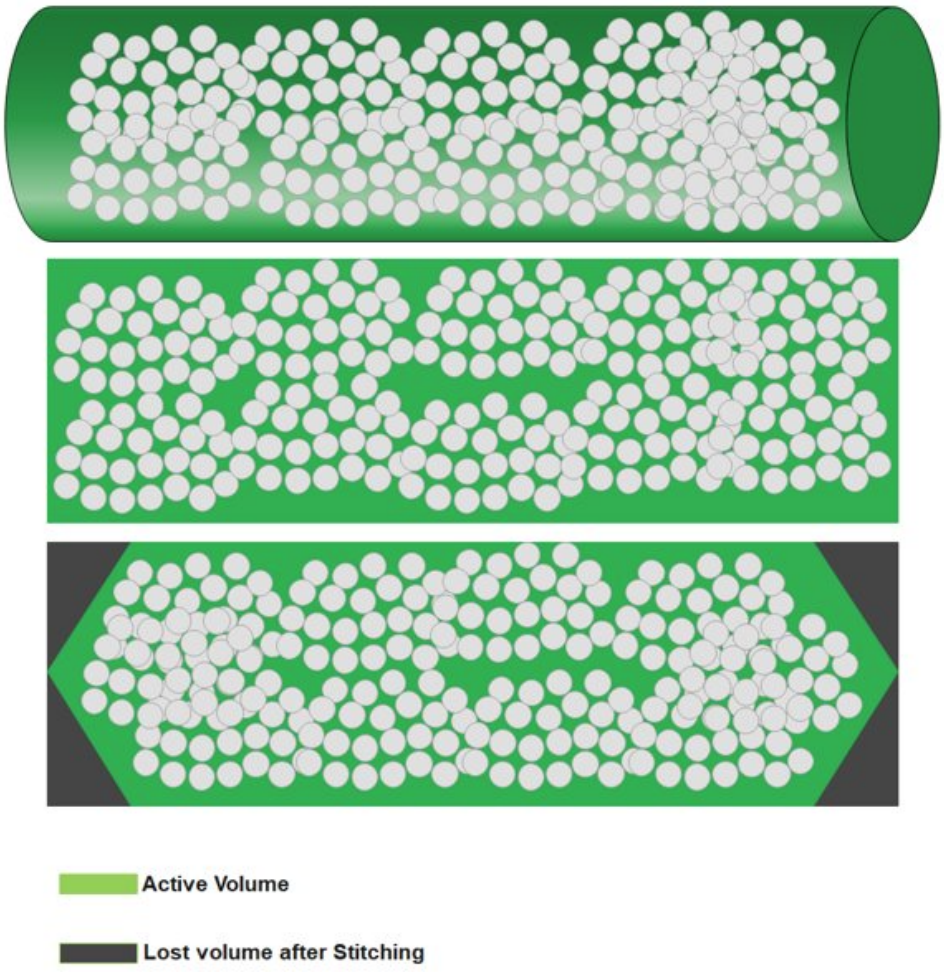

Figure 12.9: Volume Loss after Stitching Tailings Disposal Bag

- Boulder volume before crushing = $4m^3$
- Boulder volume after packing = $4m^3$ + 0.36 (porosity) * $4m^3$ = $5.44m^3$
- Bag volume after stitching = $5.44m^3$ + 0.05 (volume loss) * $5.44m^3$ = $5.712m^3$
- Bag mass per m^2 = $400g/m^2$
- Bag mass per $4m^3$ boulder = $2284.8g$

Thus, it was assumed that the mass per bag is approximately 2.3kg. This figure is multiplied by the total number of boulders to get the overall mass budget allotment for the tailings disposal bags.

12.10 Overall Processor Controls Acknowledgement

Like the gripper, while no preliminary controls analysis for the processor was completed at this stage, some acknowledgements of various control systems that would be required within the processor were outlined. These are summarized for the various components/subsystems of the processor as shown below in Table 12.8.

Table 12.8: Controls Acknowledgement

Control	**Function**
Telescopic arms	Change distance based on mass in the processor
Processor RPM	Maintain feedrate
Tailings unit	Monitor tailings, collection and bagging
Docking and Undocking on other vehicles	Autonomous controls to dock and undock
Cold fingers	Maintain temperature and condensation

Chapter 7: Mission Cost Estimate

12 Cost Estimate and Breakdown

The outlined mission in Section 8 was designed for a $1.5 billion dollar budget, with $300 million allocated for two Falcon Heavy launches to get the mission started. That leaves $1.2 billion for the construction and operation of the craft, between labour and non-labour costs. The labour costs would consist of about 50% of the non-launch cost budget which comes out to $600 million dollars and is distributed into four phases, 10% for the 1st phase, 25% for the 2nd phase, 35% for the 3rd phase, and 30% for the final 4th phase. These four phases and their $600 million budget include the expenses of continued operations for the duration of the mission. This leaves $600 million for materials and testing equipment and any non-labour expenses for the mission. Typical space mission budgets are much larger than this figure, but if the terrestrial technologies can be proven for space, and commercial off the shelf (COTS) parts can be utilized, it may be feasible to meet such a budget.

Table 12.1 below summarizes both the labour and non-labour expenses distributed by mass for the various spacecraft. Parts of the budget will go towards materials and testing equipment, and parts towards construction and testing labour, as well as operations, as outlined above. Note that the $1/250kg figure for water is for Toronto, Canada, and does not define the purity of the water to be used as propellant.

Table 12.1: Cost Breakdown for the Spacecraft

Cost Budget by Mass	**Mass (kg)**	**Money ($M)**
Fuel (Water) - Roughly $1/250kg	13756	$\sim$0
Mailman	2000	60.5
Mothership	19922	603.1
Minecarts (4)	3930	119.0
Water Tanks (2)	1000	30.3
Total (excluding water)	39642	1200.0
Total Minecarts	15720	475.9
Total Water Tanks	2000	60.5
Mailman	2000	60.5
Mothership	19922	603.1
Sum (excluding water)	39642	1200.0

Chapter 8: Technology Development and Demonstration

13 Impactor

Because of Bennu's poorly consolidated surface, it requires relatively little energy to displace a large amount of material. The OSIRIS-REx TAGSAM sampling even displaced approximately 12 cubic metres of material [7]. Gun-type impactors have been successfully used to investigate the subsurface of asteroid 162173 Ryugu and as such have been developed to TRL 9 [81].

Although Bennu's surface is poorly consolidated, there is evidence that it may have a more rigid interior below 10m depth [82] [7]. Examination of the impact crater and ejecta curtain from the impactor deployed by the Hayabusa-2 mission to Ryugu were able to determine numerous physical properties including surface strength, boulder sizes, geologic structure, and variations of properties at depth. A sufficiently energetic impactor could excavate a crater 10m deep on Bennu, allowing direct measurement of the cohesion and other properties beyond the unconsolidated surface.

Several impactor designs have been developed to TRL 9 including gun-type kinetic impactors and mission profiles where an entire spacecraft is disposed of by impacting the surface [81]. A demonstration mining mission also offers several opportunities for new impactor design. The spacecraft will need to be able to capture an manipulate boulders, which opens the possibility of capturing a boulder from the surface and accelerating it into Bennu. Similarly, processing boulders will produce tailings that require disposal and could be accelerated toward Bennu to produce impact craters. Using local materials as impactors could potentially allow for multiple impacts, characterizing properties in different locations, and could be more massive than an impactor transported from earth due to lower delta-V requirements. Finally, the processing spacecraft itself could be used as an impactor at the end of the mission. If the processing unit was filled with material prior to crashing into Bennu, it could allow for a very high energy impact.

14 Thrusters

As outlined in detail in Section 4.4, BE-7 thruster would be suitable for this mission, but to use the mined water as fuel, there are complicated steps to get LOX and LH2. These include: water purification, electrolysis, and condensation/cooling. There are many methods on Earth for water purification, giving it TRL 6, as it would need to be demonstrated in space. This does assume the technology can be easily applied in a different environment, and the procedure does not have to significantly change. Similarly, there are many ways to accomplish electrolysis on Earth. Most commonly, this is done by passing current through water via an anode and cathode, which creates hydrogen and oxygen gas. This is a very energy intensive process, but the mailman or mothership could use solar power to drive this process. Again, this would have a TRL 6, but need space testing and qualification.

Finally, and most challengingly, there needs to be a condenser/cooler, to condense LOX and LH2 into their liquid states. This could be accomplished actively or passively; however, active cooling would be near impossible, as liquid hydrogen temperature is between 14 - 33K. Liquid oxygen temperature is between 56 - 90K, so this may be possible via active cooling, but would be extremely energy intensive. One possible passive solution is to have the condensation chamber facing deep space, which has an average temperature

of 2.7K, use this to cool the gasses into liquid. This would be an untested technique and technology, so would require extensive testing and have a low TRL.

Even if separately all of these technologies are feasible, one complication is rate matching the purification and electrolysis with the condensation. The electrolysis and condensing rate would need to be faster than or equal to propellant consumption rate, as if not there would be hydrogen leakage and boil-off losses. It is also important to note, as mentioned in Section 4.4, 1 kg of water produces 0.888 kg of oxygen and 0.112 kg of hydrogen. This is a ratio of 7.93:1 oxygen to hydrogen, and typical typical LOX-LH2 mixture ratios are 5.88:1 oxygen to hydrogen. This would result in a slight excess of oxygen, but this could be sold as well.

15 Gripper

The gripper has only been designed to a preliminary stage at this point in the design, placing it around a TRL 2 level. While robotic manipulators have a long tested history in space operations, finger-claws have less of a presence. There are current developments being made for such technologies for space debris capture, but currently nothing has been flown. These future technologies could be leveraged and adjusted for this application. As mentioned in Section 11.3, many of the controls aspects of such a gripper are the most challenging. While robotic manipulator controls are well known and understood, the controls required for the actuation of multiple fingers of the claw, and the synchronization of these actuators is not a trivial task. This would require future development and testing on its own, and testing with a Bennu boulder or boulder simulant would also be necessary to know how the system interacts with its target object.

16 Processor

The processor concept presented makes use of current technologies and technologies that are currently in development. For the processor to work as intended, it is required that all these technologies work reliably over the long mission cycle. The processor elements used in the processor and their current TRL levels are shown in Table 16.1 below.

The inflatable solar optics which includes the thin film solar concentrators, light tubes and deploying mechanisms are key to deliver the power to the processor oven. This technology has been demonstrated on ground and extensive ground studies have been performed by a few companies like L'Garde Inc [83] [84]. This technology has a TRL of 6 and would require demonstrations in space. The optical mining technology is also well researched and extensive research and testing is in progress from TransAstra, putting this at a TRL level of 5.

The telescopic members used on the processor have a TRL level of 9 since they have been successfully deployed on many spacecrafts and satellites. The boulder loading mechanism, inflatable boulder crushing unit and tailing collection units are unique concepts developed for this project and have never been tested or demonstrated before. The cold finger water transport mechanism is a well established technology on Earth for volatile collection in thermal vacuum chambers, but it has not been used of vast distances, and has not been demonstrated or researched in the microgravity environment.

Finally, it should be noted that none of these elements have been demonstrated in Bennu's environment or on a similar simulated environment. All these elements are central to the success of this mission and will require extensive testing in the appropriate environment.

Table 16.1: Processor TRL Assessment

Element	TRL	Comments
Inflatable optics	6	Multiple tests conducted in space environment and ground
Optical mining	5	TransAstra
Telescopic members	9	Multiple satellites use telescopic members
Inflatable boulder loading bags	3	
Tailing collection unit	2	
Cold finger water transport	4	

16.1 TBM Crusher Face

As described in Section 12.2, the TBM face is only roughly worked out at this stage. The final face would need to be tested on either direct Bennu regolith or a regolith simulant. When the OSIRIS-REx sample is returned, many more properties about the regolith will be known and will influence the design. One factor that shows some support for a TBM face as the crusher, is its previous application on rock types will low ultimate compressive strength. Such an example includes the TBM used for the Chunnel, as this TBM bored through limestone, which is one of the closest weak chalky-like rocks on Earth to Bennu boulders. This places a farily high TRL around 5 for the TBM, but the exact geometry and design of the TBM for this application would need to be developed and demonstrated to reduce mission risk, as crushing is a key element of the water extraction process.

16.2 Tailings Disposal

Currently, the tailings disposal subsystem has a TRL of 2. The TRL is relatively low since there are no current examples of mining tailings disposal in space. The next steps required to move to TRL 3 would be to use the CAD developed for TRL 2 to create and test a physical proof-of-concept.

Another important consideration is the interface between the tailings disposal unit and the minecart. Firstly, the physical interface must be designed and tested to ensure that the minecart can securely collect the tailings bag. Secondly, the timing of this maneuvre must be analyzed. For the purposes of the proposed design, it was assumed that the minecart would collect the tailings back and deposit it on the surface at some point in the operation, but the specific timing was not confirmed. It must be determined whether the minecart must collect the tailings bag immediately after it is filled and sealed to allow for a subsequent bag to be fille to facilitate continuous processing, or whether the tailings bag can stay attached to the tailings disposal unit until the minecart is ready to make a trip to the surface to collect a boulder, and it can deposit the tailings bag while at the surface.

Once the physical model is created, testing for both of these aspects can confirm firstly that the tailings disposal unit is able to perform its independent functions, and secondly that its interfaces with the processer unit and the minecart are appropriately timed and functional. This testing can be incorporated into the demo mission.

Chapter 9: Conclusion

This report outlines the motivation for and proposed design to mine the asteroid Bennu for water. First, the background is presented with a focus on relevant reference missions and existing methods and technologies. A discussion of the properties of the boulders on Bennu is also included here. Following the review of the literature, the trade studies are conducted. These are broken down into trades on the Mission Architecture, and trades on specific mechanisms such as the Gripping, Loading, Crushing, and Processing of boulders, and Tailings Disposal.

Next, the overall mission concept is presented. This comprises the mission-level requirements, the boulder target selection, and a concept of operations. The requirements are derived based on the required revenue, timescale, and launch breakdown. The finalized systems for the mission are then outlined in further detail, with key subsystems overviewed in two subsequent chapters. The system-level and subsystem-level requirements are derived and the details of the design are illustrated in the form of SHDs, SBDs and CADs. Key detailed analysis is outlined, and complicated controls mechanisms are acknowledged.

The mission cost estimate is presented in Chapter 7. The proposed design has a $1.5 billion dollar budget, which is broken down by the launches, mass of the spacecraft, and labour and non-labour costs of construction, testing, and operations. Finally, a discussion of the technology development and demonstration is presented, outlining the need for a “Demo Mission”. The next steps for key technologies, and ways to learn more about Bennu’s surface, are outlined.

There is a certain level of confidence in the launch and timeline calculations, and the processor method leverages current technologies. However, as previously mentioned, some elements of this mission must be extended in the future. These include the development of the thrusters, fleshing out the TBM concept in further detail, and developing physical models of the tailings disposal unit for testing.

Overall, the Khepri Project outlines a preliminary concept that would allow humanity to leverage Bennu’s abundant water resources for the benefit of future space missions.

References

[1] A. Praet, M. A. Barucci, B. E. Clark, H. H. Kaplan, A. A. Simon *et al.*, "Hydrogen abundance estimation and distribution on (101955) bennu," *Icarus*, vol. 363, 7 2021.

[2] D. S. Lauretta, S. S. Balram-Knutson, E. Beshore, W. V. Boynton, C. D. d'Aubigny *et al.*, "Osiris-rex: Sample return from asteroid (101955) bennu," pp. 925–984, 10 2017.

[3] M. Beckman, B. W. Barbee, B. G. Williams, K. Williams, B. Sutter *et al.*, "Trajectory and mission design for the origins spectral interpretation resource identification security regolith explorer (osiris-rex) asteroid sample return mission." [Online]. Available: http://neo.jpl.nasa.gov/neo/groups.html,

[4] E. Jawin, T. McCoy, K. Walsh, H. Connolly, R.-L. Ballouz *et al.*, "Global geologic map of asteroid (101955) bennu indicates heterogeneous resurfacing in the past 500,000 years," *Icarus*, vol. 381, p. 114992, 7 2022.

[5] H. H. Kaplan, D. S. Lauretta, A. A. Simon, V. E. Hamilton, D. N. Dellagiustina *et al.*, "Bright carbonate veins on asteroid (101955) bennu: Implications for aqueous alteration history," *Science*, vol. 370, 11 2020.

[6] R. L. Ballouz, K. J. Walsh, O. S. Barnouin, D. N. DellaGiustina, M. A. Asad *et al.*, "Bennu's near-earth lifetime of 1.75 million years inferred from craters on its boulders," *Nature*, vol. 587, pp. 205–209, 11 2020.

[7] K. J. Walsh, R.-L. Ballouz, E. R. Jawin, C. Avdellidou, O. S. Barnouin *et al.*, "Near-zero cohesion and loose packing of bennu's near subsurface revealed by spacecraft contact," p. 6229, 2022. [Online]. Available: https://www.science.org

[8] E. R. Jawin, T. McCoy, A. Ryan, H. Kaplan, R. l Ballouz *et al.*, "Boulder classification on bennu based on morphology and albedo."

[9] E. R. Jawin, K. J. Walsh, O. S. Bar-nouin, T. J. McCoy, R.-L. Ballouz *et al.*, "The geology of bennu's biggest boulders."

[10] B. Rozitis, A. J. Ryan, J. P. Emery, P. R. Christensen, V. E. Hamilton *et al.*, "Asteroid (101955) bennu's weak boulders and thermally anomalous equator," *Science Advances*, vol. 6, 10 2020. [Online]. Available: https://www.science.org/doi/full/10.1126/sciadv.abc3699

[11] K. Ishimaru, D. S. Lauretta, N. Porter, D. R. Golish, M. A. Asad *et al.*, "Apparently layered boulders with multiple textures on bennu's surface."

[12] E. R. Jawin, K. J. Walsh, T. J. Mccoy, H. C. Connolly, A. J. Ryan *et al.*, "The geology of (101955) bennu from the first year of osiris-rex observations: Diverse boulders and recent mass movement."

[13] B. Rozitis, A. J. Ryan, J. P. Emery, M. C. Nolan, S. F. Green *et al.*, "High-resolution thermophysical analysis of the osiris-rex sample site and three other regions of interest on bennu," *Journal of Geophysical Research: Planets*, 6 2022. [Online]. Available: https://onlinelibrary.wiley.com/doi/10.1029/2021JE007153

[14] F. Merlin, J. D. Deshapriya, S. Fornasier, M. A. Barucci, A. Praet *et al.*, "In search of bennu analogs: Hapke modeling of meteorite mixtures," *Astronomy and Astrophysics*, vol. 648, 4 2021.

[15] V. E. Hamilton, A. A. Simon, H. H. Kaplan, D. C. Reuter, P. R. Christensen *et al.*, "The global mineralogy of (101955) bennu from vnir and tir observations during the detailed survey phase of the osiris-rex mission."

[16] V. E. Hamilton, H. H. Kaplan, H. C. Connolly, C. A. Goodrich, N. M. Abreu *et al.*, "Gro 95577 (cr1) as a mineralogical analogue for asteroid (101955) bennu," *Icarus*, vol. 383, p. 115054, 9 2022. [Online]. Available: https://linkinghub.elsevier.com/retrieve/pii/S001910352200166X

[17] H. H. Kaplan, A. A. Simon, V. E. Hamilton, M. S. Thompson, S. A. Sandford *et al.*, "Composition of organics on asteroid (101955) bennu," *Astronomy and Astrophysics*, vol. 653, 9 2021.

[18] D. Lauretta, C. Hergenrother, S. Chesley, J. Léonard, J. Pelgrift *et al.*, "Episodes of particle ejection from the surface of the active asteroid (101955) bennu," *Advancement of Science*, vol. 366, 2019.

[19] A. E. Rubin, J. M. Trigo-Rodríguez, H. Huber, and J. T. Wasson, "Progressive aqueous alteration of cm carbonaceous chondrites," *Geochimica et Cosmochimica Acta*, vol. 71, pp. 2361–2382, 5 2007.

[20] V. E. Hamilton, A. A. Simon, P. R. Christensen, D. C. Reuter, B. E. Clark *et al.*, "Evidence for widespread hydrated minerals on asteroid (101955) bennu," *Nature Astronomy*, vol. 3, pp. 332–340, 4 2019.

[21] C. Che, T. D. Glotch, D. L. Bish, J. R. Michalski, and W. Xu, "Spectroscopic study of the dehydration and/or dehydroxylation of phyllosilicate and zeolite minerals," *Journal of Geophysical Research E: Planets*, vol. 116, 2011.

[22] K. J. Walsh, E. R. Jawin, R. L. Ballouz, O. S. Barnouin, E. B. Bierhaus *et al.*, "Craters, boulders and regolith of (101955) bennu indicative of an old and dynamic surface," *Nature Geoscience*, vol. 12, pp. 242–246, 4 2019.

[23] R. L. Ballouz, K. J. Walsh, P. Sánchez, K. A. Holsapple, P. Michel *et al.*, "Modified granular impact force laws for the osiris-rex touchdown on the surface of asteroid (101955) bennu," *Monthly Notices of the Royal Astronomical Society*, vol. 507, pp. 5087–5105, 11 2021.

[24] P. T. Metzger, C. D. Immer, C. M. Donahue, B. T. Vu, R. C. Latta *et al.*, "Jet-induced cratering of a granular surface with application to lunar spaceports," *Journal of Aerospace Engineering*, vol. 22, pp. 24–32, 1 2009.

[25] J. Vessaire, G. Varas, S. Joubaud, R. Volk, M. Bourgoin *et al.*, "Stability of a liquid jet impinging on confined saturated sand," *Liquid Jet Impinging on Confined Saturated Sand. Physical Review Letters*, vol. 2020. [Online]. Available: https://hal.archives-ouvertes.fr/hal-02929125

[26] Z. Bo, Y. Feng, W. Huang, and Y. Cui, "Diffusion phenomenon of lunar soil particles under a plume in a vacuum environment by numerical simulation," *Acta Astronautica*, vol. 171, pp. 403–414, 6 2020.

[27] S. K. Mishra, K. D. Prasad, P. Nath, D. Agarwal, S. S. Kumar *et al.*, "Effect of lunar landing on its surface, surrounding environment and hardware: A numerical perspective," *Planetary and Space Science*, vol. 211, 2 2022.

[28] D. Fontes, J. G. Mantovani, and P. Metzger, "Numerical estimations of lunar regolith trajectories and damage potential due to rocket plumes," *Acta Astronautica*, vol. 195, pp. 169–182, 6 2022.

[29] M. Raeisi, M. Mohammadi-Amin, and R. Zakeri, "Direct simulation monte carlo of counter flow jet interaction with reentry capsule rarefied flow," *Proceedings of 9th International Conference on Recent Advances in Space Technologies, RAST 2019*, pp. 173–180, 6 2019.

[30] T. J. Scanlon, E. Roohi, C. White, M. Darbandi, and J. M. Reese, "An open source, parallel dsmc code for rarefied gas flows in arbitrary geometries," *Computers and Fluids*, vol. 39, pp. 2078–2089, 12 2010.

[31] E. B. Bierhaus, J. T. Songer, B. C. Clark, R. D. Dubisher, S. L. Deden *et al.*, "Bennu regolith mobilized by tagsam: Expectations for the osiris-rex sample collection event and application to understanding naturally ejected particles," *Icarus*, vol. 355, 2 2021.

[32] Z. Zhao, S. Wang, D. Li, H. Wang, Y. Wang *et al.*, "Development of an anchoring system for the soft asteroid landing exploration," *International Journal of Aerospace Engineering*, vol. 2019, 2019.

[33] T. A. Newson, F. W. Smith, and P. Brunning, "Silt and siltation," 2001.

[34] K. Zacny, P. Chu, J. Craft, M. M. Cohen, W. W. James *et al.*, "Asteroid mining," 2013.

[35] "Robotic asteroid prospector (rap) staged from l1: Start of the deep space economy nnx12ar04g astrotecture™," 2013.

[36] "The physical characteristics of surface earth-like planets, dwarf and small (asteroids) planets, and their companions, according to distance studies — request pdf." [Online]. Available: https://www.researchgate.net/publication/303666129_The_physical_characteristics_of_surface_Earth-like_planets_dwarf_and_small_asteroids_planets_and_their_companions_according_to_distance_studies

[37] "Is it dangerous asteroids?" [Online]. Available: https://www.researchgate.net/publication/267764844_Is_it_dangerous_asteroids

[38] A. J. Brearley, Brearley, and A. J., "Nebular versus parent-body processing," *TrGeo*, vol. 1, p. 711, 12 2003. [Online]. Available: https://ui.adsabs.harvard.edu/abs/2003TrGeo...1..247B/abstract

[39] D. J. Barber, "Matrix phyllosilicates and associated minerals in c2m carbonaceous chondrites," *Geochimica et Cosmochimica Acta*, vol. 45, pp. 945–970, 6 1981.

[40] H. Campins, K. Hargrove, N. Pinilla-Alonso, E. S. Howell, M. S. Kelley *et al.*, "Water ice and organics on the surface of the asteroid 24 themis," *Nature 2010 464:7293*, vol. 464, pp. 1320–1321, 4 2010. [Online]. Available: https://www.nature.com/articles/nature09029

[41] J. D. Macdougall, G. W. Lugmair, and J. F. Kerridge, "Early solar system aqueous activity: Sr isotope evidence from the orgueil ci meteorite," *Nature 1984 307:5948*, vol. 307, pp. 249–251, 1984. [Online]. Available: https://www.nature.com/articles/307249a0

[42] D. S. Lauretta, D. N. DellaGiustina, C. A. Bennett, D. R. Golish, K. J. Becker *et al.*, "The unexpected surface of asteroid (101955) bennu," *Nature*, vol. 568, pp. 55–60, 4 2019.

[43] D. Takir, J. P. Emery, H. Y. Mcsween, C. A. Hibbitts, R. N. Clark *et al.*, "Nature and degree of aqueous alteration in cm and ci carbonaceous chondrites," *Meteoritics Planetary Science*, vol. 48, pp. 1618–1637, 9 2013. [Online]. Available: https://onlinelibrary.wiley.com/doi/full/10.1111/maps.12171https://onlinelibrary.wiley.com/doi/abs/10.1111/maps.12171https://onlinelibrary.wiley.com/doi/10.1111/maps.12171

[44] E. Quirico, F. R. Orthous-Daunay, P. Beck, L. Bonal, R. Brunetto *et al.*, "Origin of insoluble organic matter in type 1 and 2 chondrites: New clues, new questions," *Geochimica et Cosmochimica Acta*, vol. 136, pp. 80–99, 7 2014.

[45] E. Quirico, L. Bonal, P. Beck, C. M. Alexander, H. Yabuta *et al.*, "Prevalence and nature of heating processes in cm and c2-ungrouped chondrites as revealed by insoluble organic matter," *Geochimica et Cosmochimica Acta*, vol. 241, pp. 17–37, 11 2018.

[46] V. E. Hamilton, A. A. Simon, P. R. Christensen, D. C. Reuter, B. E. Clark *et al.*, "Evidence for widespread hydrated minerals on asteroid (101955) bennu," *Nature Astronomy*, vol. 3, pp. 332–340, 4 2019.

[47] T. Yada, A. Fujimura, M. Abe, T. Nakamura, T. Noguchi *et al.*, "Hayabusa-returned sample curation in the planetary material sample curation facility of jaxa," *Meteoritics Planetary Science*, vol. 49, pp. 135–153, 2 2014. [Online]. Available: https://onlinelibrary.wiley.com/doi/full/10.1111/maps.12027https://onlinelibrary.wiley.com/doi/abs/10.1111/maps.12027https://onlinelibrary.wiley.com/doi/10.1111/maps.12027

[48] T. Nakamura, T. Noguchi, M. Tanaka, M. E. Zolensky, M. Kimura *et al.*, "Itokawa dust particles: A direct link between s-type asteroids and ordinary chondrites," *Science*, vol. 333, pp. 1113–1116, 8 2011. [Online]. Available: https://www.science.org/doi/10.1126/science.1207758

[49] Z. Jin and M. Bose, "New clues to ancient water on itokawa," *Science Advances*, vol. 5, 5 2019. [Online]. Available: https://www.science.org/doi/10.1126/sciadv.aav8106

[50] A. S. Rivkin, E. S. Howell, J. P. Emery, and J. Sunshine, "Evidence for oh or h2o on the surface of 433 eros and 1036 ganymed," *Icarus*, vol. 304, pp. 74–82, 4 2018.

[51] E. Jarosewich, "Chemical analyses of meteorites: A compilation of stony and iron meteorite analyses," *Meteoritics*, vol. 25, pp. 323–337, 12 1990. [Online]. Available: https://onlinelibrary.wiley.com/doi/full/10.1111/j.1945-5100.1990.tb00717.xhttps://onlinelibrary.wiley.com/doi/abs/10.1111/j.1945-5100.1990.tb00717.xhttps://onlinelibrary.wiley.com/doi/10.1111/j.1945-5100.1990.tb00717.x

[52] K. Zacny, P. Chu, G. Paulsen, A. Avanesyan, J. Craft *et al.*, "Mobile in-situ water extractor (miswe) for mars, moon, and asteroids in situ resource utilization." American Institute of Aeronautics and Astronautics Inc., 2012.

[53] W. F. Bottke, A. Cellino, P. Paolicchi, and R. P. Binzel, "Asteroids iii - titles," *Asteroids III*, vol. 98, pp. 55–69, 2002. [Online]. Available: https://books.google.com/books/about/Asteroids_III.html?id=NobvAAAAMAAJ

[54] M. J. Gaffey, E. A. Cloutis, M. S. Kelley, and K. L. Reed, "Mineralogy of asteroids," *Asteroids III*, pp. 183–204, 8 2002.

[55] K. Lodders, "Principles and perspectives in cosmochemistry," *Astrophysics and Space Science Proceedings*, vol. 0, p. 46, 2010. [Online]. Available: http://arxiv.org/abs/1010.2746

[56] J. R. Brophy, R. Gershman, D. Landau, J. Polk, C. Porter *et al.*, "Asteroid return mission feasibility study."

[57] J. R. Brophy and B. Muirhead, "Near-earth asteroid retrieval mission (arm) study by the jet propulsion laboratory (jpl) in collaboration with."

[58] N. Anthony, J. Frostevarg, H. Suhonen, C. Wanhainen, A. Penttilä *et al.*, "Laser processing of minerals common on asteroids," *Optics and Laser Technology*, vol. 135, 3 2021.

[59] "A techno-economic analysis of asteroid mining." [Online]. Available: https://www.researchgate.net/publication/328189258_A_Techno-Economic_Analysis_of_Asteroid_Mining

[60] J. C. Sercel, "Asteroid provided in-situ supplies (apis): A breakthrough to enable an affordable nasa program of human exploration and commercial space industrialization niac phase i final report," 2016. [Online]. Available: www.transastracorp.com

[61] C. S. Cockell, R. Santomartino, K. Finster, A. C. Waajen, L. J. Eades *et al.*, "Space station biomining experiment demonstrates rare earth element extraction in microgravity and mars gravity," *Nature Communications*, vol. 11, 12 2020.

[62] R. Santomartino, L. Zea, and C. S. Cockell, "The smallest space miners: principles of space biomining," *Extremophiles 2021 26:1*, vol. 26, pp. 1–19, 1 2022. [Online]. Available: https://link.springer.com/article/10.1007/s00792-021-01253-w

[63] F. Gòdia, J. Albiol, J. L. Montesinos, J. Pérez, N. Creus *et al.*, "Melissa: A loop of interconnected bioreactors to develop life support in space," *Journal of Biotechnology*, vol. 99, pp. 319–330, 11 2002.

[64] "Interstellar water and interstellar ice."

[65] A. M. McDonnell, D. Beving, A. Wang, W. Chen, and Y. Yan, "Hydrophilic and antimicrobial zeolite coatings for gravity-independent water separation," *Advanced Functional Materials*, vol. 15, pp. 336–340, 2 2005.

[66] M. Damak and K. K. Varanasi, "Electrostatically driven fog collection using space charge injection," 2018. [Online]. Available: https://www.science.org

[67] J. Nijhuis, S. Schmidt, N. N. Tran, and V. Hessel, "Microfluidics and macrofluidics in space: Iss-proven fluidic transport and handling concepts," *Frontiers in Space Technologies*, vol. 2, 1 2022.

[68] T. Fay, "Freeze protection for natural gas pipeline systems and measurement instrumentation."

[69] I. Staff, *2017 14th International Conference on Ubiquitous Robots and Ambient Intelligence (URAI).* IEEE, 2017.

[70] F. Alibay, "Evaluation of multi-vehicle architectures for the exploration of planetary bodies in the solar system," 2009.

[71] J. L. Molaro, K. J. Walsh, E. R. Jawin, R. L. Ballouz, C. A. Bennett *et al.*, "In situ evidence of thermally induced rock breakdown widespread on bennu's surface," *Nature Communications 2020 11:1*, vol. 11, pp. 1–11, 6 2020. [Online]. Available: https://www.nature.com/articles/s41467-020-16528-7

[72] H. Rein and S. F. Liu, "Rebound: An open-source multi-purpose n-body code for collisional dynamics," *Astronomy and Astrophysics*, vol. 537, 2012.

[73] J. N. Larson and G. Sarid, "An n-body approach to modeling debris and ejecta off small bodies: Implementation and application," *MNRAS*, vol. 000, pp. 1–13, 2021.

[74] K. A. Holsapple, "The scaling of impact processes in planetary sciences," *Annual Review of Earth Planetary Sciences*, vol. 21, pp. 333–373, 1993.

[75] K. R. Housen and K. A. Holsapple, "Ejecta from impact craters," *Icarus*, vol. 211, pp. 856–875, 1 2011.

[76] J. E. Richardson, H. J. Melosh, C. M. Lisse, and B. Carcich, "A ballistics analysis of the deep impact ejecta plume: Determining comet tempel 1's gravity, mass, and density," *Icarus*, vol. 190, pp. 357–390, 10 2007.

[77] K. Stoy, K. Walker, S. A. Nielsen, P. Ayres, M. K. Heinrich *et al.*, "A large-scale, light-weight, and soft braided robot manipulator with rapid expansion capabilities." Institute of Electrical and Electronics Engineers Inc., 4 2021, pp. 495–500.

[78] R. Stevens, *Mining and Mineral Exploration Essentials*, 1st ed. Pakawau GeoManagement Inc., 2010.

[79] D. R. Golish, N. K. Shultz, T. L. Becker, K. J. Becker, K. L. Edmundson *et al.*, "A high-resolution normal albedo map of asteroid (101955) bennu," *Icarus*, vol. 355, 2 2021.

[80] X. Huang, L. Zhang, and P. Li, "Classification and extraction of spatial features in urban areas using high-resolution multispectral imagery," *IEEE Geoscience and Remote Sensing Letters*, vol. 4, pp. 260–264, 4 2007.

[81] T. Kadono, M. Arakawa, R. Honda, K. Ishibashi, K. Ogawa *et al.*, "Impact experiment on asteroid (162173) ryugu: Structure beneath the impact point revealed by in situ observations of the ejecta curtain," *The Astrophysical Journal*, vol. 899, p. L22, 8 2020.

[82] D. J. Scheeres, S. G. Hesar, S. Tardivel, M. Hirabayashi, D. Farnocchia *et al.*, "The geophysical environment of bennu," *Icarus*, vol. 276, pp. 116–140, 2016.

[83] F. H. Redell, J. Kleber, D. Lichodziejewski, and G. Greschik, "Inflatable-rigidizable solar concentrators for space power," 2022.

[84] G. Grossman and G. Williams, "Inflatable concentrators for solar propulsion and dynamic space power," 1990.

Appendix

A List of Lecturers and Participants

Lecturers

Joanne Leung

Joanne Leung is a Project Engineer on the Robotic Services System at MDA. She has 17 years of space robotics experience, specializing in systems and project engineering for development programs, commercialization of robotic solutions, mission operations planning and execution, and proposals and costing. She holds a BASc in Engineering Science, Aerospace, from the University of Toronto.

Adam Philip

Adam Philip is a senior member of the technical staff at MDA, specializing in controls engineering. He is a licensed P. Eng, holding B.A.Sc and M.A.Sc degrees in Mechanical and Aerospace Engineering. His works include control systems for space and medical robots, such as planetary rovers and micro-satellites. Notable projects he has been a part of include the Next Generation CANADARM and CANADARM2.

Peter Krimbalis

Dr. Peter P. Krimbalis is Staff MTS and Hardware Lead in the Department of Mechanical Engineering at MDA. He has provided technical & programmatic engineering services to over 10 spaceflight missions, including GSFC's OSIRIS-REx, GSFC's OSAM-1, and most recently CSA's Canadarm3 for Gateway as part of NASA's Artemis program. Formerly an academic, Peter previously served as Research Officer at National Research Council's Aerospace Research Centre, specializing in composites and novel airframe materials.

Chris Herd

Chris Herd is an internationally recognized expert in the study of meteorites, their origin, mineralogy, and organic geochemistry. Since 2003 he has been a professor in the Department of Earth and Atmospheric Sciences at the University of Alberta, and the Curator of the University's meteorite collection - the largest university-based collection in Canada and home to the only cold curation facility for meteorites and other astromaterials.

Mike Lipsett

Mike Lipsett is a Professor of Mechanical Engineering at the University of Alberta researching automating diagnostics to improve the reliability of systems. Mike designs and develops robotic systems for remote and hazardous environments. He previously conducted research for Syncrude Canada Ltd., including on mining automation and extraction processes.

Dan Sameoto

Dan Sameoto is a Professor of Mechanical Engineering at the University of Alberta. For over 10 years, Dan has specialized in MEMS/microfabrication and nanotechnology, with a strong focus on novel fabrication technologies. Dan is currently working on mechatronics-based projects, using bioinspired engineering to produce artificial gecko-like adhesives for micro-assembly, micro-fluidics, and space applications.

Erik Asphaug

Erik Asphaug is a professor and principal investigator for the SpaceTREx laboratory at the University of Arizona. His research focuses on giant impacts, which dominate the late stage of planet formation. Erik also studies the small bodies, origin of chondrules, lunar volatiles, and patterned ground on mars.

Dante Lauretta

Dante Lauretta is an expert in near-Earth asteroid formation and evolution and the leader of NASA's OSIRIS-REx mission. Dante is a Regents Professor of Planetary Science and Cosmochemistry at the University of Arizona's Lunar and Planetary Laboratory, running a research program in Cosmochemistry and Meteoritics.

Mike Nolan

Mike Nolan is the OSIRIS-REx Science Team Chief, and is based at the University of Arizona. He has worked extensively on asteroids throughout his career and was the director of Arecibo Observatory, where he studied asteroids, comets, and meteors with radar observations to constrain the delivery of meteorites to Earth. For this, he received the NASA Outstanding Leadership Award.

Anjani Polit

Anjani Polit is the Mission Implementation Systems Engineer for the OSIRIS-REx mission where she is involved in mission planning and ensures the success of science goals. Prior to joining the OSIRIS-REx mission she was the uplink operations lead for the HiRISE instrument on the Mars Reconnaissance Orbiter.

Jekan Thanga

Jekan Thanga is an associate professor and heads the SpaceTREx and ASTEROIDS laboratories at the University of Arizona. His current research focuses on control systems encompassing a wide range of space technologies including propulsion, deployable structures, and communications. He previously worked at MDA where he was involved in both CANADARM projects.

Mark Barnet

Mark Barnet has an extensive background in spacecraft systems engineering and operations engineering. He was the lead systems engineer on several MDA space programs including Canadarm3 integration with Gateway, and has taught systems engineering at MDA, Bruce Power, and UTIAS. Mark now works at the Dunlap Institute for Astronomy and Astrophysics at the University of Toronto, leading the systems engineering effort on a new instrument for the Gemini North 8m telescope.

Chris Damaren

Chris Damaren is the director of the Institute for Aerospace Studies at the University of Toronto. Chris' research focuses on the development of spacecraft control systems including for formation flying spacecraft and utilizing Earth's magnetic field for control torque. He previously conducted research on flexible manipulators.

Tim Newson

Tim Newson is currently Western's Geotechnical Research Centre Director. He has worked from the UK to Australia on engineering projects for the offshore, mining, environmental, and civil engineering industries. His research interests include constitutive disposal of mine wastes, centrifuge and laboratory testing techniques, and soft soil and clay engineering.

Panelists

Gavin Hay

Gavin Hay has 20 years of technical and leadership experience in the proposal, development, build, and test of complex robotic systems for human safety critical, government, scientific, and commercial applications for use in spaceflight, nuclear, and medical environments. A precursor 7 years as a naval diesel mechanic in the Royal Canadian Navy provided the team leadership and hands-on technical skills to benefit his professional roles in the spaceflight/aerospace industry.

Carlos Lange

Carlos Lange is an associate professor for the Mechanical Engineering Department of the Faculty of Engineering at the University of Alberta. He holds a PhD from Friedrich-Alexander University Erlangen-Nuremberg. His main area of expertise is Computational Fluid Dynamics. His research interests range from simulations of the lung, such as drug deposition, airway surface liquid concentration of deposited drugs, aerosol generation from cough, to simulations of winds and the water cycle on Mars.

Benoit Rivard

Benoit Rivard is a Professor for the Earth & Atmospheric Sciences division of the Faculty of Science at the University of Alberta. He is a leading expert in the development of hyperspectral imaging applications in resource exploration. Dr. Rivard's research interest lies in the development of applied geological remote sensing.

Leonard Vance

Leonard Dean Vance is a PhD graduate in Aerospace and Mechanical Engineering at the University of Arizona, and a retired Senior Fellow from Raytheon Missile Systems. His 33-year career at Hughes Aircraft and Raytheon Missile Systems includes Systems Engineering lead, Chief Engineer and Program manager for a variety of forward leaning projects, including the LEAP kinetic kill vehicle, the AIM-9X sidewinder missile, Kinetic Energy Interceptor and program manager for the SeeMe imaging microsatellite. He also holds a Master of Engineering and six patents.

Brandon DeHart

Brandon DeHart is a Sessional Instructor, Adjunct Assistant Professor, and RoboHub Manager at the University of Waterl oo. He holds a MASc and PhD in Electrical and Computer Engineering from the University of Waterloo. His research interests span a wide range of topics connected to robotics, from tensegrity structures and bioinspired robot design to interactive architecture and morphological computation.

Gordon "Oz" Osinski

Gordon Osinski is a Professor in the Department of Earth Sciences at the University of Western Ontario. His research interests are diverse and interdisciplinary in nature, motivated by understanding the evolution of the surface of the Earth and other planetary bodies as well as the origin and evolution of life. He is also involved in several past and ongoing exploration-related activities, specifically science instrument and rover development for the Moon and Mars.

Participants

Gowtham Boyala

Gowtham is a 2nd year MSc in Mechanical Engineering at the Univeristy of Alberta. His background is in machine design, product development and systems and microgravity fluid dynamics. He has over 2 years of professional experience working with an Aerospace company. He is proficient in CAD, CAM, FEA, CFD.

Email: boyala@ualberta.ca
LinkedIn: linkedin.com/in/gowtham-boyala-ba25a5b9

Adam Gremm

Adam is a recent graduate of the Mining Engineering program at the University of Alberta. His co-op experiences saw him working as a survey and material testing student at Rio Tinto (Diavik) and a long-range mine planner at Teck Resources (FRX). Adam is passionate about automation and optimization in the mining industry, working with companies such as RPM Global to develop innovative mine planning tools.

Email: gremm@ualberta.ca
LinkedIn: https://www.linkedin.com/in/adamgremm/

Ahmet Gungor

Ahmet has a solid background in Mechanical Engineering. Currently, he is a PhD candidate at the University of Alberta. His main area of research is bio-inspired design of systems of oscillating foils using Computational Fluid Dynamics (CFD). He is passionate about developing fundamental understanding in flow physics and other fluid related phenomena.

Email: gungor@ualberta.ca
LinkedIn: https://www.linkedin.com/in/ahmet-g%C3%BCng%C3%B6r-abb5b216b/

Amirhossein Taghipour

Amir is pursuing his Ph.D. degree at the University of Alberta majoring in Mechanical Engineering. His current research is on the application of membrane technologies for water and wastewater treatment and desalination. Currently, as a member of the advanced water research lab (AWRL), he is working on the investigation of a novel technique for the fabrication of thin-film composite (TFC) membranes (RO application).

Email: taghipo1@ualberta.ca
LinkedIn: https://ir.linkedin.com/in/amirhossein-taghipour

Massimo Biella

Massimo is a second-year Aerospace Engineering Master's student at the University of Arizona. He has a solid background in fluid-mechanics applied to fundamental Hypersonic Boundary Layer transition research and he recently started transitioning to GNC and system's engineering. He is fluent in MATLAB, CFD software, FORTRAN, CAD and HPC computing.

Email: maxb24@email.arizona.edu
LinkedIn: https://www.linkedin.com/in/massimobiella/

Jiawei "Jackson" Qiu

Jackson is going into his second year for a PhD degree in Aerospace Engineering at the University of Arizona. He got his bachelor's degree in Physics and Astronomy at the University of Waterloo. He is interested in space system design and space mission concept designs. He is currently investigating the establishment of the early stages of the lunar base.

Email: jqx@arizona.edu
LinkedIn: https://www.linkedin.com/in/jiaweiqiu/

Athip Thirupathi Raj

Athip Thirupathi Raj is currently pursuing a PhD in Aerospace Engineering from the University of Arizona and holds a Master's Degree in Space Systems Engineering. He has worked on projects with JPL, Kennedy Space Center, and the Indian Institute of Technology Madras. His research interests include Small Satellites, Autonomous Rendezvous and Docking, Off-World bases, and human habitats.

Email: athipt@email.arizona.edu
LinkedIn: https://www.linkedin.com/in/athip-thirupathi-raj-94ba4170/

Arjun Chhabra

Arjun is a recent graduate of the Engineering Science program at the University of Toronto. With a major in Robotics Engineering and a minor in Artificial Intelligence Engineering, Arjun is passionate about building autonomous aerospace systems. He is especially interested in developing novel techniques for autonomous navigation of spacecraft and will be attending Princeton University for a PhD focused towards the same.

Email: arjun.chhabra@princeton.edu
LinkedIn: https://www.linkedin.com/in/chhabra-arjun/

Saanjali Maharaj

Saanjali is a recent graduate of U of T's Engineering Science program (Aerospace Major). Her thesis focused on Model Predictive Control. Saanjali will pursue an MASc. at U of T's Insititute for Aerospace Studies. She has interned at NASA Ames Research Center (autonomous drone design) and Intel Corporation (thermal-mechanical engineering). Saanjali is also the Rocketry Aerodynamics Lead of the U of T Aerospace Team.

Email: saanjali.maharaj@mail.utoronto.ca
LinkedIn: https://www.linkedin.com/in/saanjali-maharaj/

Adam Gee

Adam recently completed his undergraduate degree in Engineering Science, majoring in Aerospace Engineering, at the University of Toronto. He is passionate about mathematical modelling, skills he developed while working at the National Research Council's Gas Turbine Laboratory. He completed an undergraduate thesis modelling controls for a retractable water sampling UAV, illustrating his breadth of knowledge and his passion for design and fabrication.

Email: adam.gee@mail.utoronto.ca
LinkedIn: https://www.linkedin.com/in/adam-gee/

Erin Richardson

Erin studied Aerospace Engineering at the University of Toronto and is starting her PhD in Bioastronautics at the University of Colorado Boulder. Erin interned at MDA, working on Canadarm3 collision avoidance, OLA operations, flight procedures for on-orbit assembly, and systems design for rovers. She also conducted a life sciences experiment on a parabolic flight, completed her Private Pilot License, and represented young Canadians to the UN at Space Generation Congress.

Email: erin.richardson@mail.utoronto.ca
LinkedIn: https://www.linkedin.com/in/erinrichardson24/

Haidar Ali Abdul-Nabi

Haidar Ali is going into his third year of mechanical engineering at the University of Western Ontario. He is very enthusiastic about space and loves working together with his colleagues to solve problems. He is also a prospective Astrophysics dual degree student and hopes to pursue a masters in aerospace engineering. He is fluent in programming in Matlab and very experienced in CAD.

Email: habdulna@uwo.ca
LinkedIn: https://www.linkedin.com/in/haidar-ali-abdulnabi/

Erika Frost

Erika is a third-year undergraduate student studying Environmental Engineering at the University of Western Ontario. Her fascination with space combined with her passion for sustainability has led her to a prospective career in the aerospace industry where she hopes to work in the development of green technologies. Erika is involved with Western Engineering's Solar Car Team (Sunstang), where she is the current VP of Operations. She is proficient in various CAD softwares and MATLAB.

Email: efrost6@uwo.ca
LinkedIn: https://www.linkedin.com/in/erika-frost-8ba882218/

Lindsay Richards

Lindsay is a mineral exploration geologist and upper-level undergraduate student at Vancouver Island University. He works closely with the Institute for Earth and Space Exploration at Western University and is a student member of the Canadian Space Agency topical team on space resources. Lindsay's research emphasizes combining remote sensing methods with traditional prospecting.

Email: lindsay.richards@walkaboutexploration.ca
LinkedIn: www.linkedin.com/in/lindsay-richards-geologist

Ariyaan Talukder

Ariyaan is going into his second year of mechanical engineering at the University of Western Ontario. He has many robotics and coding projects under his belt and has proficient experience in CAD. He is very passionate about the aerospace industry and sees his future career there.

Email: atalukd2@uwo.ca
LinkedIn: https://www.linkedin.com/in/ariyaan-talukder/

Julia Elizabeth Empey

Julia was most recently a Mission Systems Intern at MDA Robotics & Space Operations, responsible for writing and testing all script procedures for MDA's SPIDER satellite assembly mission & creating a virtual organizer for all aspects of the Gateway External Robotics System & CANADARM project for both MDA and external staff. Currently studying Honours Physics & Astrophysics at the University of Waterloo.

Email: JEmpey@UWaterloo.ca
LinkedIn: www.linkedin.com/in/juliaempey